RAL-93-001

Science and Engineering Research Council
Rutherford Appleton Laboratory
Chilton DIDCOT Oxon OX11 0QX

RAL-93-001

Particle Physics Experiments Report 1992

Compiled by B A Roberts

March 1993

PARTICLE PHYSICS EXPERIMENTS

1992

COMPILED BY: B A ROBERTS

INTRODUCTION

This report describes work carried out in 1992 on experiments approved by the Particle Physics Experiments Selection Panel. The contents consist of unedited contributions from each experiment.

Rutherford Appleton Laboratory
Chilton
Didcot
OXON
OX11 0QX

Science and Engineering Research Council

PARTICLE PHYSICS EXPERIMENTS

Accelerator	Year of Running	Status (Dec 1992)	Spokesman	Experiment Code
SPS	1983	Analysis	G Myatt	WA21
Reactor ILL	1980-1992	Analysis	K F Smith	PN5
SPS	1978-1989	Complete	R Barate D Websdale	NA14
SPS	1983-1986	Analysis	E Paul	WA69
	1987-1992	Running and Analysis	D H Perkins	SOUDAN II
ISIS	1988-1992	Running and Analysis	R Maschuw	KARMEN
SPS	1982-1992	Running and Analysis	J B Kinson	WA76/WA91
SPS	1985-1990	Analysis	K Peach	NA31
SPS	1984-1987	Analysis	J B Kinson	WA77

Accelerator	Year of Running	Status (Dec 1992)	Spokesman	Experiment Code
FNAL	1985-1988	Analysis	G T Jones	E632
SPS	1986-1989	Analysis	N A McCubbin	NA34
SLAC	1992	Running and Analysis	M Breidenbach	SLD
COLLIDER	1987-1990	Analysis	L Di Lella	UA2
LEAR	1991-1992	Running and Analysis	E Gabathuler	PS195

Accelerator	Year of Running	Status (Dec 1992)	Spokesman	Experiment Code
BNL	1986-1990	Analysis	P L Roberts J Lowe	AGS E811
LEAR	1989-1991	Running and Analysis	H Koch	PS197
		Preparation	P F Smith	
SPS	1987-1988	Analysis	D J Crennell	WA84
SPS	1990-1991	Analysis	G Romano D H Davis	NA34/P213 EMU09
SPS	1987-1993	Running and Analysis	J Kinson	WA85/WA94
		Preparation	N W Tanner	SNO

Accelerator	Year of Running	Status (Dec 1992)	Spokesman	Experiment Code
	1991 - 1992	Running and Analysis	J Lowe	AGS E813,836, 886
FNAL	1990	Analysis	V Smith	E761
	1992 -	Running and Analysis	D M Websdale	WA92
		Preparation	K Peach	NA48
SPS	1994	Preparation	J B Kinson	WA97
LEP	1989-1992	Running and Analysis	J Steinberger P R Norton	ALEPH
LEP	1989-1992	Running and Analysis	A Michelini R M Brown	OPAL

Accelerator	Year of Running	Status (Dec 1992)	Spokesman	Experiment Code
LEP	1989-1992	Running and Analysis	U Amaldi W Venus	DELPHI
HERA	1992	Running and Analysis	F Eisele R Marshall	H1
HERA	1992	Running and Analysis	G Wolf R J Cashmore	ZEUS
LHC		Development	D J Munday	SITP

Accelerator	Year of Running	Status (Dec 1992)	Spokesman	Experiment Code
		Development	D H Saxon	RD-6
		Development	I Kenyon	RD-23
	1992	Development	K M Smith	RD-8
		Development	R J Cashmore	SDC
		Development	G Hall	RD-20
		Development	J C Thompson	RD-28
		Development	J Garvey	RD-27
	1981-1992	Development	N Booth	-
		Development	C Danson C B Edwards	-

THE STUDY OF ν AND $\bar{\nu}$ INTERACTIONS WITH PROTONS USING THE BEBC BUBBLE CHAMBER

WA21 **PROPOSAL 004**

Birmingham University, CERN, Imperial College, MPI-Munich, Oxford University, University College London.

Data taking for this experiment was completed in December 1983. The samples include approximately 19,000 ν and 11,000 $\bar{\nu}$ charged current events. These constitute the largest data set of interactions on free protons. Work published to date includes studies of inclusive structure functions and final state properties, exclusive final states, neutral current cross sections and production of strange and charmed particles.

During the past year results have been published on the multiplicity distributions of charged hadrons in charged current interactions. It is found that the distributions are well fitted by binomial functions. The data show a violation of KNO scaling and, for fixed W, the forward and backward multiplicities are found to be uncorrelated. Studies of strange particle production have been completed. They show general agreement with empirical models based on hadron interactions. The rates of strange baryon production yield the decuplet to octet baryon production ratio and allow the break-up probabilities for uu and ud systems to be assessed.

Work continues on the neutral current to charged current cross section ratios and on the study of charged current structure functions.

Publication in 1992

Multiplicity distributions of charged hadrons in νp and $\bar{\nu} p$ charged current interactions, G. T. Jones et al., Z. Phys. C 54 (1992) 45.

SEARCH FOR THE NEUTRON ELECTRIC DIPOLE MOMENT USING ULTRACOLD NEUTRONS

ILL **PROPOSAL 157**

University of Sussex; Rutherford Appleton Laboratory; Institute Laue-Langevin; University of Harvard; University of Washington

For particles to have electric dipole moments (edm), the forces concerned in their structure must show P-violation and T-violation. If we accept the CPT theorem, this also implies CP-violation. P-violation is an intrinsic feature of the weak interaction and CP-violation has been known since 1964 to occur in the K-meson decay system, but it has not yet been identified anywhere else. Such scanty information leaves a wide range of possibilities for the theories of CP-violation. Experimental measurements of particle edms, and in particular that of the neutron, are providing some of the strongest additional constraints on such theories. The standard model of the electroweak interaction is calculated to give a contribution to the neutron edm of the order of 10^{-31} to 10^{-33} e cm. This contribution is second order in the weak interaction and very small. For various reasons many people have speculated on extensions to the Standard Model such as adding extra Higgs fields, right handed fields, and/or supersymmetric partners, any of which amounts to 'new physics'. Such additions invariably give rise to dipole contributions which are first order in the weak interaction and therefore much larger and of order 10^{-25} to 10^{-27} e cm. Such large dipole moments might also come from CP-violation in the strong interaction. Calculations with QCD predict $3 \times 10^{-16}\ \theta$ e cm for the neutron edm. A priori, the parameter θ would be of order unity but from the experimental results on the edm given below, θ is clearly less than 3×10^{-10}. It has been pointed out recently that in a class of supergravity theories $\theta = 10^{-11}$ and hence they predict an edm of 3×10^{-27} e cm. A summary of the various theoretical possibilities and the existing experimental limits is given in Fig. 1.

The most recent experimental result from our collaboration, published in 1990 was $d_n = -(3 \pm 2 \pm 4) \times 10^{-26}$ e cm. The latest result of the group at the Leningrad Nuclear Physics Institute, published in 1992 is, when similarly rounded to single digits, $d_n = +(3 \pm 4 \pm 2) \times 10^{-26}$ e cm. The statistical error is followed by the systematic error in each case. Combining the two results, one can set an upper limit of 5×10^{-26} e cm for the magnitude of the neutron EDM with 90% confidence.

The best limit on the edm of the proton from thallium fluoride molecular beam experiments remains about three orders of magnitude larger than the above limit on the neutron.

Measurements on the edm of the ^{199}Hg atom have recently advanced to the point where errors less than 10^{-27} e cm are envisaged. To obtain the sensitivity to the edm of the odd neutron in the ^{199}Hg nucleus one has to allow for an attenuation factor of about 10^4 for the shielding of the applied electric field by the atomic electrons and a predicted factor of 60 enhancement of the neutron edm by the rest of the nucleons in the nucleus through a T-violating component of the internucleon force. If this enhancement really exists, the sensitivity of the mercury experiments to a neutron edm could be comparable to that of the free neutron experiments. If the neutron edm is big enough to be seen in the near future,

then it may be seen in both types of experiment, which would be very valuable input for the theories of CP violation. The nuclear enhancement effect would also cause the experiments for the proton to be more sensitive too.

However the free neutron edm continues to be the cleanest and most profitable of these measurements to pursue. The experiment being reported on here, is situated at the ILL, Grenoble. It is now three years into a rebuilding phase which has the aim of improving the performance with respect to both the statistical errors and the systematic errors. Overall, it is hoped to reduce the limit on the neutron edm by a further factor of ten. The neutron storage and measurement cell has already been increased in volume by a factor of four to increase the average neutron counting rate and further increases in size are possible and an atomic mercury magnetometer has been introduced to measure the magnetic field in the same storage cell volume as the neutrons and reduce systematic errors (see figure 2). About 70% of the equipment is new.

The experiment is carried out by storing neutrons for about 150 seconds while their spin precession rate in a constant weak magnetic field is measured using a magnetic resonance technique. The electric dipole moment is measured by looking for the change in this precession rate when an electric field in the cell is reversed relative to the magnetic field.

To enlarge the neutron storage cell we had to build a new larger vacuum chamber and the inner layer of the magnetic shield had to be removed to make room for it, leaving only four layers. The first neutron Ramsey resonances using the new cell were obtained in the period January-March 1991 just before the ILL reactor ceased to operate. The reactor is scheduled to restart in July of 1994 after a new reactor vessel is installed. The magnetic resonance obtained, using a 150s resonance time, was found to be satisfactory. The neutron counting statistics were already a little better than in our previous measurement in spite of using neutron guides with unsuitable surface coatings. Guides with the appropriate nickel-58 coatings have now been obtained and when the neutrons return we hope to have a considerably enhanced neutron counting rate.

From April 1991 the project work has been concentrated on the development of the mercury magnetometer. The first spin precession signals of mercury in the same 20 litre neutron storage cell at ILL were obtained in August 1991. Continuous monitoring of the ^{199}Hg nuclear spins revealed by the absorption of a horizontal beam of ultraviolet mercury resonance radiation passing through the cell gave a signal to noise of 160 with a band width of 2 Hz. Improvements made in the last year have increased this signal-to-noise to 900. This figure is adequate but further improvement is desirable and probably achievable. For example, a new larger diameter quarter wave plate, needed for the circular polariser of the optical pumping beam, should provide further gains. A significant part of the improvements already obtained this last year came from the use of large high efficiency calcite crystal polarisers manufactured for us in Russia.

Another area of work for the magnetometer has been to improve the mercury spin relaxation time during storage. In particular, the affects of gas discharges on the deuterated polystyrene cell surface have been examined. The only gas found to make an improvement was oxygen. In this case the relaxation time has been increased from 16 s to about 70 s. We have the impression that small numbers of single atoms of hydrogen or deuterium on the surface can have a catalytic action for relaxing the mercury spin by forming a short lived paramagnetic

diatomic molecule HgH. With a 70 s relaxation time and a signal to noise of 1800 the mercury will provide a measurement of the magnetic field, for each four minute machine storage cycle, with an RMS noise of 1 nanogauss. The corresponding precision obtained with the neutrons will be about 3 nanogauss so that on subtracting the mercury field measurement from the neutron field measurement, to correct for any unwanted changes of magnetic field, the noise power added by the mercury will be unimportant. One snag remains, however, in that we have not yet learned to produce the 70 s relaxation time performance as reliably as we would like. Over the last few months we have gained the first experience of running the magnetometer continuously for periods of several days and we have been pleased by its reliability. We have also been running our rubidium magnetometers and find that in quiet hours the field measurement noise on this system is only 2 nanogauss. It appears that the removal of the fifth magnetic shield layer has not caused this figure to deteriorate (although we are more sensitive to specific events like crane movements). It also means that we have a good chance to see the best mercury performance directly without having to infer it from the differences in neutron and mercury magnetic field measurements. During the next year besides finished the mercury development program we will be testing the high voltage system for the electric field and then using the mercury magnetometer to look for any changes in the magnetic field which correlate with the electric field during simulated edm measurements runs.

In the UK we will be continuing to search for ways to improve the storage cell by employing better materials and larger dimensions.

Publications

1 Surface density profiles and the rate of loss of stored ultracold neutrons
M Chouder, J M Pendlebury and K F Smith
Nucl. Instrum. Meths. **A311** (1992) 287-292.

2 Steps to improve the measurement of the neutron electric dipole moment
J M Pendlebury
Nuclear Physics **A546** (1992) 359c-368c.

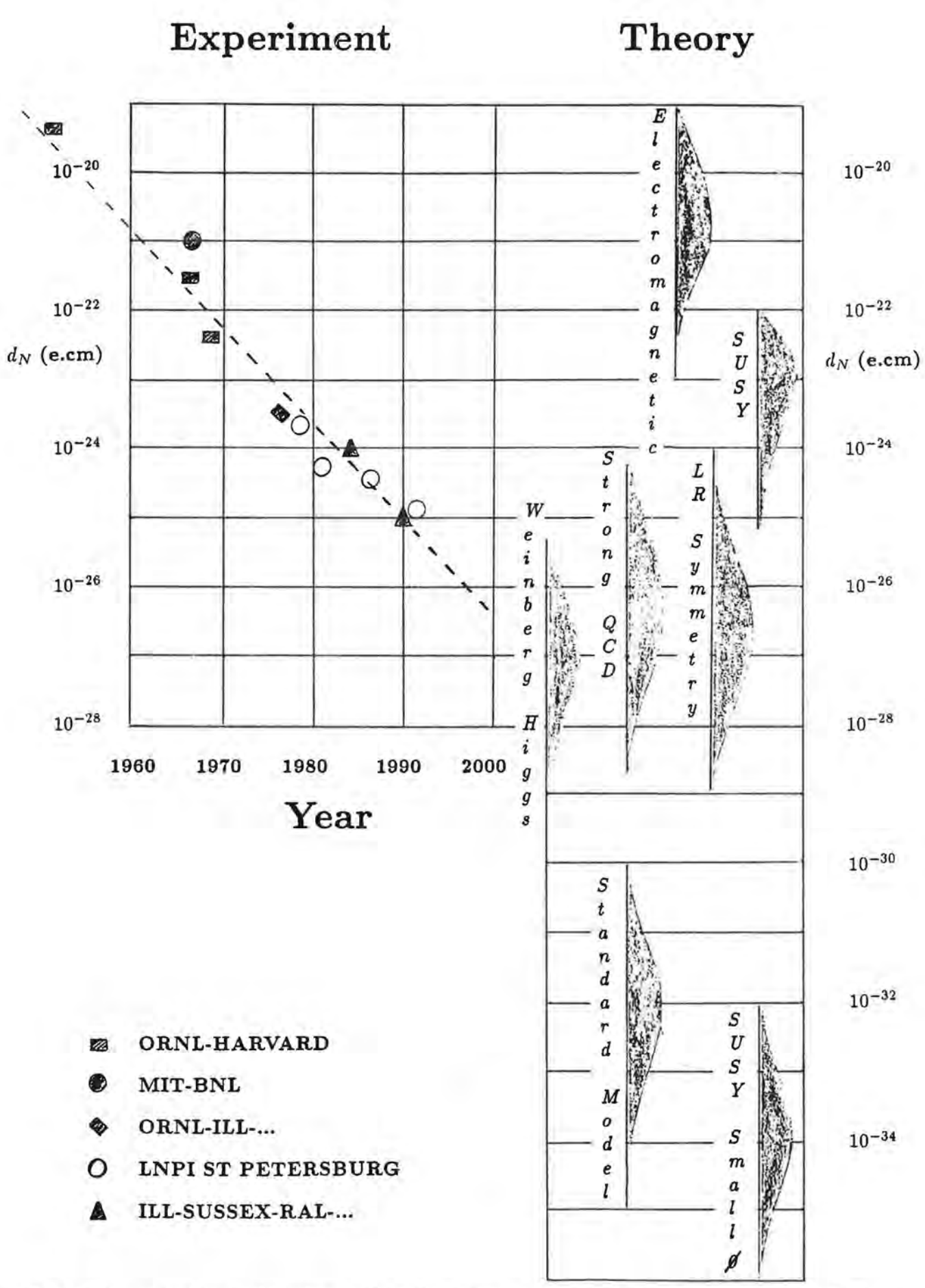

Fig. 1 The experimental limits to the edm of the neutron obtained over the last few decades are shown together with a variety of theoretical possibilities. The theoretical models of CP violation are labelled generically and reflect the range of predictions found in the literature.

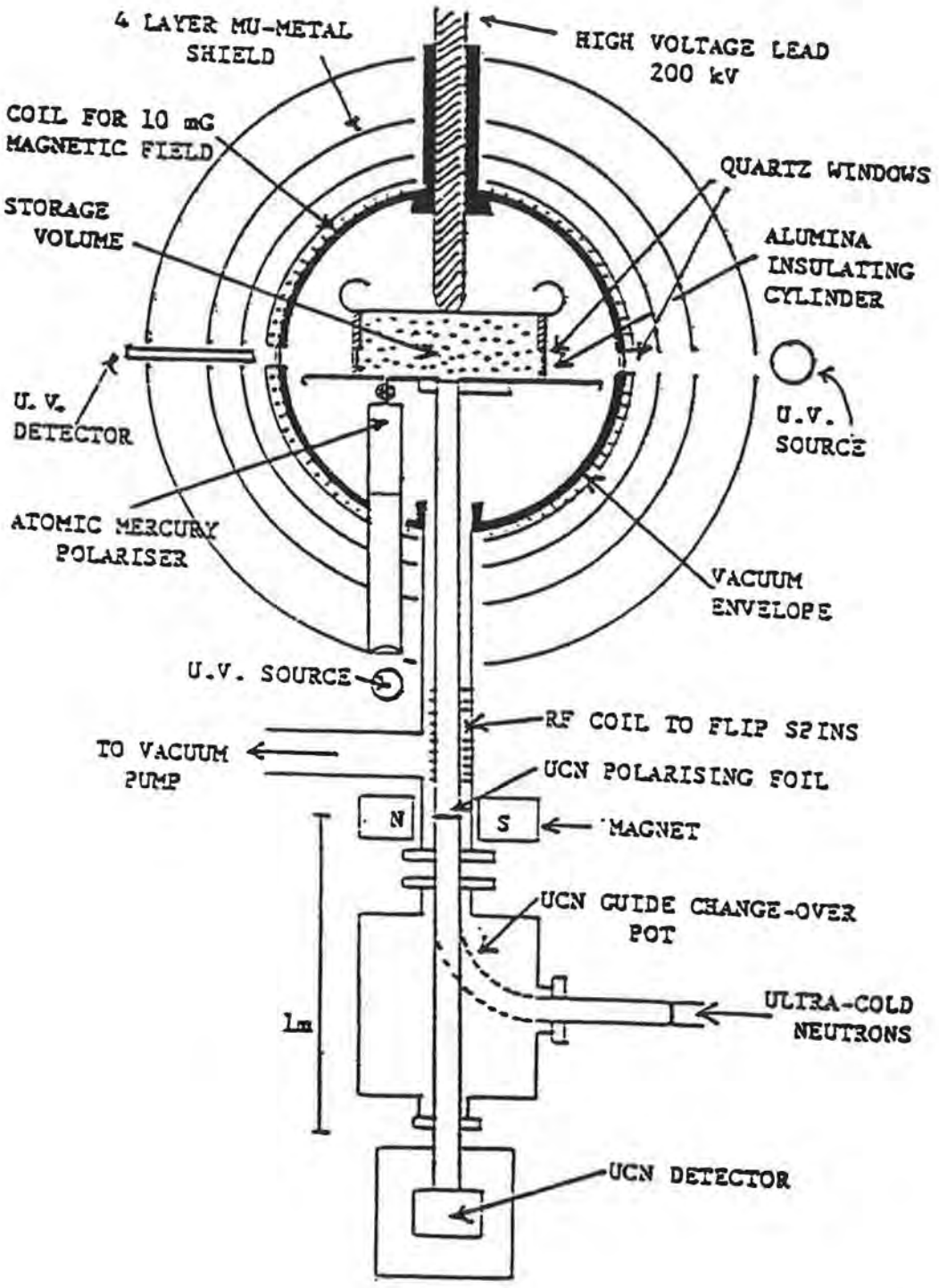

Fig.2 A schematic of the re-constructed experimental layout for the edm apparatus which has now been assembled at ILL.

AN EXPERIMENT ON PHOTOPRODUCTION AT HIGH ENERGY

NA14 **Proposal 215**

Athens, CEN-Saclay, CERN, College de France, Ecole polytechnique, Imperial College, LAL-Orsay, Southampton, Strasbourg and Warsaw Collaboration

The NA14 photoproduction experiment used the CERN tagged photon beam BEG, a high intensity bremsstrahlung beam (10^7 photons per pulse) with energy in the range 50 - 150 GeV. Analysis of data from this experiment is now complete.

Data were collected from photon hard scattering processes - deep inelastic QED Compton scattering and QCD Compton scattering, and photoproduction of heavy quark states. The detector consisted of two magnets giving 4 Tm of bending power, proportional wire chambers, electromagnetic calorimeters and two threshold gas Cerenkov counters. An iron filter downstream was used to identify muons. A silicon vertex detector, comprising a multilayer active target and a microstrip tracking chamber, was used to detect short-lived heavy-flavour states.

Photon hard scattering

The physics topics addressed in this first phase of the experiment include:

Inclusive prompt photons and QED Compton scattering.
Inclusive π^0 production and QCD Compton scattering.
Charged hadron photoproduction at high p_t
Topological studies of the high p_t photoproduction events.
Elastic and Inelastic photoproduction of J/Ψ.

The interpretation requires a point-like description of the photon in its coupling to quarks. The data are entirely consistent with the standard model of fractionally charged quarks and QCD. Corrections to the Born - term calculations have been included in this comparison and are found necessary to obtain agreement with the data.

Heavy flavour photoproduction

The second phase of the NA14 experiment was directed towards a study of charmed particle decays and an understanding of their photoproduction mechanism. Using a hadronic interaction trigger we recorded on tape 18 million events. The silicon vertex detector was used to select events with secondary decay vertices. About 2000 fully reconstructed charmed particle decays were obtained in a variety of channels.

D^0 --> $K\pi$, $K\pi\pi^0$, $K\pi\pi\pi$, KK and $\phi\pi\pi$
D^+--> $K\pi\pi$, $\phi\pi$ and $\phi\pi\pi^0$
D_s --> $\phi\pi$, $\eta'\pi$ and K*K
Λ_c --> $pK\pi$.

The following lifetimes were measured:

D^0	$.417 \pm .018 \pm .015$ ps
D^+	$1.03 \pm .08 \pm .06$ ps
D_s	$0.33 \pm .10 \pm .03$ ps
Λ_c	$0.18 \pm .03 \pm .03$ ps

and Branching ratios for several decay channels of the charmed meson decays were measured.

A sample of events containing two fully reconstructed charm decays has been used to compare the observed correlations with those predicted from the QCD photon-gluon fusion process and a Lund description of the hadronisation . Together with the inclusive cross-section measurements and the relative production yields of the various states a charmed quark mass of about 1.5 GeV/c^2 is favoured.

NA14 - Publications and theses: 1991 - 92

"Branching ratios and properties of D-meson decays"
Z. Phys C50 (1991) 11-20

"Results concerning the Decay $D_s^{\pm}$ ---> $\eta'\pi^{\pm}$"
Physics Letters B255 (1991) 639

"$\bar{D}D$- Correlations in Photoproduction"
Physics Letters B(1992)385-392

"Study of Charm Photoproduction Mechanisms"
Submitted to Z. Phys C

"Charmed particle Photoproduction "
M.Koratzinos, Imperial College.
University of London PhD thesis (1991)

Photoproduction in the energy range 70-180 GeV

WA69 Proposal 231

Bonn, CERN, Lancaster, Manchester, RAL, Sheffield, Yerevan

The WA69 experiment has been carried out by the Omega Photon Collaboration, using the Omega Spectrometer in the West Hall at CERN. Data taking was completed in 1986.

An important aim of the experiment is the study of the production of single particles and clusters of particles as a function of P_T up to P_T of 5 GeV/c, with the object of isolating the direct processes which should be present in photoproduction from the generally softer background due to hadronic processes. The photon interacts by both soft and hard processes, but the hard QCD Bethe Heitler and QCD Compton scattering processes which contribute to the latter should not be present in hadron induced reactions.

Charged particles produced by interaction of the beam with a proton in the Hydrogen target are detected and reconstructed in the Omega Spectrometer. These charged particles are identified in the downstream RICH (Ring Image Cherenkov) and TRAD (Transition Radiation) detectors, which have been constructed by the WA69 collaboration and CERN. This combination allows π and K to be efficiently separated over a wide momentum range, and provides important information on the flavour content of high P_T events. Neutral particles are detected and reconstructed in the main Omega Electromagnetic Calorimeter and a special inner Plug Calorimeter constructed for WA69 using lead/scintillating fibres.

About 20M events, with an open trigger, have been obtained with photon beams in 1985 and a further 20M with hadron beams (75% π, 25% K) at corresponding energies in 1986. Comparison of these data, which were taken using essentially identical trigger and hardware and have been analysed with the same software, has allowed a measurement of the hard QCD component due to the 'point like' interaction of the photon without the usual systematic uncertainties involved in the comparison of data from different experiments.

Results from analysis of these data have been published (a) and show an excess of photoproduced charged particles at high P_T which is in reasonable agreement with the QCD predictions, both in magnitude and dependence upon X_F. A more detailed analysis of the 'energy flow' within such high P_T events (b) and of the contribution from 'Higher Twist' (d) provide additional confirmation of the QCD model predictions. A study of forward charge asymmetry as a function of X_F and P_T, for π and K identified using the RICH/TRAD system, has produced results (c) which can be understood in terms of a Parton Recombination Model and comparisons of the photo- and hadro-production of π^0 (1), η (2) and ρ^0 mesons (3) have shown evidence for contributions from hard parton-parton scattering.

(a) Inclusive Photoproduction of Single Charged Particles at High P_T.
Apsimon et al Zeitschrift für Physik C43 (1989) 63.

(b) A Study of the point-like interactions of the Photon using energy-flows in photo- and hadro-production for incident energies between 65 and 170 GeV.
Apsimon et al, Zeitschrift für Physik C46 (1990) 35.

(c) Forward charge asymmetry in low P_T photoproduction of hadrons.
Apsimon et al, Zeitschrift für Physik C47 (1990) 397.

(d) Separation of Minimum and Higher Twist in Photoproduction of high P_T Mesons.
Apsimon et al, Zeitschrift für Physik C5O (1991) 179.

Publications since 1991 PPEXP Report

(1) Inclusive Production of π^o - mesons in πp, kp and γp collisions at energies around 100 GeV.
Apsimon et al, Zeitschrift für Physik C52 (1991) 397.

(2) Inclusive production of η-mesons in πp, kp and γp collisions at energies around 100 GeV.
Apsimon et al, Zeitschrift für Physik C54 (1992) 185.

(3) Comparison of photon and hadron induced production of ρ^o mesons in the energy range of 65 to 175 GeV.
Apsimon et al, Zeitschrift für Physik C53 (1992) 581.

(4) Production of f_2 (1270) and f_o(975) mesons by photons and hadrons of energy 65-175 GeV.
Apsimon et al, CERN-PPE/92-135.

The Soudan 2 Experiment

Proposal 240

Argonne - Minnesota - Oxford - RAL - Tufts Collaboration

The forefront of particle physics research today is the search for breakdowns in the remarkably successful Standard Model. Grand Unified Theories that go beyond the standard model in attempting to unify the strong and electroweak interactions, predict both the instability of nucleons and that neutrinos will have non-zero masses. The observed matter-antimatter asymmetry of the Universe provides a cosmological motivation for the existence of a baryon number violating interaction which could lead to nucleon decay with lifetimes beyond 10^{32} years. There have been two strong experimental indications of mixing of neutrino species (and therefore non-zero masses). The observation of fewer interactions of electron neutrinos from the sun than predicted by the standard solar model has been interpreted as the result of electron neutrino oscillations into other species (sterile at these low energies). The deficit of muon neutrino interactions from cosmic ray produced neutrinos observed by the Kamiokande and IMB water cherenkov experiments has similarly been interpreted as the oscillation of muon neutrinos into tau neutrinos. This year the first data has come from the Soudan 2 experiment bearing on these problems and over the next few years the experiment will make major contributions in these areas.

Searches for nucleon decay and atmospheric neutrino interactions require the observation of a large mass for an extended period in a low background environment, such as that provided by an underground laboratory. The Soudan laboratory is now an efficient and smooth running facility for such experiments.

The Soudan 2 detector is a fine-grained tracking calorimeter designed to record the maximum quantity of information per event. More than three-quarters of the 4.3 ton calorimeter modules are now installed and operating. with a current total mass of 757 tons. The modular nature of the detector allows operation while construction and maintenance work proceeds. The experiment currently takes data approximately 80% of the time, and has over 1 fiducial kiloton year of exposure recorded. Completion of module production is scheduled for the end of December 1992, with assembly of the full 960 ton detector anticipated by mid 1993

Atmospheric neutrino interactions and proton decays appear as events completely contained within the detector. The atmospheric neutrino events are background to

proton decay and a background to both exists from neutral particles entering the detector from cosmic ray muon interactions in the surrounding rock. The detector takes data at a rate of about 0.5Hz. About half the events are produced by cosmic ray muons and half are random noise coincidences. Atmospheric neutrino interactions take place at a rate of about 100 events per kiloton year of exposure. The enormous data reduction process is done in several stages; firstly automatically by a reconstruction program, then later by human scanning. The analysis of the first 0.5 kiloton years of data has been completed in the past year. It involved the double scanning of around 20000 events with around 700 possible contained event candidates undergoing further detailed analysis, finally yielding 290 fully contained events. The background from rock interactions is flagged by the presence of hits in the proportional tube shield that completely surrounds the main detector. Neutrino interactions will, of course, have no hits in the shield. We are left with 43 such events (38 after a 200Mev cut on showering events). An example of a shower with a recoil proton is shown in figure 1, well illustrating the fine detail available in this detector.

The events are divided into single track events (mostly muons from quasi-elastic muon neutrino interactions), single shower events (mostly quasi-elastic electron neutrino interactions) and multiprong events (inelastic and neutral current events). Table 1 gives the number of raw data events in each catagory and the numbers after small corrections for shield inefficiency and randoms. These numbers may be compared with a Monte Carlo calculation which simulates atmospheric neutrino production and interaction in Soudan 2.

Table 1

	Tracks	Showers	Multiprongs
Data (raw)	13	14	11
Data (corrected)	10.9	13.9	11
Monte Carlo	21	14.5	17
Monte Carlo (with neutirino oscillations)	12.5	14	14

It can be seen that we agree qualitatively with Kamioka and IMB in that the predicted and observed numbers of showers agree but the number of muons (and in our case the number of multiprongs) is less than expected. The chisquared between the data and Monte Carlo numbers is 12 for 3 degrees of freedom. Alternatively following Kamioka and calculating the "ratio of ratios" (R) which is defined as

$$R = (\text{data tracks}/\text{data showers})/(\text{MC tracks}/\text{MC showers})$$

and is insensitive to the absolute cosmic ray neutrino flux, we find

$$R = 0.55 \pm 0.29$$

R should obviously equal 1.0 if the MC accurately represented the data. Our result is in good agreement with those of Kamioka and IMB

$$R(\text{Kamioka}) = 0.60 \begin{matrix} +0.07 \\ -0.06 \end{matrix} \pm 0.05$$

$$R(\text{IMB}) = 0.54 \pm 0.05 \pm 0.12$$

though obviously as yet with less statistical precision. A model in which half of the muon neutrinos have oscillated into tau neutrinos, which are usually below threshold for charged current interactions, predicts the numbers given in the last line of table 1. These are in much better agreement with our data. However changes in the incident flux would also provide a better chisquared though they would not appreciably change R. The analysis of our second 0.5 kton-year of data is under way.

An initial proton decay analysis, on the first half kiloton year exposure, has been performed to search for events containing a charged kaon. [4] No candidates were found. Analysis of other modes will start in earnest when the full kiloton-year of data is analysed.

In addition to proton decay, the high resolution, large fiducial volume, and low background environment of the Soudan 2 detector allow studies of a wide range of other phenomena to be made.

The primary cosmic ray composition at very high energies, around 10^{15} ev, can be studied by analysis of the muon multiplicity in data from the main detector itself and in the veto shield that surrounds it[7]. This work is complemented and extended by the use of a surface array of proportional tubes that has come into full operation this year. The possible addition of a Cherenkov telescope to further enhance this measurement is being studied.

A search has been made for highly ionizing tracks, characteristic of GUT monopoles [2]. In three years of running no anomalously heavily ionizing tracks have been observed. This gave the best published limit to date of monopoles in ionisation detectors of

$$\text{flux}(90\%\ \text{cl}) < 8.7 \times 10^{-15}\ \text{cm}^{-2}\ \text{s}^{-1}\ \text{sr}^{-1} \text{ for Beta} > 2 \times 10^{-3}.$$

Claims have been made for the existence of underground muon excesses associated with particular discrete astrophysical objects. We have reported muon excesses correlated with radio flares of Cygnus X-3 [1], and further studies of other objects have been made[3]. To date over 12 million muons have been recorded, with surface energies of over 0.7 TeV. The background and systematics are well understood, and

work is progressing on the analysis of the entire sky visible in underground muons at Soudan 2.

A search has been made for high energy neutrinos coming from Active Galactic Nuclei (AGN)[6]. A limit which is close to the theoretical prediction has been set. With a further 4 years data a limit of around 2% of the theoretical prediction will be achieveable.

A proposal has been made for a long baseline neutrino oscillation experiment, using a neutrino beam from the Main Injector at Fermilab aimed at Soudan 2 (P822). This proposal will enable oscillation experiments, in a similar regime of the oscillation parameters dm^2 and $\sin^2(\text{theta})$ to those producing the atmospheric muon neutrino deficit (if this explanation is valid), to be carried out under controlled accelarator conditions. The distance from Fermilab to Soudan is approximately 750 km and several hundred events a year will be recorded in Soudan 2. An extended region of parameter space could be studied by constructing a new, coarser grained, 6-10 kton detector in the Soudan laboratory. Detailed design studies for such a detector are under way [8]. The experiment has received considerable encouragement from the Fermilab management and formal approval decisions are expected in November 1993.

Papers published since the 1991 report:

Journals:

1 "The observation of underground muons from the direction of Cygnus X-3 during the January 1991 radio flare," M.A. Thomson et al., Physics Letters B 269, 220-226 (1991).

2 "A search for magnetic monopoles with the Soudan 2 detector," J.L. Thron et al., to be published in Physical Review D, ANL-HEP-PR-92-49.

Theses:

3 M.A. Thomson, "An experimental study of the possible association of deep underground muons with astronomical point sources," University of Oxford, February 1992.

4 D.J. Schmid, "First nucleon decay results from the Soudan 2 detector ," University of Minnesota, May 1992.

5 D.M. Roback, "Measurement of the atmospheric neutrino flavor ratio with the Soudan 2 detector," University of Minnesota, August 1992.

Conference proceedings:

6 "Search for AGN nu's with the Soudan 2 detector," W.W.M. Allison et al., paper submitted to the proceedings of the Workshop on High Energy Neutrino Astrophysics, Honolulu, Hawaii, 23-26 March 1992,

7 "Correlations with multiple muon bundles observed at 2090 mwe," N. Sundaralingam, talk at the Washington APS Meeting, 20-24 April 1992, Bull. Am. Phys. Soc. Vol. 37, No. 2, p. 1032 (1992)

8 Papers in the proceedings of the Workshop on Long-Baseline Neutrino Oscillations, Fermilab, November 17-20, 1991, edited by Maury Goodman:

"Prospects for long-baseline neutrino oscillation experiments," M. Goodman, p. 53-89.

"Report from the large area detector working group and the R-nu = NC/CC working group," D. Cockerill, p. 93-108.

"Status of a search for atmospheric neutrino oscillations with the Soudan 2 detector, D. Roback, p. 171-175.

"Update of P822 - The Soudan 2 proposal for a long baseline neutrino oscillation experiment," E. Peterson, p. 243-244.

"Possible upgrades of Soudan 2," P. Litchfield, p. 387-400.

"Neutrino Beam Geodesy," R. Milburn, p. 459-472.

"Construction of delta m2 - sin2 2theta plots," R. Snyder, M. Goodman, p. 491-49.

"Advantages of a fine-grain detector for long baseline neutrino oscillation experiments," W. Oliver, J. Schneps, p. 499-509.

9 "Beyond the standard model, underground," P. Litchfield, submitted to the proceedings of the 27th Rencontres de Moriond, March 1992, 12 pages.

10 "Results from the Soudan 2 detector," J. Thron, submitted to the proceedings of the XXVI International Conference on HEP, Dallas, Texas, August 6-12, 1992, ANL-HEP-CP-92-85

11 "Underground muons from point sources," M. Marshak, submitted to the proceedings of the XXVI International Conference on HEP, Dallas, Texas, August 6-12, 1992.

Figure Captions

Fig 1 An example of a ν_e quasi-elastic interaction in Soudan 2. The circles correspond to hit drift tubes in the detector. A 500 MeV shower straddles two detector modules and a short recoil proton is clearly visible in the top view.

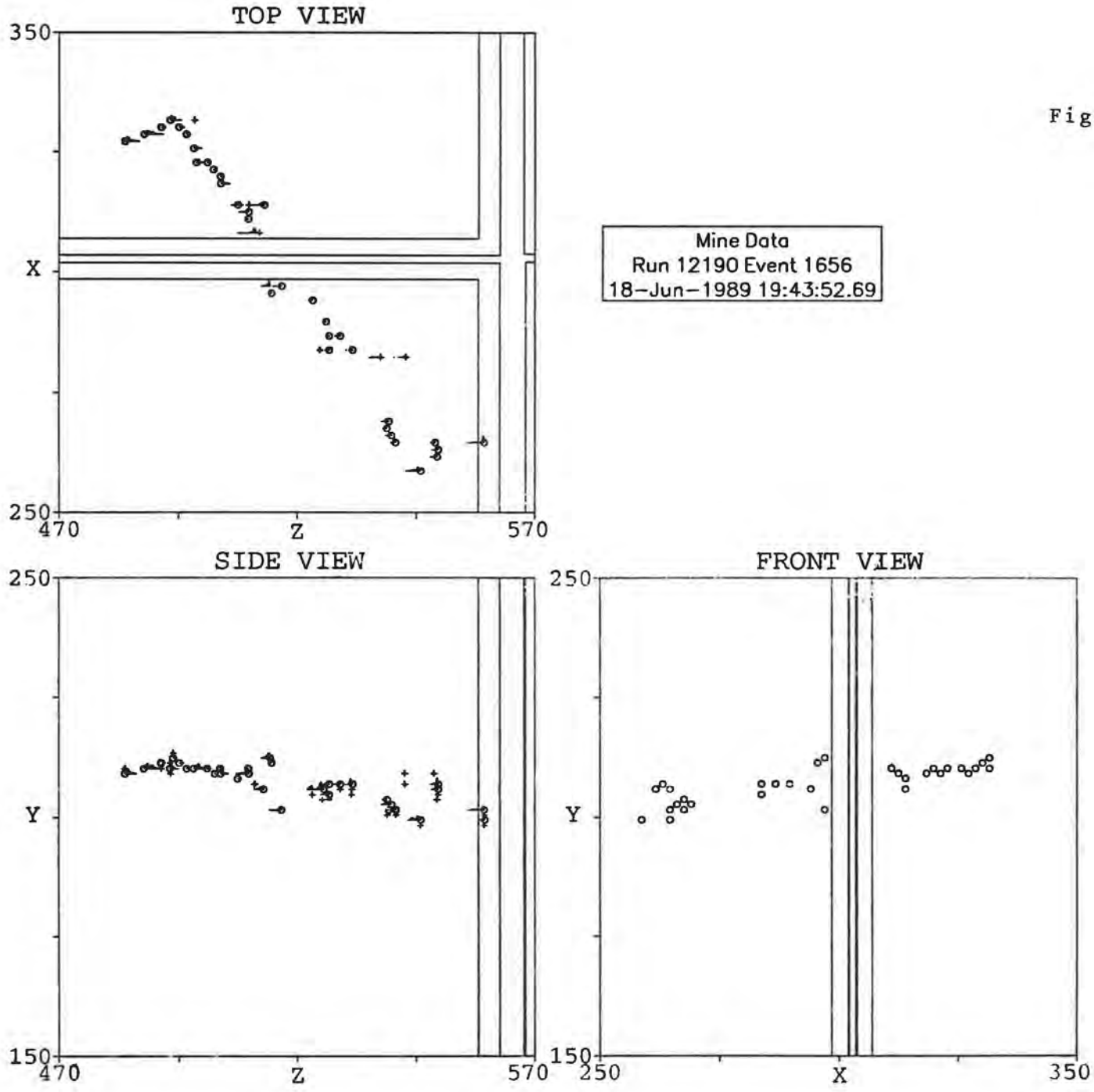
TOP VIEW
350
X
250
470
Z
570
Mine Data
Run 12190 Event 1656
18-Jun-1989 19:43:52.69
SIDE VIEW
250
Y
150
470
Z
570
FRONT VIEW
250
Y
150
250
X
350

Fig. 1

NEUTRINO EXPERIMENTS AT ISIS

Proposal 244

The KARMEN Collaboration
(Queen Mary & Westfield College, Kernforschungszentrum Karlsruhe,
Universität Erlangen-Nürnberg, Rutherford Appleton Laboratory, Oxford University)

Abstract

The KARMEN experimental program at the pulsed beam-stop source ISIS studies the interactions of neutrinos with energies up to 53 MeV in a 56 tonne scintillation calorimeter. Major aims include studies of specific weak couplings, weak nuclear form factors, and ν_μ - ν_e universality, by the measurement of charged current (CC) and neutral current (NC) neutrino interactions with ^{12}C, and a search for neutrino oscillations $\nu_\mu \rightarrow \nu_e$ and $\bar{\nu}_\mu \rightarrow \bar{\nu}_e$. We present results from the first two years of data taking.

INTRODUCTION

The KARMEN experiment is performed at the neutron spallation facility ISIS at Rutherford Appleton Laboratory. The decay of stopped pions, produced in the U/D_2O target by the 800 MeV pulsed proton beam, yields equal fluxes of ν_μ, ν_e and $\bar{\nu}_\mu$ with energies up to 52.8 MeV according to the sequence $\pi^+ \rightarrow \mu^+ + \nu_\mu$; $\mu^+ \rightarrow e^+ + \nu_e + \bar{\nu}_\mu$. The combination of a narrow proton spill (2 x 130 ns bunches at 50 Hz) with the different π^+, μ^+ lifetimes results in a prompt ν_μ burst within ~0.5 μs of beam-on-target, followed by ν_e,$\bar{\nu}_\mu$ emission, unaccompanied by ν_μ, at later times. The duty factor $\sim 10^{-4}$ allows highly effective suppression of cosmic background. A high resolution calorimeter[1] containing 56 t of organic liquid scintillator is housed in a 6000 t steel bunker at a mean distance from the production target of 18 m of which 8 m is steel, reducing neutron fluxes by $\sim 10^{-16}$. The calorimeter, with >98% active mass, serves as a live target for studying various ν-induced reactions on ^{12}C and ^{1}H.

NEUTRINO REACTIONS ON ^{12}C: THEORY

Figure 1 shows the superallowed transitions linking the ground state of ^{12}C to the $(1^+,1)$ analogue states of the $A = 12$ system. There have been several[2-5] calculations of the transition amplitudes of which those[3-5] that use the elementary particle treatment[6] are model-independent, requiring as input only the four weak nuclear form factors $F_M(q^2)$, $F_A(q^2)$, $F_P(q^2)$ and $F_T(q^2)$. In the absence of second-class currents, matrix elements for the charged (CC) and neutral (NC) current reactions are related, assuming isospin symmetry, by the Wigner-Eckart theorem. The form factors therefore contain all specifically nuclear information.

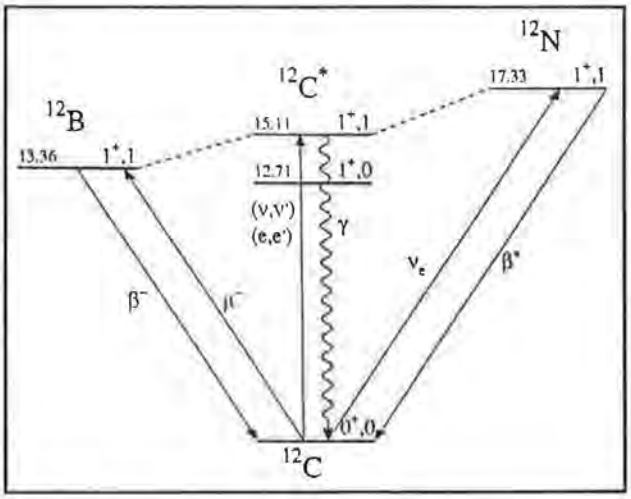

Figure 1. Transitions in the A=12 system.

The value of the weak magnetism form factor F_M at $q^2=0$ is related by the CVC hypothesis to the rate of the M1 γ-decay of the 15.1 MeV state in ^{12}C. The ft-values and angular distributions of β-decays of the analogue states in ^{12}B and ^{12}N allow $F_A(0)$ and $F_T(0)$ to be calculated; the latter is found to be small. Measurements of inelastic electron scattering and of μ^- capture on ^{12}C give the q^2 dependence of F_M and F_A respectively, with the result that $F_A(q^2) \propto F_M(q^2)$; different authors[4,5] use similar explicit forms which differ from dipole dependence by <5% in the low q^2 range accessible to KARMEN. The same form is taken for $F_T(q^2)$ and the contribution of the pseudoscalar term F_P is ignored on account of its m_e^2-dependent coefficient. Thus the axial vector form factor $F_A(q^2)$ dominates. The ability of KARMEN to measure CC and NC reactions $^{12}C(\nu_e,e^-)^{12}N_{g.s.}$ and $^{12}C(\nu,\nu')^{12}C^*(1^+,1)$ permits detailed study of ν-nucleus interactions, of the structure of weak currents, ν_μ-ν_e universality, and neutrino oscillations.

RECENT RESULTS FROM KARMEN

The exclusive CC reaction $^{12}C(\nu_e,e^-)^{12}N_{g.s.}$

Detection of this exclusive reaction is based on a spatially correlated delayed coincidence between an electron from the inverse β-decay of ^{12}C during the ν_e time window and a positron from the subsequent ^{12}N decay, which uniquely identifies ν-induced transitions to the ground state of ^{12}N. The data sample used for the present analysis was taken between April 1990 and June 1992 representing 2641 C of protons on target. Software cuts[7] on the time, energy and spatial correlation of the prompt and delayed signals selected 130 coincidence events. Proof that these ν-candidates are indeed due to exclusive CC reactions is given by Figure 2; the measured time and energy distributions of the prompt and delayed signals are in very good agreement with what one expects from the reaction sequence $^{12}C(\nu_e,e^-)^{12}N_{g.s.} \rightarrow ^{12}C+e^+ + \nu_e$. In particular the time distribution of the prompt

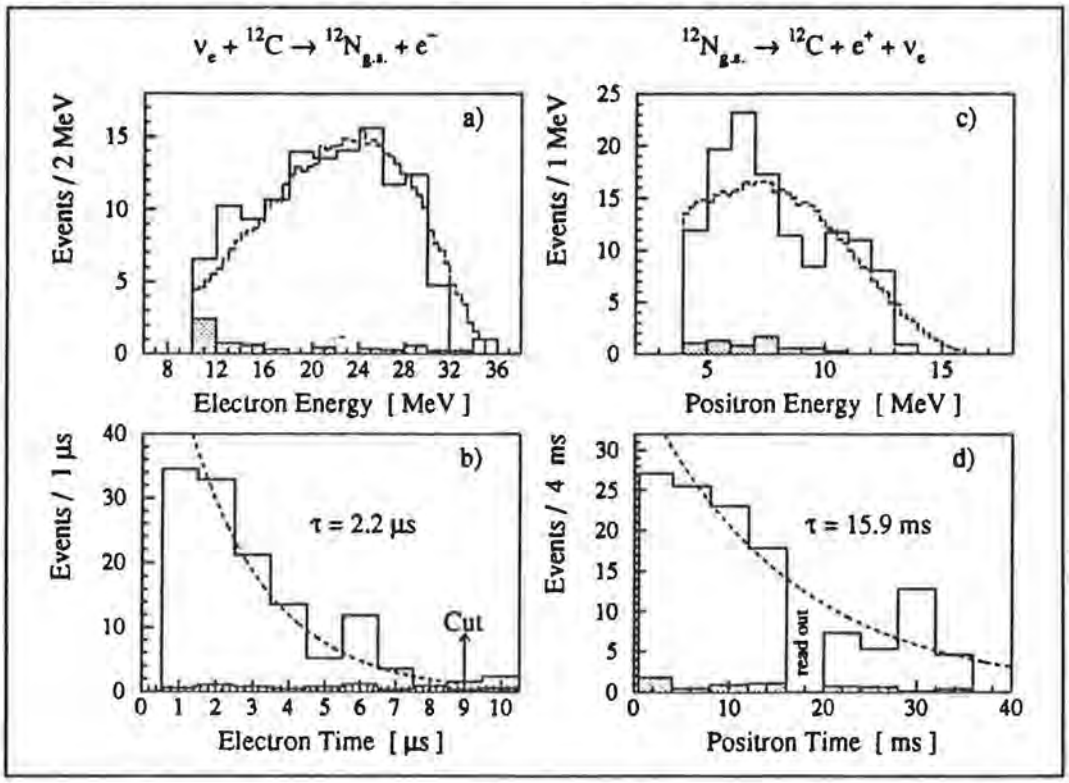

Figure 2. Energy and time distributions of prompt and delayed signals following cuts to select CC reactions on ^{12}C. Energy spectra are compared to Monte Carlo simulations of $^{12}C(\nu_e,e^-)^{12}N_{g.s.}$ (broken lines), time distributions are shown with the decay curves of μ^+ and ^{12}N superimposed. Normalised background with beam off is shown shaded.

signal, Figure 2(b), clearly shows these events to have been induced by ν_e from μ^+-decay. From 123.7 ± 11.4 events left after background subtraction (signal:background ≈ 20:1) the cross section flux-averaged over the energy distribution of the ν_e was deduced to be

$$\langle\sigma_{excl\ CC}\rangle = [8.0 \pm 0.75_{stat} \pm 0.75_{syst}] \times 10^{-42}\ cm^2$$

Calculations[2,4,5] yielding values in the range (8.0-9.4) x 10^{-42} cm^2, with 10% uncertainties, are in good agreement, as is a lower resolution experiment[8] at LAMPF.

The excellent energy resolution of our detector allowed the neutrino energy distribution to be reconstructed from the energy spectrum of prompt electrons, and the CC cross section evaluated in four energy intervals (Figure 3). This first measurement of energy dependence of a ν-nucleus cross section shows clearly the threshold behaviour, while better statistics will allow study of the q^2 dependence of F_A.

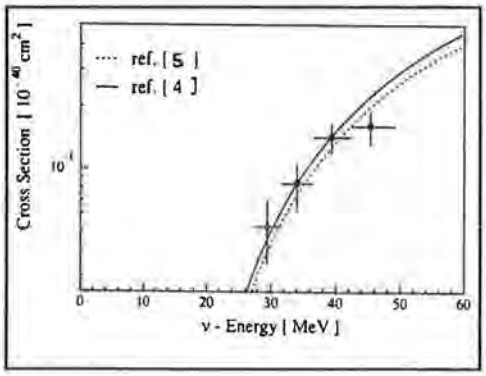

Figure 3. Energy dependence of $^{12}C(\nu_e,e^-)^{12}N_{g.s.}$

The NC reaction $^{12}C(\nu,\nu')^{12}C^*(1^+,1;15.1\ MeV)$

Improved trigger conditions since July 1990 have enabled us to make the first observation of a weak nuclear excitation, namely this NC transition between discrete nuclear states. The signal for this process is detection of a localised scintillation event of 15 MeV visible energy from photons emitted as the (1^+1) analogue state of ^{12}C decays back to the ground state with a 94% γ-decay branching ratio. In order to optimise the signal:background ratio evaluation[9] was restricted to the $\nu_e,\bar{\nu}_\mu$ time window of 0.5-3.5 μs after beam-on-target. The energy spectrum of events satisfying these criteria is shown, with "beam off" background subtracted, in Figure 4. Above 17 MeV there is a broad distribution of events attributable to inclusive CC reactions. Between 11 and 16 MeV lies a distinct peak which we ascribe to the reaction $^{12}C(\nu,\nu')^{12}C^*(1^+,1)$. The time distribution in this energy interval shows an exponential decrease with a time constant of 2.2 μs indicating that these events are indeed induced by ν_e and $\bar{\nu}_\mu$ from μ^+ decay. We find 68 ± 13 such events leading to a flux averaged cross section for the sum of ν_e and $\bar{\nu}_\mu$ transitions of

$$\langle\sigma_{NC}\rangle = [9.5 \pm 1.8_{stat} \pm 1.35_{syst}] \times 10^{-42}\ cm^2$$

again in good agreement with theory[2,3,5].

The inclusive CC reaction $^{12}C(\nu_e,e^-)^{12}N^*$

The broad structure in the energy spectrum of Figure 4 is almost all assigned to inclusive CC reactions on ^{12}C. The time distribution of events above 17 MeV again shows the 2.2 μs decay constant of μ^+ decay showing that they too are ν-induced. There are small contributions from ν-e scattering and from the inclusive reaction $^{13}C(\nu_e,e^-)^{13}N^*$. The former is calculable with confidence, the latter is less well understood but scales roughly with the (natural) isotopic composition of the scintillator. Together they amount to only a few percent of the events with visible energy above 17 MeV. The number of transitions to the ^{12}N ground state is directly known from our measurement of the exclusive channel, and the kinematic distribution is well reproduced by a Monte Carlo simulation (*cf* Figure 2(a)). The remaining events are thus ascribed to CC transitions to excited states of ^{12}N, all of which are proton unstable. Their energy spectrum is well fitted

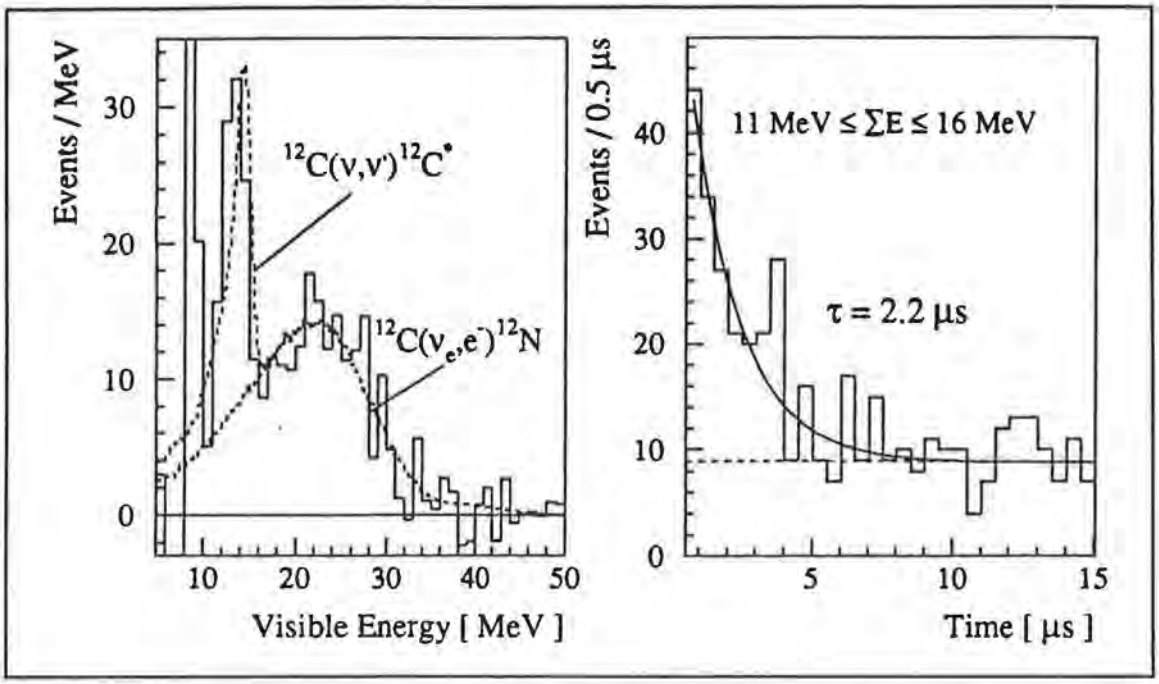

Figure 4. Spectra of single prong events satisfying the criteria described in the text. Left: Visible energy after background subtraction; broken lines show Monte Carlo simulations for NC excitation of ^{12}C, and inclusive CC reactions. Right: Time with respect to beam-on-target, cosmic background (broken line) *not* subtracted.

by a simulation which takes into account the known level structure of ^{12}N. From 108 ± 18.5 events we determine the flux-averaged cross section for the reaction $^{12}C(\nu_e,e^-)^{12}N^*$ to be

$$\langle\sigma_{CC\ exc.N}\rangle = [12.3 \pm 2.2_{stat} \pm 1.5_{syst}] \times 10^{-42}\ cm^2$$

contrdicting theoretical estimates of $3.7\times10^{-42}cm^2$ [2] and $6.4\times10^{-42}cm^2$ [10], and substantially larger than expected from measurements[8] at LAMPF of the exclusive, and total inclusive, cross sections. This discrepancy is unresolved and demonstrates a need, here and in similar situations in ν-astrophysics, for further study of ν-induced transitions to excited nuclear states.

EQUALITY OF $\bar{\nu}_\mu$-ν_e NC COUPLING

Apart from an isospin factor $1/\sqrt{2}$, the matrix elements of the dominant isovector axial vector currents are the same[4,5] for the NC (CC) reactions $^{12}C(\nu,\nu')^{12}C^*(1^+,1)$ and $^{12}C(\nu_e,e^-)^{12}N_{g.s.}$ As the former is induced by fluxes of $\bar{\nu}_\mu$, ν_e of equal intensity, the ratio

$$R = \sigma_{NC}(\nu_e+\bar{\nu}_\mu)/\sigma_{CC}(\nu_e)$$

is about 1, provided that ν_e and $\bar{\nu}_\mu$ couple in the same way to the Z^o. The exact expectation for this ratio, taking into account both the small ν-$\bar{\nu}$ difference in the NC matrix elements and the slightly different energy spectra of ν_e and $\bar{\nu}_\mu$, is[4] R = 1.08, whereas from our measurements we get R = 1.19 ± 0.26. Better statistics will soon improve this flux independent test of flavour universality in the neutrino NC coupling.

A NEW LIMIT ON SCALAR COUPLING

Muon decay is described in the standard model by a chiral hamiltonian in which the left-handed vector coupling constant g^V_{LL}=1, all other couplings being zero. Measurements on charged leptons in μ^+ decay are consistent with this; in particular the Michel parameter

$$\rho = \tfrac{3}{4}\{1-[|g^V_{LR}|^2+|g^V_{RL}|^2+2|g^T_{LR}|^2+2|g^T_{RL}|^2 +\Re(g^S_{LR}g^{T\,*}_{LR}+g^S_{RL}g^{T\,*}_{RL})]\}$$

describing the positron energy spectrum is found to have its *V-A* value of ¾. Fetscher has recently remarked[11], however, that the good energy resolution of the KARMEN calorimeter allows a direct measurement of the ν_e energy spectrum described by the analogous parameter

$$\omega = 3/16\{ |g^S_{LL}|^2+|g^S_{RR}|^2+4|g^V_{LR}|^2+4|g^V_{RL}|^2 + |g^S_{LR}+2g^T_{LR}|^2+|g^S_{RL}+2g^T_{RL}|^2\}$$

and that an experimental upper limit on ω would for the first time set an upper limit on the left-handed scalar coupling constant $|g^S_{LL}|$.

In deriving the energy dependence of the inverse β-decay $^{12}C(\nu_e,e^-)^{12}N_{g.s.}$ (Figure 3) we have implicitly assumed the *V-A* form for μ decay. However Fetscher shows[11] that a non-zero value of ω has a significant effect only near the maximal ν energy and that the slope of the excitation function is otherwise almost independent of ω, allowing the effect of $\omega \neq 0$ to be disentangled. By parametrising our results he finds $\omega \leq 2.6\times10^{-2}$ and derives a new limit of

$$|g^S_{LL}| \leq 0.37 \text{ (68\% c.l.)}.$$

NEUTRINO OSCILLATIONS

KARMEN is measuring, simultaneously, the probabilities *P* for both $\nu_\mu \rightarrow \nu_e$ and $\bar{\nu}_\mu \rightarrow \bar{\nu}_e$ oscillations. Each has a distinct signature. The first would lead to reactions $^{12}C(\nu_e,e^-)^{12}N_{g.s.}$ induced by mono-energetic (30 MeV) ν_e during the first 0.5 μs after beam-on-target. No event has been found, when 56 would be expected if *P*=1. One expects 0.4 and 0.3 events due to contamination by ν_e from μ^+ decay, and beam-off background, respectively; we conclude that

$$P(\nu_\mu \rightarrow \nu_e) < 4.1\times10^{-2} \text{ (90\% c.l.)}$$

In the absence of $\bar{\nu}_e$, except at a level $\sim10^{-4}$ from π^- decays in flight, the reaction $^1H(\bar{\nu}_e,e^+)n$ is a signal for oscillation. It is detected by a delayed coincidence with $Gd(n,\gamma)$. Four such events have been found, when 206 would be expected if *P*=1. The background is 2.2 events leading to a limit of

$$P(\bar{\nu}_\mu \rightarrow \bar{\nu}_e) < 2.8\times10^{-2} \text{ (90\% c.l.)}$$

These early results, though not yet competitive with other experiments, have clear signatures and excellent calibration and normalisation *via* the co-existing ν_e flux.

CONCLUSIONS

In its first two years the KARMEN experiment has made a precision measurement of an allowed CC nuclear transition and confirmed the dominance of the axial vector form factor. A measurement of reactions leading to excited states reveals deficiencies in the understanding of ν-induced forbidden transitions. We have made the first observation of a NC transition between nuclear states, and confirmed the assumption of minimal breaking of isospin symmetry. Our data provide a direct, flux-independent test of the universality of ν-Z^o couplings, and enable a new upper limit to be set on scalar couplings in the weak interaction. Well-normalised limits to $\nu_\mu \rightarrow \nu_e$ and $\bar{\nu}_\mu \rightarrow \bar{\nu}_e$ oscillations have been set.

REFERENCES

1. G.Drexlin *et al*, *Nucl.Inst.Meth.* **A289** (1990) 490
2. T.W.Donnelly, *Phys.Lett.* **B34** (1973) 93; and private communication (1992)
3. J.Bernabéu&P.Pascual,*Nucl.Phys.***A324**(1979)365
4. M.Fukugita, Y.Kohyama and K.Kubodera, *Phys.Lett.* **B212** (1988) 139
5. S.L.Mintz *et al*, in *Prog.Nucl.Phys.* (Elsevier, 1991) p.290
6. C.W.Kim & H.Primakoff, in *Mesons in Nuclei I* (North-Holland,1979) p.67
7. B.Bodmann *et al*, *Phys.Lett.* **B280** (1992) 198
8. D.A.Krakauer *et al*, *Phys.Rev.* **C45** (1992) 2450
9. B.Bodmann *et al*, *Phys.Lett.* **B267** (1991) 321
10. E.Kolbe *et al*, *Nucl.Phys.* **A540** (1992) 599
11. W.Fetscher, preprint, ETH Zürich (1992)

PUBLICATIONS

B.Bodmann *et al*, "First observation of the neutral current excitation $^{12}C(\nu,\nu')^{12}C^*(1^+,1)$", *Phys.Lett.* **B267** (1991) 321

B.Bodmann *et al*, "Cross section of the charged current reaction $^{12}C(\nu_e,e^-)^{12}N_{g.s.}$", *Phys.Lett.* **B280** (1992) 198

KARMEN collaboration: "Results from the KARMEN neutrino experiment", to appear in Proceedings of:

Workshop on Massive Neutrinos, Moriond, 1992

International Conference on Weak and Electromagnetic Interactions in Nuclei, Moscow, 1992

Nuclear Physics Conference of the German Physical Society, Wiesbaden, 1992

26th International Conference on High Energy Physics, Dallas, 1992

A. Malik, "A laser calibration and monitoring system for a neutrino detector" (PhD thesis, University of London, 1992)

A SEARCH FOR GLUEBALLS IN THE CENTRAL REGION

WA76/WA91 Proposal 246

Athens : Bari : Birmingham : CERN : Paris.

Experiment WA76 was designed to study exclusive final states formed in the reaction

$$pp \rightarrow p_f(X^0)p_s \quad (1)$$

where the subscripts f and s indicate the fastest and slowest particles in the laboratory respectively, and X^0 represents the central system which is presumed to be produced by a double exchange process. At high centre-of-mass energies these double exchange processes are believed to be dominated by Double Pomeron Exchange (DPE), where the Pomeron is thought to have a large gluonic content, leading to the conclusion that Pomeron-Pomeron scattering could be a source of gluonic states.

The data taken with π^+ and p incident at 85 GeV/c allowed good separation of many exclusive channels [1]. Several resonances suggested as gluonium candidates were seen with good signal to background ratios whereas well-known $q\overline{q}$ states seem to be suppressed in the central region relative to other production mechanisms.

During 1986 12 million triggers were obtained at an incident momentum of 300 GeV/c. The CERN Ω Spectrometer, equipped with MWPC and drift chambers, was used to measure tracks with momentum up to about 30 GeV/c. Particle identification was provided by a system of threshold Cerenkov counters, and a fine grain electromagnetic calorimeter was used to allow detection of neutral particles, as shown in fig. 1. To maintain the good separation of exclusive channels, microstrip detectors [2] were used to measure the beam particle and the fast track (fig. 2). Results from the 300 GeV/c data have been presented in previous reports. As this phase of the experiment has almost been completed, we summarize the principal results below.

A detailed study of the $\pi^+\pi^-$ mass spectrum has been performed [3]. The spectrum is shown in fig. 3, and shows clear evidence for $S^*/f_0(975)$ production. A good description of the $\pi^+\pi^-$ mass spectrum was obtained using a coupled channel (Flatté) formalism, and allowing the $S^*/f_0(975)$ to interfere coherently with the S-wave background. The $S^*/f_0(975)$ parameters were determined to be $m_0 = 979 \pm 4$ MeV, $g_\pi = 0.28 \pm 0.4$, $g_K = 0.56 \pm 0.18$, giving a pole position on sheet II at $(1001 \pm 2) - i(36 \pm 4)$ MeV. The corresponding contribution in the $K\overline{K}$ channel is easily accommodated in the mass spectrum.

The principal interest in the $K\overline{K}$ spectrum lies in the observation of the $\theta/f_2(1720)$ [4], the first such observation in hadroproduction. The K^+K^- spectrum is shown in fig. 4, where a peak corresponding to the $\theta/f_2(1720)$ is clearly seen. As a signal is also seen in the $K^0_SK^0_S$ mass spectrum, it is concluded that the spin of the object is either 0^{++} or 2^{++}. The decay angular distributions for the $f'(1525)$ and the $\theta/f_2(1720)$ are found to be qualitatively similar, suggesting that the $\theta/f_2(1720)$ and the $f'(1525)$ have the same spin. A density matrix analysis assigns $80 \pm 4\%$ of the signal to the D wave.

The $K\overline{K}\pi$ mass spectrum in the 1.4 GeV mass region has been of long standing interest in this experiment [1,5,6]. The $K^0_SK^{\pm}\pi^{\mp}$ mass spectrum is shown in fig. 5, and shows very prominent signals for the D/$f_0(1285)$ and E/$f_1(1420)$ mesons. While the status of the D/$f_0(1285)$ is not controversial, that of the E/$f_1(1420)$ has aroused much interest in recent years. It now appears that there are three states in this mass region. The one seen by WA76 has been found to have $M = 1429 \pm 3$ MeV and $\Gamma = 58 \pm 8$ MeV. A Dalitz plot analysis has shown its J^{PG} to be 1^{++}, decaying to $K^*\overline{K}$ [5]. More recently [6], its observation in our $K^0_SK^0_S\pi^0$ data has fixed its C-parity to be +, from which we deduce its isospin to be zero. We have searched for the E/$f_1(1420)$ in our 4π [7], $\eta\pi^+\pi^-$ [8] and $\rho^0\gamma$ [9] channels. Although the D/$f_0(1285)$ is clearly seen in all channels, as can be seen from fig. 6, there is no evidence for production of the E/$f_1(1420)$ in any of them.

An interesting result observed in the 300 GeV/c data is that many vector-vector channels are observed [10,11]. We have extracted signals corresponding to $\phi\phi$, $K^*_0\overline{K}^*_0$, $\rho^0\omega$, $\omega\omega$, $\rho^0\rho^0$ and $\rho^+\rho^-$ production. The preliminary results are summarized in the vector-vector mass spectra shown in fig. 7. Further work on the analysis of vector-vector channels is in progress.

FUTURE PLANS (WA91)

As a result of the interesting results obtained at 85 GeV/c and subsequently at 300 GeV/c, we have been approved for 100 days at 450 GeV/c under the new experiment code WA91. In the new configuration the acceptances for fast and slow particles are each increased by a factor of about two, which in conjunction with the recently improved Omega data acquisition system should allow us to obtain a large increase in statistics. We intend to take 100 million triggers. The gain in slow proton acceptance requires the use of a new slow proton hodoscope built at RAL and Birmingham. the refurbished OLGA calorimeter is used for γ detection, giving improved acceptance for neutral particles such as π^0, η, η' and ω. 20 million triggers were obtained in two weeks of effective data taking in 1991. A second, longer period of data taking began at the end of September 1992.

REFERENCES

1. T.A. Armstrong et al., Phys. Lett. **146B** (1984) 273.
   T.A. Armstrong et al., Phys. Lett. **166B** (1986) 245.
   T.A. Armstrong et al., Phys. Lett. **167B** (1986) 133.
   T.A. Armstrong et al., Z. Phys. C **34** (1987) 23.
   T.A. Armstrong et al., Z. Phys. C **35** (1987) 167.
2. T.A. Armstrong et al., Nucl. Inst. and Meth. **A274** (1989) 165.
3. T.A. Armstrong et al., Z. Phys. C **51** (1991) 351.
4. T.A. Armstrong et al., Phys. Lett. **227B** (1989) 186.
5. T.A. Armstrong et al., Phys. Lett. **221B** (1989) 216.
6. T.A. Armstrong et al., CERN/PPE 92-94, submitted to Z. Phys. C
7. T.A. Armstrong et al., Phys. Lett. **228B** (1989) 536.
8. T.A. Armstrong et al., Z. Phys. C **52** (1991) 389.
9. T.A. Armstrong et al., Z. Phys. C **54** (1992) 371.
10. T.A. Armstrong et al., Phys. Lett. **221B** (1989) 221.
11. T.A. Armstrong et al., Z. Phys. C. **46** (1990) 405.
10. T.A. Armstrong et al., Phys. Lett. **221B** (1989) 216.

Publications (October 1991 to September 1992)

1. Search for glueballs in Omega.
   I.J. Bloodworth, J.N. Carney, R. Childs, J.B. Kinson,
   M.T. Trainor, O. Villalobos Baillie and M.F. Votruba;
   with Athens, Bari, CERN, and Paris.

   Proc. XXVIth Rencontres de Moriond, Les Arcs, 1991, 469-475.

2. Study of the $\eta\pi\pi$ system centrally produced in the
   reaction $pp \rightarrow p_f(\eta\pi\pi)p_s$ at 300 GeV/c.

   R.P. Barnes, I.J. Bloodworth, J.N. Carney, D. Evans,
   J.B. Kinson, O. Villalobos Baillie, and M.F. Votruba; with Athens
   Bari, CERN, and Paris.

   Z. Phys. C **52** (1991) 389-395.

3. Central Meson Production.

   R.P. Barnes, I.J. Bloodworth, J.N. Carney, C.J. Dodenhoff,
   D. Evans, J.B. Kinson, O. Villalobos Baillie, and M.F. Votruba;
   with Athens, Bari, CERN, and Paris.

   Proc. Europhysics Conference on High Energy Physics, Geneva, July 1991, pp 73-76.

4. A Study of the $f_1(1285)$ and E/$f_1(1420)$ in central production.

   R.P. Barnes, I.J. Bloodworth, J.N. Carney, C.J. Dodenhoff, D. Evans, J.B. Kinson, O. Villalobos Baillie, and M.F. Votruba; with Athens, Bari, CERN, and Paris.

   Proc. 4th Int. Conf. on Hadron Spectroscopy, Maryland, August 1991, pp. 30-33.

5. Study of the $\pi^+\pi^-\gamma$ system centrally produced in the reaction $pp \to p_f(\pi^+\pi^-\gamma)p_s$ at 300 GeV/c.

   R.P. Barnes, I.J. Bloodworth, J.N. Carney, C.J. Dodenhoff, D. Evans, J.B. Kinson, O. Villalobos Baillie, and M.F. Votruba; with Athens, Bari, CERN, and Paris.

   Proc. 4th Int. Conf. on Hadron Spectroscopy, Maryland, August 1991, pp. 26-29.

6. Study of the $\pi^+\pi^-\gamma$ system centrally produced in the reaction $pp \to p_f(\pi^+\pi^-\gamma)p_s$ at 300 GeV/c.

   R.P. Barnes, I.J. Bloodworth, J.N. Carney, C.J. Dodenhoff, D. Evans, J.B. Kinson, O. Villalobos Baillie, and M.F. Votruba; with Athens, Bari, CERN, and Paris.

   Z. Phys. C **54** (1992) 371-376.

7. Further Study of the E/$f_1(1420)$ Meson in Central Production.

   I.J. Bloodworth, J.N. Carney, C.J. Dodenhoff, J.B. Kinson, O. Villalobos Baillie, and M.F. Votruba; with Athens, Bari, CERN, and Paris.

   CERN/PPE 92-94. Submitted to Z. Phys. C.

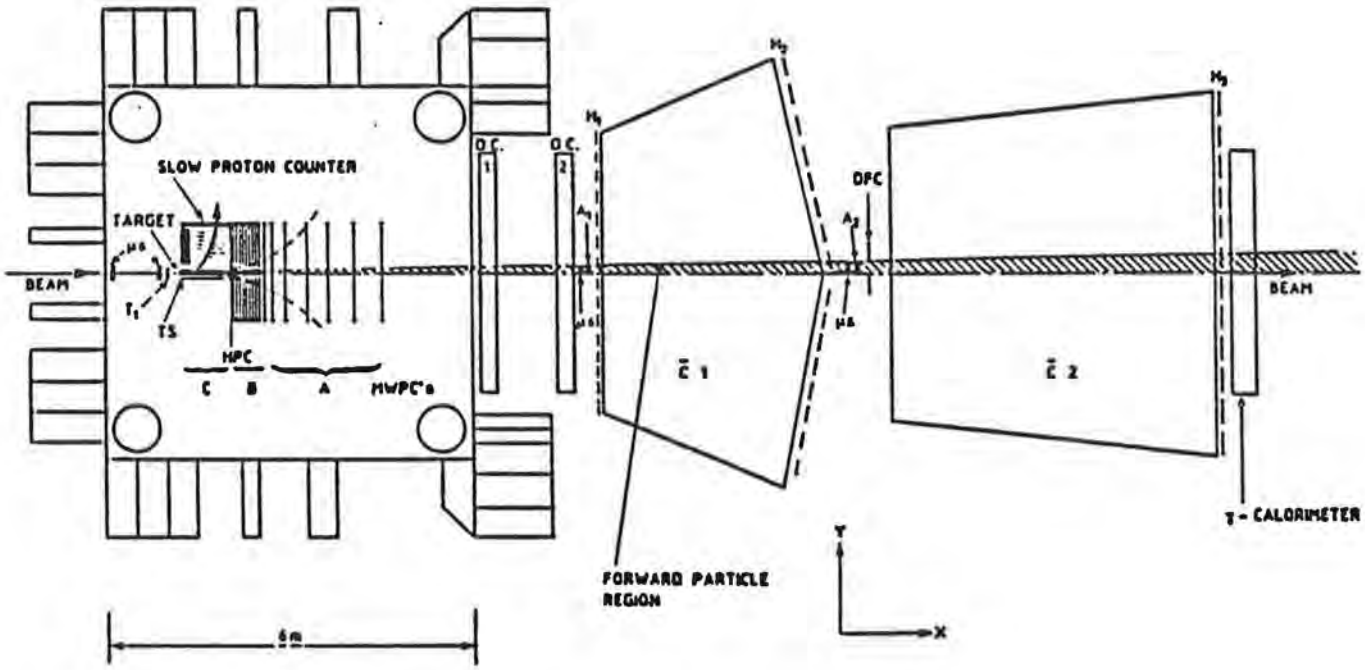

Fig. 1. Layout of the CERN Ω Spectrometer as used for the WA76 experiment.

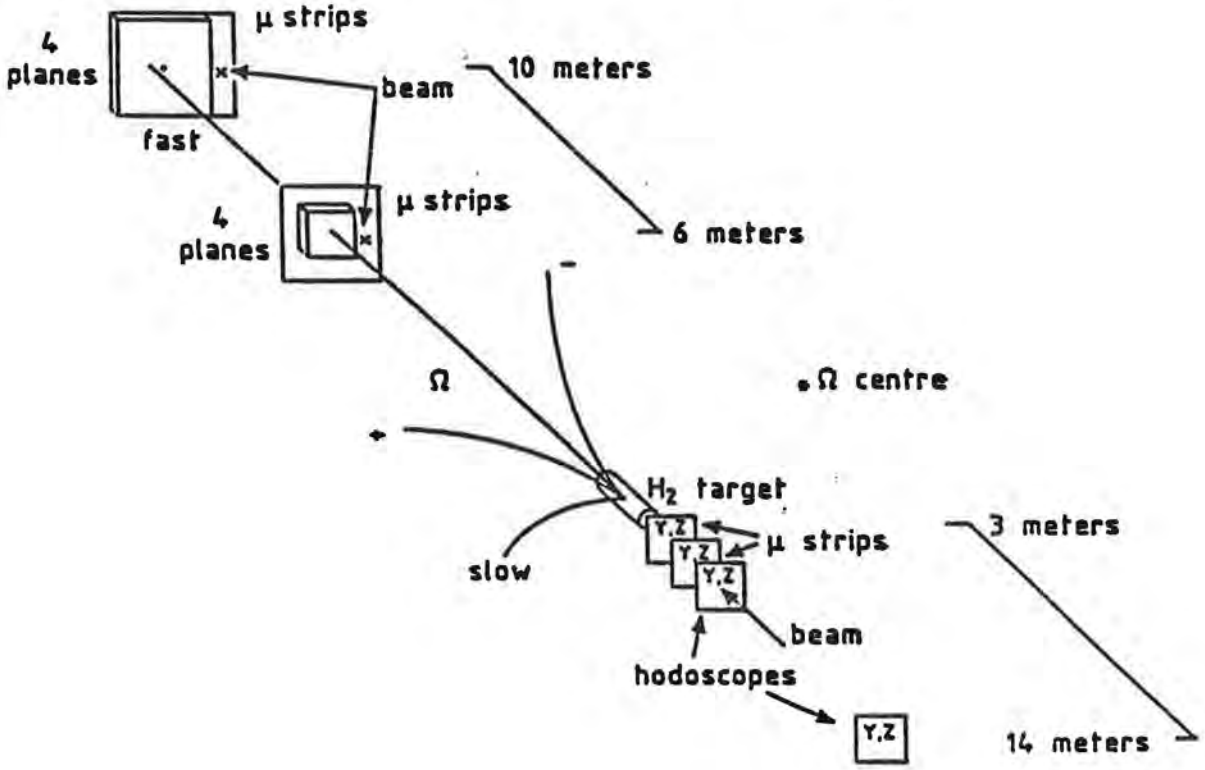

Fig. 2 Layout of the μ-strips and scintillators used to measure the beam and the fast particle.

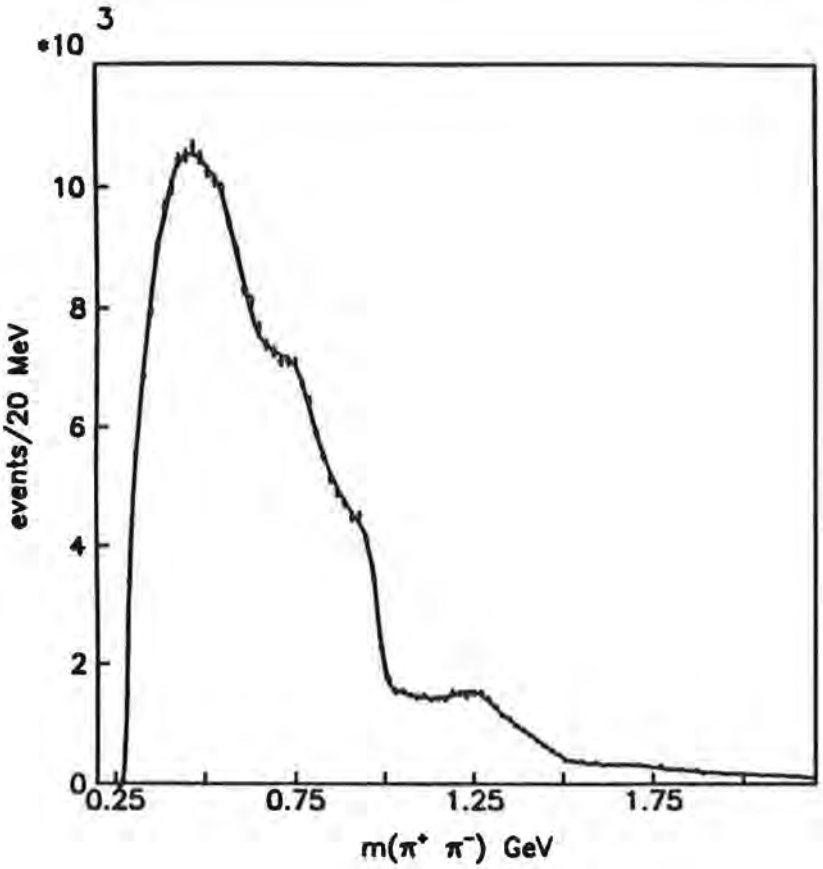

Fig. 3. $\pi^+\pi^-$ effective mass distribution at 300 GeV/c. The fit is described in the text.

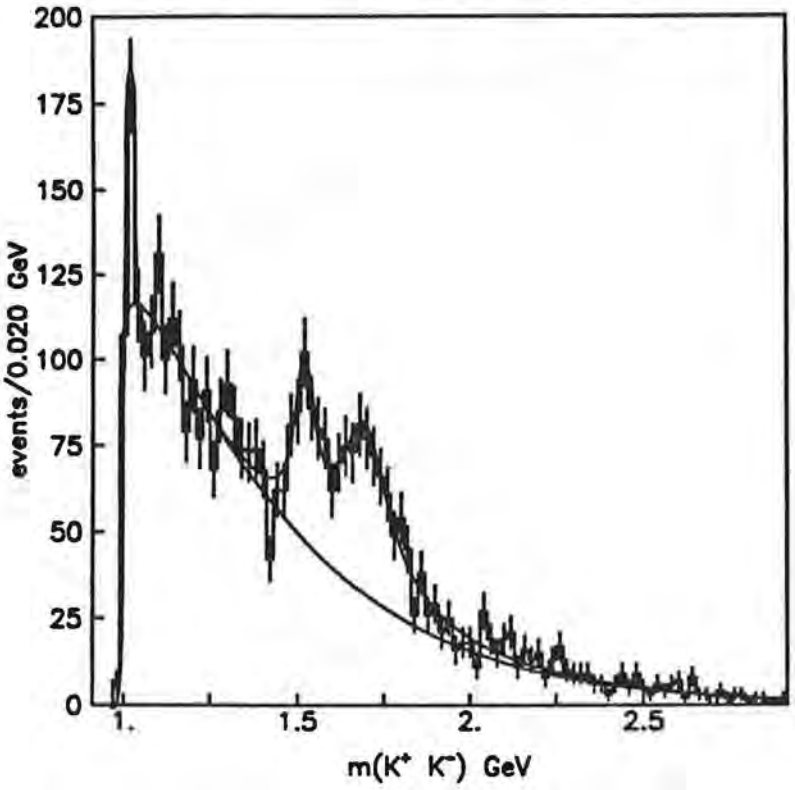

Fig. 4. K^+K^- effective mass distribution at 300 GeV/c. The fit is described in reference 4.

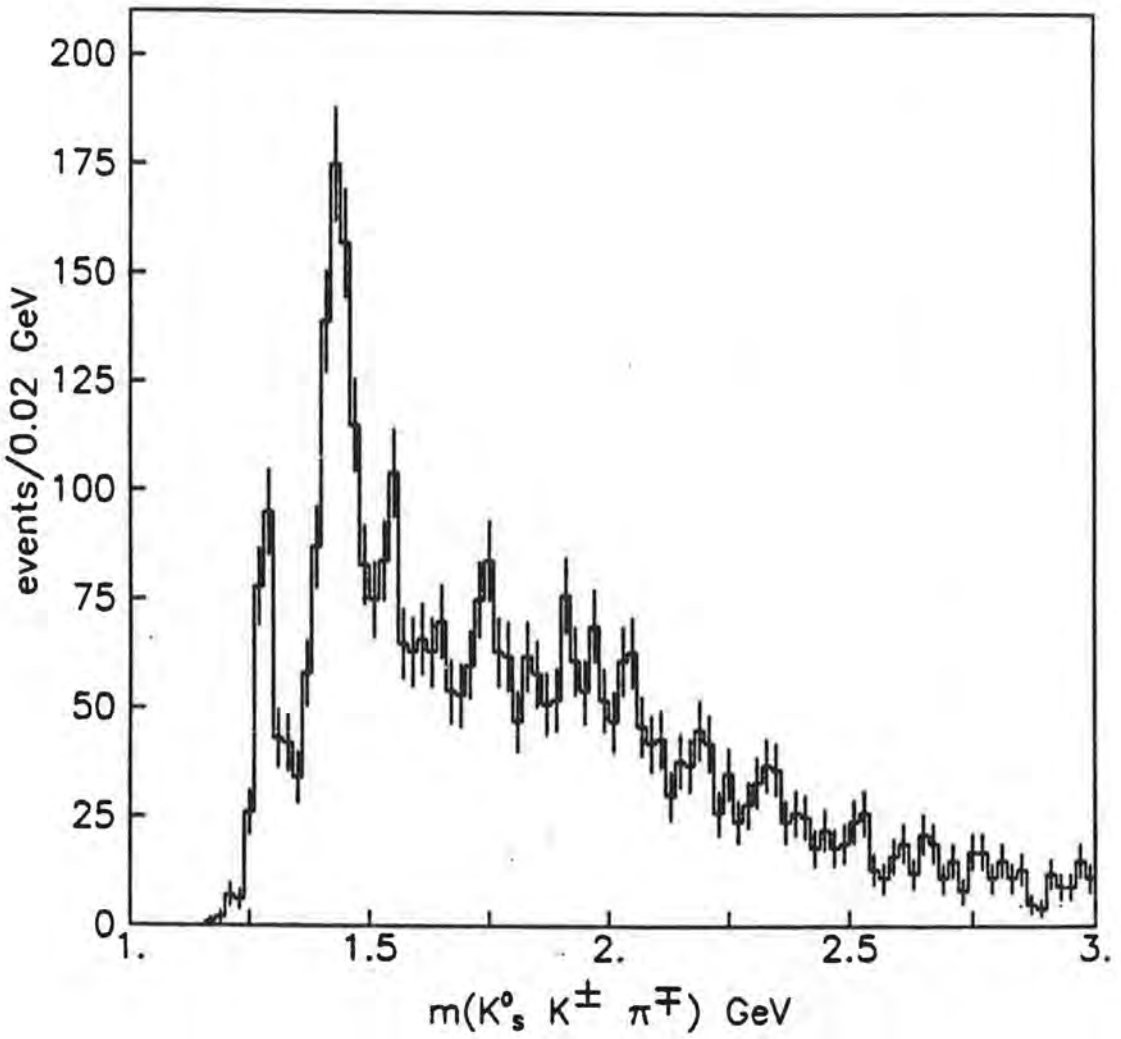

Fig. 5 $K^0_S K^{\pm}\pi^{\mp}$ effective mass spectrum at 300 GeV/c.

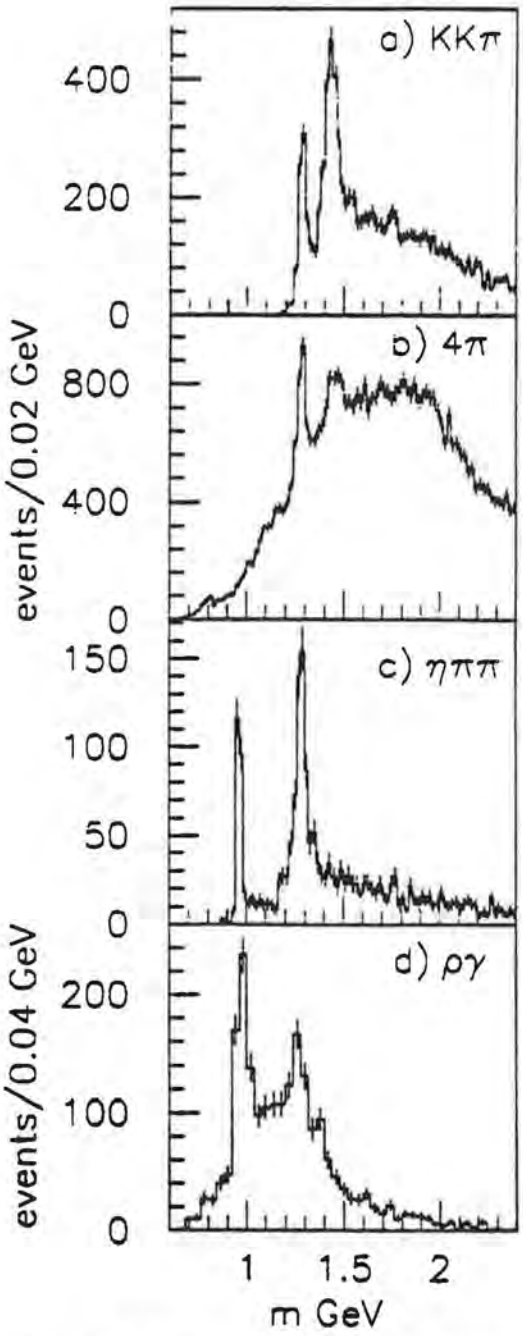

Fig. 6. Effective mass distributions for $(a)\ K^0_S K^{\pm}\pi^{\mp}$, $(b)\ \pi^+\pi^-\pi^+\pi^-$, $(c)\ \eta\pi^+\pi^-$ and $(d)\ \rho^0\gamma$ channels.

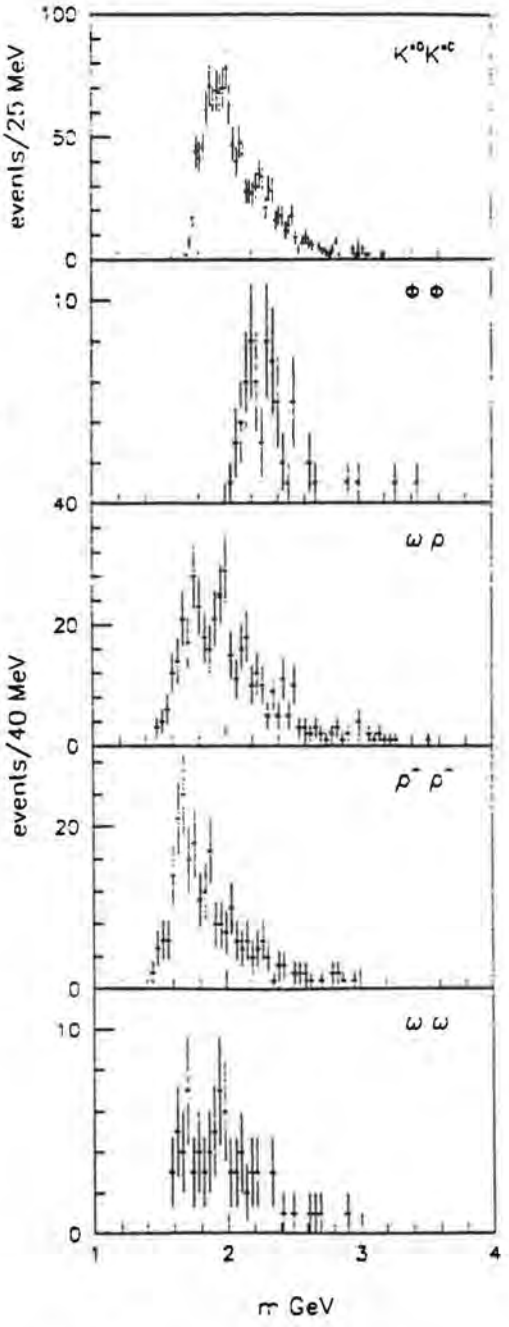

Fig. 7. Vector-Vector mass spectra for 300 GeV/c data.

NA31 Proposal 252

A Precise Measurement of $|\eta_{00}/\eta_{+-}|^2$

CERN, Edinburgh, Mainz, Orsay, Pisa, Siegen Collaboration

The main aim of this experiment is to measure precisely the strength of CP-violation in the decay amplitude relative to the dominant CP-violation in the K^0 mass matrix, by comparing the ratio of decays into two charged and two neutral pions for K_S and K_L. Data taking took place between 1986 and 1989, obtaining a sample of more than 300 000 $K_L \to 2\pi^0$ events.

The results of the analysis indicate a small, positive value for the parameter $\epsilon'/\epsilon = 1 - \frac{1}{6}|\eta_{00}/\eta_{+-}|^2$ of 0.0023 ± 0.0007, consistent with the results published earlier on the 1986 data alone. Calculations of the expected magnitude of ϵ'/ϵ, taking account of electroweak effects, within the standard model are sensitive to the mass of the top quark. However, recent calculations show that, for reasonable values of the top quark mass (and certainly for those consistent with the precise measurements at the Z^0), ϵ'/ϵ must be positive, and probably in the range 0.0005-0.0002.

The experiment has also searched for rare neutral kaon decays, knowledge of which is important for estimating the CP-conserving contribution to, for example, the decay $K_L \to \pi^0 e^+ e^-$. In particular, measurements of the decays $K_L \to \pi^0\gamma\gamma$ and searches for the decay $K_S \to \pi^0 e^+ e^-$. During the past year, a new measurement of the former has been made, and much reduced upper limits placed on the latter. The conclusion from these is that the primary contribution to the decay $K_L \to \pi^0 e^+ e^-$ is likely to be direct CP-violation.

Publications

1. GD Barr *et al*
   A measurement of the decay $K_L \to \pi^0\gamma\gamma$
   (to be published in Physics Letters B)

2. GD Barr *et al*
   Search for the decay $K_S \to \pi^0 e^+ e^-$ (to be published in Physics Letters B)

SEARCH FOR DIRECT PRODUCTION OF MESON STATES IN HIGH p_T π^-N COLLISIONS AT 150 AND 300 GeV/c

WA77 Proposal 253

Athens : Bari : Birmingham : CERN : Paris.

The purpose of this experiment is to search for evidence of direct production of mesons by QCD higher twist processes. Detailed predictions exist for the direct production cross sections for $L = 0$ and $L = 1$ $q\bar{q}$ mesons, and also for $L = 0$ glueball states [1]. The experiment is designed to observe the decays of such resonances to two charged particles. To this end a unique multiparticle high p_T trigger was developed [2], which selects events where 3 particles with $p_T > 1$ GeV/c are produced in π^- Be interactions. There were two data taking periods, at 300 GeV/c (7×10^6 triggers), and at 150 GeV/c (14×10^6 triggers). An electromagnetic calorimeter was used for the 150 GeV/c data in order to measure neutral channels.

The mass spectrum for pairs of high p_T particles assumed to be pions shows clear signals in the $\rho^0(770)$ and $f^0(1270)$ mass regions. In direct production the directly produced meson is balanced in p_T by a jet opposite in p_T. In order to exploit this feature, the data have been analyzed in terms of the variable $x_E = p_T^{opposite}/p_T^{pair}$, where direct production is favoured at low x_E. Analysis of the $\pi\pi$ spectrum shows that the ρ^0 behaves differently from the $\pi\pi$ background as a function of x_E [3]. The Lund model is able to reproduce the x_E behaviour of the background, but not the ρ^0 signal. However, the behaviour of the ρ^0 signal can be described by combining a higher twist contribution with the minimum twist one. A special Monte Carlo has been written to describe the higher twist contribution [4]. The fact that this combined model is required to describe the ρ^0 signal is interpreted as evidence for direct ρ^0 production *via* QCD higher twist processes.

The high p_T trigger also allows the study of fragmentation phenomena. A paper on short range flavour correlations has been published this year [5], and a second one describing vector meson p_T spectra at $p_T > 2$ GeV/c is in preparation.

Analysis of the data from the electromagnetic calorimeter is also in progress. High p_T $\eta\prime$ production is of particular interest, as evidence has already been found for direct $\eta\prime$ production in a study of published ISR data [6]. It is important to establish further direct production signals in our data, as a comparison of the differential cross sections for direct production of different mesons allows detailed tests of the production mechanism to be made.

REFERENCES

1. M. Benayoun et al., Nucl. Phys. **B268** (1987) 653.
2. W. Beusch et el., Nucl. Inst. and Meth. **A249** (1986) 391.
3. M. Benayoun et al., Phys. Lett. **183B** (1987) 412.
4. G. Ingelman. DESY 86-131 (1986).
5. A. Bellogianni et al.. Z. Phys. C. **54** (1992) 535.
6. M. Benayoun et al., Phys. Lett. **192B** (1987) 447.

Publications (October 1991 to September 1992)

1. Short-range correlations in hadron pair production at $p_T \geq 2$ GeV/c.

   I.J. Bloodworth, J.N. Carney, J.B. Kinson, M.T. Trainor,
   O. Villalobos Baillie and M.F. Votruba; with Athens, Bari, CERN,
   and Paris.

   Z. Phys C **54**, 535-548 (1992).

An exposure of the 15-foot bubble chamber filled with a Ne/H_2 mixture to a quad-triplet beam from the TEVATRON running at 800 GeV/c.

FNAL E632 Proposal 254

Berkeley - Birmingham - Brussels - CERN - Chandigarh - FNAL-
Hawaii - IHEP(Serpukhov) - Illinois - Imperial College London - ITEP (Moscow) -
Jammu - MPI Munich - Moscow State University - Oxford -
RAL - Rutgers - Saclay - Tufts

For the majority of the original groups of the experiment, data-processing finished during 1992. However, IHEP(Serpukhov), ITEP(Moscow) and Moscow State University are in the process of measuring a large unbiassed sample. This should provide sufficient data at the highest-ever neutrino energy for many comparisons to be made with experiments at lower neutrino energies - fragmentation studies, energy dependences in strange particle production, neutral currents, etc.

Several new analyses are under way and the results should be published in the near future.

Publications since 1 October 1991

• Study of high-energy neutrino neutral-current interactions
Phys. Rev. D45 (1992) 2232- 2243.
• Strangeness production in neutrino interactions
Proc. of XXVIth International Conference, Dallas, 1992.
• Neutral Secondary Vertices Associated to High Energy Neutrino Interactions
Proceedings of International Conference on Neutrino Physics and Astrophysics, Granada, 1992.

PhD theses since 1 October 1991

1. Holography in the FNAL 15-foot Bubble Chamber and Particle Density Fluctuations in Neutrino Interactions.

   Ludo Verluyten; Antwerp University.

2. Coherent Production of Pions and Rho Mesons in Neutrino Charged Current Interactions on Neon Nuclei at the Fermilab Tevatron.

   Stéphane Willocq; Tufts University.

STUDY OF LEPTON PRODUCTION IN HADRONIC COLLISIONS

HELIOS (NA34) - CERN SPS (H8 beam) PROPOSAL 260

Bari University
Brookhaven National Lab.
CERN
Ferrara
Heidelberg University
Lebedev Institute, Moscow
Lund University
McGill University
Montreal University
Munich
NIKHEF, Amsterdam
Novosibirsk Inst. Nucl. Phys.
PEI, Moscow
Pittsburgh University
Roma University
Rutherford Appleton Lab.
Stockholm University
Tel-Aviv University
Torino University
University College, London

The aim of the HELIOS experiment is to study lepton and photon production in hadronic collisions, with particular emphasis on the 'soft' radiation at low lepton-pair mass and transverse momentum.

The main feature of the detector is the combination of electron, photon, and muon identification, together with energy measurement over the full solid angle by calorimetry.

The final data taking of the experiment was carried out during the SPS Fixed Target running at the end of 1989. The final publications from the experiment should appear during 1993.

Figure 1 shows the di-muon mass spectrum and the various channels which contribute to it. By taking proper account of all these contributions we have been able to show that they match the experimental data, and there is no need to invoke any "anomalous" source of di-muons. A similar conclusion is obtained from the di-electron spectrum.

Publications October 1991 to September 1992:
(includes publications from those parts of the Helios Heavy Ion experiment in which there was substantial UK involvement.)

1) A search for weakly interacting neutral particles in missing energy events in 450 GeV/c pN collisions.
T.Åkesson et al. Z.Phys. C52, 219 (1991)

2) Proton distributions in the target fragmentation region in proton-nucleus and nucleus-nucleus collisions at high energies.
T.Åkesson et al. Z.Phys. C53, 183 (1992)

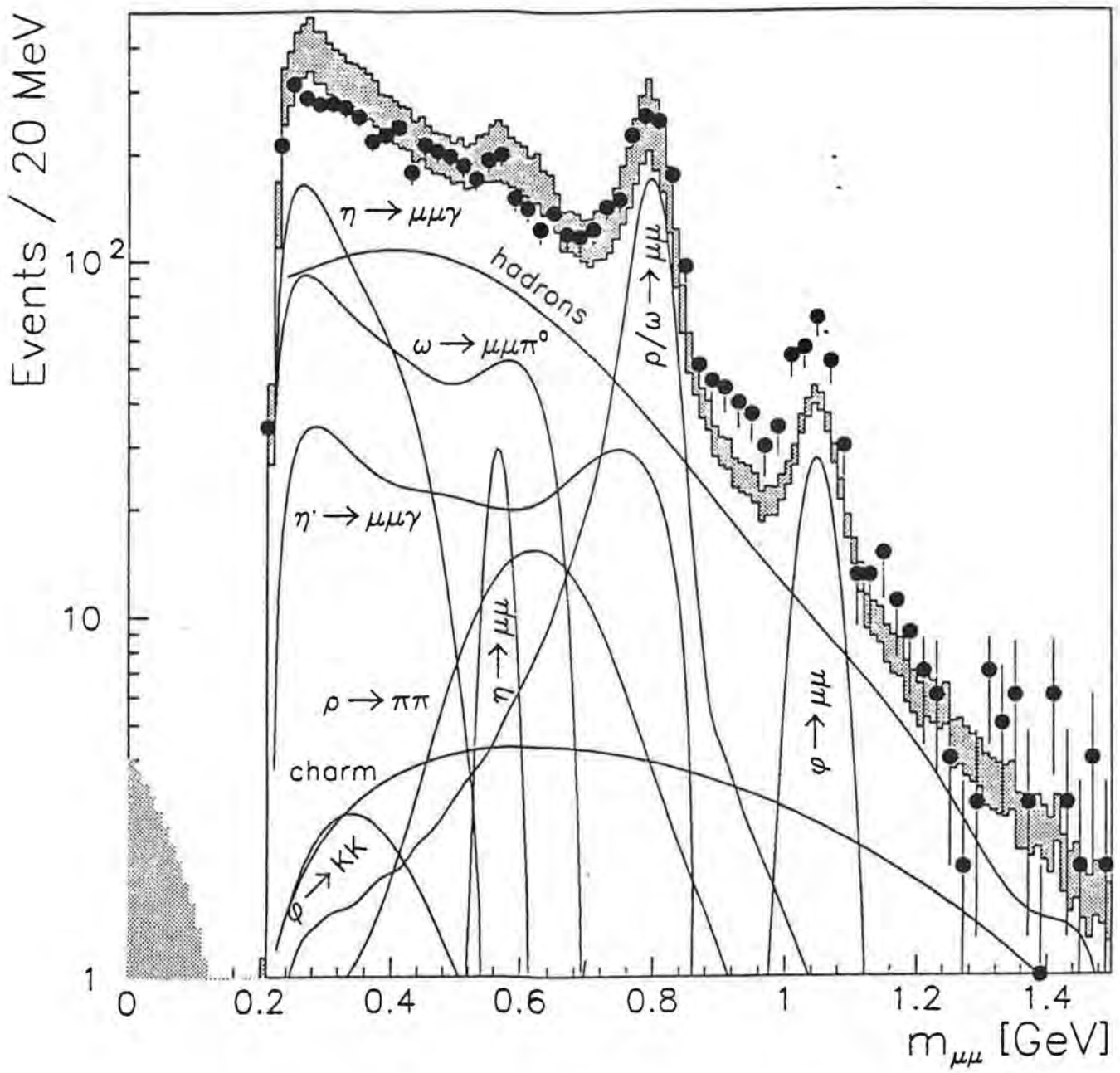

Figure 1. The di-muon mass spectrum (black dots) in pBe collisions at 450 GeV/c. The various physical processes which contribute to the di-muon spectrum are also shown. They are sufficient to explain the data.

SLD Collaboration at SLC

Proposal 263

Bologna, Boston, Brunel, Caltech, Cincinnati, Colorado, Colorado State, Columbia, Ferrara, Frascati, Illinois, Massachusetts, MIT, Nagoya, Northeastern, Northridge, Oregon, Padova, Perugia, Pisa, Rutgers, RAL, Santa Barbara, Santa Cruz, SLAC, Tennessee, Tohoku, Vanderbilt, Washington, Wisconsin, Yale.

SLD had its initial physics run in 1992. After a lengthy commissioning phase, the SLAC Linear Collider (SLC) has been brought under control and even exceeded the goals for the run.

I. SLC Performance

The major challenges were to improve the machine luminosity and reliability, and at the same time to provide SLD with longitudinally polarized electrons, since this gives the best chance of beginning to reveal the physics which lies beyond the Standard Model.

The commissioning of the polarized electron system was accomplished at lightning speed during April, and SLD started the physics run on May 2. By the end of the run, SLC had delivered 11,000 Z^0s on tape to SLD, with a polarization of about 24%. The luminosity improved steadily during the run, repeating the results of previous years which demonstrate the rewards of a sustained effort on the part of the SLC team. By the end of the run, the machine was up to one third of the design luminosity.

A prestigious DoE Panel has just recognised the special physics opportunities at SLD by strongly recommending further SLC upgrades and a continuation of the running for at least the next two years. It is anticipated that SLD will accumulate around 70,000 Z^0s per year during this time, with increasing polarization, possibly as high as 75% for the run in 1994.

Finally, the deep understanding of the linear collider technology afforded by the SLC experience has resulted in a clearly defined plan for building a future machine up to 1.0 TeV in CM energy and with the required luminosity for physics. This is a real triumph on the part of all who have contributed to the SLC enterprise, and provides the particle physics community with a wonderful opportunity to break through to a detailed study of the New Physics beyond the Standard Model.

II. SLD Status and Plans

All essential elements of SLD are in place and working well. The 120 Mpixel vertex detector was taken from RAL to SLAC in October 1991, installed and fully commissioned before the start of data taking in May 1992. Preliminary physics results reported at the Dallas Conference included a measurement of A_{LR} (not yet sufficient statistics to challenge the Standard Model), QCD physics (where one is not statistics limited, so suffers no disadvantage with respect to LEP), and first results of heavy flavour physics. The beautiful decays (τ, b, c) seen with the powerful vertex detector, in conjunction with the beam polarization, offer interesting physics opportunities complementary to those at LEP.

While SLD will never compete with LEP in terms of number of Z^0s, the experience being accumulated with the detector (as for the accelerator) is providing a firm foundation for the next linear collider system, for which the physics case is exciting enthusiasm internationally. SLC/D forms the cornerstone of a major R & D effort which is expected over the next two years to lead to a fully workable design for a collider/detector complex able to carry the detailed study of e^+e^- interactions into an energy regime which will never be accessible to storage rings.

University of Bern, Cambridge University, CERN, University of Dortmund, University of Heidelberg, University of Melbourne, INFN Milan, University of Paris (Orsay), University of Pavia, University of Perugia, University of Pisa, CEN (Saclay)

The aim of the upgraded UA2 experiment has been to search for the top quark and new phenomena such as those suggested by supersymmetric and composite models, to carry out further tests of QCD, especially in W + jets and in multijet studies, and to provide improved tests of the electroweak model. This has been made possible by the high luminosity of proton-antiproton interactions provided by the Antiproton Accumulator Complex (AAC) for the CERN Collider, and a new apparatus which included a scintillating fibre detector and inner and outer silicon detectors for which Cambridge shared direct responsibility. By the end of 1990 data-taking was complete and in the course of 1992 the final analysis of that data was essentially finished. A summary of new results follows. Complete accounts can be found in the papers listed below. This list includes all papers published or submitted for publication since the last progress report.

1. Search for the charged Higgs. Important searches for the top quark including that carried out by the UA2 experiment have been able to set a lower limit on the mass m_t based on the lack of observed semileptonic decays such as $t \rightarrow e^+\nu b$. On the other hand, if charged Higgs bosons ($H^\pm$) exist, as implied by simple extension of the minimal standard model, and if $m_t > m_H + m_b$, then the decay $t \rightarrow H^+b$ competes with the standard decay $t \rightarrow W^+b$ (where the W can be virtual) and in fact dominates in the mass region accessible at the CERN $\bar{p}p$ Collider, $m_W > m_t + m_b$. Therefore in order to validate top quark mass limits set by searches for (for example) $W^+ \rightarrow t\bar{b}$, $t \rightarrow e^+\nu b$, it is important to study the question, crucial in its own right, of the existence of the charged Higgs.

In 1992, UA2 published the results of a search for $t \rightarrow H^+b$, $H^+ \rightarrow \tau^+\nu$, $\tau^+ \rightarrow$ hadrons $+\bar{\nu}$, and for its charge conjugate. Using data corresponding to an integrated luminosity of $13pb^{-1}$ at the CERN $\bar{p}p$ Collider, the numbers of electrons and taus accompanied by large missing transverse momentum were determined. With the assumption of e-τ universality, the number of electrons was used to predict the number of taus from W decay and this prediction was carefully compared with the data. The lack of significant excess of taus made it possible to exclude the above decays involving the charged Higgs in new regions of the m_H - m_t plane. This is shown in Fig.1. In addition, the ratio of couplings of the τ and electron to the W was measured to be

$$g_\tau^W / g_e^W = 1.02 \pm 0.04 \pm 0.04$$

which is consistent with e-τ universality.

2. W Physics. The results of two major studies in this area were published in 1992, one concerned with a W decay branching ratio and the other bearing on self-interactions among gauge bosons.

The UA2 experiment has observed the decay $W^\pm \rightarrow e^+\nu$ and the hadronic decay in the quark-antiquark channel. In the same experiment, a search has also been made for the decay $W^\pm \rightarrow \pi^\pm\gamma$. In the framework of the standard model, this decay is highly suppressed and the partial width ratio is estimated to be

$$R = \frac{\Gamma(W^\pm \rightarrow \pi^\pm\gamma)}{\Gamma(W^\pm \rightarrow e^\pm\nu)} < 3 \times 10^{-8}$$

However, if one extends to W decay the method used to calculate the $\pi^0 \rightarrow \gamma\gamma$ amplitude, much larger values of R are obtained, corresponding to a branching ratio of the order of 0.1 for the decay $W^\pm \rightarrow \pi^\pm\gamma$.

The signature of the $W^\pm \rightarrow \pi^\pm\gamma$ is a photon and a charged pion opposite in azimuth with an invariant mass compatible with the W mass. The background for this process is due mainly to direct photon production where an associated jet is mis-identified as a single charged pion, and two-jet events where one jet fakes a photon and the other is taken to be a single pion. Studies of shower containment and profiles in the calorimeter, together with associated tracks and consideration of acceptance, enable cuts to be established and efficiencies determined. The result is that no events compatible with the decay $W^\pm \rightarrow \pi^\pm\gamma$ survive the selection criteria. Using Monte-Carlo techniques and reasonable assumptions, R can be calculated to be $< 4.9 \times 10^{-3}$ (95% C.L.) and $< 3.8 \times 10^{-3}$ (90% C.L.). This represents more than a factor of ten improvement in the limit obtained previously by the UA1 Collaboration at the collider. A limit on the

branching ratio BR($W^{\pm} \rightarrow \pi^{\pm}\gamma$) can be derived assuming the standard model value for BR($W^{\pm} \rightarrow e^{\pm}\nu$) as computed for $m_t > m_W - m_b$: BR($W^{\pm} \rightarrow \pi^{\pm}\gamma$) $< 5.4 \times 10^{-4}$ (95% C.L.). This result is similar to the limit obtained by LEP experiments for the branching ratio of the decay $Z \rightarrow \pi^o\gamma$ which is also suppressed in the standard model.

In another analysis, a first direct measurement of the coupling of the W boson to the photon has been made by UA2. The reaction $\bar{p}p \rightarrow W\gamma+X$ is studied because the angular distribution of the W's is particularly sensitive to the magnetic dipole moment, μ_W. This can be written in terms of parameters κ and λ in the form $\mu_W = (e/2M_W)(1+\kappa+\lambda)$ in the standard model. Similarly, the electric quadrupole moment of the W, can be expressed as $Q_W = -(e/M_w^2)(\kappa-\lambda)$. Experimentally, $\bar{p}p \rightarrow e\nu\gamma$ was studied by looking for an electron accompanied by missing transverse momentum and a photon. The main source of background was $W \rightarrow e\nu$ decays associated with jets, where a jet is mis-identified as a photon. Using the entire UA2 data sample, 16 events were observed and the number of background events computed to be 7 ± 1. Two different Monte-Carlo calculations yielded predictions in close agreement for any values of κ and λ. These in turn were compared with experimental results to yield $-3.5 < \kappa < 5.9$ and $-3.6 < \lambda < 3.5$ with 95% confidence limits. The measurements are thus in good agreement with expectations from the standard model ($\kappa=1$ and $\lambda=0$) and do not depend on any cutoffs or regularization schemes.

3. Prompt photon production. The production of prompt photons in hadron-hadron collisions is a particularly direct way to obtain information about the constituents of hadronic matter and their interactions. The photons are produced directly, in lowest order in the strong coupling constant α_s, through two quantum chromodynamics (QCD) processes: compton scattering ($qg \rightarrow \gamma q$) and annihilation ($\bar{q}q \rightarrow \gamma g$). Calculations are available for leading and next-to-leading order for both single and double prompt photon production.

In 1992, the UA2 collaboration completed measurements of the single and double prompt photon cross sections and the gluon structure function $G(x,Q^2)$ at the CERN $\bar{p}p$ Collider. In the cross section measurements, the main source of background was high transverse momentum hadron jets, which often contain one or more π^o or η mesons which decay to unresolved photon pairs. However, it proved to be possible to develop effective isolation criteria so that with the entire data sample, the cross section for prompt photon production was determined with higher statistics than in previous measurements. In addition, a signal from double prompt proton production was observed with a statistical significance of 4.3 standard deviations. The measurements, spanning a transverse momentum range of 10 – 31 GeV at $\sqrt{s} = 630$ GeV, were found to be in good agreement with perturbative QCD. The gluon structure function was determined for $0.049 \leq x \leq 0.207$ in a Q^2 range of 280 GeV^2 to 3670 GeV^2 by measuring both the photon and the recoiling jet and using the known quark distribution function $F(x,Q^2)$ and theoretical parton-parton QCD cross sections. The results are in agreement with the gluon density function obtained indirectly by extrapolating from deep inelastic neutrino-nucleon scattering data.

During the last seven years, the upgraded UA2 experiment has used an innovative and reliable apparatus to exploit successfully a large and important area of physics potential at the CERN $\bar{p}p$ Collider. The results have been reported in scores of meetings and conferences and have been fully published in over thirty major research papers. The results published in 1992 were essentially the final ones, and marked an end to the involvement of Cambridge in the experiment.

Publications

UA2 Collaboration, "A study of multi-jet events at the CERN $\bar{p}p$ collider and a search for double parton scattering", *Phys. Lett. B* **B268**, 145 (1991).

UA2 Collaboration, "A measurement of electron-tau universality from decays of intermediate vector bosons at the CERN $\bar{p}p$ collider", *Z. Phys. C* **52** 209 (1991).

UA2 Collaboration, "Study of electron pair production below the Z mass at the CERN $\bar{p}p$ collider", *Phys. Lett. B* **B275**, 202 (1992).

UA2 Collaboration, "A search for scalar leptoquarks at the CERN $\bar{p}p$ collider", *Phys. Lett. B* **B274**, 507 (1992).

UA2 Collaboration, "A measurement of the W and Z production cross sections and a determination of Γ_W at the CERN $\bar{p}p$ collider", *Phys. Lett. B* **B276**, 365 (1992).

UA2 Collaboration, "An improved determination of the Ratio of W and Z masses at the CERN $\bar{p}p$ collider", *Phys. Lett. B* **B276**, 354 (1992).

UA2 Collaboration, "Experimental limit on the decay $W^{\pm} \rightarrow \pi^{\pm} \gamma$ at the CERN $\bar{p}p$ collider", *Phys. Lett. B* **B277**, 205 (1992).

UA2 Collaboration, "Direct measurement of the W–γ coupling at the CERN $\bar{p}p$ collider", *Phys. Lett. B* **B277**, 194 (1992).

UA2 Collaboration, "A search for charged Higgs from top quark decay at the CERN $\bar{p}p$ collider", *Phys. Lett. B* **B280**, 137 (1992).

UA2 Collaboration, "A measurement of single and double prompt photon production at the CERN $\bar{p}p$ collider", *Phys. Lett. B* . **288**, 386 (1992).

UA2 Collaboration, "Measurement of the gluon structure function from direct photon data at the CERN $\bar{p}p$ collider", submitted to *Phys. Lett. B* .

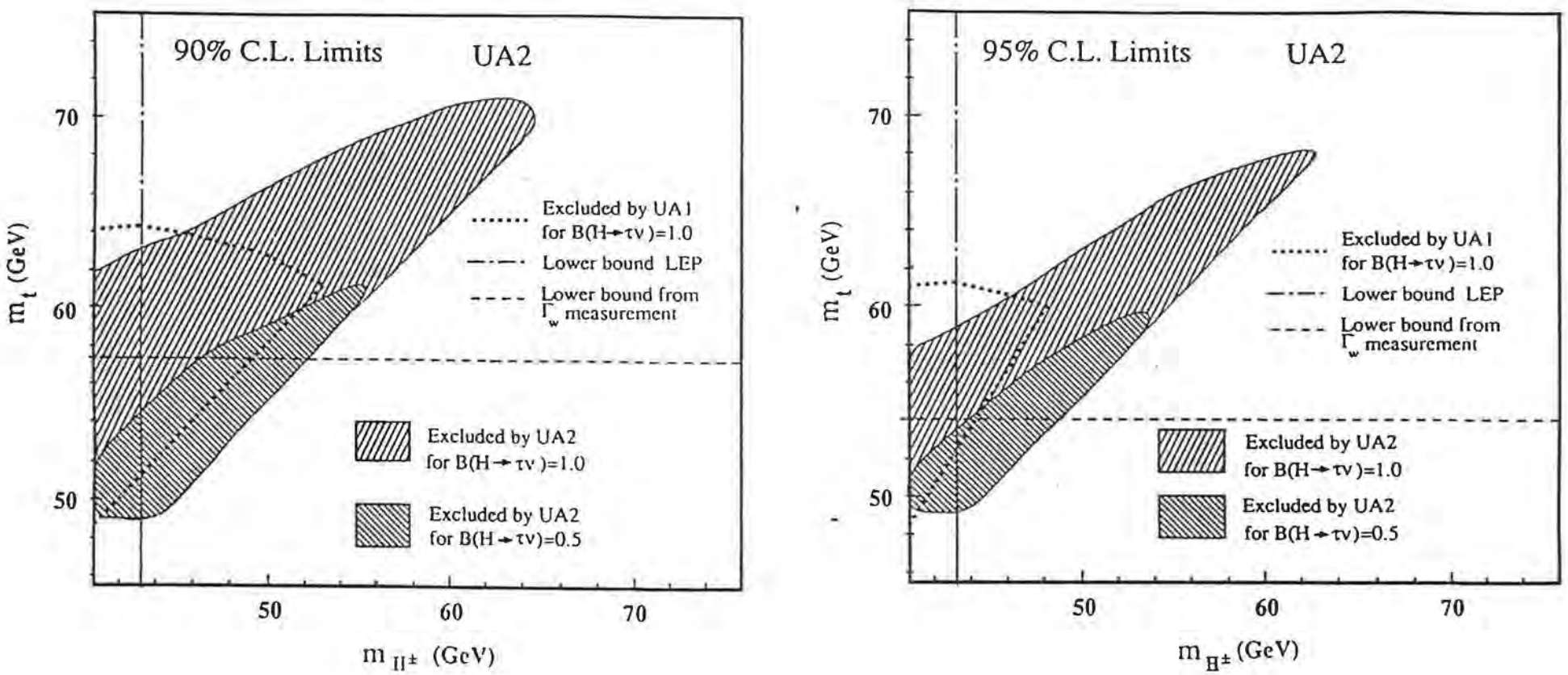

Fig. 1. Regions of the $m_H - m_t$ plane excluded at the confidence limits indicated.

The LEP bound is for the branching B = 1, 95% confidence limit.

THE STUDY OF CP VIOLATION IN THE NEUTRAL KAON SYSTEM AT LEAR

PS 195 Proposal 265

Athens, Basel, Boston, CERN, Coimbra, Delft, ETH Zurich, Fribourg, Ioannina, Liverpool, Lubljana. Marseille, Orsay, PSI, Saclay, Stockholm, Thessalonika.

Introduction

Traditionally CP violation has been investigated using beams of high energy K^0_L and K^0_S, and has only been detected in the 2 pion and semileptonic decay modes of K^0_L and their interference with the corresponding decays of K^0_S. CPLEAR adopts a fundamentally different approach, where CP violation is detected by observing the asymmetry between the decays of initially pure K^0 and $\bar{K}^0$ states.

The initial neutral kaon is produced in a state of definite strangeness by antiproton annihilation at rest in a high pressure (16 bar) gaseous hydrogen target via the reactions

$$\bar{p}p \rightarrow K^+ \pi^- \bar{K}^0 , \quad \bar{p}p \rightarrow K^- \pi^+ K^0$$

The strangeness of the neutral kaon is tagged by observing the sign of the charged kaon. This method has the considerable advantage of simultaneous and symmetric production of K^0 and $\bar{K}^0$ and symmetric detection of their decay products. Thus systematic corrections and uncertainties are reduced to a very low level.

This method also enables, at least in principle, CP violation to be detected in all possible decay modes of the neutral kaon. Of particular importance in this experiment are the following:-

$$K^0 \rightarrow \pi^+\pi^-, \pi^0\pi^0 \qquad (1)$$
$$K^0 \rightarrow \pi^\pm \ell^\mp \nu \qquad (2)$$
$$K^0 \rightarrow \pi^+ \pi^- \pi^0 \qquad (3)$$

Study of (1) in the $\pi^+ \pi^-$ channel will enable a determination to be made of the magnitude and phase of η_{+-} with a precision significantly better than the present world average. In the $\pi^0\pi^0$ channel the phase φ_{00} of η_{00} should be determined to better than 1°. These channels will also enable a precise measurement of the K^0_S lifetime to be made. Study of (2) will enable a precise test of the $\Delta S = \Delta Q$ rule to be made, as well as the first measurement of direct T violation. It will also provide an accurate determination of $\Delta m = m_L - m_S$. Finally analysis of the three pion decay mode (3) will provide the first direct measurement of CP violation in the decay of K^0_S.

Status of the Detector and Trigger

The detector is shown in fig. 1. It has cylindrical geometry and is mounted inside a solenoid of 3.6 m length which produces a magnetic field of 0.44 T parallel to the $\bar{p}$ beam. Tracking of the annihilation products is performed by two layers of proportional chambers, 6 layers of drift chambers and two layers of streamer tubes. The proportional and drift chambers provide rapid on-line r-φ co-ordinates while the streamer tubes provide on-line axial (z) co-ordinates, all of which are used by the event trigger. More precise off-line z co-ordinates are provided by cathode strip readout from the drift chambers. Particle identification is provided by a 32-sector scintillator - threshold Cerenkov - scintillator sandwich (the PID), while an 18-layer gas-sampling electromagnetic calorimeter provides high spatial resolution detection of photons and electrons.

The detector has been complete and fully equipped with readout electronics since the late summer of 1991. Data has been taken with the complete system during two running periods in late 1991 and also during running which started in August 1992. The desired "golden" channels ($K^{\pm}\pi^{\mp}K^{\circ}$) represent only about 4 x 10^{-3} of the total $\bar{p}p$ annihilation rate. Hence, to achieve the physics goals of this experiment in a reasonable length of time, it is necessary to run at a $\bar{p}$ annihilation rate of about 1 MHz. In order to pick out the desired events from the large unwanted background, a sophisticated multi-level trigger has been designed based on several sequential decisions provided by fast trigger processors.

The main advance which has been made this year is the implementation of further stages of this trigger. The pre-trigger and P_T cut, which select charged kaon candidate tracks, have been working for some time, as has the track launcher which permits triggering on final states of any chosen multiplicity. The additional stages which have been introduced in the past year are as follows. The "track follower" determines whether each track candidate has sufficient wire-chamber hits for off-line reconstruction and determines track parameters such as total momentum. The kinematics processor then places a cut on the sum of the primary kaon and pion momenta which helps eliminate events with extra π°'s at the primary vertex. The "HWP2" processor then confirms particle identification using dE/dX information from the inner scintillator and pulse-height information from the Cerenkov in conjunction with the track momentum. Finally the "HWP2.5" processor determines the number of showers in the calorimeter and enables a cut to be placed on this. The introduction of these further stages of trigger processing has lead to a significant reduction in the rate at which data are written to magnetic tape through the elimination of unwanted background events.

<u>Status and Data Analysis</u>

Most progress in the past year has been made in the analysis of the $\pi^{+}\pi^{-}$ channel where the complete data sample up to the end of 1991 has been analysed. Fig. 2 shows the measured lifetime distribution of these events after acceptance correction using Monte Carlo data. A 3-parameter fit to these data (solid curve) yields a K°_S lifetime of $(0.99 \pm 0.01)\tau_S$ and a K°_L level at long lifetimes which is 1.7 ± 0.2 times greater than that expected from CP violating $K^{\circ}_L \rightarrow \pi^{+}\pi^{-}$ decays (dashed curve), showing that some residual 3-body decays remain. The statistical accuracy of the K°_S lifetime measurement is presently limited by the availability of Monte Carlo data.

The asymmetry parameter A_{+-} is shown as a function of K° lifetime in fig. 3. A fit of these data for the magnitude and phase of η_{+-} assuming the 3-body background contamination determined from fig. 2 is shown by the solid curve. The results of the fit are printed on the plot and show excellent agreement with the present world average values. The dashed curve is a fit to the points assuming no 3-body background.

The analysis of semileptonic decays is still at a preliminary stage since, so far, only low momentum electrons have been identified using the PID. However, the results already show some very striking features and are shown in fig. 4. Here are shown various asymmetries which can be obtained from the decays of initial K° and $\bar{K}^{\circ}$ mesons to final states containing positively and negatively charged leptons, together with the best fits to the data. The asymmetry $A_{\Delta m}$ is sensitive to $\Delta m = m_L - m_S$ and yields the result $\Delta m\tau_S = 0.475 \pm 0.019 \pm 0.013$ which is in excellent agreement with the present world average value, although with a much larger error. Asymmetries A_x and A_t are both sensitive to $\Im m(x)$, where x measures violation of the $\Delta S = \Delta Q$ rule. The fits give a best value for $\Im m(x)$ of $-0.016 \pm 0.028 \pm 0.010$, which is already comparable in accuracy to the present world average value. The asymmetry A_T is a direct measure of T violation. If T is violated along with CP, so that CPT is conserved, then the expected value of A_T is 4 $\Re e(\varepsilon)$. The fit gives a result which is in good agreement with this expected value, although with large errors on it.

The analysis of the $\pi^0\,\pi^0$ and $\pi^+\,\pi^-\,\pi^0$ channels is at an even more preliminary stage and work is continuing to improve algorithms for identifying photon shows in the calorimeter and reconstructing π^0's. However, good progress is being made as is shown in figs. 5 and 6, where the invariant masses of identified $\pi^0\pi^0$ and $\pi^+\pi^-\pi^0$ events are shown.

Conclusion

The apparatus is working well and considerable progress has been made in the on-line trigger processing and in off-line data analysis. With the large amount of data which is being taken during 1992 with this improved trigger, and with improved algorithms for the identification of charged and neutral showers in the calorimeter, considerable progress in the analysis of all the physics channels listed will be made.

Ph.D. Theses (Liverpool University)

J. M. Bennett	A measurement of η_{+-} using strangeness tagging at LEAR.
P. D. Maley	A determination of delta(m) from tagged neutral kaons
S. Vlachos	Evaluation of real-time event selection mechanisms for the CPLEAR experiment.

Publications

First determination of CP violation parameters from K^0 - $\bar{K}^0$ decay asymmetry.
Phys. Lett. B286 (1992) 180 - 186.

Figure Captions

1. Schematic plan view of the CPLEAR detector. Also shown is a typical event decaying at long lifetime with the track fit superimposed.

2. Lifetime distribution for the sum of K^0 and $\bar{K}^0$ events decaying to $\pi^+\pi^-$.

3. The asymmetry $A_{+-}(t)$ between initial K^0 and $\bar{K}^0$ states decaying to $\pi^+\pi^-$.

4. Various asymmetries between initial K^0 and $\bar{K}^0$ states decaying to semileptonic states containing positively and negatively charged leptons.

5. The reconstructed secondary invariant mass of K^0 and $\bar{K}^0$ events decaying to $\pi^0\pi^0$, using the calorimeter to identify and reconstruct the π^0's.

6. The reconstructed secondary invariant mass of K^0 and $\bar{K}^0$ events decaying to $\pi^+\pi^-\pi^0$ for events with at least 1 photon shower in the calorimeter.

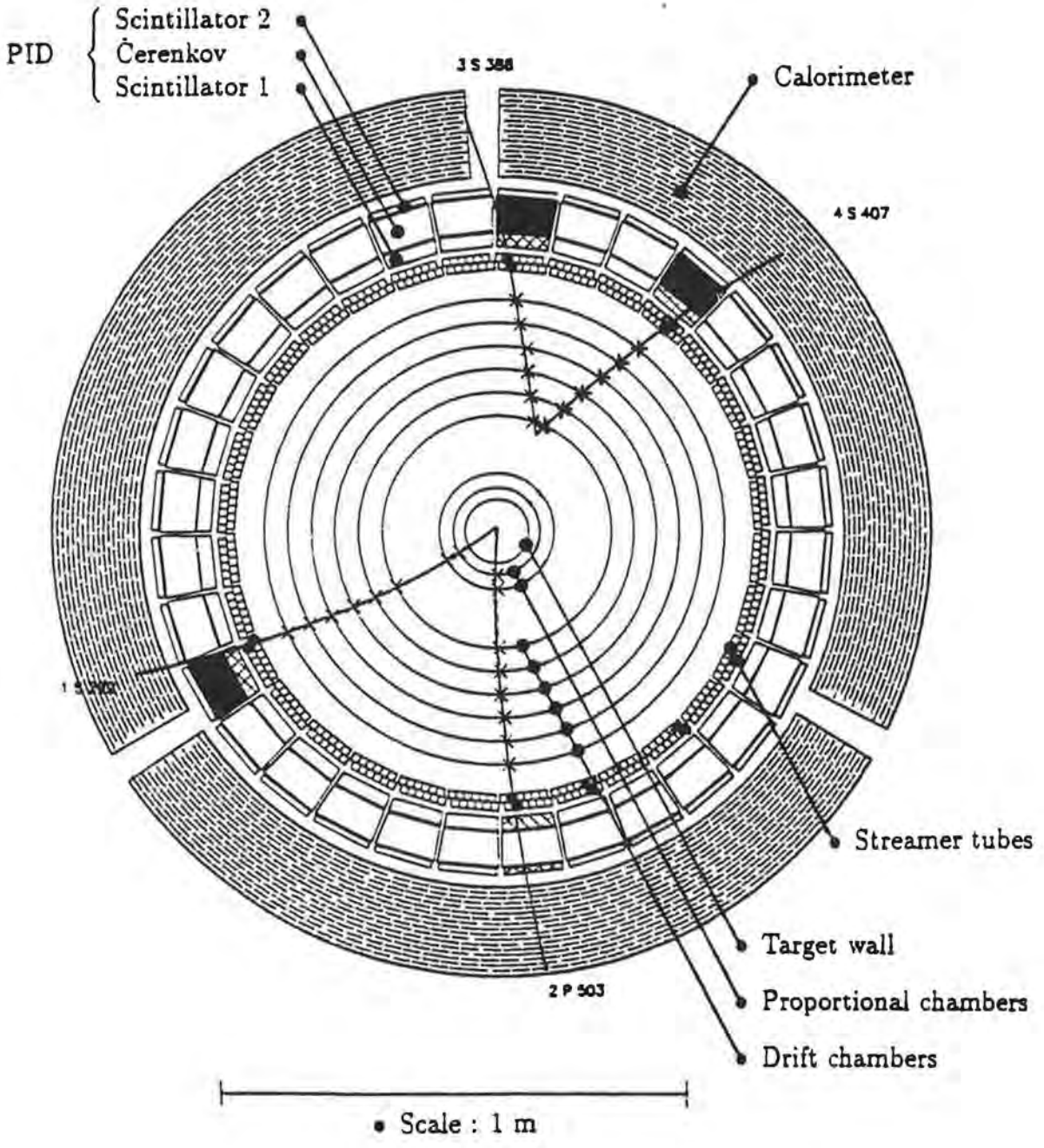
PID
Scintillator 2
Čerenkov
Scintillator 1
3 S 388
Calorimeter
4 S 407
1 S 262
Streamer tubes
Target wall
2 P 503
Proportional chambers
Drift chambers
Scale : 1 m

Figure 1.

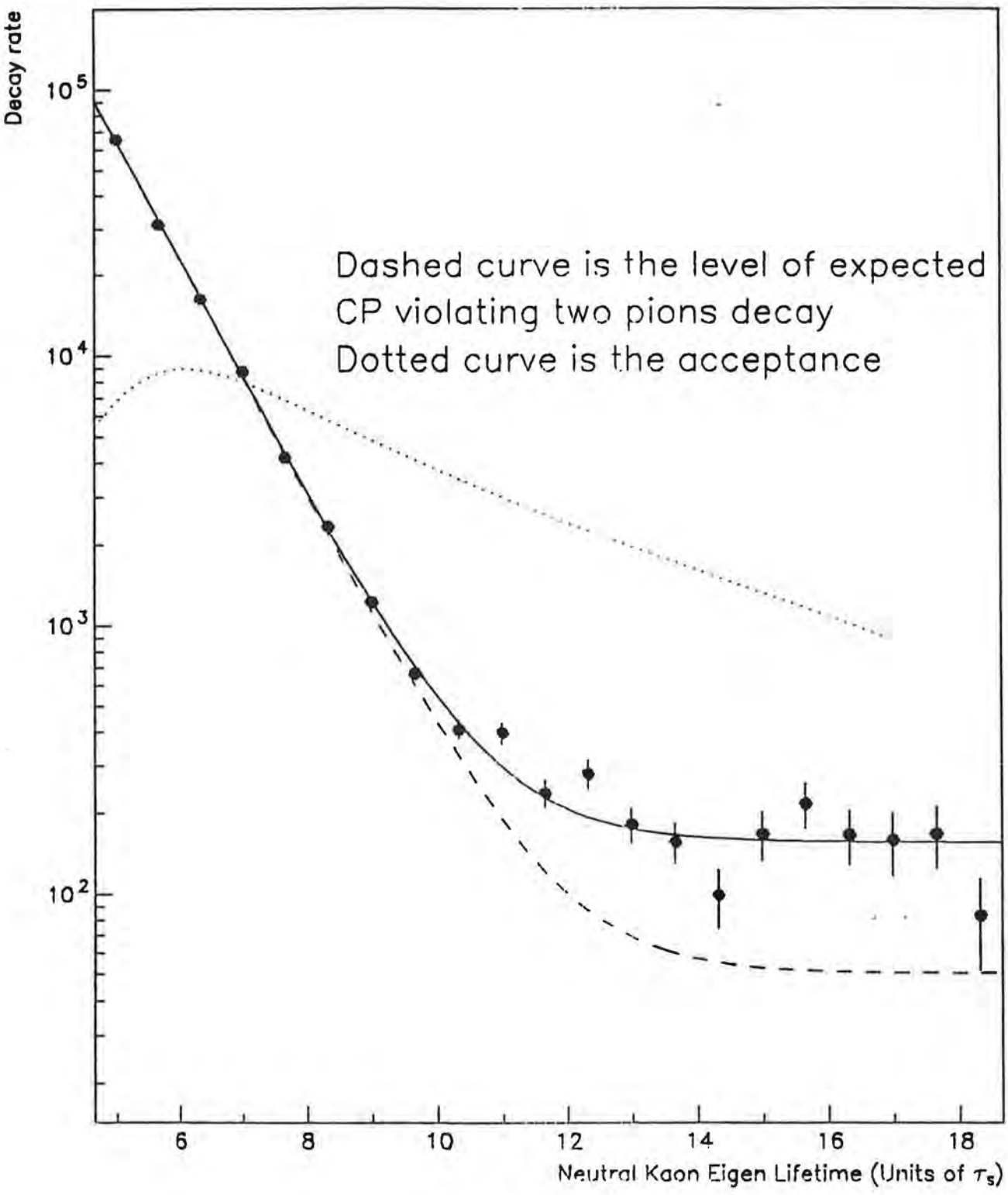
Decay rate
10^5
10^4
10^3
10^2
Dashed curve is the level of expected
CP violating two pions decay
Dotted curve is the acceptance
6
8
10
12
14
16
18
Neutral Kaon Eigen Lifetime (Units of τ_S)

Figure 2.

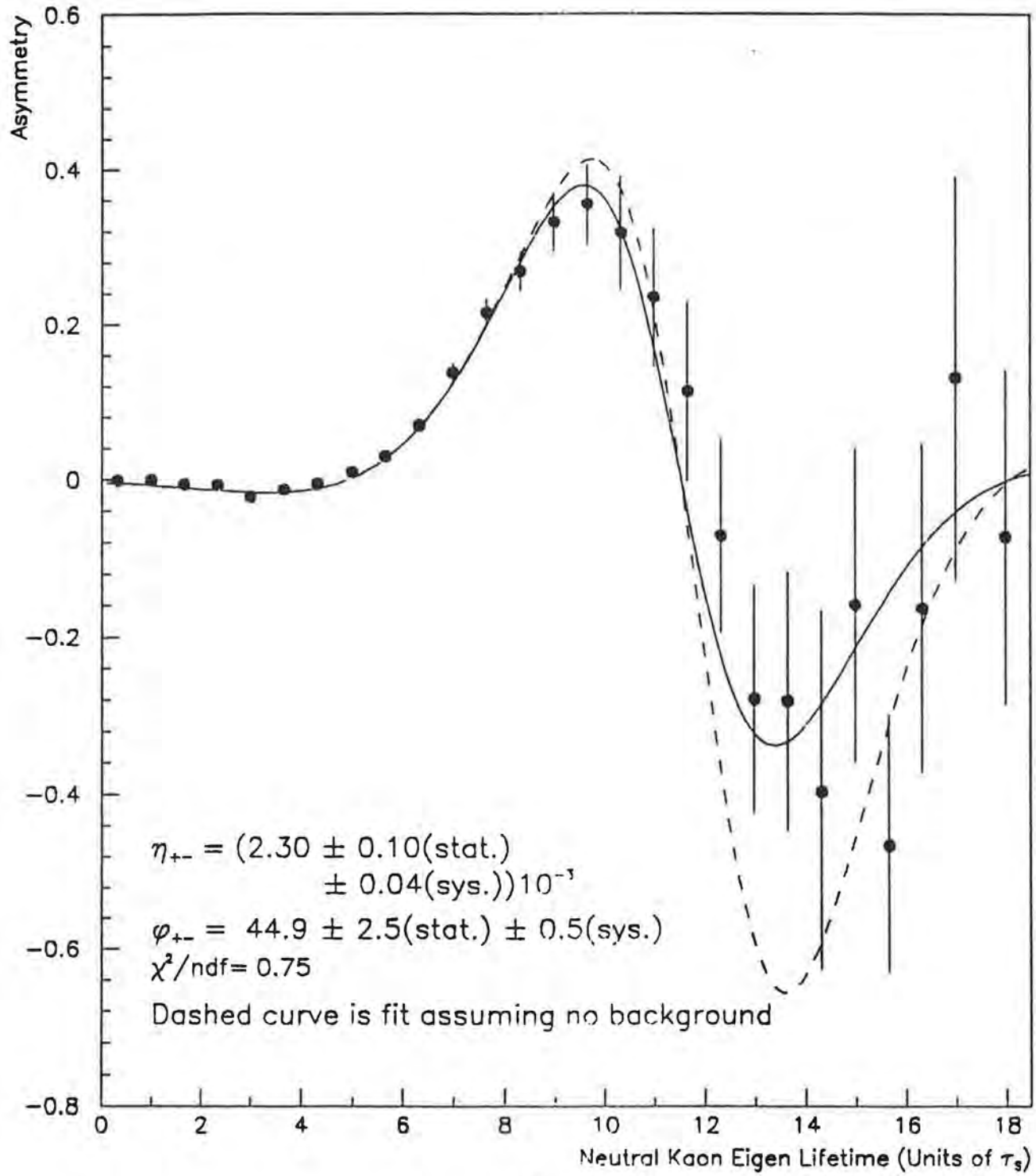
Asymmetry
0.6
0.4
0.2
0
−0.2
−0.4
−0.6
−0.8
0
2
4
6
8
10
12
14
16
18
Neutral Kaon Eigen Lifetime (Units of τ_S)
η_{+-} = (2.30 ± 0.10(stat.)
± 0.04(sys.))10^{-3}
φ_{+-} = 44.9 ± 2.5(stat.) ± 0.5(sys.)
χ^2/ndf= 0.75
Dashed curve is fit assuming no background

Figure 3.

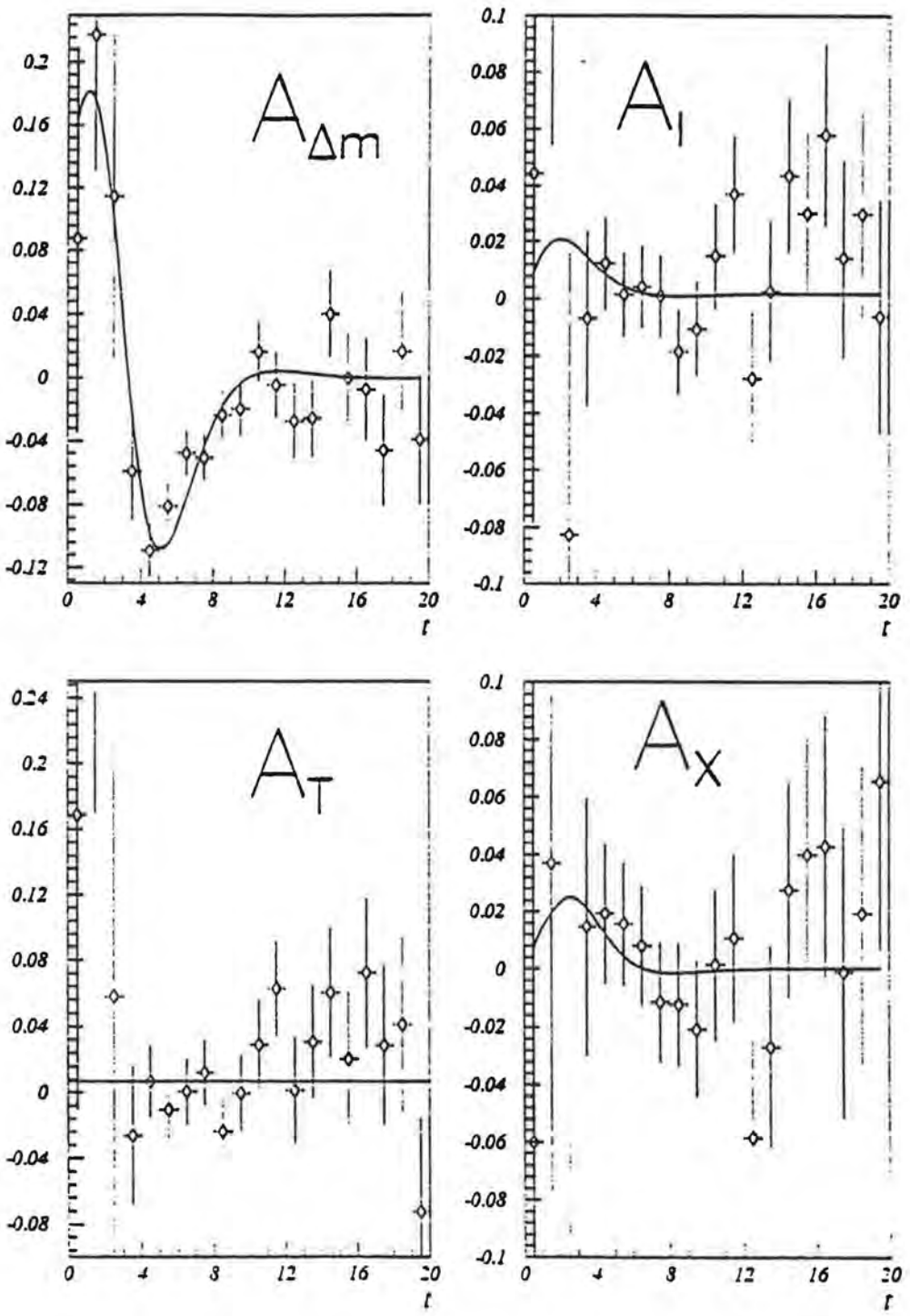

Figure 4.

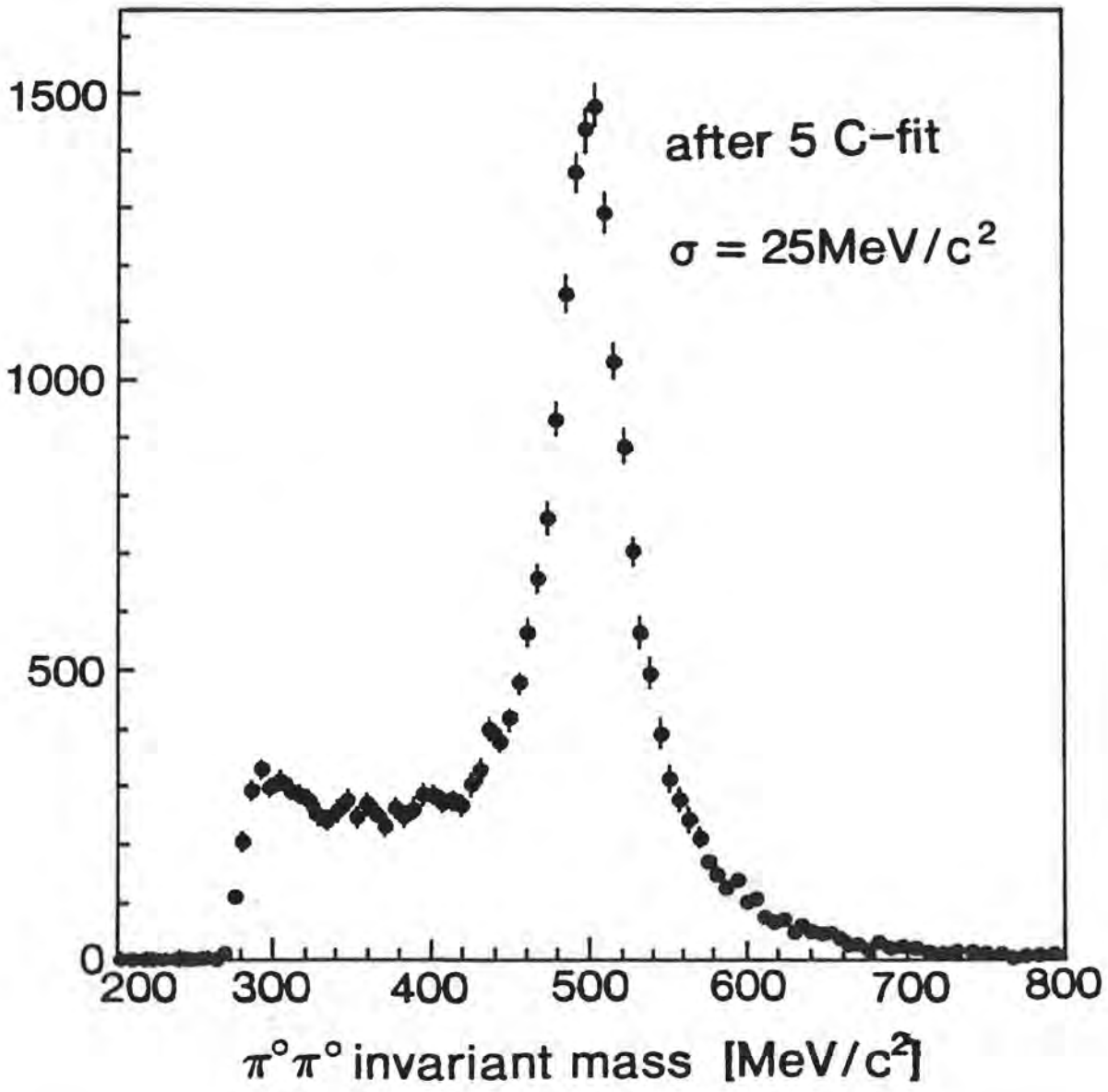
1500
1000
500
0
200
300
400
500
600
700
800
after 5 C-fit
σ = 25MeV/c²
π°π° invariant mass [MeV/c²]

Figure 5.

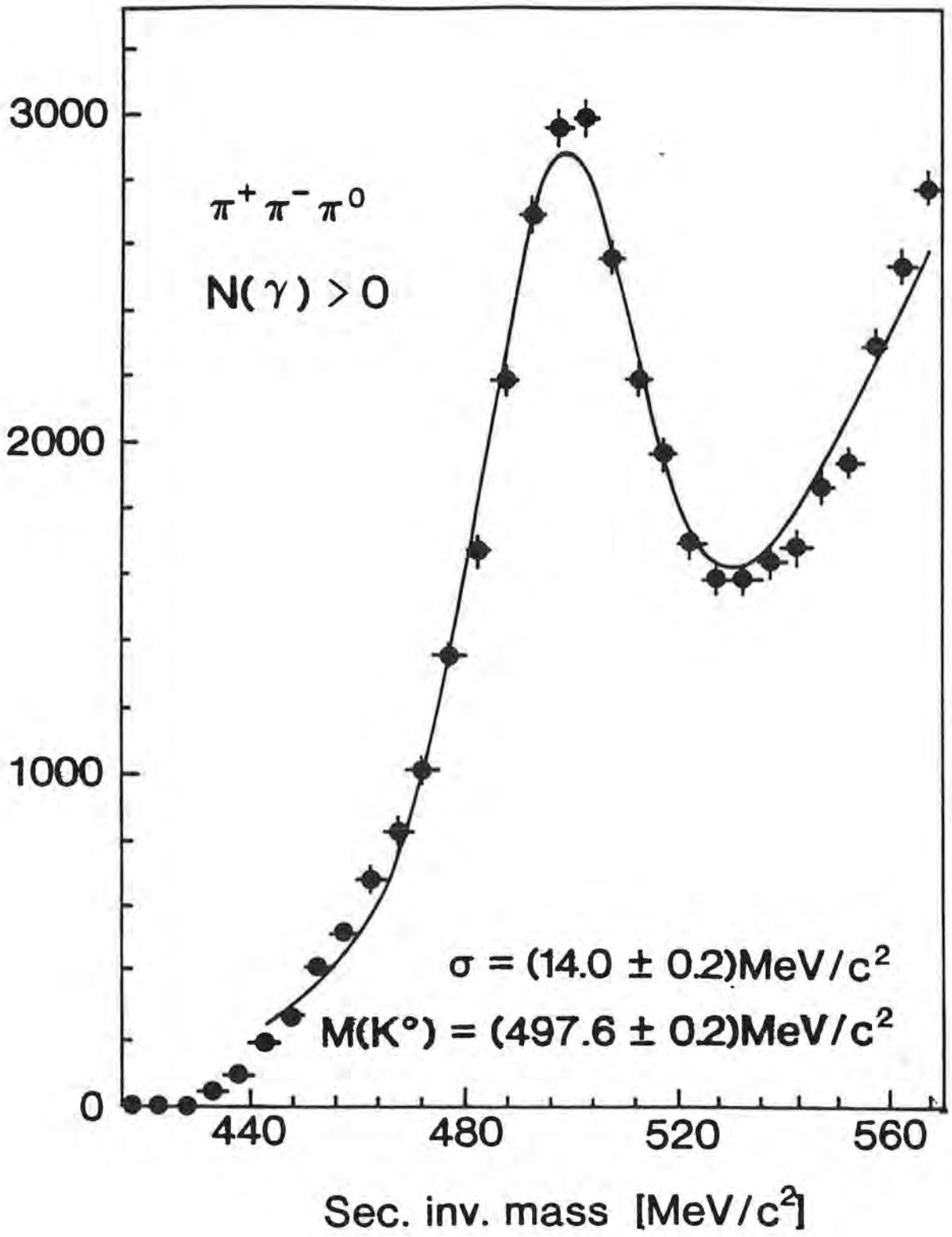
3000
2000
1000
0
$\pi^+\pi^-\pi^0$
N(γ) > 0
σ = (14.0 ± 0.2)MeV/c²
M(K°) = (497.6 ± 0.2)MeV/c²
440
480
520
560
Sec. inv. mass [MeV/c²]

Figure 6.

A. The weak radiative decay, $\Lambda \to n\gamma$ and the radiative kaon capture, $K^-p \to \Sigma(1385)\gamma$; B. π^-p interactions near threshold

Birmingham University, Boston University, Brookhaven National Laboratory,
Case Western Reserve University, KFKI Budapest, Nottingham University,
Oxford University, Triumf, University of New Mexico

A. The weak radiative decay, $\Lambda \to n\gamma$; Radiative capture, $K^-p \to \Sigma(1385)\gamma$

Running on these experiments, part of Brookhaven E811, finished in 1989 and all analysis is now complete. The last two papers have been submitted during the past year; one[1] has been published in Phys. Rev. Letters and the other[2] is in press in Physical Review.

B. Pion production near threshold and chiral symmetry breaking.

The experimental part of this work, Brookhaven E857, consisted of measurements of the reaction $\pi^-p \to \pi^0\pi^0 n$ near threshold. These were completed and published in 1990. Following this work, a global analysis of the world supply of data on $\pi N \to \pi\pi N$ reactions near threshold was carried out. The results of this have been published during the past year[3,4,5].

This work has been taken up again now that new data on $\pi^+p \to \pi^+\pi^0 p$ are emerging from the University of Virginia group. At present, only preliminary results from this group are available but they have already had a very significant effect on the analysis in that they have removed a puzzling ambiguity in the earlier fits.

The analysis of our data, together with the University of Virginia data on $\pi^+p \to \pi^+\pi^0 p$ to give $\pi\pi$ phase shifts across the σ-meson region is continuing.

References

1. A measurement of the $\Lambda \to n\gamma$ branching ratio, A.J. Noble, K.D. Larson, B. Bassalleck, W.J. Fickinger, J.R. Hall, A.L. Hallin, M.D. Hasinoff, D. Horvath, J. Lowe, E.K. McIntyre, D.F. Measday, J.P. Miller, B.L. Roberts, D.K. Robinson, M. Sakitt, M. Salomon, C.E. Waltham, T.M. Warner, D.A. Whitehouse and D.M. Wolfe, Phys. Rev. Lett. **69**, 414 (1992).

2. The weak radiative decay, $\Lambda \to n\gamma$; the radiative capture $K^-p \to \Sigma(1385)\gamma$ K.D. Larson, A.J. Noble, B. Bassalleck, H. Burkhardt, W.J. Fickinger, J.R. Hall, A.L. Hallin, M.D. Hasinoff, D. Horvath, J. Lowe, E.K. McIntyre, D.F. Measday, J.P. Miller, B.L. Roberts, D.K. Robinson, M. Sakitt, M. Salomon, C.E. Waltham, T.M. Warner, D.A. Whitehouse and D.M. Wolfe, submitted to Phys. Rev.

3. A global analysis of $\pi N \to \pi\pi N$ data, H. Burkhardt and J. Lowe, πN Newsletter no. 3, September 1991, ed. R.E. Cutkosky, G. Höhler, W. Kluge and B.M.K. Nefkens, p.43.

4. A global analysis of $\pi N \to \pi\pi N$ data, H. Burkhardt and J. Lowe, Phys. Rev. Lett. **67**, 2622

(1991).

5. Amplitudes for $\pi N \rightarrow \pi\pi N$ reactions, H. Burkhardt and J. Lowe, πN Newsletter no. 6, April, 1992, ed. R.E. Cutkosky, G. Höhler, W. Kluge and B.M.K. Nefkens, p.121.

Publications and conference contributions

The reaction $\pi^- p \rightarrow \pi^0\pi^0 n$ near threshold and chiral symmetry breaking, J. Lowe, B. Bassalleck, H. Burkhardt, W.J. Fickinger, J.R. Hall, M.D. Hasinoff, D. Horvath, G. Koch, K.D. Larson, J.P. Miller, A.J. Noble, B.L. Roberts, D.K. Robinson, M. Sakitt, M.E. Sevior, N.W. Tanner, C.E. Waltham, T.M. Warner and D.M. Wolfe, πN Newsletter no. 3, September 1991, ed. R.E. Cutkosky, G. Höhler, W. Kluge and B.M.K. Nefkens, p.47.

A global analysis of $\pi N \rightarrow \pi\pi N$ data, H. Burkhardt and J. Lowe, πN Newsletter no. 3, September 1991, ed. R.E. Cutkosky, G. Höhler, W. Kluge and B.M.K. Nefkens, p.43.

A global analysis of $\pi N \rightarrow \pi\pi N$ data, H. Burkhardt and J. Lowe, Phys. Rev. Lett. **67**, 2622 (1991).

Amplitudes for $\pi N \rightarrow \pi\pi N$ reactions, H. Burkhardt and J. Lowe, πN Newsletter no. 6, April, 1992, ed. R.E. Cutkosky, G. Höhler, W. Kluge and B.M.K. Nefkens, p.121.

A measurement of the $\Lambda \rightarrow n\gamma$ branching ratio, A.J. Noble, K.D. Larson, B. Bassalleck, W.J. Fickinger, J.R. Hall, A.L. Hallin, M.D. Hasinoff, D. Horvath, J. Lowe, E.K. McIntyre, D.F. Measday, J.P. Miller, B.L. Roberts, D.K. Robinson, M. Sakitt, M. Salomon, C.E. Waltham, T.M. Warner, D.A. Whitehouse and D.M. Wolfe, Phys. Rev. Lett. **69**, 414 (1992).

The weak radiative decay, $\Lambda \rightarrow n\gamma$; the radiative capture $K^- p \rightarrow \Sigma(1385)\gamma$ K.D. Larson, A.J. Noble, B. Bassalleck, H. Burkhardt, W.J. Fickinger, J.R. Hall, A.L. Hallin, M.D. Hasinoff, D. Horvath, J. Lowe, E.K. McIntyre, D.F. Measday, J.P. Miller, B.L. Roberts, D.K. Robinson, M. Sakitt, M. Salomon, C.E. Waltham, T.M. Warner, D.A. Whitehouse and D.M. Wolfe, Phys. Rev., in press.

Λ hyperon weak radiative decay, B. Bassalleck *et al.*, contribution to Baryons 92, Yale University, June 1992.

CRYSTAL BARREL EXPERIMENT

PS197 **PROPOSAL 268**

Queen Mary & Westfield College, London; Rutherford Appleton Laboratory; Lawrence Berkeley Laboratory; UCLA; University of Bochum; University of Budapest; CERN; University of Hamburg; University of Karlsruhe; University of Mainz; University of Munich; CRN Strasbourg; University of Zurich.

The main physics aim of the crystal barrel experiment is a detailed study of light quark spectroscopy with a particular emphasis on the search for glueballs, hybrids and multi-quark states produced in $\bar{p}p$ (and $\bar{p}n$) annihilations. Subsidiary aims are studies of radiative and rare meson decays and a study of $\bar{p}p$ annihilation dynamics from atomic S and P states.

The experiment is mounted at the LEAR facility, CERN and uses antiproton beams over the momentum range 0.2 to 2.0 GeV/c. Since many of the exotic states are expected to decay to neutrals such as π^0 and η, which then decay to γ's, good detection and measurement of photons over a large solid angle is essential. The apparatus is mounted inside a solenoidal magnet which gives fields up to 1.5 T. Antiprotons enter the apparatus along its symmetry axis and pass through beam defining and monitoring counters before entering the liquid hydrogen target. The target is surrounded by two cylindrical multiwire proportional chambers (PWC) which provide the trigger for outgoing charged particles. Surrounding these wire chambers is a cylindrical jet drift chamber (JDC) used to measure the momenta of outgoing charged particles; ionization sampling in the chamber can be used to discriminate between π's and K's for momenta below 500 MeV/c. Nearly all neutrals and charged particles are detected in a modular (1380 element), barrel shaped, CsI detector covering 97% x 4π solid angle.

The RAL group is responsible for the ADC and discriminator systems associated with the CsI detector and for the beam defining and veto counters. During 1992 the experiment had its first long data-taking run using 1.2 and 1.9 GeV/c antiprotons to study $\bar{p}p$ interactions in-flight. (Previous runs had mostly used 0.2 GeV/c beams to study $\bar{p}p$ interactions at rest). This required the provision of new 1 mm thick Si beam counters which were made specially for the experiment. Since less than 1% of the incident high energy beam interacts in the target, a high efficiency veto counter to identify annihilation events in the target was required and again this was developed at RAL.

A particular feature of the Crystal Barrel experiment is the availability of a fast on-line trigger on charged and neutral multiplicities and on the invariant mass of secondary particles. The PWC and JDC give the multiplicity of charged particles whilst a hardware fast cluster encoder (FACE) measures for each event the total multiplicity of clusters due to photons or charged tracks in the JDC crystals. A level 2 software trigger using the CsI crystal read-out microprocessor can also be used to calculate invariant masses of all possible $\gamma\gamma$ combinations. The software trigger can then select particular combinations of final state particles (π^0 and η) which decay to γ's.

As we have already mentioned, one of the physics motivations for the Crystal Barrel experiment is the search for glueballs (gg), exotic ($qq\bar{q}\bar{q}$) and hybrid mesons ($gq\bar{q}$). A possible candidate hybrid meson is the M(1405) 1^{-+} resonance which, because of its quantum numbers, cannot be a normal ($q\bar{q}$) meson or glueball. It has been observed to decay into $\pi^0\eta$, although the evidence for the resonance is not well established. In order to investigate such a potentially rare state a special software trigger was used by the QMW group to study the channel $\bar{p}p \to \pi^+\pi^-\eta$ at rest. The trigger for accepted events required between 3 and 5 clusters in the CsI barrel, 2 charged tracks in the PWC and JDC and that the $\gamma\gamma$ invariant mass should lie within a window around the η mass (549 MeV).

360K events were taken in less than 1 day of running. Figure 1 shows the $\gamma\gamma$ effective mass distribution of events passing the pre-selection criteria. The inset, using an expanded scale, shows the η peak with a mass resolution (σ) of 17 MeV/c^2. The lower mass peak is due to $\gamma\gamma$ combinations corresponding to the π^0. The observed rate of $\pi^+\pi^-\eta$ events is in reasonable agreement with the predictions of trigger studies. Kinematic fitting reduces the above sample to about 10K events. Figure 2 shows, for these events, a Dalitz plot distribution of the $\pi^-\eta$ effective mass versus the $\pi^+\eta$ effective mass. The strong diagonal band is due to $\rho\eta$, whilst the horizontal and vertical axes show the production of $a_0(980)$ and $a_2(1320)$ intermediate resonances decaying to $\pi^\pm\eta$. A partial wave analysis of the data will be carried out to investigate the possible existence of the M(1405) resonance.

The QMW group has also analysed data taken at an antiproton momentum of 1.2 GeV/c to study the channel $\bar{p}p \to \pi^+\pi^-\pi^0\eta$. Again a special trigger was used, but with rather loose cuts since the Crystal Barrel experiment had not previously run at high momenta and the detectors acceptance was not well understood. In addition photons produced by high energy π^0's may have such a small opening angle that the software trigger photon recognition routine sees just one photon. The trigger used selected two long tracks, 4 to 9 energy clusters in the crystals (including those produced by the charged tracks) and a wide energy window around the total energy deposited in the crystals for $\bar{p}p$ annihilations in flight.

Using the above trigger, 2M events were recorded. Of these 10K are expected to fulfil the requirements, including kinematic fitting, needed to identify the $\pi^+\pi^-\pi^0\eta$ channel. Figure 3 shows the effective mass plot for $\pi^+\pi^-\pi^0$ and has a clear peak at the ω mass (782 MeV) corresponding to the reaction

$$\bar{p}p \to \eta\,\omega \quad (\eta \to 2\gamma;\ \omega \to \pi^+\pi^-\pi^0 \to 2\gamma)$$

A reaction of particular interest is

$$\bar{p}p \to \pi^0 X \quad (X \to a_2^{\pm}(1320)\pi^{\mp} \to \pi^{\pm}\eta)$$

since for this decay process, X will give a signal with quantum numbers 2^{-+} which is allowed for both normal ($q\bar{q}$) mesons and glueballs. Figure 4 shows, for part of the data, the effective mass plot for $\pi^{\pm}\eta$ and has indications of a peak at 1320 MeV corresponding to the a_2 meson. Analysis of the complete data set for the reaction $\pi^+\pi^-\pi^0\eta$ at 1.2 GeV/c incident momentum is still in progress. Data for the same process at 1.9 GeV/c was taken during 1992 and analysis will again be carried out by the QMW group.

Publications

1 E Aker et al.
The Crystal barrel Spectrometer at LEAR
Preprint CERN-PPE/92-126
Nuclear Instruments and Methods **A321** (1992) 69.

2 C Amsler et al.
Proton-proton annihilation into $\eta\eta\pi$- observation of a scalar resonance decaying into $\eta\eta$
Preprint CERN-PPE/92-114
Physics Letters **B291** (1992) 347.

3 C Amsler et al.
The pseudoscalar mixing angle θ_{PS} from η and η' production in $\bar{p}p$ annihilations at rest
Preprint CERN-PPE/92-147
Physics Letters **B294** (1992) 451.

4 C Amsler et al.
P-versus S-wave $\bar{p}p$ annihilation in LH_2
Physics Letters (accepted for publication).

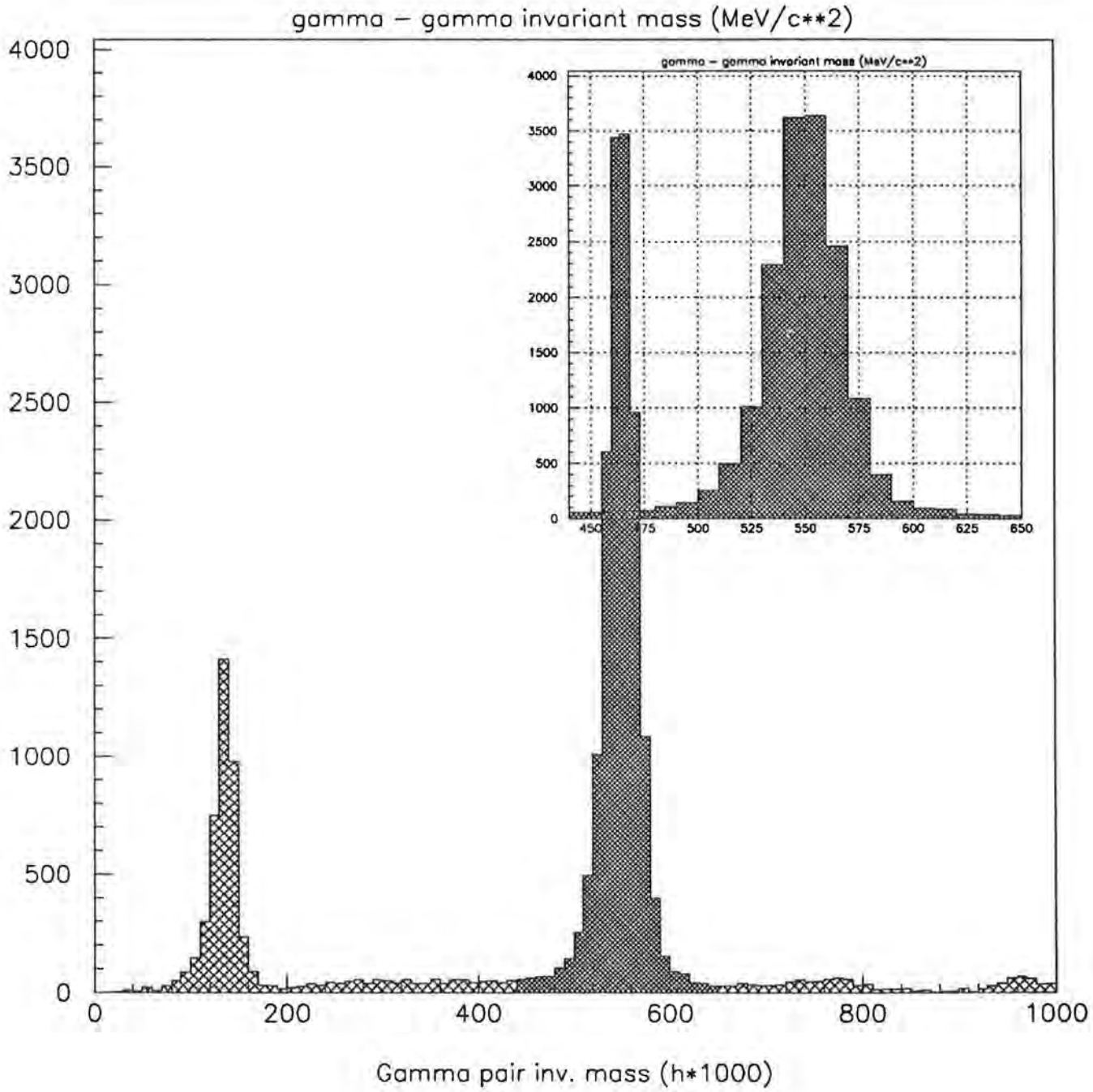

Figure 1 $\gamma\gamma$ effective mass distribution for $\pi^+\pi^-\gamma\gamma$ events obtained using a special trigger to select the reaction $\bar{p}p \rightarrow \pi^+\pi^-\eta$.

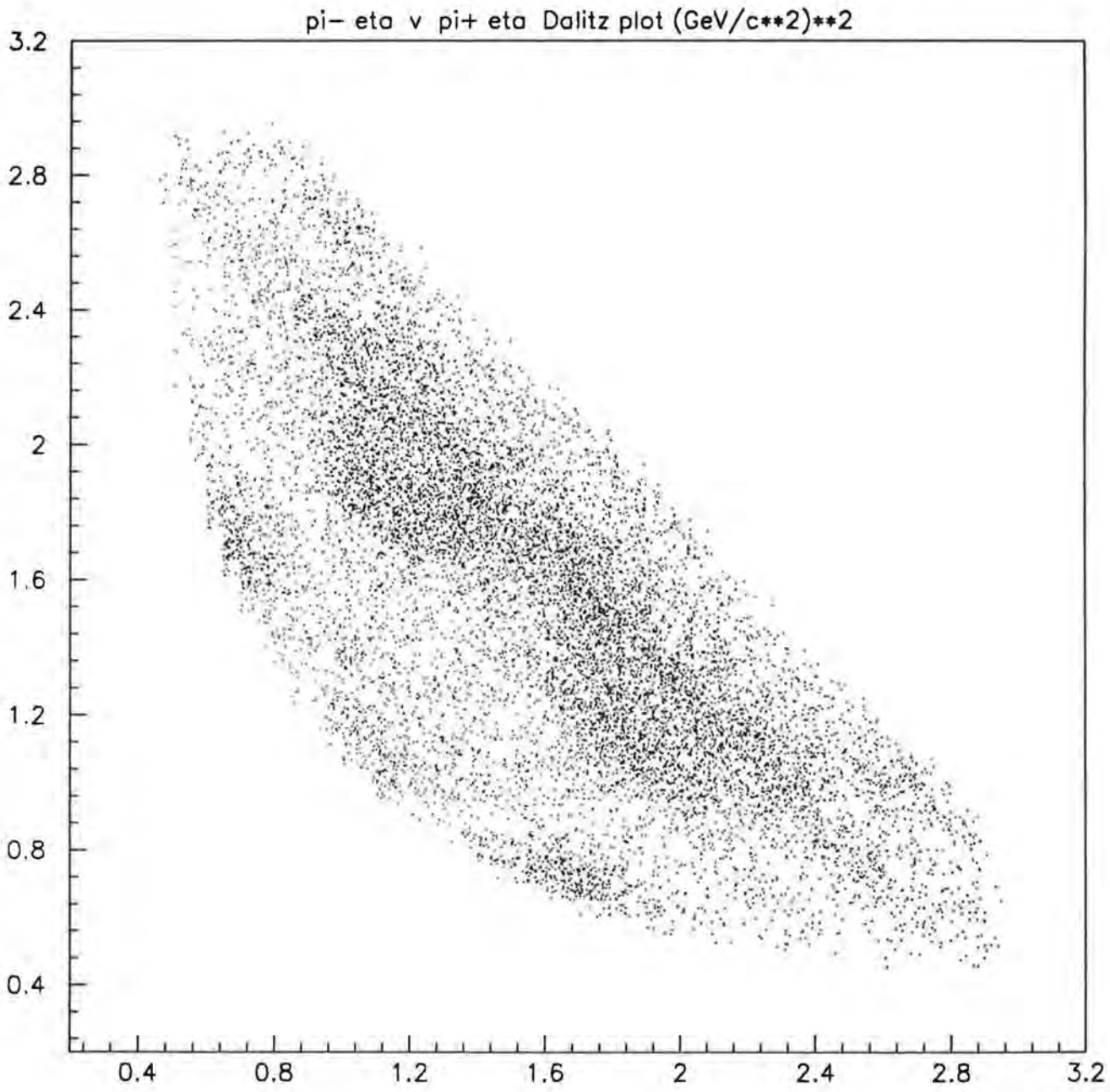

Figure 2 Dalitz plot distribution of $\pi^-\eta$ effective mass versus the $\pi^+\eta$ effective mass for $\pi^+\pi^-\eta$ events.

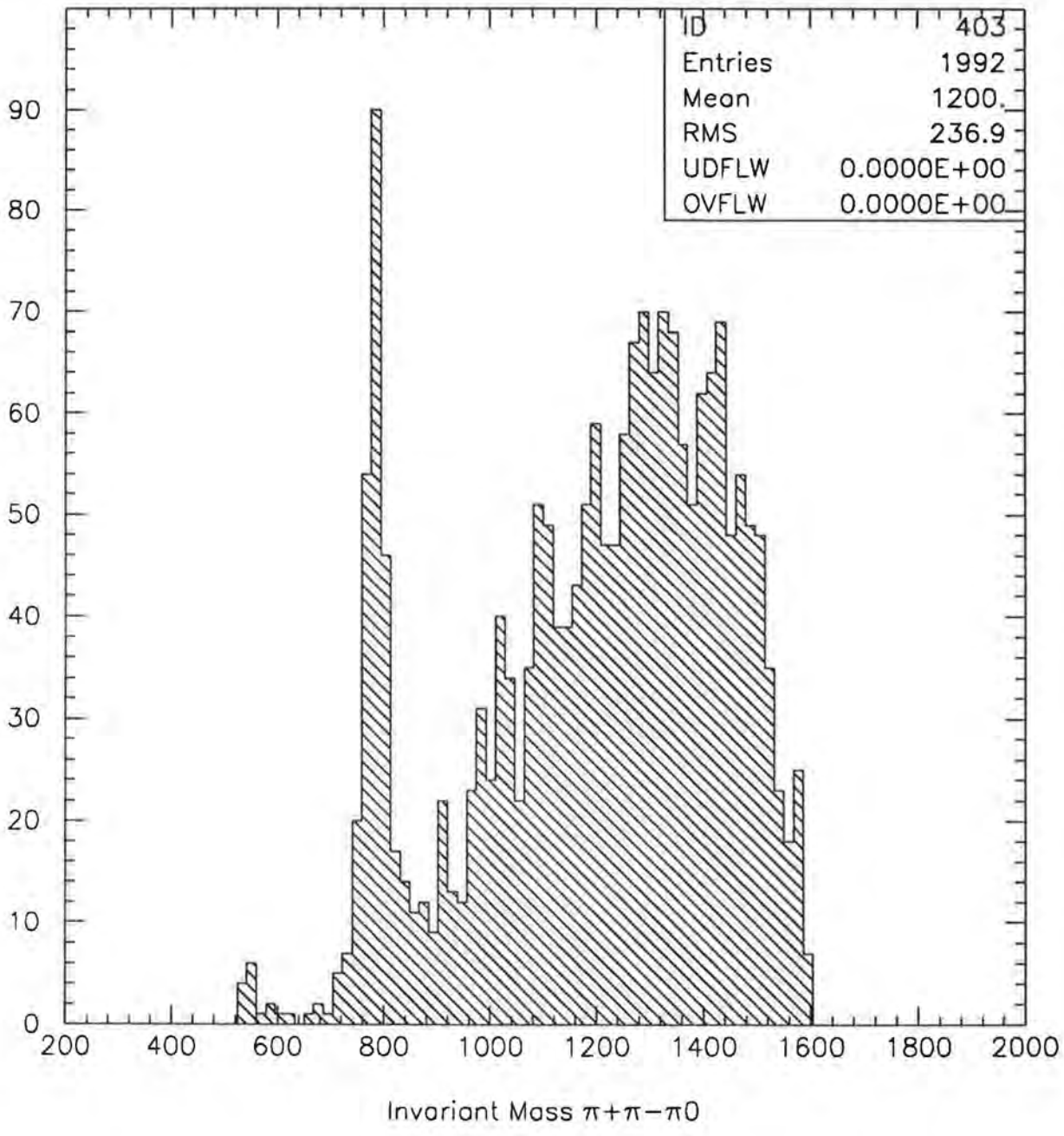

Figure 3 Effective mass plot of $\pi^+\pi^-\pi^0$ obtained for $\pi^+\pi^-\pi^0\eta$ events. The clear peak at the ω mass (782 MeV) corresponds to the reaction $\bar{p}p \rightarrow \eta\omega$.

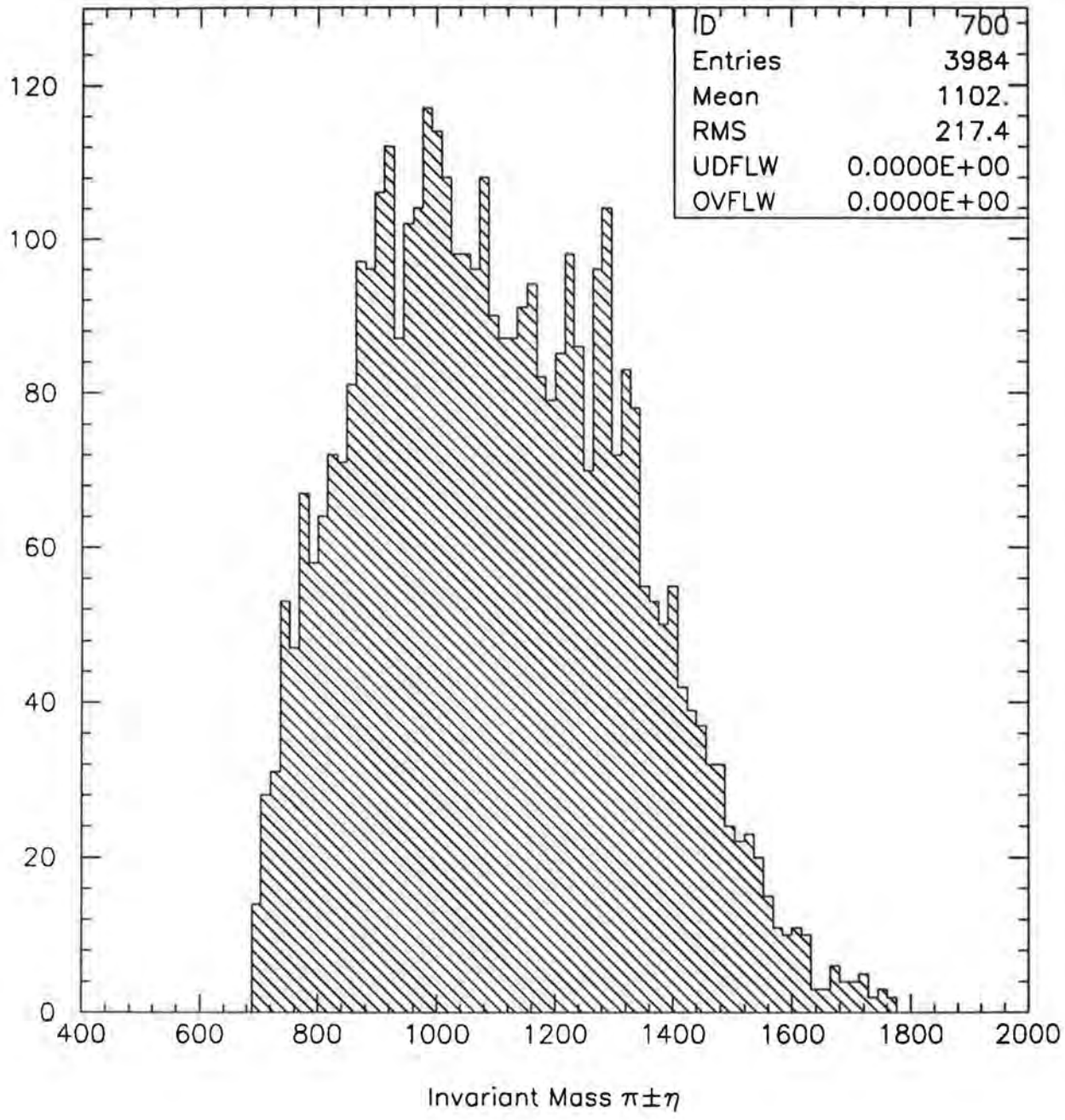

Figure 4 Effective mass plot of $\pi^{\pm}\eta$ obtained for $\pi^+\pi^-\pi^0\eta$ events. The indications of a peak at 1320 MeV correspond to production of the a_2 meson, (see text).

DARK MATTER EXPERIMENTS

Proposal 270

Particle Physics/ Astrophysics / Low Temperature Physics collaboration
Imperial College London (Astrophysics, Particle Physics, Solid State Physics)
Birkbeck College London (Cosmic Ray Physics)
University of Nottingham (Cosmic Ray Physics, Low Temperature Physics)
Royal Holloway and Bedford New College (Low Temperature Physics)
Oxford (Astrophysics)
RAL (Particle Physics, Astronomy, Technology)

A major unresolved problem at the interface of particle physics and cosmology is the identity of the "dark matter" which is known to comprise 90% of the mass of our own Galaxy and up to 99% of the universe as a whole. There is also evidence that the dark matter may be non-baryonic, and could thus consist of relic stable elementary particles. Candidate particles include non-zero mass neutrinos, axions, or hypothetical new heavy particles such as the photino.

An experimental programme to investigate the heavy particle hypothesis is now funded jointly by NP and APS Boards. The experiments will search for nuclear recoil events from the interactions of dark matter particles, either by the resulting ionization or from the thermal pulses produced in targets operating at very low temperature. The nuclear recoil events would be in the 1-100keV energy range, and the planned experiments will be sensitive to event rates of order 0.1-10/day/kg.

To eliminate neutron background from cosmic ray muons, the experiments will be carried out in a cavern (Fig 1) at a depth of 3000mwe in a salt mine at Boulby (near Whitby, UK). Further shielding from radioactivity in the cavern walls has been provided by means of a 6m diameter tank of pure water, in which several detector systems can be suspended (Fig 1). Installation of this tank is now complete together with associated water purification equipment and other underground facilities (Fig 2).

Initial experiments will be based on scintillation and ionization detectors using target materials with nuclear spin (for sensitivity to axially-coupled particles). First detectors have been based on the materials NaI and GaAs. During 1992, attempts to set up a sodium iodide detector in the low background underground environment were delayed by engineering problems with the water shielding system and by the presence of small quantities of radioactive cement in the crystal assemblies supplied by Harshaw. These problems are now fully diagnosed and the first low background detector tests are expected by the end of 1992.

As a second stage, it is planned to achieve sensitivity to very low event rates (1–10/day) by new detectors capable of discriminating between nuclear recoil events and electron recoil events (from background photons and beta decay in the target). The first under construction is a liquid xenon detector, capable of discrimination through the differences in light pulse decay time. At energies as low as 10–100keV, this involves working at the level of only a few photons and analysis of their arrival times. A second possibility is the use of undoped sodium iodide at a temperature of 100K, where both uv and visible light contribute to the signal, but in different proportions for nuclear recoil events. Both of these new techniques are unique to the UK programme.

Recent publications

Demonstration Of nuclear recoil discrimination by measurement of ionization/thermal energy ratio in a low temperature Si target
N J C Spooner et al., Phys. Lett. B273 (1991) 333

Investigation of voltage amplification of thermal spectra in a low temperature calorimetric detector.
N J C Spooner, G J Homer, P F Smith, Phys Lett B278 (1992) 382

The race to detect dark matter
N Hall, P F Smith, New Scientist 134 (1992) 37

GaAs ionization detectors and their application to dark matter searches
N J C Spooner et al., Proc Int workshop on GaAs detectors in HEP (Erice 1992)

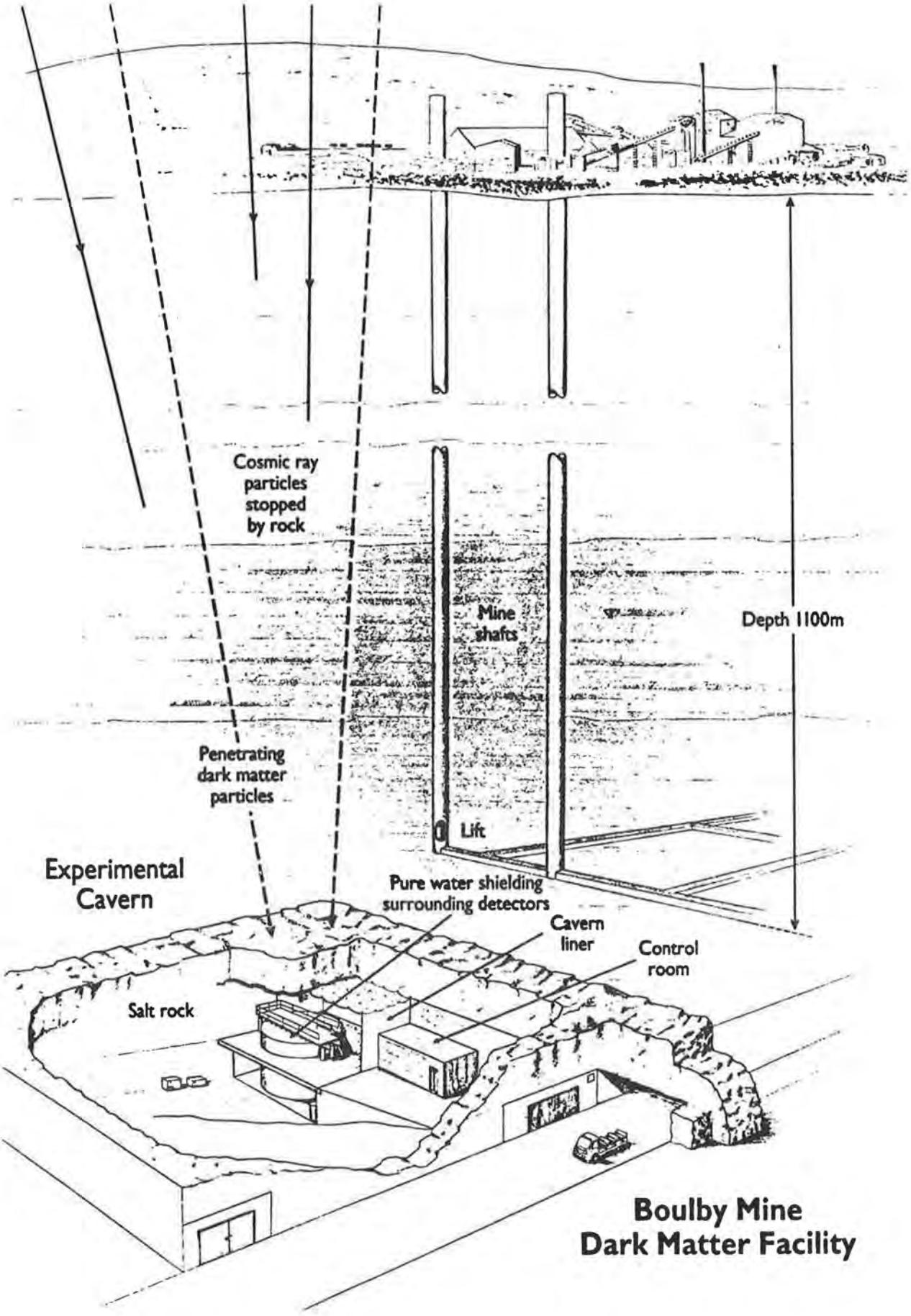

Fig 1 Artists impression of Boulby Mine dark matter facility

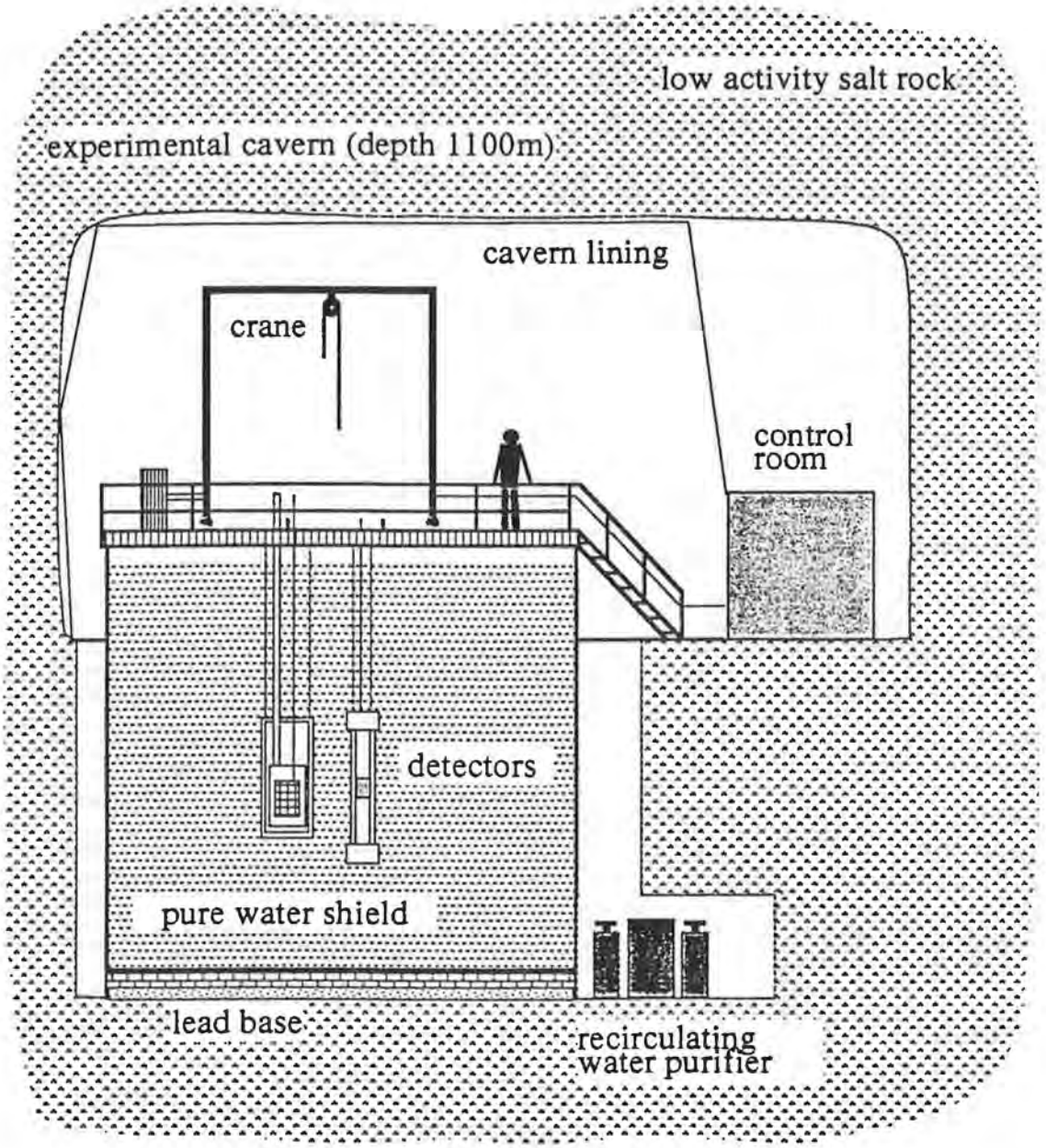

Fig 2. Arrangement of water shielding facility in underground cavern

Development of a Scintillating Optical Fibre Microvertex Detector for Beauty Particle Studies

WA84 **Proposal 271**

CERN; JINR; IHEP; Imperial College; Pisa; RAL; Rome; Southampton

This project concerns an R&D study of particle tracking using bundles of scintillating fibres (SCIFI).

During the last few years we have tested SCIFI devices based on bundles of 30,000 - 100,000 fibres, where each fibre has a diameter of 15 - 30 μm. The typical bundle cross-section is 5x5 mm^2 and its length between 40 and 500 mm.The fibres were tested in charged particle beams where images of the tracks were recorded using an optoelectronic chain followed by a charged coupled device (CCD) equipped with ADC read-out. Measurements were made of the parameters relevant to the specific application as a vertex detector for short-lived particles.

Three different types of SCIFI have been tested:

1. Cerium doped glass fibres.
2. PMP (1-phenyl-3-mesityl-2-pyrazodine) doped plastic fibres.
3. Glass capillaries filled with liquid scintillators.

1. The glass fibres were drawn with a core of GS1 glass containing cerium oxide which is tolerant to radiation doses ~ 10^4Gy. Cross-talk between fibres is eliminated using extra-mural absorber (EMA) which surrounds each fibre. The presence of long lived components in the scintillation emission time restricts their use to low rate applications, furthermore the light attenuation is severe (attenuation length λ ~ 20 mm), resulting in a low light output ~0.6 hits/mm after propagation over 20 mm in the fibre.

2. The plastic fibres had cores of polystyrene doped with PMP. Their radiation hardness is somewhat lower than GS1 (~10^3 Gy) but the light output was fast (~3 ns). The attenuation was greatly reduced compared with GS1 and a light output ~2 hits/mm was obtained. However, no technique of incorporating EMA into the structure without degrading this light output could be developed. Without EMA the cross-talk between fibres contributes noise comparable with the track signal.

3. Glass capillaries of 20 - 25μm bore with 2μm thick walls are now available in 1m lengths. Filled with liquid organic scintillators these combine the best features of 1. and 2. above. Time response and light attenuation are similar to plastic SCIFI, while insertion of black glass fibres between capillaries eliminates cross-talk. A dose of 10^6 Gy results in a factor two loss in light yield. With 20μm capillaries a spatial precision of σ ~ 12μm was obtained. The attenuation length is λ ~ 20 cm for distances < 10 cm where hit densities of 5 hits/mm were obtained. For distances > 20 cm, λ ~ 80 cm was measured.

Thus the capillaries are fast, precise and radiation hard. The hit density corresponds to 2x10^3 hits per unit of radiation length which compares favourably with that obtained using other types of high spatial precision tracking detectors.

WA84 - Publications 1991 - 92

1. "Application of a scintillating-fibre detector to the study of short-lived particles"
   Nucl. Instr. and Methods A310 (1991) 485 - 489

2. "A high-resolution tracking detector based on capillaries filled with liquid scintillator"
   Nucl. Instr. and Methods A311 (1992) 91 - 97

3. "Use of a high-resolution, scintillating-fibre, tracking detector in recording π -nucleon interactions at $\sqrt{s}$ = 26 GeV"
   Nucl. Instr. and Methods A315 (1992) 67 - 73

4. "Progress on high-resolution tracking with scintillating fibres: a new detector based on capillaries filled with liquid scintillator"
   Nucl. Instr. and Methods A315 (1992) 177 - 181

Studies of Heavy Ion Collisions

NA34/P213/EMU 09 **Proposals 273, 278**

Aichi College - Aichi University - Bari - CERN - University College, Dublin - Gifu - University College London - Nagoya University - Nagoya Institute - Roma - Salerno - Toho - Torino - Utsonomiya - Yokohama.

The initial exploratory study of heavy ion collisions (experiment NA34) has been completed. The main thrust of this experiment was an attempt to identify the onset of quark-gluon plasma formation in central heavy ion collisions with nuclei by locating and analysing in nuclear emulsions events exhibiting features such as high transverse energy flow in the downstream Helios calorimeters. As with other experiments no unequivocal evidence for quark-gluon plasma formation was found, the results obtained being well explained by the superposition of many nucleon-nucleon interactions at high energy.

A detailed study of a randomly selected sample of interactions in emulsion was also made and the extent of projectile fragmentation and target fragmentation, and shower multiplicities was recorded. The correlations between these features were as expected from a simple geometrical model.

The important contribution of electromagnetic dissociation to the total cross section was established and cross sections for exclusive channels of projectile break-up (with no isotope separation) were measured and compared to those obtained in real photodisintegration experiments.

The earlier apparent anomaly that our results indicated much larger than expected electromagnetic (γ,α) cross sections for both ^{16}O and ^{32}S projectiles was explained, at least in the case of the oxygen sample, by establishing that the origin of the majority of these events was an hadronic diffraction process.

The run of the CERN experiment EMU 09 and the necessary initial calibration procedures have been completed. In this experiment it is hoped to determine the variation of the total and exclusive channel EMD cross sections for ^{32}S projectiles using a variety of foil targets, namely Ag, Cu and Pb. A total of 100 modules with a variety of targets and foil thicknesses were exposed to the 200 GeV A ^{32}S beam. Each of these consisted of CR39 plastic detectors placed fore and aft of the target foil-emulsion assembly which were used to select those events in which the charge of the incident projectile is reduced in transit. An emulsion plate immediately beyond the target foil enables nuclear and electromagnetic interactions in the foil to be separated. Further emulsion plates allow the angular separation of the tracks and their curvature in a magnetic field of induction of 2.5T to be determined, such that discrimination between hydrogen and helium isotopes among the projectile fragments may be made.

The analysis both of the etch pits in the CR39 detectors and of events in emulsion is underway but progress at present is slow.

However, provided the areas of the etch pits are calibrated locally to those of beam particles, measurements of a single etch pit are sufficient to discriminate easily charges of various ions in the region of ^{32}S (Z=16).

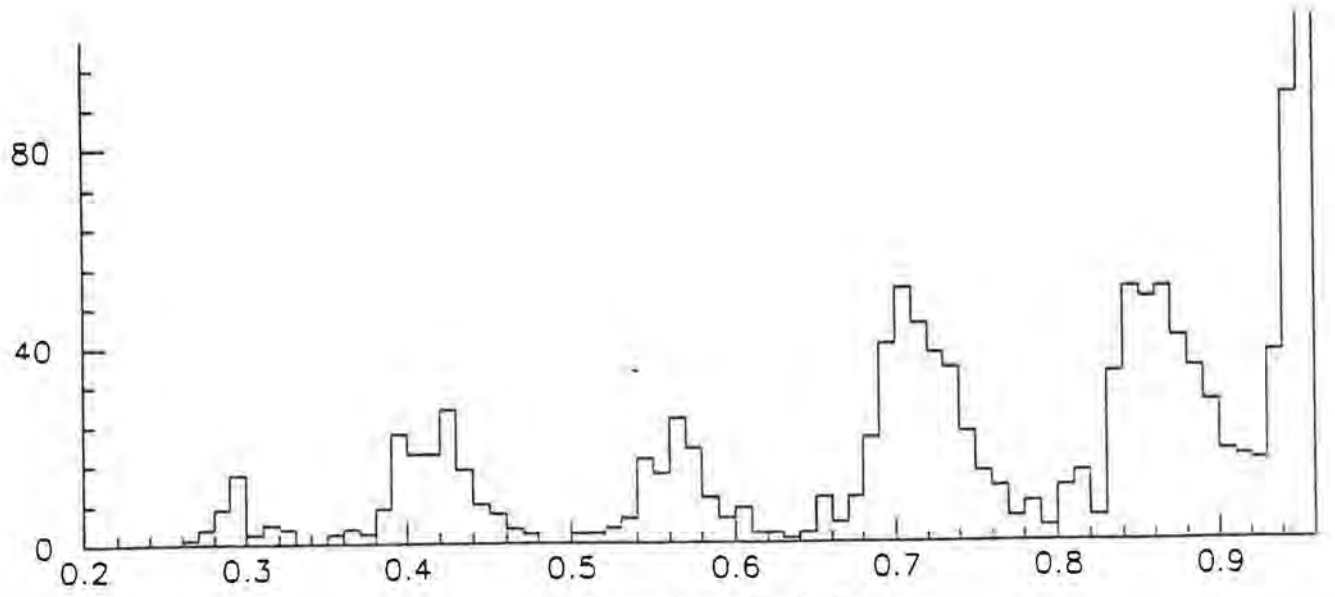

Fig 1

Fig 1 clearly shows peaks for ions with Z in the range 15 to 11, the huge peak for beam particles is not shown, being at a normalized pit area of 1.0.

Measurements made in emulsion have shown that protons may be clearly distinguished from other hydrogen isotopes but separation of deuterons from tritons is more problematical.

Publications

1. The production of charmed particles in high energy ^{16}O - emulsion central interactions. Physics Letters B224 441 (1989).

2. An emulsion study of ^{16}O and ^{32}S interactions at 200 GeV per nucleon selected by transverse energy. Nuclear Physics B342 279 (1990).

3. Electromagnetic dissociation of 200 GeV/N ^{16}O and ^{32}S ions in nuclear emulsions. Nuclear Physics A516 67 (1990).

4. A search for multiplicity fluctuations in high energy nucleus-nucleus collisions. Physics Letters B252 303 (1990).

5. Interactions of 200 GeV/nucleon ^{16}O and ^{32}S ions in nuclear emulsions. Nuclear Physics A531 691 (1991).

6. The electromagnetic and hadronic diffractive dissociation of ^{16}O ions. Nuclear Physics A540 646 (1992).

Ph.D. thesis - University of London (1992) - Simon K.C. Yuen. A study of the interactions of 200 A GeV ^{16}O and ^{32}S ions in nuclear emulsion.

WA85/WA94 **Proposal 275**

Athens; Bari; Bergen; Birmingham; CERN; Kosice; Legnaro; Madrid; Padova;
Paris; Serpukhov; Strasbourg; Trieste

Hyperon production is expected to be a useful probe of the dynamics of hadronic matter under the extreme conditions realised in central heavy ion collisions [1]. In particular, the onset of a Quark-Gluon Plasma (QGP) phase during the collisions is expected to enhance the antihyperon yield with respect to normal hadronic interactions and to give rise to a large $\overline{\Xi^-}/\overline{\Lambda}$ ratio [2]. WA85 is the only experiment which has obtained results on the production of cascades in heavy ion interactions.

The WA85 experiment [3] was performed using the CERN Omega Spectrometer with a 200 GeV/c per nucleon beam of ^{32}S ions incident on a tungsten target. The aim is to study strangeness production at $p_T > 1$ GeV/c and central rapidity. The Omega multiwire proportional chambers were modified to select only high p_T tracks so that only a few tracks are recorded out of the several hundred produced in a central collision, making reconstruction of both strange and multi-strange baryons possible in this kinematic region. The apparatus and trigger, which select central collisions, have been discussed previously [4].

The method of reconstructing Λ[4] and Ξ^- [5] decays has already been described. Fig. 1 shows a fully reconstructed $\overline{\Xi^-}$ candidate, and Fig. 2 shows the mass distributions for Λ, $\overline{\Lambda}$, Ξ^- and $\overline{\Xi^-}$candidates from our 1987 S W data (10 million triggers). We see clear peaks with little background at both Λ and Ξ^- masses and select Λ candidates in a 50 MeV mass interval centred on the Λ mass, giving 13,307 Λ and 3,407 $\overline{\Lambda}$ candidates, and Ξ^- candidates in a 100 MeV mass interval centred on the Ξ^- mass, giving 108 Ξ^- and 44 $\overline{\Xi^-}$ candidates. The full phase space window used for Λs and $\overline{\Lambda}$s is $2.3 < y_{lab} < 3.0$ and $0.9 < p_T < 2.8$ GeV/c; for Ξ^-s and $\overline{\Xi^-}$s it is $2.3 < y_{lab} < 3.0$ and $1.1 < p_T < 3.3$ GeV/c.

The Λ and $\overline{\Lambda}$ candidates include K^0_S contamination, which is around 7% for Λs and 27% for $\overline{\Lambda}$s. For this study [6] we select only unambiguous decays ($\cos\theta^* < -0.5$) leaving us with 5,865 Λs and 1,138 $\overline{\Lambda}$s. V^0s and cascades are then corrected for geometrical acceptance, decays outside the fiducial region, unseen decay modes and reconstruction efficiencies.

Particles from a thermal source, in a narrow rapidity window, are expected to have a transverse mass distribution given by [7]

$$\frac{1}{m_T}\frac{dN}{dm_T} \approx e^{-\beta m_T} \qquad (1)$$

where β is the inverse temperature of the source and m_T is the transverse mass ($m_T = \sqrt{p_T^2 + m^2}$). In order to study m_T distributions, we choose the narrow rapidity interval $2.4 < y_{lab} < 2.6$. The acceptance, integrated over p_T, varies little in this interval. Fig. 3 shows the invariant m_T distributions in S W interactions for Λ, $\bar{\Lambda}$, Ξ^- and h^-. Here, in addition to corrections for acceptance and reconstruction efficiency, the Λ and $\bar{\Lambda}$ distributions have also been corrected for feed-down from Ξ and $\bar{\Xi}$ decay [6]. The inverse slopes obtained from the distributions in Fig. 3, and for K^0_s[8], are all compatible with a temperature of about 230 MeV. Preliminary results for p W interactions [8] give similar slopes, and for all the species considered indicate an increase by a factor of about two in the ratio of strange particle to negative particle production in S W relative to p W interactions.

Once corrections have been made to particle production rates to allow for acceptance, reconstruction efficiency, particle identification and feed-down, it is possible to compare production rates for the hyperons and antihyperons. The hyperon-antihyperon ratios $\bar{\Lambda}/\Lambda$ and $\bar{\Xi}^-/\Xi^-$ are straightforward to calculate. However, the value obtained for the Ξ^-/Λ ratio depends on whether a cut is made in p_T or m_T owing to the different rest masses for Ξ and Λ. In Table 1, we present the ratios in terms of an m_T cut, and in the p_T range $1 < p_T < 2$ GeV/c in order to facilitate comparison with other experiments. In addition, a preliminary $\bar{\Xi}^-/\Xi^-$ ratio in p W collisions of 0.27 ± 0.06 has been reported [9]. The $\bar{\Xi}/\Xi$ ratio appears to be higher in S W than in p W, and the $\bar{\Xi}/\bar{\Lambda}$ ratio appears high in comparison with all other published values (from e^+e^-, $\bar{p}p$ and pp interactions) as shown in Fig. 4. All these results point towards a significant degree of flavour equilibration at a temperature (taken from the inverse slope of the m_T distributions) close to that which a phase transition is expected to occur.

In 1990 80 million S W and 100 million p W events were recorded. Preliminary mass distributions for Λ and cascade candidates are shown in Fig. 5 for the S W data.

The continuation of the experiment, under the new CERN experiment number WA94[10], uses a sulphur target. In 1991 100 million S S events were obtained and analysis is in progress. p W data will be taken in 1993 for comparison.

A different configuration will be used to measure protons and antiprotons and a microstrip telescope will provide good momentum resolution. Charged tracks will be traced through the telescope and the MWPCs to the upgraded Omega RICH, which will be used for particle identification. A set of MWPCs placed behind the RICH will be used to give good position accuracy for the ring centres corresponding to tracks traced from the microstrip telescope. Several precautions have been taken (raising the principal axis of the RICH above the beam line, providing an iron shield with an aperture between the RICH and the Omega magnet, and masking off part of the RICH mirror) in order to avoid an excessive number of hits in the RICH TPCs. These are described in detail elsewhere [10]. Data was successfully taken in 1992 and analysis is in progress.

References

[1] J. Rafelski and B. Müller, Phys. Rev. Lett. 48 (1982) 1066; 56 (1986) 2334.
P. Koch, B. Müller, and J. Rafelski, Phys. Rep. 142 (1986) 167.
J. Ellis and U. Heinz, Phys. Lett. 233B (1989) 223.

[2] J. Rafelski, Phys. Lett. 262B (1991) 333.

[3] WA85 Proposal, A. Apostolakis et al., CERN/SPSC 84-76, SPSC/P206 (1984) and CERN/SPSC 87-18, SPSC/P206 Add.1 (1987).

[4] S. Abatzis et al., Phys. Lett. 244B (1990)130.

[5] S. Abatzis et al., Phys. Lett. 259B (1991) 508.

[6] S. Abatzis et al., Phys. Lett. 270B (1991) 123.

[7] J. Rafelski, GSI-90-37 July 1990.

[8] S. Abatzis et al., Proc. Int. Europhysics Conf. on High Energy Physics, 466, Geneva 1991.
S. Abatzis et al., Proc. Quark Matter 1991, Gatlinburg, November 1991, presented by J.B. Kinson.

[9] S. Abatzis et al., Nucl. Phys. A525 (1991) 441c.

[10] WA94 Proposal, S. Abatzis et al., CERN/SPSLC 91-57 P 257 (1991).

Table 1: Summary of relative hyperon production rates in S W interactions.

Ratio	$m_T > 1.72$ GeV	$1 < p_T < 2$ GeV/c
$\overline{\Lambda}/\Lambda$	0.13 ± 0.03	0.13 ± 0.03
$\overline{\Xi^-}/\Xi^-$	0.39 ± 0.07	0.39 ± 0.07
Ξ^-/Λ	0.20 ± 0.04	0.11 ± 0.02
$\overline{\Xi^-}/\overline{\Lambda}$	0.60 ± 0.20	0.33 ± 0.11

Publications (October 1991 to September 1992)

1. Ξ^-, $\overline{\Xi^-}$, Λ and $\overline{\Lambda}$ production in sulphur-tungsten interactions at 200 GeV/c per nucleon.
R.P. Barnes, I.J. Bloodworth, J.N. Carney, D. Evans, J.B. Kinson, O. Villalobos Baillie, M.F. Votruba; with Athens, Bari, Bergen, CERN, Paris and Trieste.
Phys. Lett. 270B, 123-127 (1991)

2. Strange (anti)baryon and K^0 production in central ^{32}S-W interactions at 200 GeV/c per nucleon.
R.P. Barnes, I.J. Bloodworth, J.N. Carney, D. Evans, J.B. Kinson, O. Villalobos Baillie, M.F. Votruba; with Athens, Bari, Bergen, CERN, Paris and Trieste.
Proc. Europhysics Conference on High Energy Physics, 466-469. Geneva, July 1991.

3. WA85 results on strangeness production in heavy ion collisions.
R.P. Barnes, I.J. Bloodworth, J.N. Carney, D. Evans, J.B. Kinson, O. Villalobos Baillie, M.F. Votruba; with Athens, Bari, Bergen, CERN, Paris and Trieste.
Physics and Applications, **16**, 94-105 (1991).

4. Recent results from the CERN WA85 experiment on strangeness production in sulphur-tungsten interactions.
R.P. Barnes, I.J. Bloodworth, J.N. Carney, D. Evans, J.B. Kinson, O. Villalobos Baillie, M.F. Votruba; with Athens, Bari, Bergen, CERN, Paris and Trieste.
Proc. Int. Symposium on High Energy Nuclear Collisions and Quark Gluon Plasma, Kyoto, Japan, 77-84, June 1991.

5. Strange particle production in sulphur-tungsten interactions at 200 GeV/c per nucleon.
R.P. Barnes, A.C. Bayes, I.J. Bloodworth, J.N. Carney, D. Evans, J.B. Kinson, O. Villalobos Baillie, M.F. Votruba; with Athens, Bari, Bergen, CERN, Paris and Trieste.
Proc. Quark Matter 1991, Gatlinburg, Tennessee, November 1991, presented by J.B. Kinson.

6. Strange particle production in relativistic heavy ion interactions.
J.B. Kinson.
Proc. Int. Conf. on Quark Matter and the Heavy Ion Collisions, Dera Ismail Khan, January 1992.

7. Production of strange and multistrange particles in sulphur-tungsten interactions at 200 GeV/c per nucleon.
R.P. Barnes, A.C. Bayes, I.J. Bloodworth, J.N. Carney, D. Evans, J.B. Kinson, O. Villalobos Baillie, M.F. Votruba; with Athens, Bari, Bergen, CERN, Paris and Trieste.
Proc. 27th Rencontres de Moriond, Les Arcs., March 1992, presented by R.P. Barnes.

8. Review of results from WA85.
R.P. Barnes, A.C. Bayes, I.J. Bloodworth, J.N. Carney, D. Evans, J.B. Kinson, O. Villalobos Baillie, M.F. Votruba; with Athens, Bari, Bergen, CERN, Paris and Trieste.
Proc. Hadron Structure 92, Stara Lesna, September 1992, presented by D. Evans.

Thesis

D. Evans (PhD Birmingham, 1992).

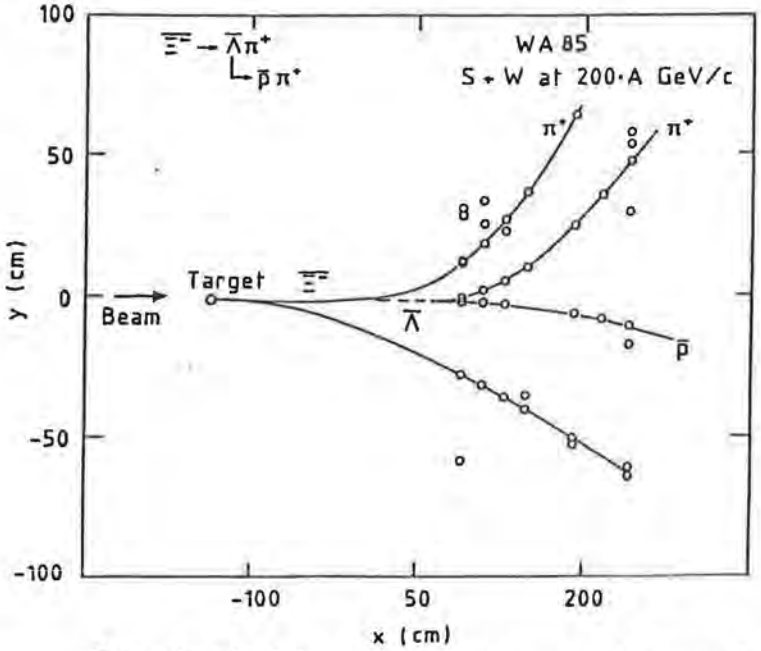

Fig. 1: Example of a fully reconstructed event with a cascade ($\bar{\Xi}^-$) candidate.

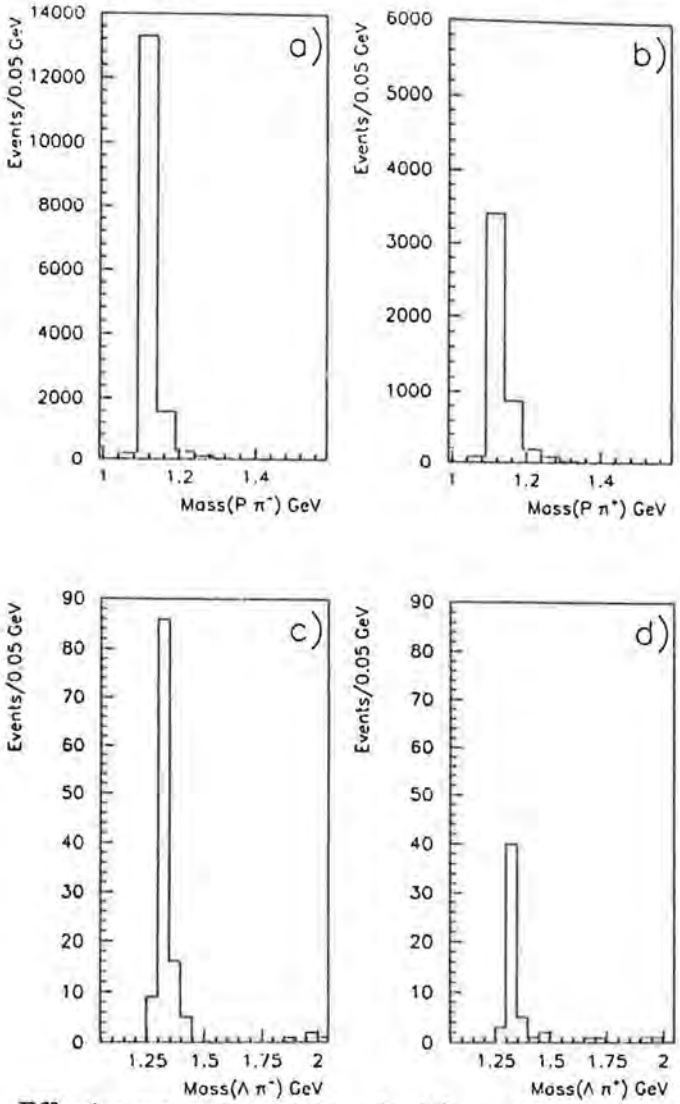

Fig. 2: Effective mass distributions for V^0 candidates as a) $p\pi^-$ and b) $\bar{p}\,\pi^+$, and cascade candidates as c) $\Lambda\pi^-$ and d) $\bar{\Lambda}\,\pi^+$.

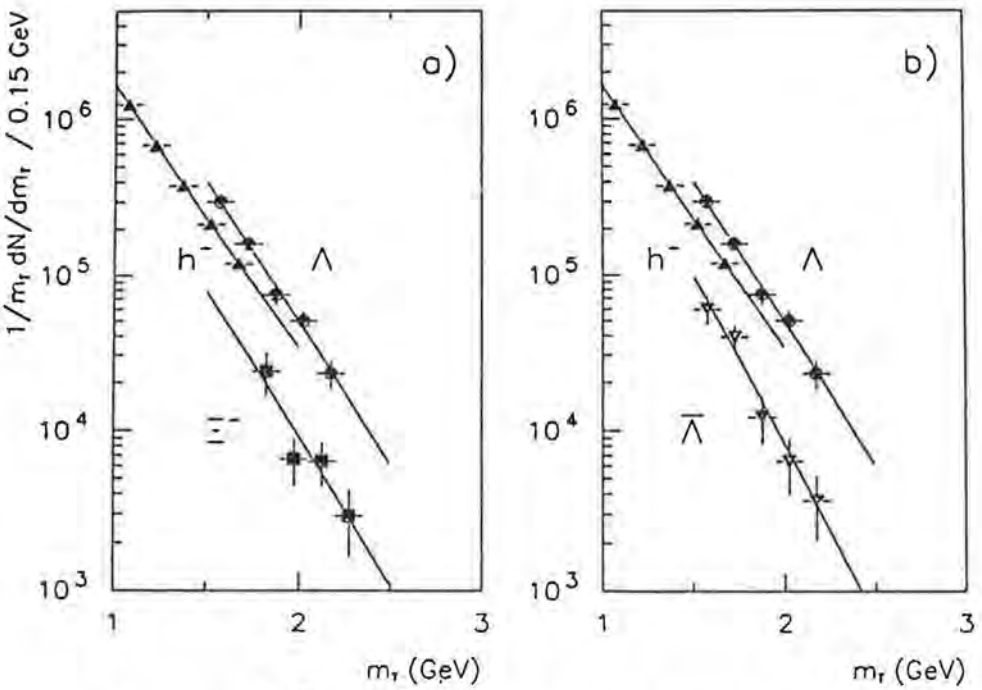

Fig. 3: $\frac{1}{m_T}\frac{dN}{dm_T}$ vs m_T in arbitary units (bin size 0.15 GeV) for
a) negative particles, h^- (mostly π^-s) Λs and $\bar{\Xi}^-$ s.
b)negative particles, h^- (mostly π^-s) Λs and $\bar{\Lambda}$ s.

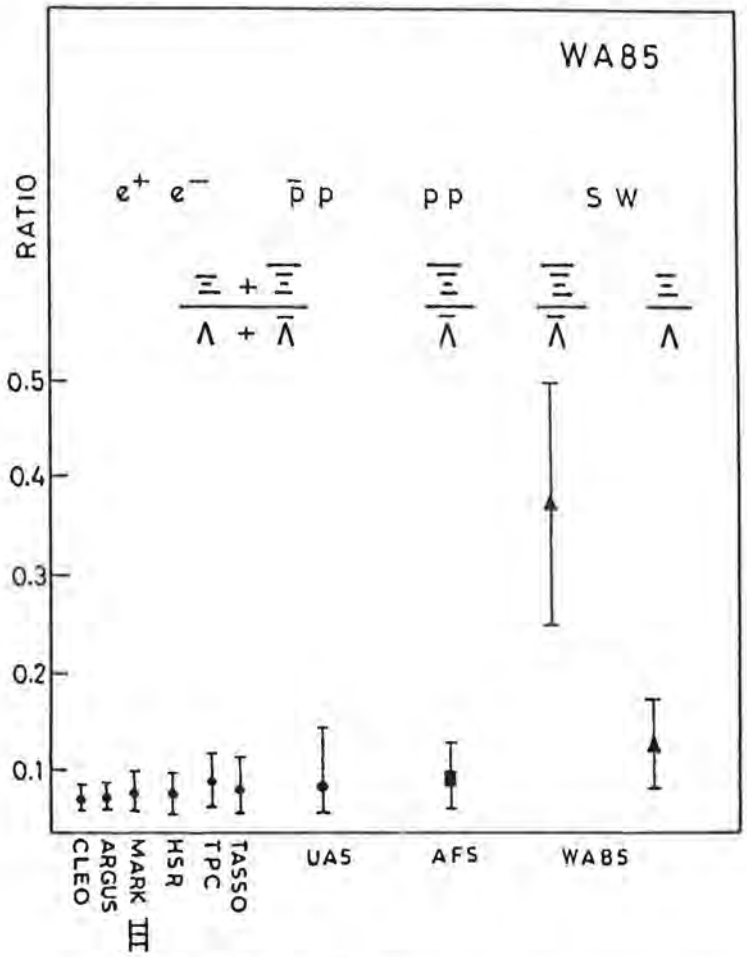

Fig. 4: $\bar{\Xi}^-/\Lambda$ and $\bar{\Xi}^-/\bar{\Lambda}$ ratios for different experiments.

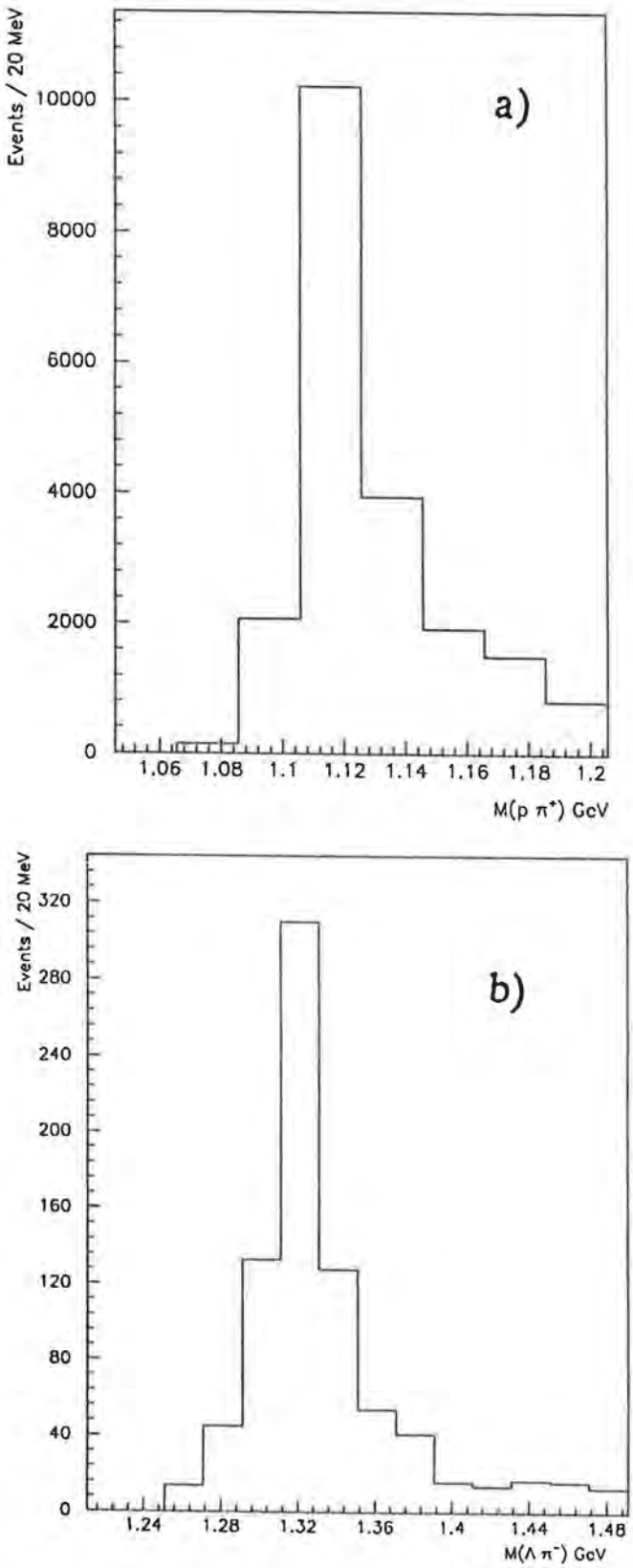

Fig. 5 Effective mass distributions from the 1990 data for *a*) lambda candidates and *b*) cascade candidates.

Sudbury Neutrino Observatory

R.A. Black, R.J. Boardman, S.J. Brice, G. Doucas, E.W. Hooper
N.A. Jelley, A.B. Knox, M.D. Lay, M.E. Moorhead, M. Omori, N.W. Tanner
R.K. Taplin, D.L. Wark and N. West.
University of Oxford

J.C. Barton and P.T. Trent
Birkbeck College, London

October 28, 1992

Physics

The discrepancy between the solar neutrino capture rate in ^{37}Cl predicted by the Standard Solar Model (SSM) and the rate measured by the Chlorine experiment in the Homestake Gold Mine has persisted for more than twenty years. Recent calculated values of the capture rate are 7.9 ± 2.6 SNU (1 Solar Neutrino Unit = 10^{-36} captures/target atom/s) in the Bahcall-Ulrich SSM[1]. This is to be compared with the measured value in the Chlorine experiment, averaged over 1970–1988, which is 2.3 ± 0.3 SNU[2]. A deficit has also now been observed by the Kamiokande II water Cerenkov counter[3], which observes only 0.46 ± 0.05 (stat.) ± 0.06 (syst.) of the rate predicted by the Bahcall-Ulrich SSM.

Solutions of the "solar neutrino problem" have been put forth which invoke either nonstandard solar models or new particle physics. The ^{37}Cl and Kamiokande experiments are primarily sensitive to the high energy ^{8}B solar neutrinos, whose production rate depends critically on the core temperature of the sun. Numerous non-standard solar models[4] which reduce the core temperature have been suggested, incorporating reduced heavy element abundances, high magnetic fields, turbulent diffusion, continuous mixing, and other effects. However, none of the nonstandard models has been able to reproduce the observed ^{8}B flux and still agree with all other observed features of the sun. Solutions which invoke new particle physics include neutrino matter oscillations (the MSW effect)[5] or neutrino magnetic moments[6]. It is interesting to note that the current results from the gallium experiment, SAGE and Gallex which detect lower-energy pp solar neutrinos (the flux of which is nearly insensitive to the core temperature of the sun) are respectively $44 \pm 15 \pm 11\%$ and $63 \pm 14 \pm 6\%$ of the SSM[7]. As long as the assumption is made that the sun is in quasi-static equilibrium and is deriving its energy primarily from nuclear fusion the firm lower limit is 61% of the SSM it is beginning to look as if the solution to the solar neutrino problem must lie within the realm of new particle physics. It is just this new physics which SNO is uniquely capable of exploring.

The planned SNO detector[8] consists of an acrylic vessel containing 1000 tons of D_2O immersed in 7000 tons of high-purity H_2O located in a cavity 6800 feet underground in the Creighton mine near Sudbury, Ontario (see Fig.1). The H_2O provides both shielding against the natural radioactivity of the surrounding rock and the optical coupling to the 9577 PMTs. These PMTs are mounted on a polygonal stainless steel/ABS plastic structure (PSUP) about 2.5m from the acrylic vessel. The primary neutrino detection reactions are:

$$\begin{aligned} &\text{(I)} && \nu_e + d \rightarrow p + p + e^- \\ &\text{(II)} && \nu_x + e^- \rightarrow \nu_x + e^- \\ &\text{(III)} && \nu_x + d \rightarrow \nu_x + p + n \end{aligned}$$

where $\nu_x = \nu_e, \nu_\mu, \nu_\tau$ (for reaction II the cross section is 6 times higher for ν_e than for ν_μ or ν_τ, while for reaction III the cross section is independent of the particle flavour and ν or $\bar{\nu}$). Reactions I and II are observed via the Cerenkov radiation emitted by the energetic electrons and are distinguished by the strongly directional correlation of the type II events (the electron trajectories point away from the sun). Reaction III is observed by detecting the neutrons (by adding NaCl to the D_2O and observing the Cerenkov radiation emitted by energetic electrons produced when the gammas created by neutron capture on Cl interact in the detector). By operating the detector with and without NaCl added the rates for all three reactions can be determined. This gives SNO the capability of measuring both the ν_e and the total ν_x flux from the sun, and if these two differ it is a direct signature of neutrino oscillations which does not depend on any prediction of the Standard Solar Model. The count rates in SNO will be far higher than for any existing experiment (given the SSM fluxes we would detect 9750, 1100 and 2800 events per annum for reaction types I, II and III respectively). These events are recorded in real time, allowing observation of any time structure in the range μseconds to years. Furthermore, if neutrino oscillations are observed these high count rates (for illustration, the non-adiabatic MSW solution favoured by current results from other experiments would produce 3750, 488 and 2800 per annum detected events for reactions types I, II and III respectively will permit a precise determination of the mixing parameters.

As an added bonus the capabilities discussed above would make the SNO detector the world's premier supernova detector. In the fortunate event of a supernova at 10 kpc it would detect in a few seconds 500 events summed over all types (dominated by the type III events), which would give unprecedented information on neutrino star formation and would permit a direct measurement of the mass of the ν_μ or ν_τ in the range 50 eV $\leq m_\nu \leq$ 100 keV.

In order to improve the light collection, and hence the signal/noise of the detector the Oxford group has developed non-imaging light concentrators to mount around the PMTs. These concentrators are a substantial development of the well-known "Winston cone" for a quasi-spherical photocathode (the Winston cone is designed to reach the theoretical limit of light collection for the case of a flat photocathode[9]). They have the twin virtues of increasing by 65% the number of photons from the D_2O detected (thus increasing the signal), while simultaneously keeping each PMT from seeing the PMTs adjacent to it. This greatly reduces the probability of a radioactive decay near one of the PMTs being misidentified as an event in the D_2O (a so-called PMT beta-gamma event), which is the major source of background at low energies. These advantages have made the concentrators central to the design of the detector.

Oxford/Birkbeck Participation in SNO

a) Light Concentrators

The design and development has been completed and agreed by the collaboration, and the main contracts have been placed for the manufacture and assembly of parts for 10,000 concentrators. The model which is being manufactured is made up of an injection moulded plastic dish which seats on the curved surface of the 200mm diameter photomultiplier and holds in place 18 strips of aluminium sheet, coated for high reflectance and preformed to the correct optical shape. For all practical purposes the assembly amounts to a cylindrically symmetric reflecting surface of aperture 275mm which, within the acceptance angle of 56° to the axis, concentrates all the light onto the photocathode, bar the reflectance loss of $\sim$ 10%, and rejects all light outside 56°. The acceptance cone of half angle 56° encloses the 12m diameter sphere of D_2O in Fig.1,

and 1m radially of H_2O. The plastic dishes of the concentrators have been designed to be a good fit in the cells of the honeycomb structure of the photomultiplier support sphere to provide a significant water flow impedance which is a necessary condition for the water flow to be radially outward everywhere over the sphere. This is important as the outer H_2O volume, where there will be turbulence convection currents, is likely to be less clean than the inner H_2O volume which is in contact with the D_2O acrylic vessel (see fig.1).

b) Simulation and Analysis

Oxford has recently undertaken full responsibility for the design and writing of the basic core of the analysis and simulation programmes, and the coordination and supervision of such programmes generally.

This work has been closely associated with the determination of the characteristics of the photomultipliers including their reflection properties, and the development of calibration sources. A Cerenkov source has been developed which permits the absolute calibration of the photomultiplier efficiencies to a few per cent accuracy.

c) Assay of Th and Ra

The background of the neutrino detector will largely originate in the decays of the ubiquitous ^{232}Th and ^{238}U chains. At 6800 feet depth cosmic rays are unimportant. Every material which is to be used in the detector has to be checked and selected for appropriately low activity, and much has has been made of the low background gamma counting facility at Birkbeck. This has included the development of low activity glass and the measurement of leaching of radio-activities from various materials.

The most stringent requirement applies to the component activities of the ^{232}Th decay chain in the D_2O which activities must be reduced below the level of one decay per ton per day, equivalent to a mass concentration of ^{232}Th of 10^{-15}. Techniques are under development for the concentration of radium and thorium in water, with or without NaCl in solution, based on the method of seeded ultrafiltration. In round numbers it is necessary to extract the radium and thorium from 100 tons of water and concentrate to the level of a few milli-grams (or equivalent) which will permit α-counting. Ultra filtration seeded with hydrous titanium oxide at a concentration of 1 ppm has been shown to extract radium quantitatively, and a pilot plant capable of handling some tons of water is being constructed.

The work on photomultipliers and water assay has been supported by CASE studentships sponsored by Thorn EMI Electron Tubes and British Nuclear Fuels.

Current Status of SNO

The photomultipliers are in production and being delivered, and the designs of the photomultiplier support structure and the acrylic have been finalized. Mining work will be completed in 1993 and will allow installation to proceed with the expectation of completion late in 1995.

Publications — Theses

M.E. Moorhead, Oxford 1992.
R.J. Boardman, Oxford 1992.

References

[1] J.N. Bahcall and R. Ulrich, Rev. Mod. Phys. **60** (12988) 297.

[2] R. Davis *et al.*, Proc. of Neutrino '88 Intl. Conf., (1988) 518.

[3] K.S. Hirata *et al.*, Phys. Rev. Lett. **65**, 1297 (1990).

[4] See articles by Schatzman (p.69), Michaud (p.75) and Roxburgh (p.88) in AIP Conf. Proc. No. 126 (1985).

[5] S.P. Mikheyev and A. Yu. Smirnov, Sov. J. Nucl. Phys. **44**, (1986) 938; L. Wolfenstein, Phys. Rev. **D17**, (1978) 2369.

[6] M.B. Voloshin *et al.*, Sov. J. Nucl. Phys. **44**, (1986) 440; L.B. Okun *et al.*, Sov. J. Nucl. Phys. **44**, (1986) 546.

[7] V.N. Gavrin at the XXVI Int. Conf. on High Energy Physics, Dallas 1992; P. Anselmann *et al.*, Phys. Lett. B. **285**, (1992) 376.

[8] For a compact but outdated view, see the Sudbury neutrino Observatory Proposal, SNO–87–12, (1987). Somewhat more current information is available from the papers presented to the Temple review in Oct. 1989 which have been copied to the SERC.

[9] W.T. Welford and R. Winston, High Collection Non-Imaging Optics, Academic Press (1989).

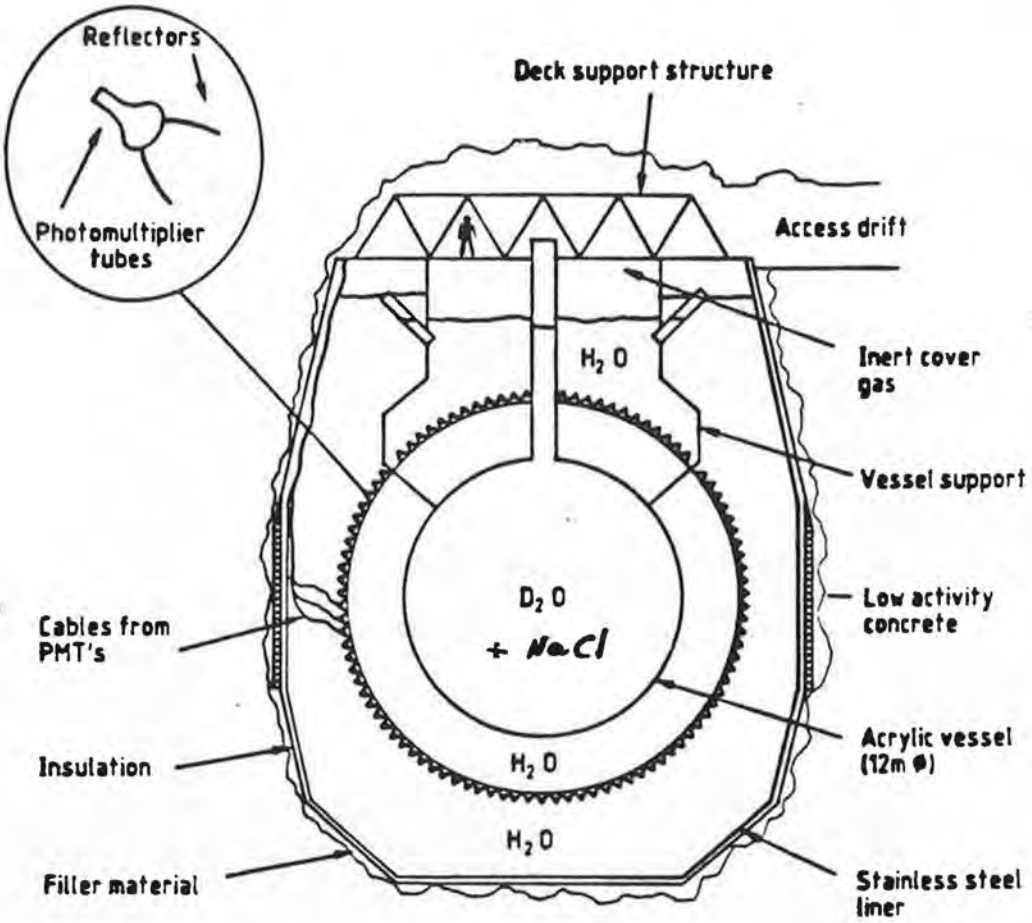

Figure 1. On overview of the SNO detector.

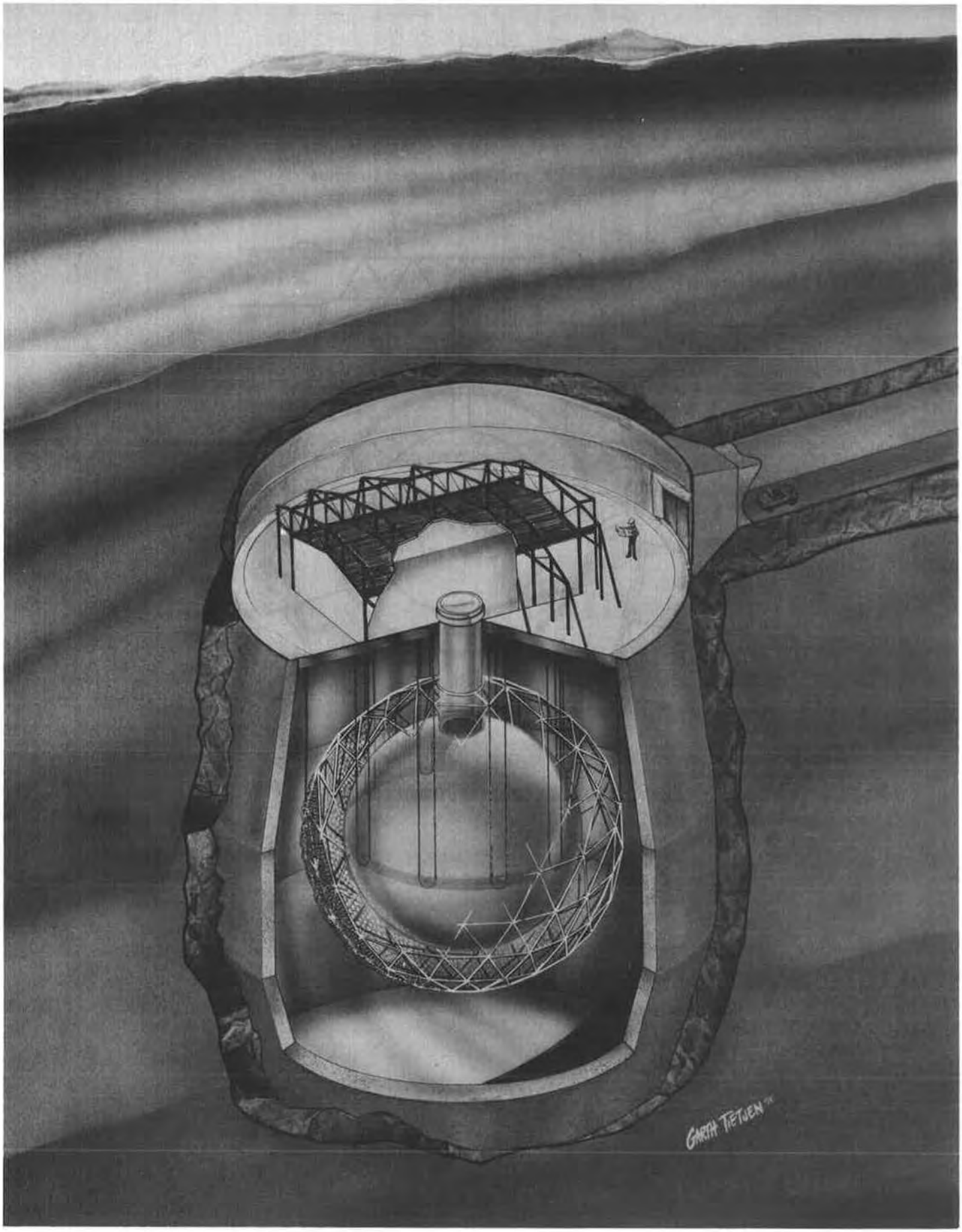
GARTH TIETJEN

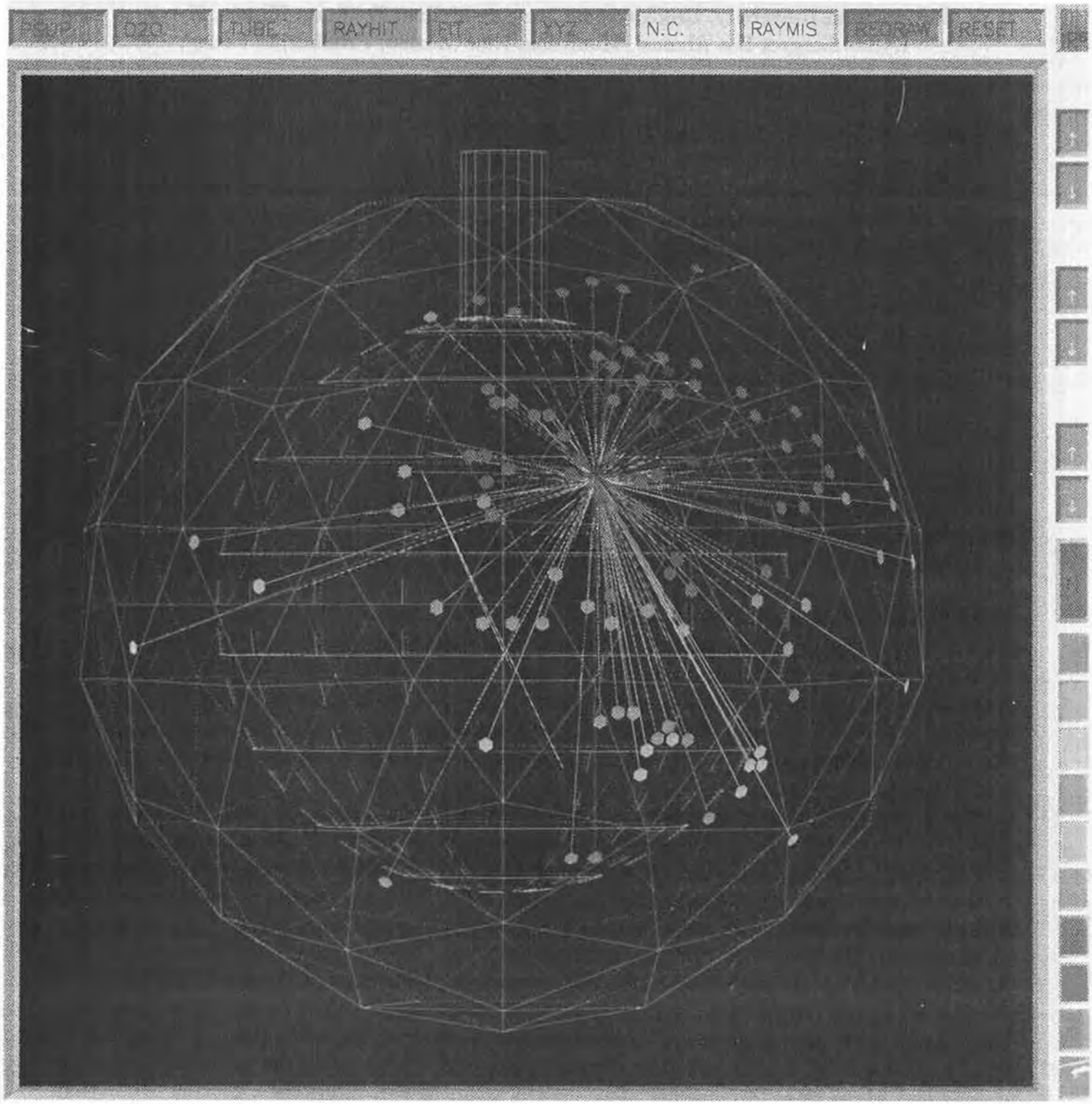

7 MeV $\nu_e d \rightarrow pp e^-$ EVENT

A search for the H-particle and other strange matter

Birmingham University, Brookhaven, Carnegie-Mellon, Freiburg, Illinois, Kyoto,
Kyoto-Sangyo, Los Alamos, Manitoba, New Mexico, Pittsburgh, Saclay,
Triumf, Vassar College

A. E813/836 - A search for the H-particle

Brookhaven E813 is a search for the H-particle, a strangeness-2 dibaryon, originally postulated by Jaffe[1] to be bound against strong decays. In E813, K^- at about 1.8 GeV/c enter a liquid hydrogen target, producing Ξ^- by the reaction

$$K^- p \rightarrow K^+ \Xi^-.$$

The K^+ is detected in a magnetic spectrometer, and the Ξ^- pass through a tungsten degrader and stop in a liquid D target, where they form $\Xi^- d$ atoms which produce H-particles via the process

$$\Xi^- d \rightarrow Hn.$$

The primary signal is a monoenergetic neutron from H formation. A schematic diagram of the layout of the apparatus is given in fig. 1.

This apparatus is installed at the end of a new high-flux 2 GeV/c kaon beam line at the AGS. Our first run with the apparatus was an engineering run in April - June, 1991. A small part of the 1991 run was devoted to data taking. However, the integrated kaon flux during the 1991 run was only about 6% of the total of 10^{12} planned for the whole experiment. This was mainly a result of slow commissioning of the beam line and poor performance of the separators. Because the expected signal from the whole experiment corresponds to at most about 100 H-particles, we would not expect to see a signal from the 1991 running. Our spectra enable us to estimate the signal-to-background to be about 4 $\times B$ where B is the $\Xi^- d$ atomic branching ratio for $\Xi^- d \rightarrow Hn$.

Fig. 2 shows a scatter plot, from a small fraction of the data from the 1991 run, of particle mass (from time-of-flight) *vs* momentum in the spectrometer. The K^+ signal is visible and its momentum, $\sim 1.15\ GeV/c$, is correct for the production of Ξ^- that can stop in the D target.

Our 1992 run took place during June and July, 1992. We have made several improvements to the apparatus:
(i) The data-acquisition dead time has been reduced.
(ii) Extra planes have been added to the drift chambers at the back of the spectrometer.
(iii) A second-level trigger was installed to reject proton triggers online on the basis of time-of-flight. An approximate momentum measurement is made from the track positions in one drift chamber and a TOF hodoscope. The time of flight is compared with the expected values for protons and kaons in a "Firecracker" fast preprocessor. If this indicates a proton, all fastbus ADCs and TDCs are fast cleared and the event is rejected.

After a slow start due to continual problems with the newly constructed AGS booster, the run went well, except that we still have problems with the separators, one of which was damaged to a point where it could not be repaired during the run. The first-pass data reduction from the 1992 run is just starting using, amongst other machines, the Dec ALPHA computer which we have just installed. To date, we have an integrated kaon flux of about 40% of the total of 10^{12} required.

B. E886 - A search for new strange particles in nucleus-nucleus collisions

An unusual form of potentially stable hadronic matter containing roughly equal numbers of up, down and strange quarks has been proposed by various authors[2]. The relatively large strangeness content of such matter is expected to result in objects, called strangelets, with anomalous mass to charge ratios, M/Z, ($M/Z \geq 4GeV/c^2$) compared to ordinary particles and nuclei. Brookhaven E886 is a search for such exotic stable particles in Si+Pt and Au+Pt collisions.

Our strategy is to use two separate spectrometers, one of which contains an electrostatic separator, in sequence to search for particles with anomalous M/Z ratios produced in relativistic heavy ion collisions. The first of these is the 2 GeV/c D6 beam line (developed for E813, the H particle search), used as a mass spectrometer. The overwhelming abundance of ordinary particles produced in these collisions (e.g. e, π, K, p, d, t, and other light nuclei) can pose a serious background for such a search. However, in our experiment the counters used for particle identification (PID) are largely shielded from high background rates due to the limited phase space acceptance of the beam line and the electrostatic deflection of ordinary particles from our acceptance by two electrostatic separators and mass slits. The second spectrometer is the 48D48 magnet and its associated detectors that constitute the spectrometer for the H-particle experiment. The beam-line and detector set-up was essentially the same as for E813 except that the hydrogen target was removed and replaced by four 2 mm-thick counters (IE1 - 4). The two electrostatic separators and associated mass slits determine an accepted range of M/Z.

We carried out a test run of 280 hours in 1992 and have been allocated a data-taking run in 1993. Production rates of strangelets in heavy ion collisions have been estimated under widely varying assumptions[3]. Based on reasonable models of hadron production we can achieve sufficient sensitivity in the 1993 Au running period ($10^{-6} - 10^{-8}$ per collision) to provide the first serious test of the more optimistic of these scenarios.

In the 1992 test runs we took data with two sets of applied fields corresponding to accepted ranges in M/Z of approximately $3.0 < m/Z < 5.0\ GeV/c^2$ and $5.0 < m/Z < 10.0\ GeV/c^2$. Particle identification is based on time of flight, momentum, Cerenkov, and pulse height information. An example of the excellent particle and charge separations from pulse height is shown in fig. 3. This shows a plot of pulse height in IE1 against time of flight in the beam line. Also shown are energy-loss curves calculated from the Landau expression and also corrected for the response of the plastic scintillator.

By measuring particle velocity from time of flight and p/Z from magnetic measurements, the ratio m/Z can be determined, which is a signature of a strangelet. With our apparatus, m/Z can be determined both from the beam-line counters and magnets and also, quite independently, from our spectrometer magnet and its associated counters. Imposing the requirement

of agreement between these two determinations (from the "front" and "back" spectrometers) gives a substantial rejection of false strangelet events due to randoms, scattering off magnet poles, etc. This is demonstrated if fig. 4 where m/Z from the front spectrometer is plotted against m/Z from the back, from a Si run. Evidently, many events appear to have high m/Z (i.e. $> 4GeV/c^2$) from either spectrometer alone, but in the region $6 < m/Z < 8\ GeV/c^2$, no events survive when agreement between the two determinations is required.

While we are still refining our background rejection techniques, very simple rejection cuts are sufficient to reject all strangelet candidates recorded in the Au data at the current statistical levels. More sophisticated background rejection analysis is currently underway to address the few remaining strangelet candidates from the much higher statistics Si data.

References

1. R.L. Jaffe, Phys. Rev. Lett. **38**, 195 (1977).

2. S.A. Chin and A.K. Kerman, Phys. Rev. Lett. **43**, 1292 (1979); E. Witten, Phys. Rev. **D30**, 272 (1984); E. Fahri and R.L. Jaffe, Phys. Rev. **D30**, 2379 (1984) and **D32**, 2452 (1985).

3. S.E. Eiseman *et al.*, Phys. Lett. **B248**, 254 (1990).

Conference contributions

A time-of-flight wall used with the K^+ spectrometer on BNL experiment 813, W.D. Ramsay and the H-particle collaboration, Bull. Am. Phys. Soc., **37**, 995, 1992.

A search for the H-particle in $\Xi^- d$ interactions, B.P. Quinn *et al.*, contribution to Baryons 92, Yale University, June 1992.

Measurements of light-particle production in Au + Pt and Si + Pt colllisions at the AGS using a fixed-angle focusing spectrometer, G.E. Diebold, J.M. Nelson, R. Zybert, D. Beavis, R.E. Chrien, P. Pile, R. Sawafta, R. Sutter, G.B. Franklin, B. Quinn, R.A. Schumacher, R. Magahiz, F. Merrill, I.R. Soukaton, V. Zeps, T. Buerger, M. Burger, J. Franz, H. Schmitt, E. Roessle, H. Enyo, T. Iijima, K. Imai, A. Masaike, N. Saito, S. Yokkaichi, K. Okada, F. Takeutchi, P.D. Barnes, B. Bassalleck, J. Lowe, A. Rusek, D.M. Wolfe and R. Stearns, Santa Fe meeting, 1992 (BAPS).

Search for strangelets and other rare objects in Au + Pt and Si + Pt collisions at the AGS using a fixed-angle focussing spectrometer, A. Rusek, B. Bassalleck, J. Lowe, A. Rusek, D.M. Wolfe, J.M. Nelson, R. Zybert, D. Beavis, R.E. Chrien, P. Pile, R. Sawafta, R. Sutter, G.B. Franklin, B. Quinn, R.A. Schumacher, R. Magahiz, F. Merrill, I.R. Soukaton, V. Zeps, T. Buerger, M. Burger, J. Franz, H. Schmitt, E. Roessle, H. Enyo, T. Iijima, K. Imai, A. Masaike, N. Saito, S. Yokkaichi, K. Okada, F. Takeutchi, P.D. Barnes, R. Stearns and G.E. Diebold, Santa Fe meeting, 1992 (BAPS).

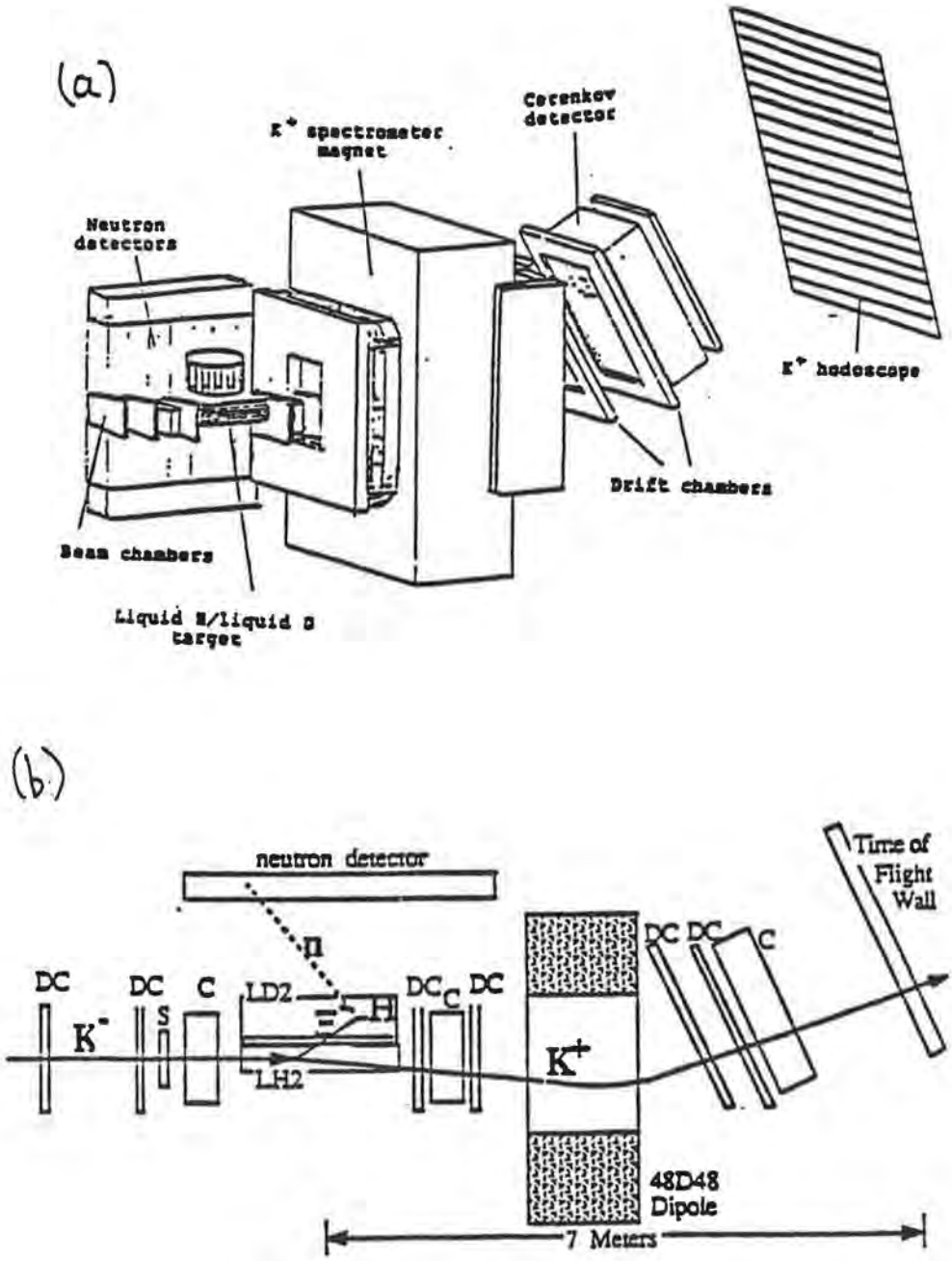

Fig. 1. Layout of the main components of the apparatus for E813/836. The perspective view, (a), shows the general layout, while the side view, (b), shows more detail. The neutron counters, some of which are not shown for clarity, surround the target on both sides. Several Cerenkov and scintillation counters are also omitted from this drawing.

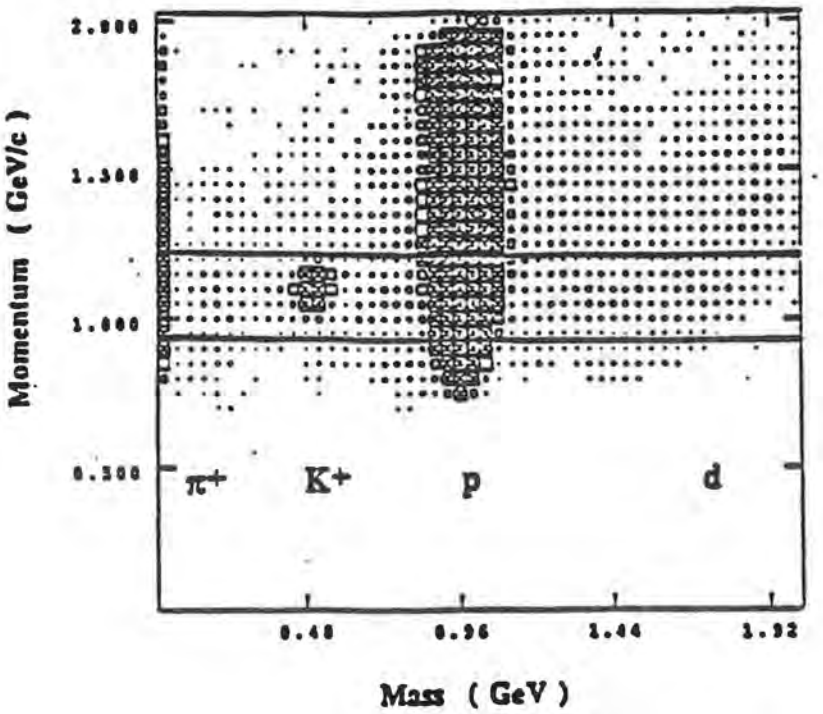

Fig. 2. Plot of secondary momentum against particle mass (from time-of-flight).

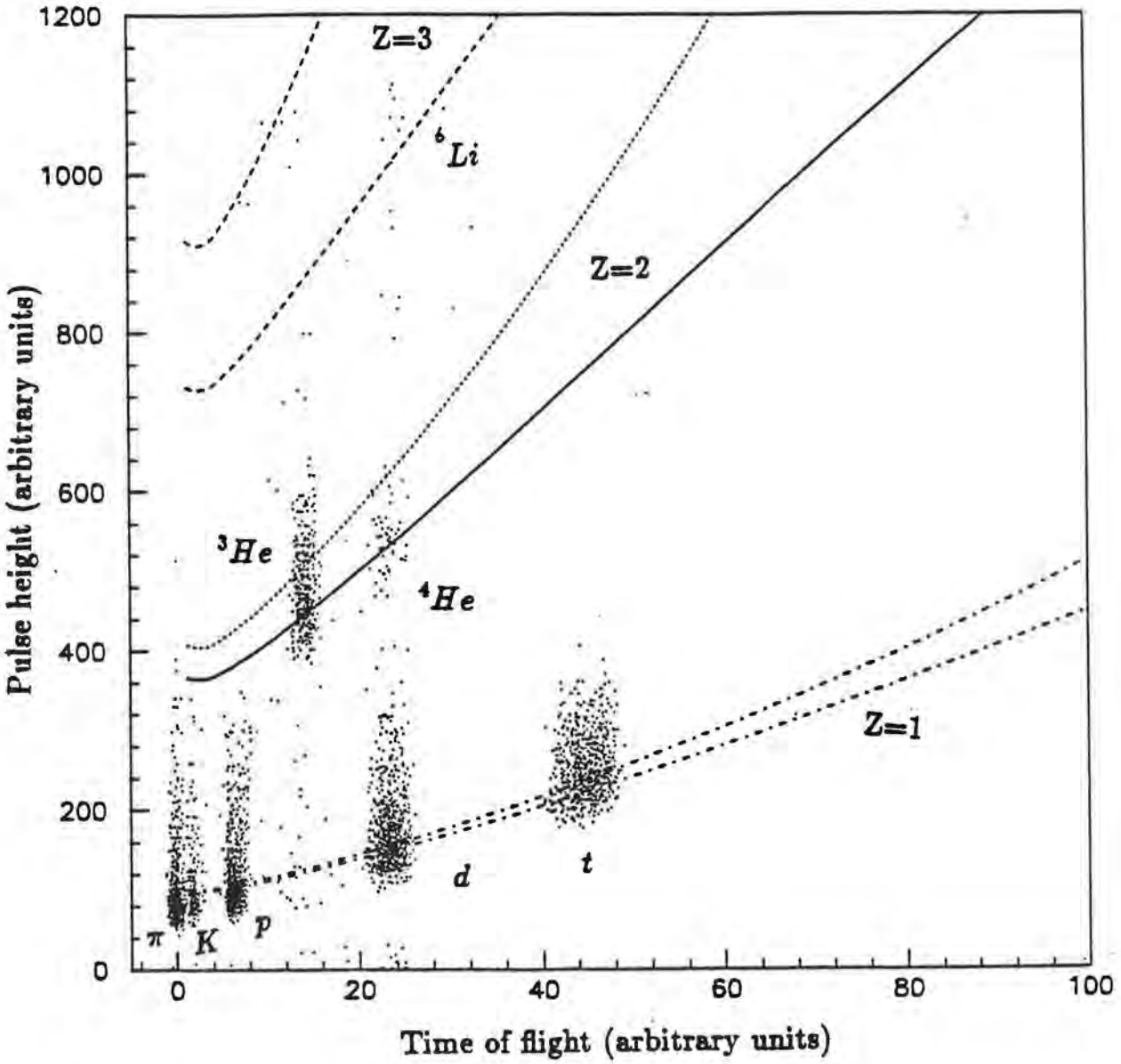

Fig. 3. Pulse height in IE1 against time of flight in the beam line. The curves are the predictions of the Landau energy-loss formula for Z=1, 2 and 3, and the lower curve of each set shows the same prediction corrected for the scintillator energy response.

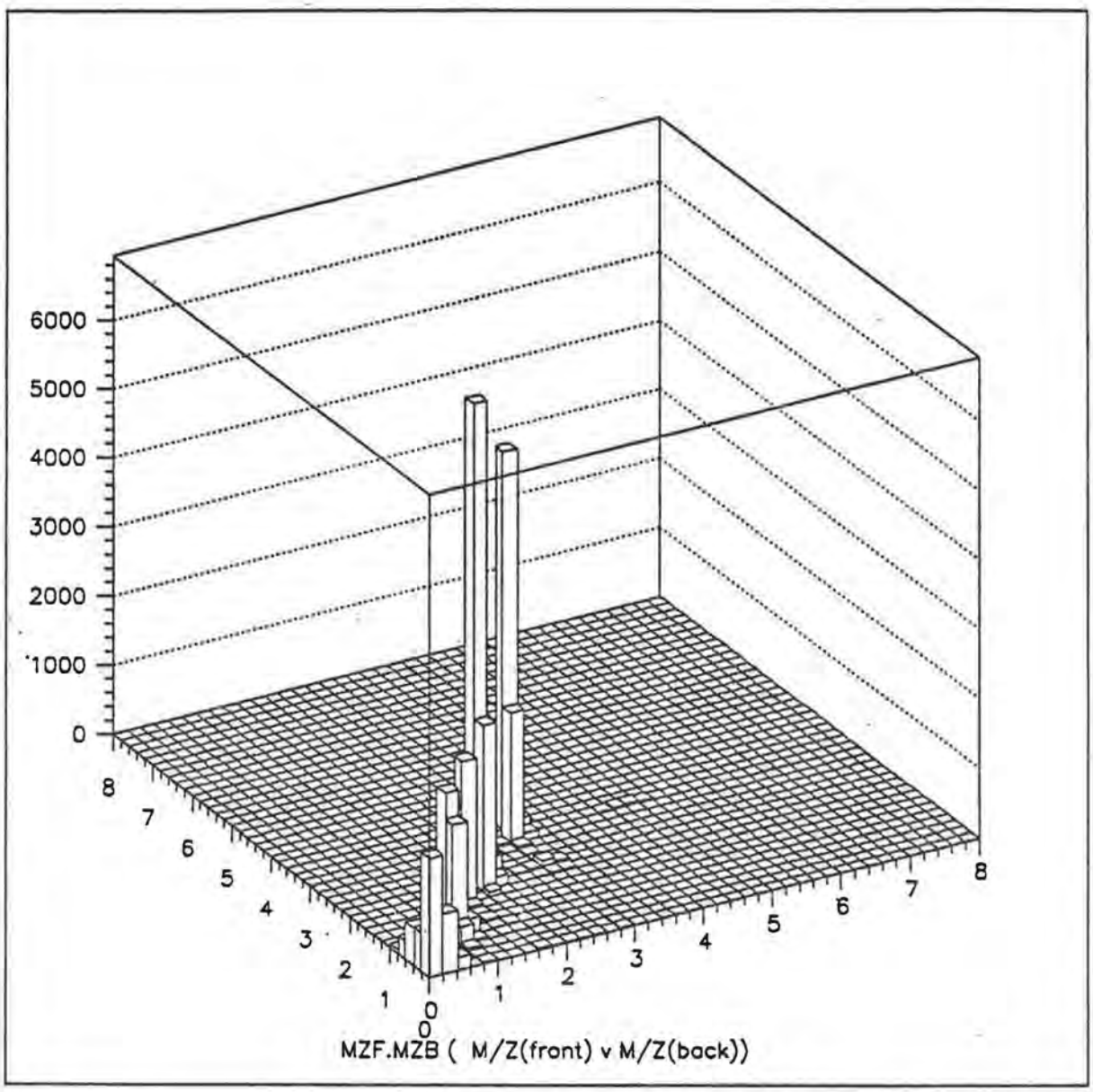

Fig. 4. Scatter plot of m/Z determined from the front spectrometer against m/Z determined from the back spectrometer. The run was taken with a triton trigger; the proton, $d + {}^4He$ and triton peaks are clearly visible.

RADIATIVE WEAK DECAYS OF Σ^+ & Ξ^- HYPERONS

Fermilab E–761 proposal 279

Rio de Janeiro (CBPF & CNPQ), São Paulo, *Brazil* Beijing (IHEP), *PRC* Bristol, *UK*
Fermilab, Iowa, SUNY–Albany, Yale, *USA* Moscow (ITEP), St. Petersburg (PNPI), *USSR*

The experiment took data in the Fermilab 1990 fixed–target run. The main purpose was the study of the decays $\Sigma^+ \to p\gamma$ and $\Xi^- \to \Sigma^-\gamma$, however the experiment also measured the production polarisation of Σ^+ and $\overline{\Sigma}^-$ and their magnetic moments. The Σ^+ magnetic moment was also measured by a novel technique, using the precession of the direction of polarisation during channelling in a bent crystal.

(a) Radiative decays :

The layout of the experiment is shown in figure 1. The parent hyperon is measured in the upstream spectrometer (two magnets and three stations of SSDs), the decay photon is converted in one of the steel plates and the shower position is measured in the TRDs, while the energy is measured in a lead-glass and BGO calorimeter. The daughter baryon is measured in the downstream spectrometer (three magnets and four stations of PWCs). For the $\Xi^- \to \Sigma^-\gamma$ mode, since the daughter Σ^- has a short decay length, the baryon spectrometer was about half as long.

The result for the $\Sigma^+ \to p\gamma$ asymmetry parameter has now been published (over 60,000 events observed — previous results were from experiments with a few hundreds), and the branching ratio result will be submitted for publication shortly. A few thousand $\Xi^- \to \Sigma^-\gamma$ events have been observed (only 11 previously), and this branching ratio will also be submitted for publication.

(b) Production Polarisation :

The background decay, $\Sigma^+ \to p\pi^0$, provides overwhelming numbers of events for a measurement of the Σ^+ polarisation. Figure 2 shows the polarisation vs. p_T for the Σ^+ and its antiparticle $\overline{\Sigma}^-$. The latter has the same sign but reduced magnitude. This is similar to the behaviour of the Ξ^- and its antiparticle (ref 1), whereas the anti-Λ is not produced polarised in proton–nucleus collisions (ref 2).

(c) Magnetic Moment :

The direction of polarisation will precess in a magnetic field, by an amount which depends on the magnetic moment of the particle. The large sample of $\Sigma^+ \to p\pi^0$ events allows a measurement with statistical precision nearly a factor of 10 better than previous measurements. The systematic error is dominated by the uncertainty of the field of the hyperon target magnet, which is being re-mapped to reduce this error. We will also measure the $\overline{\Sigma}^-$ magnetic moment. Both these measurements use the field of the hyperon target magnet (3.4 T x 7.3 m), which precesses the spin by approx 700°. In a subsidiary experiment, a fraction of the Σ^+ beam was channelled in a bent Silicon crystal, giving an effective field of 45 T (but only 4.5cm long). Two measurements of the precession angle were made, which are both consistent with the known magnetic moment (see figure 3). This is the first observation of the precession of the spin of channelled particles.

References :

(1) Ho *et al*, Physical Review Letters **65**, 1713 (1990)

(2) Heller *et al*, Physical Review Letters **41**, 607 (1978)

Figure 2

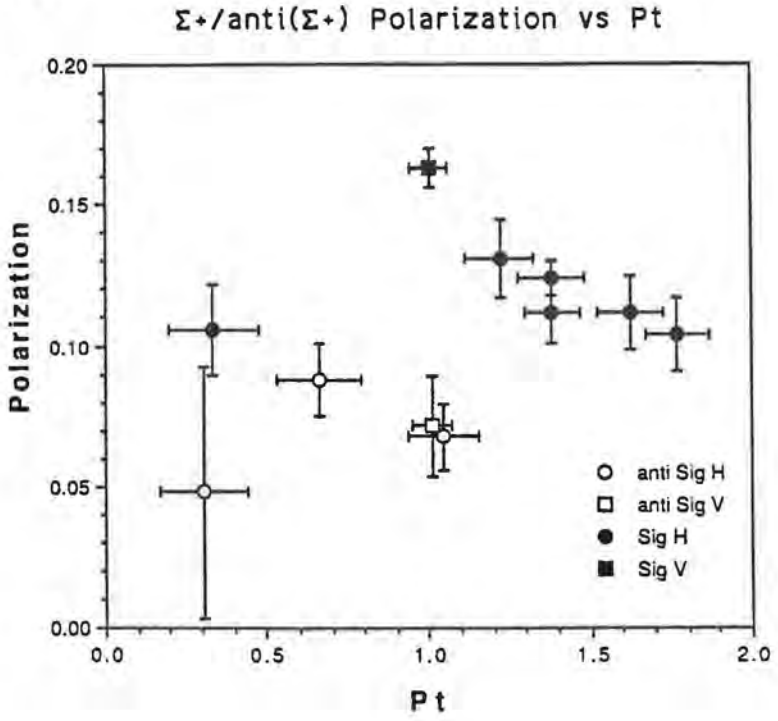

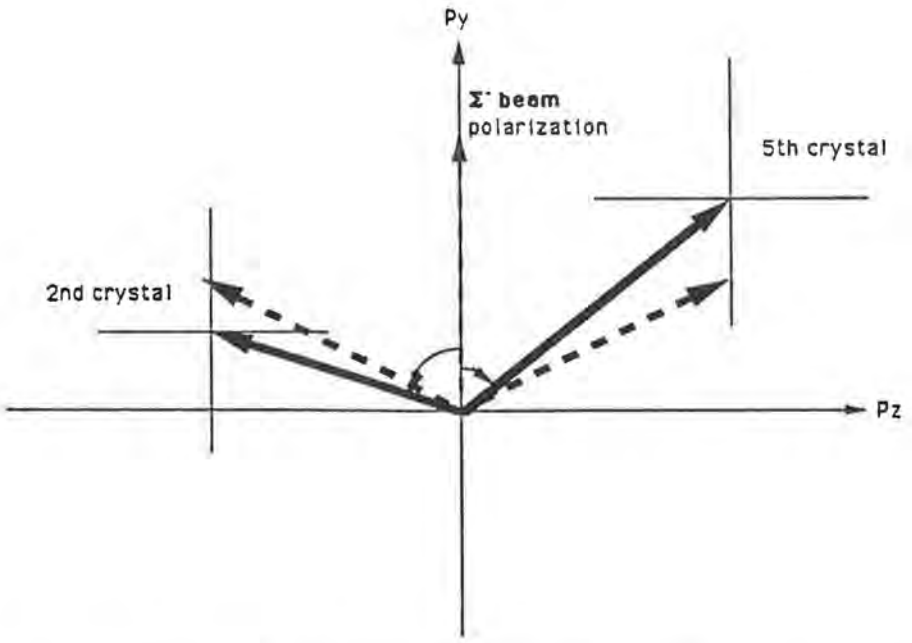

Figure 3 : Measured polarisation directions (full lines) and predicted directions (dotted) for Σ^+ precession in bent crystal. The original direction is vertical.

Publications :

(1) "Measurement of the Asymmetry Parameter in the Hyperon Radiative Decay $\Sigma^+ \rightarrow p\gamma$", M.Foucher *et al*, Physical Review Letters **68**, 3004–3007 (1992)

(2) "A Measurement of Hyperon Radiative Decay", V.J.Smith, on behalf of the E-761 collaboration, published in proceedings of the Hadron '91 International Conference, Ed. D C Peaslee & S Oneda, World Scientific, 1992.

Theses :

(1) "The Asymmetry Parameter and Branching Ratio of Sigma Plus Radiative Decay", Maurice Foucher, PhD thesis, Yale University, 1992.

(2) "The Measurement of the Magnetic Moment of Sigma Plus Using Channeling in Bent Crystals", Dong Chen, PhD thesis, State University of New York at Albany, 1992.

(3) "Measurement of the Polarization and Magnetic Moment of the Σ^+ and $\overline{\Sigma}^-$ Hyperons", Antonio Morelos, PhD thesis, CINVESTAV–IPN, Mexico D.F., 1992.

Figure 1

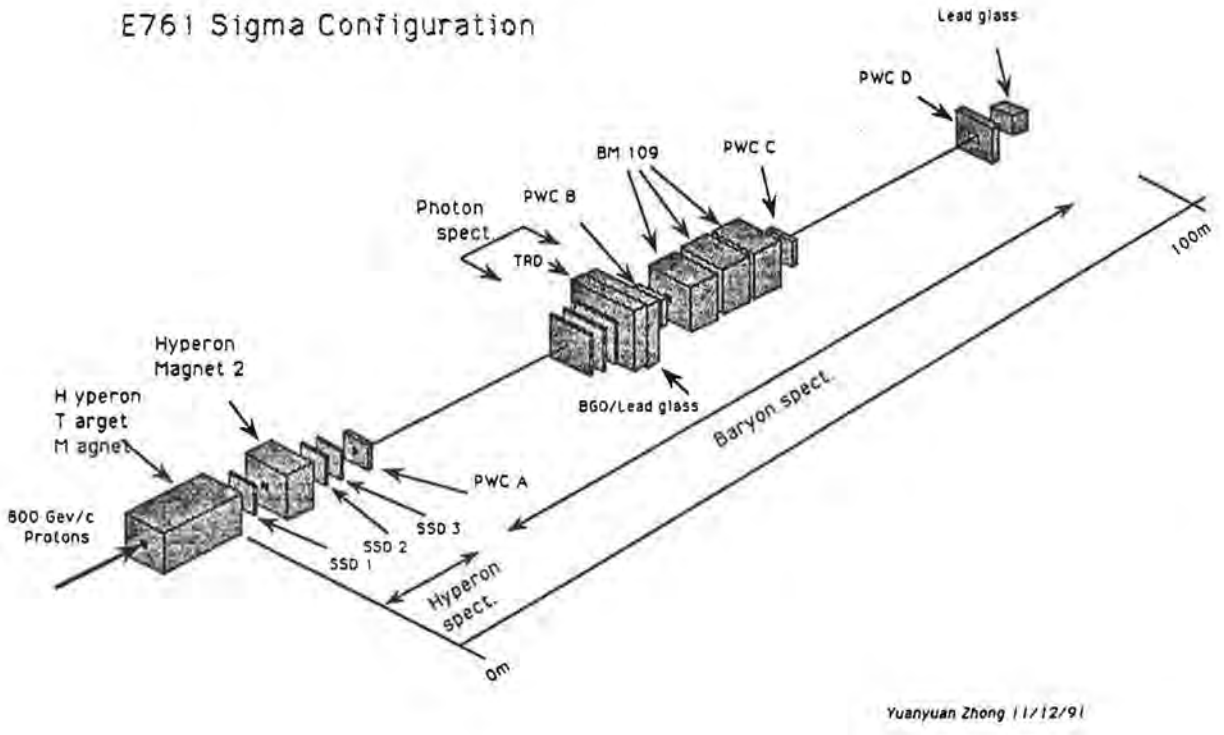

Measurement of Beauty Particle Lifetimes and Hadroproduction Cross-section

WA92 **Proposal 280**

Bologna; Brussels; CERN; Genoa; Imperial College; Mons; Moscow; Pisa; Rome; Southampton

This experiment uses a 350 GeV negative pion beam incident on a tungsten target at the CERN Omega Spectrometer. Its aim is to identify a sample of B mesons, large enough to address several important physics issues, including measurements of the lifetimes of charged and neutral B mesons, the B hadroproduction cross-section, and possibly, $B\bar{B}$ mixing.

The experiment will also be valuable within the context of R&D for prospective B-physics at future high energy hadron colliders. Many features of the proposed LHC fixed target experiments can already be tested.

Although hadronic interactions provide a strong source of B particles the signal / noise is, at presently available fixed target energies, small ($< 10^{-6}$), and the success of the experiment relies on the strategy used for triggering and identifying the beauty events. The WA92 trigger is designed to select events with evidence for leptons or high transverse momentum particles emerging from secondary vertices and the identification of beauty particles relies on the observation of the sequential b-->c decay chain within a silicon decay detector, which provides a spatial precision $< 3\mu m$.

During 1992, 90M triggers were recorded during a 60-day data taking period. The trigger algorithm enriches (by factors ~20 - 30) the Beauty fraction of the data while maintaining a high (~50%) acceptance. On reasonable assumptions for the B cross-section we estimate that more than 1000 B's are on tape. Appropriate off-line filters and event reconstruction are now underway to identify the B-decays.

WA92 - Publications 1991 - 92

" A fast tracking μ - detector"
Nucl. Instr. & Methods A315 (1991) 485 - 489

"WA92: A fixed target experiment to study Beauty in hadronic interactions"
Nuclear Physics B(Proc Suppl) 27 (1992) 251-256

"A Microstrip Decay Detector for Beauty Physics"
submitted to Nucl. Instr. & Methods A

NA48 Proposal 283

A Precision Measurement of ϵ'/ϵ in CP Violating $K^0 \to 2\pi$ Decays

Cagliari, Cambridge, CERN, Dubna, Edinburgh, Mainz, Perugia, Pisa, Saclay, Siegen, Torino, Vienna Collaboration

This is a new experiment, approved in 1991, whose main main aim is to measure precisely the strength of CP-violation in the decay amplitude relative to the dominant CP-violation in the K^0 mass matrix, by comparing the ratio of decays into two charged and two neutral pions for K_S and K_L. The technique, while similar in some respects to that of the NA31 experiment, is very different to that of previous experiments.

There are several challenges. A new neutral kaon beam system has to be built in the high-intensity experimental hall in the North Area of the SPS at CERN, which will deliver nearly collinear K_L and K_S beams concurrently. The $\pi^+\pi^-$ decays will be detected and measured in a classical magnetic spectrometer while the $2\pi^0$ decays will be detected and measured in a novel electromagnetic calorimeter using liquid krypton as the ionizing medium. Advanced triggering and readout systems must be developed to process the very high trigger and data rates required.

Design, prototype and test work is in progress for the various detectors and ancillary systems. The UK effort is centered around the muon veto system, and the advanced electronics required for the readout of the muon veto system and the other detectors. The design of a new data acquisition architecture is well advanced.

Reports on technical progress with the liquiud krypton calorimeter were presented to the Vienna Wire Chamber Conference, and on the data acquisition architecture to the Computing in High Energy Physics Conference in Annecy.

STUDY OF LEAD LEAD INTERACTIONS AT 160GeV/c PER NUCLEON

WA97 ***Proposal 285***

Athens; Bari; Bergen; Birmingham; CERN; Paris; Genoa; Kosice; Legnaro; Padua; Rome; Salerno; Serpukhov; Strasbourg; Trieste.

This experiment intends to measure the spectra of hyperons and antihyperons produced in ultrarelativistic lead-lead interactions over a wide phase space window. The experiment will make use of the 160 GeV/c per nucleon Pb beam expected to become available at CERN in 1994. The principal aim is to compare the production of baryons carrying one unit of strangeness (Λ) with those carrying two (Ξ^-) and three units of strangeness (Ω^-). The possibility of a comprehensive study of the spectra of various hyperon and antihyperon species will constitute a unique feature of our experiment.

In addition we shall measure the spectra of protons and antiprotons in a smaller but overlapping phase space window. This will enable us to compare the spectra of baryons carrying zero, one, two and three units of strangeness under the same trigger conditions.

The ultimate goal of the heavy ion programme is to find evidence for a new state of matter, the Quark-Gluon Plasma (QGP). A transition from normal hadronic matter to the QGP is predicted to occur in head-on collisions of heavy ions because of the large energy and baryon densities obtainable over a relatively large volume.

Hyperons are expected to be a useful probe for the dynamics of hadronic matter under such extreme conditions. In particular, the onset of a Quark-Gluon Plasma phase during the collision is expected to enhance the hyperon yield [1] with respect to normal hadronic interactions. The enhancement is expected to be more marked for those hyperons (*e.g.* Ξ^- and Ω^-) which carry more than one unit of strangeness.

The detection of Ξ^- and Ω^- decays in heavy ion interactions is not easy because of the large event multiplicities; several experiments have succeeded in measuring Λ spectra, but Ξ^- spectra have only been obtained by the WA85 experiment [2] . The first results are very encouraging. The WA85 results for S W interactions at 200 GeV/c per nucleon indicate not only that the ratios of Λ and $\overline{\Lambda}$ to pions are enhanced with respect to those in *p* W interactions [3], but also that Ξ^- and in particular $\overline{\Xi^-}$ production [4] are larger than is predicted by non-QGP models. No measurements have yet been possible for Ω^- spectra.

The proposed experiment aims to extend WA85 study to heavier projectiles, *i.e.* to larger reaction volumes, which should increase the likelihood for the onset of a phase transition from hadronic matter to QGP during the collision. In addition it will use a larger phase space window than WA85, in particular covering lower transverse momenta, and will have a better acceptance for Ω^- detection.

We intend to measure the hyperon and charged particle spectra by using an array of silicon microstrips, silicon pads and pad cathode readout MWPCs located in the Omega magnet [5]. The same apparatus will also be used to measure proton and antiproton spectra in conjunction with the Omega RICH.

The principal challenge is to handle the large number of secondaries produced in central Pb Pb interactions. Our strategy is (*i*) to use a restricted kinematic window, which can be moved over the required phase space region, while retaining the advantages of low multiplicity in the detector elements, and (*ii*) to have a setup capable of high event rates to get good statistics in our kinematic window.

The apparatus consists of a number of elements all currently under development, which will be tested prior to the start of the lead beam programme using sulphur and proton beams. We expect the apparatus to be ready to take good physics data from the startup date for lead beams.

References

[1] J. Rafelski and B. Müller, Phys. Rev. Lett. 48(1982)1066; 56(1986)2334.
P. Koch, B. Müller and J. Rafelski, Phys. Rep. 142(1986)167.
J. Ellis and U. Heinz, Phys. Lett. 233B(1989)223.
J Rafelski, Phys. Lett. 262B(1991)333

[2] Proposal 275, this volume.

[3] S. Abatzis et al., Nucl. Phys. A525(1991)445c.
S. Abatzis et al., Phys. Lett. 244B(1990)130.

[4] S. Abatzis et al., Phys. Lett. 259N(1990)508.
S. Abatzis et al., Phys. Lett. 270B(1991)123.
S. Abatzis et al., Proc. Quark Matter 1991, Gatlinburg, November 1991.
Presented by J.B. Kinson.

[5] WA97 Proposal, CERN/SPSLC 91-29, SPSLC/P263(1991).

Annecy; Barcelona; Bari; Beijing; CERN; Clermont-Ferrand; Copenhagen; Demokritos; Ecole Polytechnique; Edinburgh; Firenze; Florida; Frascati; Glasgow; Heidelberg; Imperial College; Innsbruck; Lancaster; Mainz; Marseille; MPI Munchen; Orsay; Pisa; Royal Holloway & Bedford New College; Rutherford-Appleton Laboratory; Saclay; Santa Cruz; Sheffield; Siegen; Trieste; Wisconsin.

Introduction

The ALEPH experiment has continued to record data at LEP. At the time of writing 577000 Z hadronic decays have been observed in 1992. By mid-September the total number of Z decays seen in ALEPH since 1989 exceeded 1 million. Thanks to excellent integrated luminosities from LEP recently and improvements in ALEPH experimental efficiencies, the number of events recorded this year has comfortably surpassed 1991 already. The overall operational efficiency of ALEPH has been 88% since the start of the year, where even losses arising from intolerably high LEP backgrounds have been taken into account. The results reported here will include publications and preprints based on the data taken up to the end of 1991, together with some preliminary and new results including data taken this year and presented to the International Rochester conference in Dallas in August.

The apparatus is essentially the same as in past years. Inside a large superconducting solenoid, a TPC records charged particle tracks, and an electromagnetic calorimeter of high granularity identifies electrons and photons. At the heart of the apparatus is a beryllium beam pipe of 5.30cm inner radius surrounded by a two-layer double-sided silicon strip vertex detector to exploit the extra space available close to the interaction point. The inner tracking chamber, between the vertex detector and the TPC, acts as a link between the two for tracking and also provides the sole tracking element in the first-level trigger. The return yoke of the magnet is a hadron calorimeter of iron and streamer tubes; further outside are two layers of muon chambers, fully instrumented since early 1991. An important addition to the apparatus was installed in September, namely two cylindrical solid-state luminosity calorimeters which extend the measurement of Bhabha scattering events to even smaller angles (24.3mrad) from the interaction point as well as extending the coverage of the calorimeters down to very small angles. This detector has an important role to play in reducing systematic and statistical errors in luminosity measurements. Fig 1 shows a typical ALEPH event in beam's eye view recorded off-line by the DALI package.

Hardware items in ALEPH supplied by the UK have all functioned very well throughout the year.

As has been reported in previous years, the responsibilities of the UK groups are as follows:

Electromagnetic calorimeter and front-end electronics (RAL, Glasgow, RHBNC, Lancaster, Sheffield)
ITC (Imperial College)
Level 2 trigger using TPC (RHBNC)
Laser calibration of TPC (Glasgow)

In addition to carrying out the responsibilities of maintenance of these items, physicists from the UK have been prominent in all aspects of the experiment: run management and co-ordination, data quality assurance, data acquisition, shift leadership, distribution of processed data to all institutes, management and co-ordination of physics analysis, as well as the individual physics analyses themselves.

The remainder of this report concentrates on the physics output of ALEPH in 1992. So far, there have been 16 published papers in the journals and 4 CERN preprints awaiting publication. This output is classified into the broad headings below, where selected topics are highlighted:

Z lineshape and electroweak parameters

ALEPH's original papers (2) on a detailed study of fits to the Z lineshape for hadronic and leptonic decays have been updated to include all the data taken up to the end of 1991. The quantities fitted are the mass and width of the Z, the cross section at the Z peak, and the ratio R of the hadronic and leptonic decay widths. The following results were presented to the Dallas conference based on 452000 multihadronic and 55000 leptonic Z decays:

M_Z = 91.187 ± 0.007 (exp) ± 0.006 (LEP) GeV

Γ_Z = 2501 ± 12 MeV

σ^0_{had} = 41.60 ± 0.23 nb

R = $\Gamma_{had}/\Gamma_{l^+l^-}$ = 20.78 ± 0.13

From the measured value of $[\Gamma_Z - \Gamma_{had} - 3\,\Gamma_{l^+l^-}]/\Gamma_{l^+l^-} = 5.91 \pm 0.11$ and the standard model value for $\Gamma_{l^+l^-}/\Gamma_\nu$, the inferred number of light neutrino species is 2.97 ± 0.05. The errors quoted are the smallest of the 4 LEP experiments. Without the assumption of lepton universality, a fit to all the cross sections and the leptonic FB asymmetries at the Z peak employs 9 parameters. These fits allow the individual axial and vector couplings of the e, μ and τ leptons to the Z to be determined, provided the average τ polarisation and τ polarisation asymmetry are used as a constraint. The results are plotted in Fig 2 with probability contours at 68% CL. Also shown is the result assuming lepton universality and a comparison with the Standard Model for a range of top quark masses from 50 to 250 GeV. The agreement is excellent with a high top mass preferred. The above leptonic couplings can be used to determine the effective weak mixing angle $\sin^2\theta_W(M_Z^2)$ giving:

$$\sin^2\theta_W(M_Z^2) = 0.2320 \pm 0.0028$$

This measurement from the peak lepton asymmetries can be improved by including four other asymmetry measurements from quark charge, τ polarisation and polarisation asymmetry, and $b\bar{b}$ and $c\bar{c}$ FB asymmetries. The combined result is:

$$\sin^2\theta_W(M_Z^2) = 0.2328 \pm 0.0016$$

which is substantially more accurate than the result quoted in 1991 of 0.2296 ± 0.0023.

This angle can also be obtained separately from the leptonic partial width assuming a Standard Model value for k_{eff} which represents Z self-energy and vertex corrections across the resonance. This method gives:

$$\sin^2 \theta_W(M_z^2) = 0.2305 \pm 0.0016$$

which is in good agreement with the former method and comparable in precision. Alternatively, k_{eff} can be determined from the data by comparing $\sin^2 \theta_W(M_z^2)$ from the asymmetries with $\Gamma_{l^+l^-}$. This result is plotted in Fig 3 again with probability contours. The value of k_{eff} is found to be 0.0131 ± 0.0082 compared with a Standard Model value of 0.0053 ± 0.0016 calculated when $M_{Top} = 175$ GeV and $M_{Higgs} = 300$ GeV. These measurements will enable a severe test of the Standard Model to be made when M_{Top} is known to good precision. Currently ALEPH measurements alone constrain M_{Top} to be:

$$M_{Top} = 175 \begin{matrix} +30+17 \\ -36-20 \end{matrix} \quad \text{(Higgs) GeV/c}^2$$

when $\alpha(s)$ is put at 0.125 ± 0.005 (11).

<u>τ physics</u>

In addition to the study of $Z \rightarrow \tau\tau$ for the measurement of $\Gamma_{l^+l^-}$, A^0_{FB} and P_τ, final results have been published on τ decay branching fractions and lifetime. There were two anomalies reported in τ decays:

(a) the identified one prong decay modes did not saturate the inclusive one prong branching fraction, and
(b) the measured lifetime disagreed with the one calculated from the measured leptonic branching ratio and the calculated partial width.

The ALEPH published results resolve these anomalies. Making full use of the particle-identification capability of the ALEPH detector, the sum of exclusive branching ratios of the $\tau = 100.4 \pm 1.9\%$ ruling out any new undetected decay modes beyond 2.1% with 95% CL. The published τ lifetime is 291 ± 13 (stat) ± 6 (sys) fs consistent with the world average and with $B(\tau \rightarrow e \nu \bar{\nu})$.

Measurements of the polarisation of τ's, P(cos θ), as a function of their production angle to the e-beam enable a precise test of e-τ universality to be made, and a value of $\sin^2 \theta_W (M_z^2)$ to be determined. Using more than 16000 τ pairs from all 1990 and 1991 data the first detailed measurements of P(cos θ) have been made and reported to the Dallas conference. The two most useful decays are $\tau \rightarrow \pi \nu$ and $\tau \rightarrow \rho \nu$ both of which need the high granularity of the ECAL to resolve photons from charged particles in tight jets. The plot of P(cos θ) is shown in

Fig 4 where the analyses of the $\pi\,\nu$, $\rho\,\nu$, $e\,\nu\,\bar{\nu}$ and $\mu\,\nu\,\bar{\nu}$ channels have been combined. P(cos θ) is related to the electron and τ asymmetry parameters A_e and A_τ as follows:

$$P_\tau(\cos\theta) = \frac{A\tau + \left(\frac{2\cos\theta}{1+\cos^2\theta}\right) Ae}{1 + \left(\frac{2\cos\theta}{1+\cos^2\theta}\right) A_\tau A_e}$$

The distribution is fitted allowing A_e and A_τ to be varied independently from which it is found that $A_e = -0.120 \pm 0.031$ and $A_\tau = -0.134 \pm 0.026$, consistent with lepton universality. Within the Standard Model these parameters are equal and are related to $\sin^2\theta_W$, which after small corrections is determined to be 0.2328 ± 0.0025.

Heavy flavour b physics

The early publication of b quark asymmetries and partial width at the Z was based on the identification of $b\bar{b}$ events by their prompt lepton decays. This year results from studies of both single and dilepton events with the full statistics up to the end of 1991 were presented to the 1992 winter conferences. This type of analysis enables the branching ratios and partial width to be disentangled, giving systematically a more accurate value of $\Gamma_{b\bar{b}}/\Gamma_{had} = (21.1 \pm 0.7$ (stat) $\pm$ 0.8 (syst))% in agreement with the Standard Model. More recently, new methods of tagging B hadrons using signed impact parameters determined from tracks reconstructed using the Silicon vertex detector have been developed.

A new value for the FB asymmetry at the Z peak, A^0_{FB} ($b\bar{b}$), has been presented corrected for mixing (12) and charm background using the high p_t lepton sample. The systematic errors are difficult to extract but a large effort is considered worthwhile as this quark asymmetry is a sensitive test of the Standard Model once M_{Top} is known. The value quoted is $A^0_{FB}(\,b\bar{b}\,) = 8.3 \pm 1.8 \pm 0.6)\%$.

A large effort has been devoted to exclusive B meson and b baryon decays and lifetime measurements in the past year. The value of a full year of running in 1991 with an operational vertex detector is increasingly evident in these analyses. An outstanding example which also employs the granularity of ECAL and energy flow determination is the measurement of the branching ratio of $B \rightarrow \tau^\pm\,\bar{\nu}X$. Hadronic Z decays with large missing energy and leptons are selected and their missing energy distributions compared with Monte Carlo which includes residual background not entirely removed by VDET tagging and other B, D decays. The final result reported to the Dallas conference is $BR(B \rightarrow \tau^\pm\,\bar{\nu}X) = (4.20 \pm 0.7 \pm 0.46)\%$ to be compared with a Standard Model value of $2.83 \pm 0.31\%$. This makes it one of the largest decay modes of the B, which was not previously observed. Theoretically, it is an interesting process which may test predictions of non-standard models.

During the year, the data reported earlier on the excess of correlated $\frac{\Lambda\, l^+}{\Lambda\, l^-}$ was published (6) as evidence for b baryons in Z decays; then later the lifetime of such particles was measured to be $1.12 \pm 0.3 \pm 0.16$ps (19). The 1991 data with the VDET operational has been used to isolate a sample of 4909 b candidates and their average lifetime extracted from a fit to the impact parameter distribution of the lepton tracks. The result is $1.49 \pm 0.03 \pm 0.06$ps (18). Also a first measurement of the lifetime of the B^0_s meson was reported to the Dallas conference using the decay mode ($B^0_s \rightarrow D^+_s X l^- \bar{\nu}$). A value of $1.05 \pm 0.37 \pm 0.09$ps was reported.

QCD and γ-γ physics

The strong coupling constant of QCD, $\alpha(s)$ is the least well-known coupling in the Standard Model, since its experimental determination is beset by systematic uncertainties in transforming from a hadronic final state to partons and the choice of renormalisation scale. However, recent theoretical progress on these problems has enabled ALEPH to publish a more precise value of $\alpha(s)$ (11). Despite this advance, the description of hadronic decays of the Z must still rely on the QCD parton shower event generators which form the core of the simulation programmes. During the year, ALEPH published detailed comparisons of the three principle generators (JETSET, ARIADNE and HERWIG) with charged particle data (15) and showed that all are in good agreement after tuning of free parameters. This agreement was conclusively shattered, however, after comparison with a high statistics sample of hadronic events each containing an isolated photon radiated from the primary quarks (20). The Cambridge based HERWIG generator proved to be the most satisfactory, shedding some light on the parton showering mechanism. Another area where the generators proved to be unreliable was in the prediction of pseudoscalar mesons in particular the η' (16), which in its contribution to the $\pi^+\pi^-$ production rate is an important reference to the study of Bose-Einstein correlations in like-sign pion pairs (8). Fig 5 shows the measured η' fragmentation function compared with 2 generators. Again, HERWIG is closer to the data than JETSET.

Finally, new results were presented on the properties of hadronic final states observed in photon-photon collisions to the International Workshop on this subject in San Diego and at the Dallas Conference. In discussions on physics at the next generation e^+e^- linear collider this subject took on a new significance following theoretical predictions of copious production of high p_T hadrons, apparently already substantiated at KEK energies by the AMY experiment. The new ALEPH data plots the distributions of visible energy W_{vis} (Fig 6a) and the transverse momentum to the beam axis of the vector sum of all hadrons in one hemisphere about the reconstructed thrust axis, p_T(thrust) (Fig 6b). Both these distributions show that a QCD based multijet model is needed to explain the excess of events not accounted for by a pure VDM approach. This is consistent with the AMY data. However, a simple combination of QPM, QCD and VDM models does not describe all the data over the full range of measured variables.

Searches for new particles

The comprehensive review based on data up to the end of 1990 was published in Physics Reports during the year (14). It covers the complete range of possible new particle searches in

the Higgs sector including Standard Model extensions, SUSY particles, composite objects, leptoquarks and new weakly interacting particles as well as rare Z decays.

Some of these analyses have been continued and extended to new channels on inclusion of the 1991 data which increases the statistics by a factor of 1.5. The all important search for the neutral standard Higgs has been pursued via the $Z \rightarrow Z^* + H^0$ process into all feasible decay channels. The mass limit has been improved from 48 GeV/c^2 to 53 GeV/c^2 at 95% CL with no indication for any signal found in a data sample of 488000 hadronic Z decays.

This year, updated limits on branching ratios of the Z have been presented to the Winter and Dallas conferences as follows:

$$\begin{aligned} Z &\rightarrow \gamma\gamma\gamma && < 0.9 \times 10^{-5} \\ &\rightarrow W+X && < 3.7 \times 10^{-5} \\ &\rightarrow W+\rho && < 2.6 \times 10^{-5} \end{aligned}$$

In addition, still no events have been found corresponding to the radiative decays of excited charged leptons or neutrinos in Z decays or even for e^* in the t-channel where the mass limit extends to 90 GeV/c^2 with 95% CL.

Finally, a study of the differential cross section for the reaction $e^+e^- \rightarrow \gamma\gamma(\gamma)$ was reported at Dallas. The angular coverage extends to $|\cos\theta| = 0.95$ producing 818 events. However, no deviation from QED which predicts 804 events has been found. This rules out the possible existence of an ee $\gamma\gamma$ contact term thus setting a limit on a new energy scale where QED breaks down of 100 GeV.

The future

Important aspects of future physics in which the UK groups plan to play an important role are:

(a) continued exploitation of the microvertex detector for heavy flavour physics and later at LEP200 in the search for Higgs etc,
(b) high statistics particle searches at the Z
(c) preparation for W^+W^- physics at LEP200
(d) electroweak physics, especially τ physics
(e) QCD and the parton showering process.

These will keep the ALEPH team busy with physics for a long time to come.

Physics publications and preprints

1. Measurement of the charged particle multiplicity distribution in hadronic Z decays.
   ALEPH D Decamp et al. Phys. Lett. B273 (1991) 18.

2. Improved measurements of electroweak parameters from Z decays into fermion pairs.
   ALEPH D Decamp et al. Z Phys. C53 (1992) 1.

3. An investigation into intermittency.
ALEPH D Decamp et al. Z Phys. C53 (1992) 21.

4. Measurement of the absolute luminosity with the ALEPH detector.
ALEPH D Decamp et al. Z Phys. C53 (1992) 375.

5. Electroweak parameters of the Z resonance and the standard model.
The LEP collaborations Phys. Lett. B276 (1992) 247.

6. Evidence for b baryons in Z decays.
ALEPH D Decamp et al. Phys. Lett. B278 (1992) 209.

7. Measurement of the τ lepton lifetime.
ALEPH D Decamp et al. Phys. Lett. B279 (1992) 411.

8. A study of Bose-Einstein correlations in e^+e^- annihilations at 91 GeV.
ALEPH D Decamp et al. Z Phys. C54 (1992) 75.

9. Measurement of τ branching ratios.
ALEPH D Decamp et al. Z Phys. C54 (1992) 211.

10. Evidence for the triple-gluon vertex from measurements of the QCD colour factors in Z decay into four jets.
ALEPH D Decamp et al. Phys. Lett. B284 (1992) 151.

11. Measurement of $\alpha(s)$ in hadronic Z decays using all-orders resummed predictions.
ALEPH D Decamp et al. Phys. Lett. B284 (1992) 163.

12. Measurement of $B\text{-}\bar{B}$ mixing at the Z using a jet-charge method.
ALEPH D Buskulic et al. Phys. Lett. B284 (1992) 177.

13. Search for a very light CP-odd neutral Higgs boson of the MSSM.
ALEPH D Buskulic et al. Phys. Lett. B285 (1992) 309.

14. Searches for new particles in Z decays using the ALEPH detector.
ALEPH D Decamp et al. Phys. Rep. 216 (1992) 253.

15. Properties of hadronic Z decays and a test of QCD generators.
ALEPH D Buskulic et al. Z. Phys. C55 (1992) 209.

16. Measurement of the production rates of η and η' in hadronic Z decays
ALEPH D Buskulic et al. Phys. Lett. B292 (1992) 210.

17. Observation of the semileptonic decays of B_s and Λ_b hadrons at LEP
ALEPH D Buskulic et al. CERN-PPE/92-73.

18. Updated measurement of the average B hadron lifetime

ALEPH D Buskulic et al. CERN-PPE/92-133.

19. A measurement of the b baryon lifetime
ALEPH D Buskulic et al. CERN-PPE/92-138.

20. Measurement of prompt photon production in hadronic Z decays
ALEPH D Buskulic et al. CERN-PPE/92-143.

Theses submitted since last year's report

Imperial College

A.M. Greene — The forward-backward charge asymmetry in $e^+e^- \rightarrow b\bar{b}$ near $s=Mz^2$

N. Lieske — Intermittency in hadronic events from Z decays

Lancaster

M. Nuttall — Tau lepton polarisation from the three charged pion decay channel (RALT 132)

Sheffield

R. Carney — Differentiation between quark induced and gluon induced hadronic jets

P. Reeves — A measurement of the inclusive cross sections and fractions of stable hadrons and a study of proton-antiproton correlations at the Z resonance

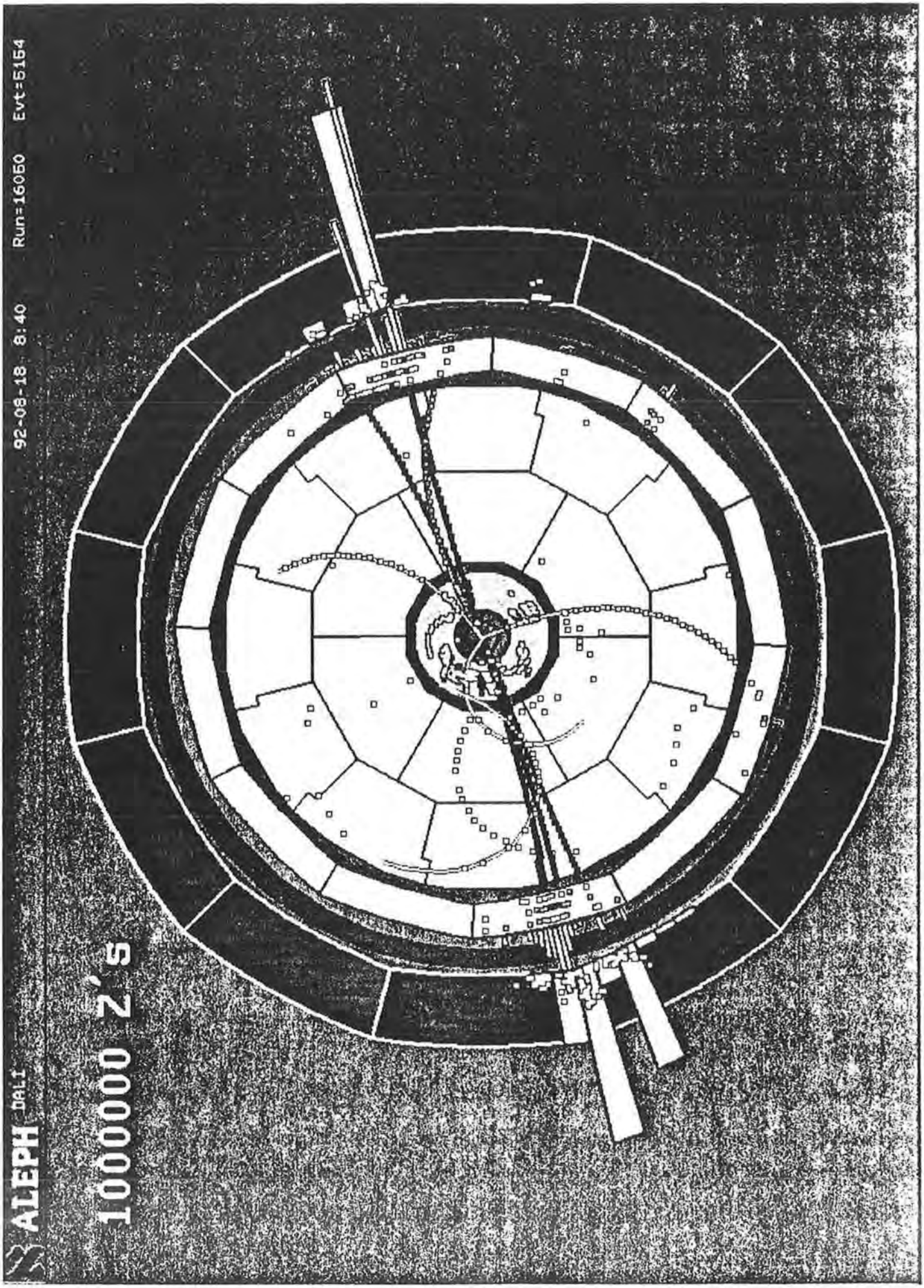

Fig 1

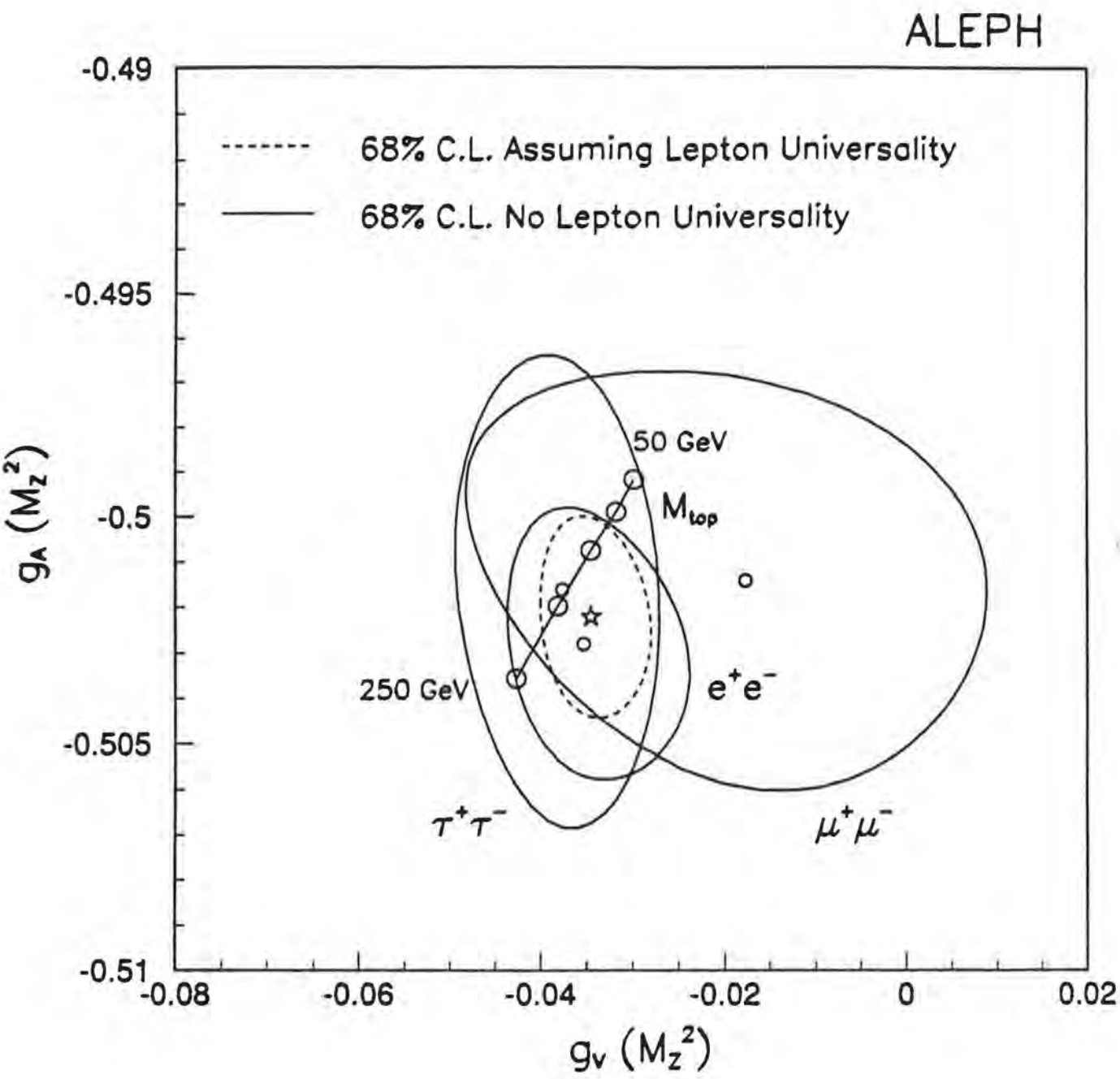

Probability contours for $g_V(M_Z^2)$ and $g_A(M_Z^2)$ for each lepton species from leptonic forward-backward asymmetries and τ polarization. Also shown is the result assuming lepton universality. The points are the expectations of the Standard Model for top masses from 50 to 250 GeV, assuming $\alpha_s = 0.125 \pm 0.005$ and $M_{\text{Higgs}} = 300$ GeV.

Fig 2

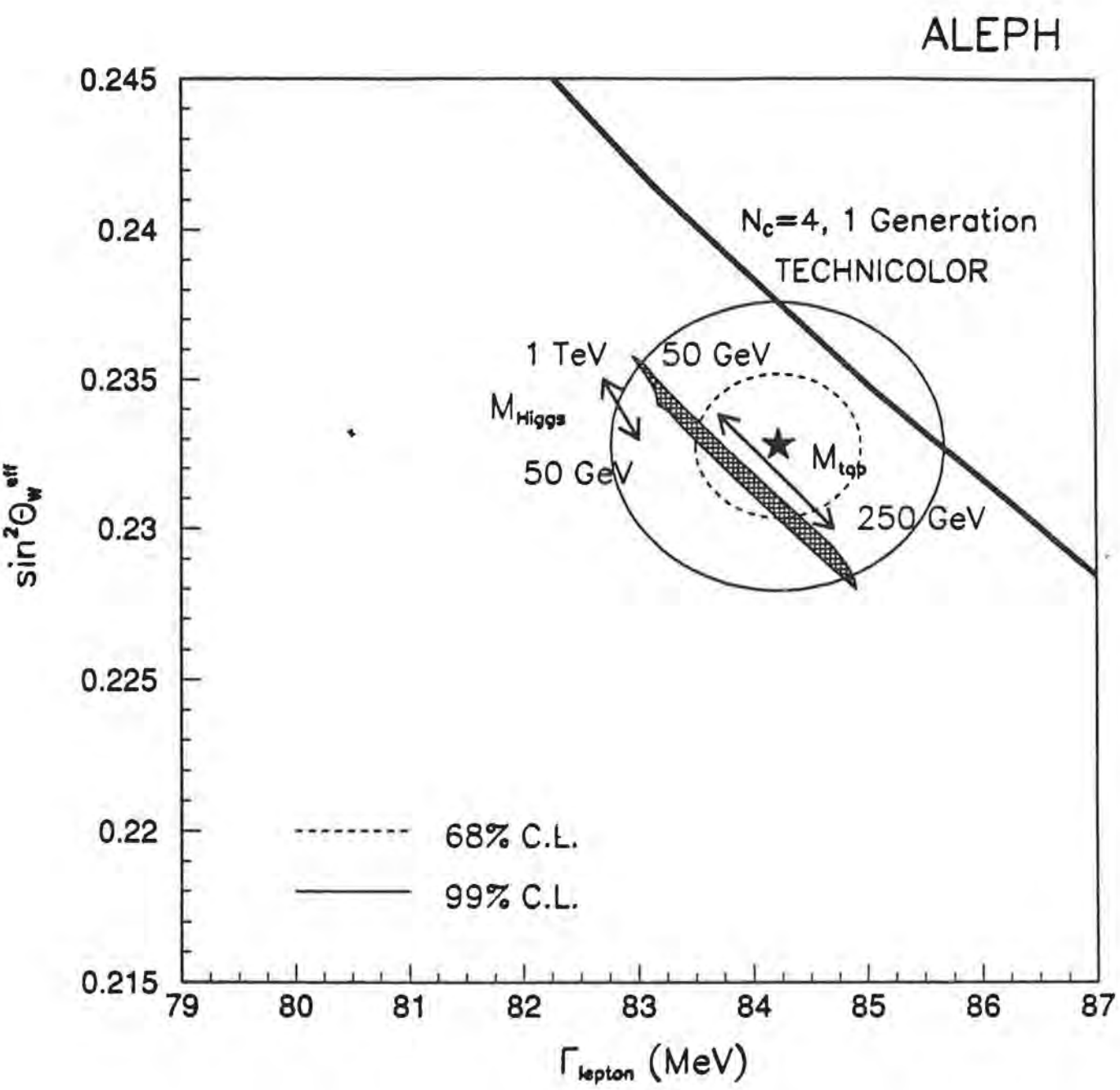

Contours of constant χ^2 for $\sin^2\theta_W^{eff}$ from asymmetry measurements versus Γ_ℓ. The Standard Model predictions as a function of M_{top} and M_{Higgs} are shown. The expectation for one generation of technifermions in $N_c = 4$ technicolor is indicated also.

Fig 3

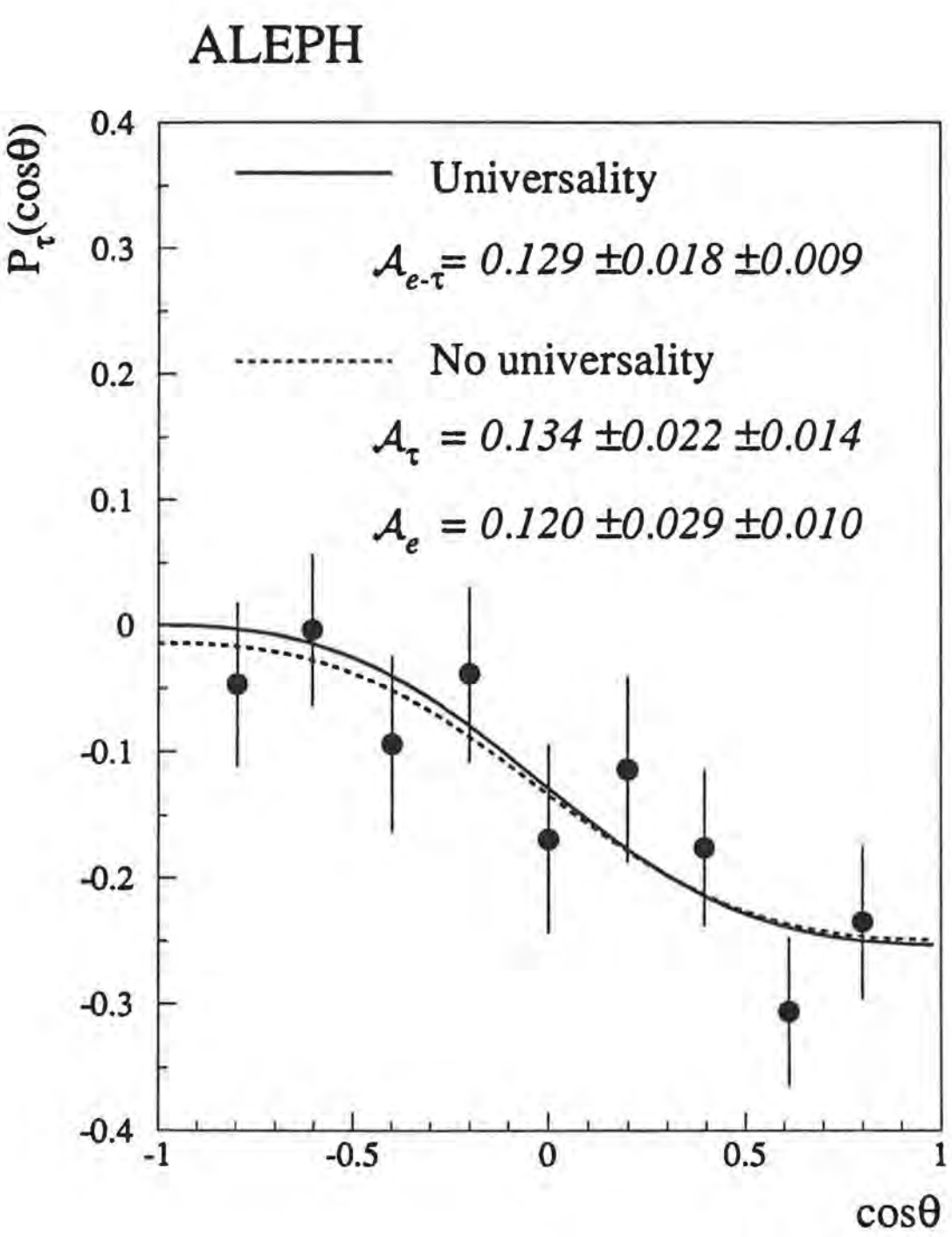

Result of global fit to $P(\cos\theta)$ for the combined 1990 and 1991 data. The overall scale is fit separately in each bin in order to avoid dependence on the Monte Carlo $\cos\theta$ distribution. The error bars show all uncertainty due to random fluctuations, including those from the data and the Monte Carlo. The solid (dashed) line shows the fit curve with (without) the assumption of tau-electron universality.

Fig 4

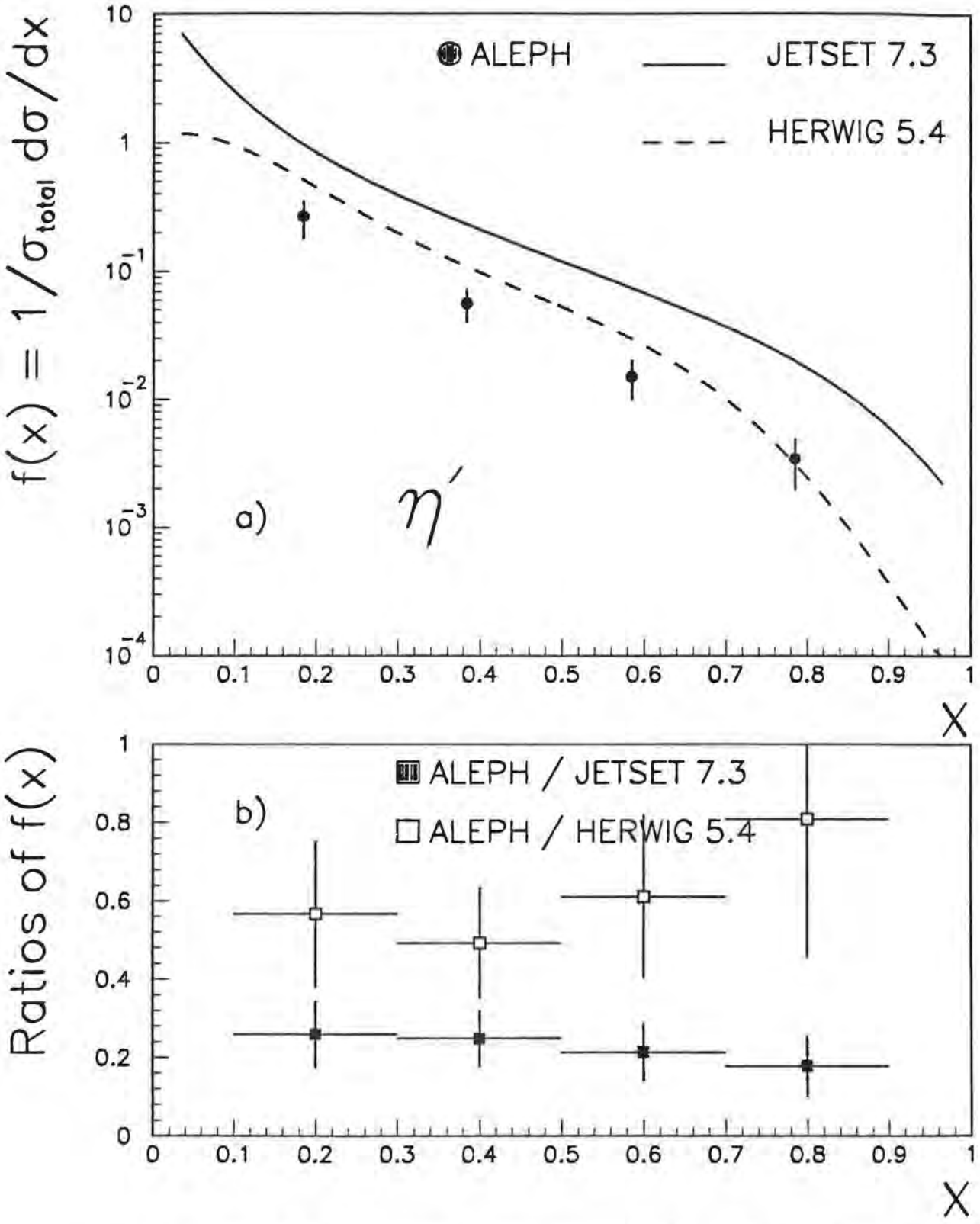

a) The corrected η' fragmentation function compared with the predictions from JETSET 7.3 and HERWIG 5.4. b) The ratios of the fragmentation functions. All errors shown are statistical only.

Fig 5

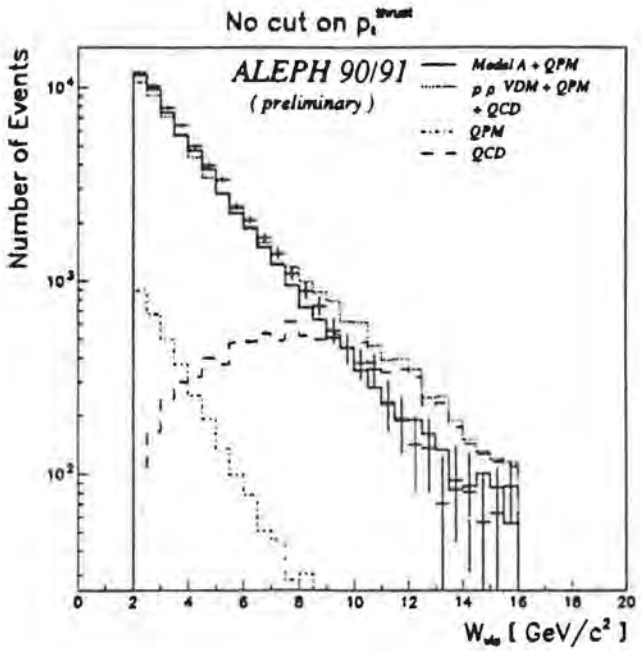

W_{vis} distribution for all events

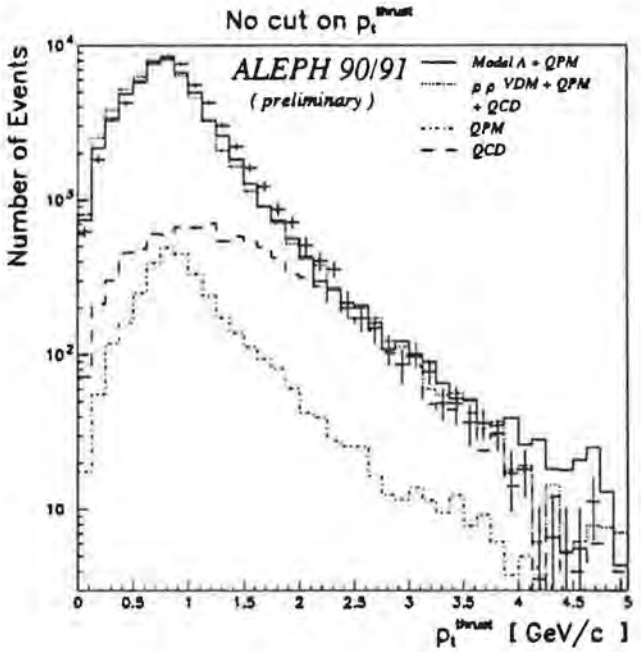

p_t^{Thrust} distribution for all events

Fig 6 a, b

THE OPAL EXPERIMENT AT LEP

PROPOSAL 720

Birmingham; Bologna; Bonn; Brunel; Cambridge; Carleton; CERN; Chicago; CRPP Canada; Freiburg; Hamburg/DESY; Heidelberg; Indiana; Manchester; Maryland; Montreal; Oregon; Queen Mary and Westfield College, London; Riverside; Rutherford Appleton Laboratory; Saclay; Technion; Tel Aviv; Tokyo; University College/Birkbeck College, London; Vancouver (UBC); Victoria; Weizmann Institute.

INTRODUCTION

The performance of LEP during the latter part of 1992 has been excellent and OPAL has operated with very high efficiency throughout the run, the third major data-taking period at LEP. Thus, despite a rather disappointing start-up of the accelerator this year, the number of $Z^0 \rightarrow$ hadron events recorded by OPAL passed 1 million before the end of September, with the 1992 run accounting for more than half the total. An impressive rate of publication of papers has been maintained and the number published or submitted for publication is now 63.

During the 1991/92 shutdown a pre-trigger stage was introduced into the OPAL trigger to allow fully efficient operation with an 11.1 μs beam-crossing interval, in preparation for 8*8 bunch operation of LEP. This required extensive modifications, not only to the global trigger logic, but also to the read-out and trigger electronics of some sub-detectors. The new system has operated successfully during all LEP test runs with 8*8 bunches.

The following sections outline the contributions made to OPAL in the past year by UK groups.

DETECTOR OPERATION

Barrel Muon Detectors

The 110 large-area drift chambers of the Barrel Muon detector were built by Manchester University, who remain responsible for their maintenance. They have continued to run smoothly and efficiently throughout 1992, providing 2-dimensional co-ordinate measurements of the tracks of particles which penetrate through to the outer part of the OPAL detector, with a resolution of 2 mm in both directions.

During the year, improvements to the readout system have increased the readout speed, lowering dead-times. It is now possible to extract the full pulse information online, significantly reducing the size of the raw data records written to storage media.

End cap Muon Chambers

The University of Birmingham is responsible for these detectors, which consist of limited streamer chambers covering an area of 12×12 m^2 at each end of OPAL. During the 1991/92 shutdown, a significant modification was made to the read-out to enable a pre-trigger to be obtained within an 11.1 μs cycle time. Additional on-line monitoring was implemented at the same time, and the new system has performed well throughout the year. Steady

progress has been made in reducing the number of inactive channels (approximately 1% of the total).

Shortening the integration time for the signals decreased the triggering efficiency, however test data collected at the end of the 1991 run demonstrated that it would be possible to compensate for this by lowering the trigger threshold, without causing an unacceptable increase in the rate of spurious triggers. As a consequence, the detector performance in 1992 has been as good as that in 1991, despite the shorter cycle time. The modified LEP optics, introduced this year, has not caused beam-induced background to increase from its previous low level.

Vertex Drift Chamber & Track Trigger

Both these devices are the responsibility in the UK of the Cambridge and QMW groups, with the support of the RAL Electronics Division. Throughout 1992, the Vertex Drift Chamber and the Track Trigger processor continued to operate to a very high standard with excellent efficiency. The drift chamber provided r-ϕ co-ordinates with a precision between 50 and 60 μm, as well as z co-ordinates with $\sigma(z)$ around 700 μm from stereo wires. The fast measurement of z from time-difference was used as input to the Track Trigger processor in the form of z/r values. A genuine event from the interaction region provides constant values of z/r for all digitizings along the trajectory of each emerging particle. By comparing such values as measured in the Vertex Chamber with those in the surrounding Jet Chamber, good events are accepted and background processes are vetoed. Prior to the 1992 running, the electronics for both the chamber and the trigger processor were modified to be compatible with 8*8 bunch operation of LEP. The read-out for the chamber was upgraded to reduce deadtime, and the processor was modified to allow the use of Track Trigger information in the event pre-trigger.

During 1992 a significant improvement in both the absolute precision and the quality of OPAL r-ϕ tracking has been achieved by integrating the chamber data with that from the new silicon strip microvertex detector. This has resulted in enhanced impact parameter resolutions for prompt tracks from the interaction point (figure 1) as well as greatly improving the reconstruction of secondary decay vertices from short-lived states.

End cap Lead Glass Calorimeters

The endcap electromagnetic calorimeter, consisting of 2264 lead glass shower counters, is the responsibility of RAL together with Cambridge and QMW. It has continued to perform extremely reliably throughout 1992. The only substantial changes to the subdetector during the Christmas shutdown were the installation of a pre-trigger (see below), to cope with 8*8 bunch running of LEP, and the addition of a second microprocessor in the acquisition system, pioneering a collaboration-wide improvement in readout times. Offline, to supplement the test beam calibration of all lead glass assemblies before installation into OPAL, 70% of the assemblies have now been calibrated in situ to 1.5%, using $e^+e^- \rightarrow e^+e^-$ events from the 1990 and 1991 data taking. Together with a fine tuning of the θ dependence of the detector response, this has improved the energy resolution by 30%, both for 45 GeV electrons in Bhabha scattering events and for photons at lower energies (figure 2).

Forward Detectors

The absolute luminosity is used to normalise all measured cross sections. Thus the determination of this quantity is a crucial ingredient in fitting the parameters of the

electroweak theory, which is based on measurements of the charged-lepton, neutrino and hadronic channels at the peak of the Z^0. University College London has been responsible for extracting the absolute luminosity for 1991 and 1992. The technique involves the use of well-surveyed drift chambers (UCL) to survey a set of proportional tubes (Brunel University/UCL) which are buried deep inside the Forward Calorimeter (U. of Maryland/UCL/Bologna). As LEP statistics have increased it has been necessary to improve the precision of this survey in order to make increasingly accurate selection cuts on the minimum (~ 60 mr) and maximum (~ 110mr) scattering angles of small-angle Bhabha scattering events. In 1992, the UCL group installed a new set of drift chambers with sense-wires close to the minimum cut angle. These chambers have been used, in conjunction with the older chambers whose wires are close to the outer cut angle, to give a luminosity measurement with a systematic error of less than 0.65%. A more precise Monte Carlo model of the Forward Detector has been developed at UCL for this analysis, and 100,000 events have been generated on the UCL and Brunel Vax clusters. For the 1992 data, the corresponding error is expected to be less than 0.5%.

Brunel and Birkbeck College are performing an independent measurement of the luminosity, using a set of precise scintillators. Birkbeck has continued to develop the Far-forward Luminosity Monitor, which gives fast feed-back on short term luminosity changes during a LEP run.

UPGRADE PROJECTS

The Silicon Microvertex Detector

The Silicon Microvertex Detector was designed by, and is the continuing responsibility of, the Cambridge and QMW groups. It has completed its second successful year as the high precision component of the OPAL inner tracking. It consists of two layers of single-sided microstrip ladders, of which there are 25 in total, situated at radii of 6.1 and 7.5 cm around a beryllium beam-pipe.

The individual silicon wafers are 300 μm thick, having implant strips separated by 25 μm, with a/c coupled readout to metallised strips at a pitch of 50 μm. These devices were designed by the Cambridge and QMW groups in association with Micron Semiconductors Ltd (UK), who manufactured them. The strips are biassed by a new FOXFET scheme that allows dynamic resistance control which provides excellent signal to noise performance, with a value of better than 22:1 for a complete OPAL ladder of three daisy-chained wafers. The r-ϕ co-ordinate is measured to a precision of 5 μm, and incorporated into physics analyses after detector alignment with an uncertainty close to 10 μm. Each ladder has a digitizing efficiency of about 97%.

Much of the associated VLSI electronics, including the MX5 readout chip and the local on-board sequencer, were designed by Cambridge and RAL.

The complete detector has performed with excellent reliability and gives r-ϕ track co-ordinates of a new quality within the OPAL experiment, resulting in new analyses, particularly in the areas of τ and b physics.

The efforts of the two UK universities are also now at the heart of an advanced project for implementing a new microstrip detector into the OPAL experiment before the 1993 running period. This will maintain the same geometry as the current scheme but each ladder

will be capable of measuring both the r-ϕ and r-z track co-ordinates, and so extend further the physics potential of the experiment.

Lead Glass Trigger Upgrade

To cope with the 8*8 bunch running of LEP during 1992, a pre-trigger system with a decision time of 4 μs was added to the original 16 μs system during the 1991/92 shutdown. For the End Cap Electromagnetic Calorimeter this necessitated a redesign of the original analogue trigger, capitalising on OPAL's experience of FADCs in the inner tracking chambers to construct a fully digital pre-trigger and trigger system. The FASTBUS digital adding matrix to form the final pre-trigger and trigger decisions was designed and manufactured at RAL, and in collaboration with the RAL group, VME FADC modules were designed and manufactured in Heidelberg. This hardware was installed and commissioned before the 1992 LEP running. Additional FASTBUS digital to analogue conversion modules, designed and manufactured by the group at RAL, were added during the year to complete the system by allowing analogue summing of localised barrel and endcap calorimeter energy. The digital trigger has proved successful, working reliably with thresholds some 50% lower than those of the original analogue system. The pre-trigger, with a threshold of 350MeV deposited electromagnetic energy, has also proved successful, allowing a combined barrel and endcap electromagnetic pre-trigger efficiency for $e^+e^- \rightarrow \mu^+\mu^-$ of 96%, and 100% for $e^+e^- \rightarrow \tau^+\tau^-$ or e^+e^-, complementing the tracking chamber pre-triggers.

Silicon-Tungsten Luminosity Monitor

To gain full benefit from the expected statistics of 10^7 Z^0s during 1993 and 1994, it will be necessary to reduce the systematic error on the absolute luminosity even further. To this end, a precision Silicon-Tungsten (Si-W) luminometer is being built for installation during the 1992/93 shutdown. It will have an inner acceptance angle of 25 mr and be able to measure shower positions to within 20 μm, reducing the systematic error on the luminosity measurement to approximately 0.1%. The UK groups are contributing vital parts of this upgrade. Birmingham and RAL are developing specialised readout and triggering electronics. UCL is designing and building support, installation and survey systems and coordinating UK cabling effort. Brunel has constructed installation stages and has worked on the beam tests which indicate that the new luminometer will achieve the predicted performance.

PHYSICS RESULTS

During the past year, studies made by OPAL of the resonance line shape and forward-backward asymmetries have continued to improve the precision of the determination of the Z^0 parameters. The Manchester and Brunel groups are active in the study of $\mu^+\mu^-$ events, and Brunel, Cambridge, QMW and RAL have contributed to the work on the e^+e^- final state. The overall work on the leptonic final states is coordinated by a member of the Manchester group. The mass of the Z^0 is now measured by OPAL to be 91.180 ± 0.007 (exp.) ± 0.006 (LEP) GeV/c^2 and the total width Γ_z is $2.483 \pm 0.011 \pm 0.005$ GeV. Figure 3 shows a test of lepton universality in Z^0 decays; the forward-backward asymmetry A_{FB} (sensitive to the vector couplings) is plotted against the cross-section ratio $R_z = \Gamma_{had}/\Gamma\ell\ell$ (mainly sensitive to the axial vector couplings). The data are also now precise enough to test the γ - Z interference which leads to energy variation of A_{FB}; the parameter $C^a_{\gamma Z}$ which governs this energy dependence is measured to be 0.216 ± 0.018, compared with the Standard Model expectation of 0.25. Central

to these studies is the measurement of luminosity, for which the UCL and Brunel groups are now fully responsible.

Measurements of the decay properties of the τ-lepton provide many important tests of the Standard Model. The measurement of the τ polarisation is a crucial ingredient in the determination of the electroweak parameters, while the measurement of the lifetime and leptonic branching ratio permit a test of lepton universality. There are also unsolved problems in obtaining a consistent picture of the branching ratios. The Cambridge and Birmingham groups have been involved in extending muon and electron identification into the endcap regions for these studies, while the Manchester group has produced the most precise measurement of the topological branching ratios, obtaining:
$B_1 = 84.48 \pm 0.27$ (stat.) ± 0.23 (syst.)% and $B_3 = 15.26 \pm 0.26 \pm 0.22$%. A study of the decay $\tau^- \to \pi^+\pi^-\pi^-\nu$ is under way at RAL. The silicon microvertex detector, involving the QMW and Cambridge groups, has proved its value in a new determination of the τ lifetime (see Figure 4), $\tau_\tau = 290.0 \pm 6.0$ fs. Combining this value with the latest OPAL measurements of the leptonic branching fraction allows the ratio of the Fermi constants for τ and μ to be determined as $G_F^\tau / G_F^\mu = 0.990 \pm 0.013$.

Heavy quark physics is an area of major activity at present. One of the standard methods for tagging b-quarks is to identify jets containing leptons of high momentum and high p_T. The Cambridge group has been working on electron identification in the endcaps, and on the measurement of A_{FB} for b-quarks using electron tagging (see Figure 5). The present OPAL measurement, based on both electrons and muons, is:
$A_{FB}^b = 0.099 \pm 0.018$ (stat.) ± 0.010 (syst.) ± 0.006 (mixing) (after correction of $B^0 - \overline{B^0}$ mixing). This measurement, which is still statistically limited, is likely soon to provide one of the most stringent tests of the Standard Model. An essential related measurement is of the $B^0 - \overline{B^0}$ mixing parameter χ, for which the current OPAL value is $0.125^{+0.017}_{-0.016} \pm 0.015$; analyses of mixing using dilepton events are being carried out in Cambridge and in Birmingham.

Another method of tagging b-quarks uses the reconstruction of secondary decay vertices. The Cambridge and QMW groups have played a leading rôle in developing these techniques using the silicon microvertex detector, and are finding very encouraging results. The microvertex detector is also proving valuable in measuring the lifetimes of b-flavoured hadrons; the Cambridge, QMW and Birmingham groups are all involved in these studies. Other tagging techniques, based on the boosted sphericity product or using neural networks, are being pursued in Manchester, while D*-lepton correlations are being used in b-fragmentation work at Birmingham.

Statistics are now sufficient for the first observations at LEP of exclusive and semi-exclusive decays of hadrons containing b-quarks to be possible. This is an area in which much progress can be expected in future. Convincing evidence for the production of the Λ_b baryon and the B_s^0 meson has been obtained through the observation of Λ^0 in association with ℓ^-, and D_s^+ in association with ℓ^- respectively, where ℓ is a high p_T electron or muon (see Fig. 6). The QMW group has been strongly involved in this work, whilst studies of lifetimes of b-hadrons using these techniques have begun at Cambridge.

OPAL has been the leading LEP experiment in studies of QCD. A recent analysis (coordinated at Cambridge) of 15 different observables yielded a value of $\alpha_s(M_{Z0}) = 0.122^{+0.006}_{-0.005}$. The values from the different observables were consistent, after accounting for all experimental and theoretical errors (Figure 7), providing an important test of QCD. This analysis included the first application of recent "resummed" QCD calculations at LEP, and further work in this interesting new area is continuing at Cambridge and Birmingham. Measurements of α_s for b-quarks are proceeding at Manchester. In the field of soft QCD the Cambridge group has pursued several studies relating to soft gluon coherence effects, including a recently published study of two-particle momentum correlations, while the RAL group has been responsible for investigations of intermittency. Studies of fragmentation phenomena have been spearheaded at Manchester with a recent publication of measurements of vector meson production ($K^*(892)^0$ and $\phi(1020)$); Manchester is now in charge of coordinating all efforts in this area.

The search for the Higgs boson has now placed a lower mass limit of 54.2 GeV/c^2 at the 95% confidence level for the Standard Model Higgs. The UCL group has been particularly responsible for the search for a possible doubly-charged Higgs particle, placing a limit of 45.6 GeV/c^2. The RAL group has been involved in the investigation of "$\ell\ell$V" events, following evidence from ALEPH of an anomalous rate of $\tau^+\tau^-$V events. OPAL has found no evidence for an anomaly, with the observed rate of $\ell\ell$V events explicable in the terms of standard processes.

A process which has proved remarkably interesting at LEP is the $q\bar{q}\gamma$ final state, which permits a determination of the couplings of charge $\frac{1}{3}$ and charge $\frac{2}{3}$ quarks to the Z^0 as well as providing interesting tests of QCD. The RAL group is now in charge of extending the acceptance for final state photons in this reaction into the endcaps. The UCL group has been responsible for coordinating OPAL work on two-photon physics. First results were presented this year, and were well described by a mixture of Vector Meson Dominance and QCD. Results on the F_2 structure function of the photon are imminent.

OPAL Publications

1 A Study of Charged Particle Multiplicities in Hadronic Decays of the Z^0
P D Acton et al., Zeit. fuer Physik **C53** (1992) 539-554.

2 Properties of Multihadronic Events with a Final State Photon at $\sqrt{s} = M_Z{}^0$
P D Acton et al., Zeit. fuer Physik **C54** (1992) 193-209.

3 Measurement of the Average B Hadron Lifetime in Z^0 Decays
P D Acton et al., Phys. Letters **B274** (1992) 513-525.

4 Measurement of $B^0 - \overline{B^0}$ Mixing in Hadronic Z^0 Decays
P D Acton et al., Phys. Letters **B276** (1992) 379-392.

5 An Improved Measurement of α_s ($M_Z{}^0$) Using Energy Correlations with the OPAL detector at LEP
P D Acton et al., Phys. Letters **B276** (1992) 547-564.

6 Search for Free Gluons in Hadronic Z^0 Decays
P D Acton et al., Phys. Letters **B278** (1992) 485-494.

7 Electroweak Parameters of the Z^0 Resonance and the Standard Model
The LEP Collaborations : ALEPH, DELPHI, L3 and OPAL
Physics Letters **B276** (1992) 247-253.

8 Test of CP-invariance in $e^+e^- \rightarrow Z^0 \rightarrow \tau^+\tau^-$ and a limit on the weak dipole moment of the τ lepton
P D Acton et al., Phys. Letters **B281** (1992) 405-415.

9 A Global Determination of α_s ($M_z{}^0$) at LEP
P D Acton et al., Zeit. fuer Physik **C55** (1992) 1-24.

10 Evidence for b-flavoured Baryon Production in Z^0 Decays at LEP
P D Acton et al., Physics Letters **B281** (1992) 394-404.

11 A Measurement of Electron Production in Hadronic Z^0 Decays and a Determination of $\Gamma(Z^0 \rightarrow b\bar{b})$
P D Acton et al., Zeit. fuer Physik **C55** (1992) 191-207.

12 A Test of Higher Order Electroweak Theory in Z^0 Decays to Two Leptons with an Associated Pair of Charged Particles
P D Acton et al., Physics Letters **B287** (1992) 389-400.

13 Measurement of the τ Topological Branching Ratios at LEP
P D Acton et al., Physics Letters **B288** (1992) 373-385.

14 A Study of Two-particle Momentum Correlations in Hadronic Z^0 Decays
P D Acton et al., Physics Letters **B287** (1992) 401-412.

15 Inclusive Neutral Vector Meson Production in Hadronic Z^0 Decays
Submitted to Zeit. fuer Physik C. CERN-PPE/92-116.

16 A Measurement of Strange Baryon Production in Hadronic Z^0 Decays
P D Acton et al., Physics Letters **B291** (1992) 503-518.

17 A Measurement of the Forward-Backward Charge Asymmetry in Hadronic Decays of the Z^0
P D Acton et al., Submitted to Physics Letter B. CERN-PPE 92-119.

18 A Search for Doubly-charged Higgs Production in Z^0 Decays
P D Acton et al., Submitted to Physics Letters B. CERN-PPE/92-144.

19 Evidence for the Existence of the Strange b-flavour Meson B_s^0 in Z^0 Decays
P D Acton et al., Submitted to Physics Letters B. CERN-PPE/92-144

20 The OPAL Silicon Microvertex Detector
P P Allport et al., accepted for publication in Nucl. Instr. and Methods A.

21 The Detector Simulation Program for the OPAL Experiment at LEP
J Allison et al., NIM A317 (1992) 47.

Conference Contributions and Review Articles by UK Physicists

1 Multiquadric Radial Basis Functions for Representing Multidimensional High Energy Physics Data -A New Smoothing Algorithm.
J Allison. CHEP92 (Computing in HEP), Annecy, 21st-25th September.

2 Current Status of the OPAL Silicon Microvertex Project
P P Allport, 3rd International Conference on Advanced Technology and Particle Physics Como Italy, June 1992.

3 Measurement of the τ topological branching ratios.
J Banks. Second workshop on τ lepton physics, Columbus, Ohio.

4 Recent Results from LEP
J R Batley, Summer School in High Energy Physics and Cosmology ICTP, Trieste, July 1992.

5 A Measurement of B^0 - $\overline{B^0}$ Mixing in Hadronic Z^0 Decays
V Gibson, XXVI Inter. Conf. on High Energy Physics, Dallas, 6-12 August.

6 The use of DEC-AVS for HEP event viewing
R Hughes-Jones, (With C Clavi). CHEP92 (Computing in HEP), Annecy, 21st-25th September.

7 Evidence for b-flavoured baryon production from OPAL.
R W L Jones XXVII Rencontre de Moriond, QCD 23-28 March 92

8 Recent Electroweak Results from LEP in Puzzles on the Electroweak Scale
B W Kennedy, Proceedings of the XIV International Warsaw Meeting on Elementary Particle Physics, Z Ajduk, S Pokorsi, A K Wroblewski (eds), world Scientific Singapore, 1992

9 Hadron Production in Singly-Tagged Two-Photon Collisions in the OPAL Experiment at LEP
B W Kennedy, Ninth International Workshop on Photon-Photon Collisions, UCSD La Jolla., California, March 1992 (In press)

10 Resonance Production in e^+e^- collisions
G Lafferty. XXVI Int. conf. on HEP, Dallas, 6 - 12 August.

11 Final State Decays of the Z^0
A J Martin, invited talk at the XII International Conference on Physics in Collision, Boulder, Colorado, June 1992.

12 Muon Production in Singly-Tagged Two-Photon Collisions in the OPAL Experiment at LEP
D J Miller, Ninth International Workshop on Photon-Photon Collisions, UCSD La Jolla., California, March 1992 (In press)

13 Higgs Searches at LEP
P Sherwood, Presented at the XXVIIth Rencontres de Moriond, Moriond, France, March 15-22 1992 (In Press)

14 Precision Tests of the Standard Model at LEP
C P Ward, XV International Warsaw Meeting on Elementary Particle Physics, Kazimierz, 25 - 29 May.

15 Tests of QCD at LEP
D R Ward, IOP Conference on HEP, Lancaster, 2 - 3 April

16 Measurements at LEP of the Forward-Backward asymmetries of quarks
T Wyatt. XXVI Int. conf. on HEP, Dallas, 6 - 12 August.

OPAL Research Theses by UK Students

1 A study of heavy quark production on the Z^0 resonance using muons at OPAL.
D L Rees, Ph.D. Thesis, Birmingham, February 1992. (RALT-129, 1992).

2 The detection and analysis of muons in leptonic decays of the Z^0 particle at OPAL
S J Hillier, Ph.D. Thesis, Birmingham, February 1992. (RALT-131, 1992).

3 Measurement of the $Z^0 \rightarrow b\bar{b}$ Branching Ratio at LEP.
S Pawley, Ph.D. Thesis, Manchester.

4 A measurement of $B^0 - \overline{B^0}$ mixing at LEP
M Moss, Ph.D. Thesis, Manchester.

5 Tests of QCD at the Z^0 Resonance
M F Turner, Ph.D. Thesis, Cambridge (December 1991) (RALT-126, 1992).

6 A Study of Tau Leptons Produced in Z^0 Decays
J Hart, Ph.D. Thesis, Cambridge (December 1991).

7 Drift Chamber Studies for the OPAL Forward Detector
K Ahmet, Ph.D. Thesis, Birkbeck College London (1992).

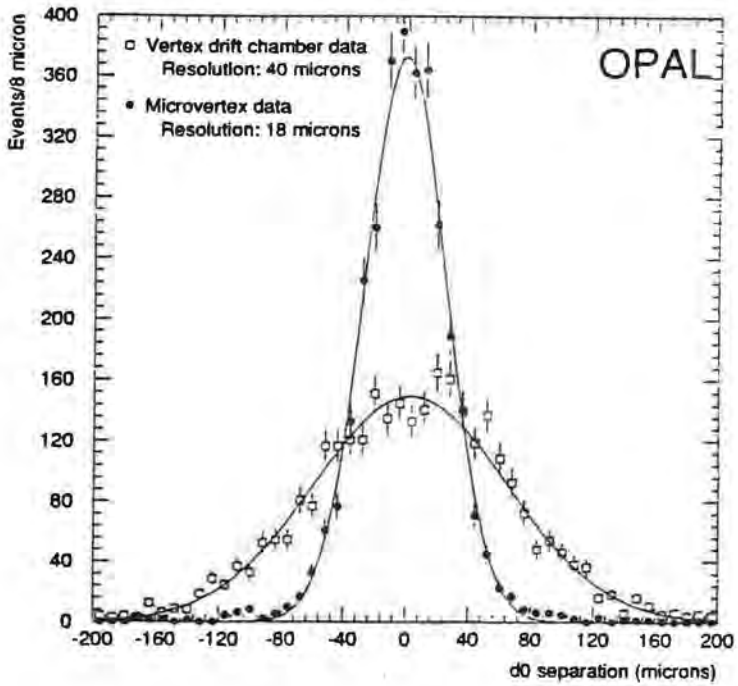

Figure 1 Measured impact parameter for $Z^0 \to e^+e^-$ and $Z^0 \to \mu^+\mu^-$ events in data with vertex drift chamber data only, and with silicon microvertex detector hits added to the tracks.

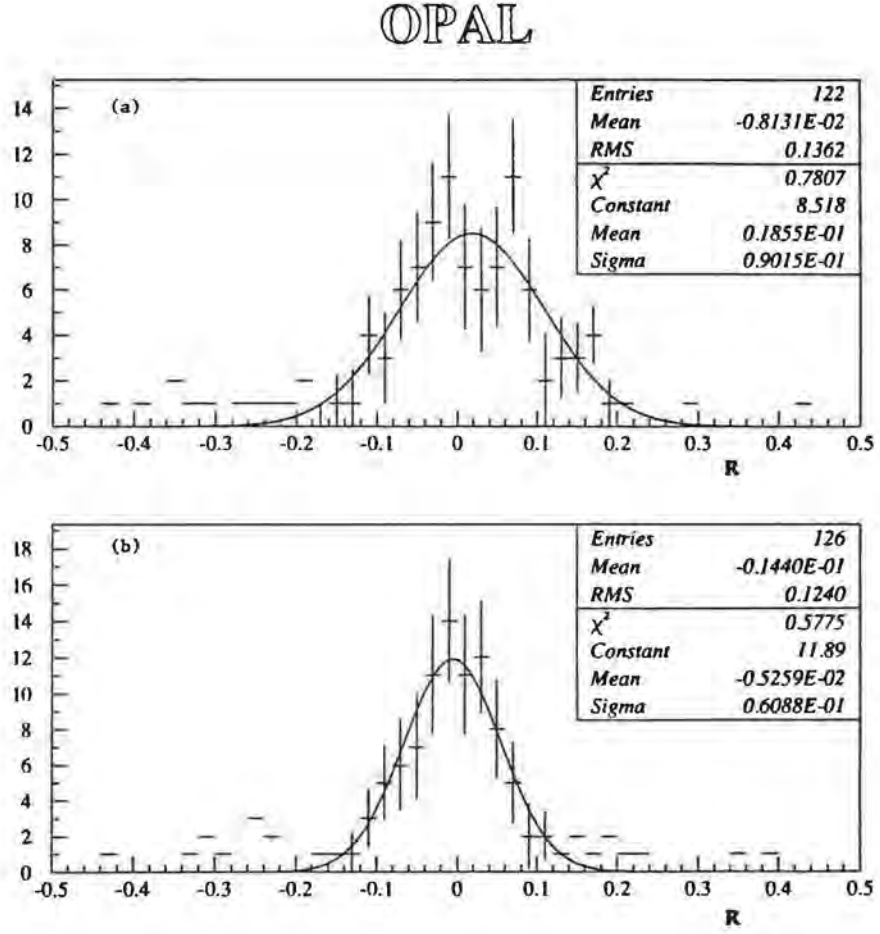

Figure 2 Distributions of the ratio $R = \frac{\text{(Measured Energy - Predicted Energy)}}{\text{Predicted Energy}}$ for photons from the reaction $e^+e^- \to e^+e^-\gamma$, with predicted energies in the range from 10 to 20 GeV, detected in the lead glass endcaps. Figure 2a was obtained using the original calibrations, measured in an electron beam before the start of the experiment; 2b shows results obtained after combining these calibrations with ones obtained from Bhabha scattering events.

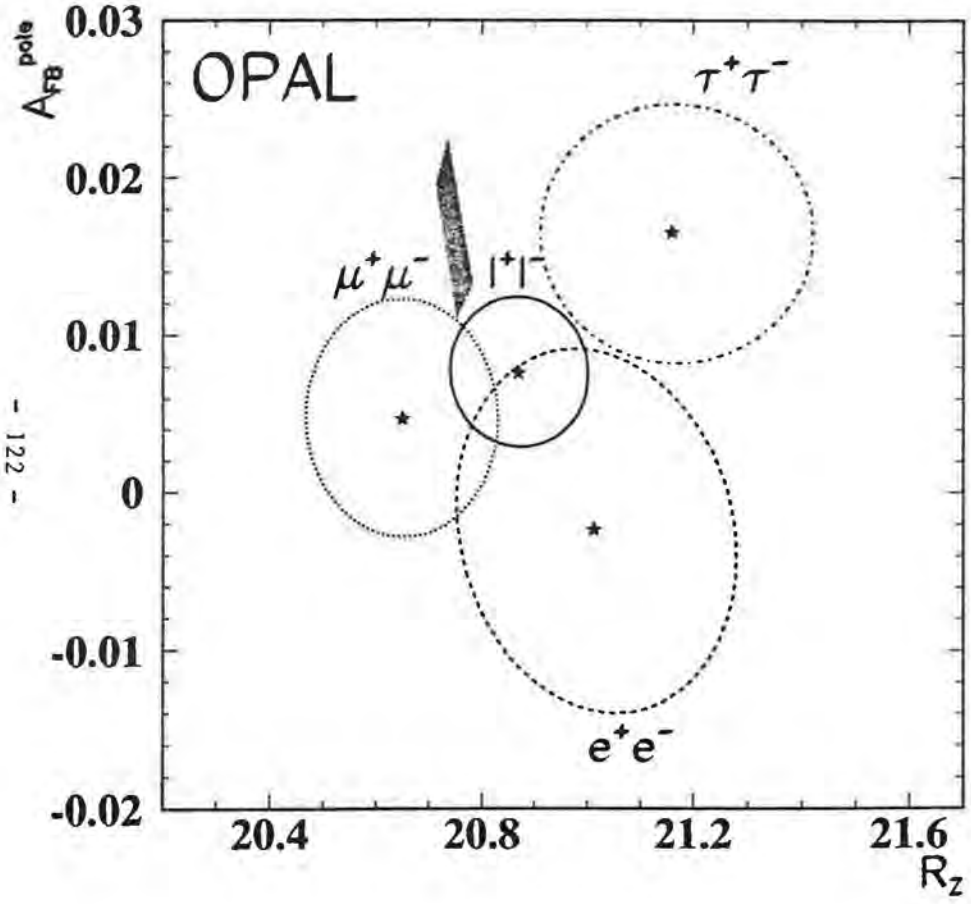

Figure 3 One standard deviation contours (38% probability) in the R_Z-A_{FB}^{pole} plane for each lepton species and for all leptons assuming lepton universality. The shaded area is the Standard Model prediction for $50 \leq M_t \leq 230$ GeV/c^2 and $50 \leq M_H \leq 1000$ GeV/c^2.

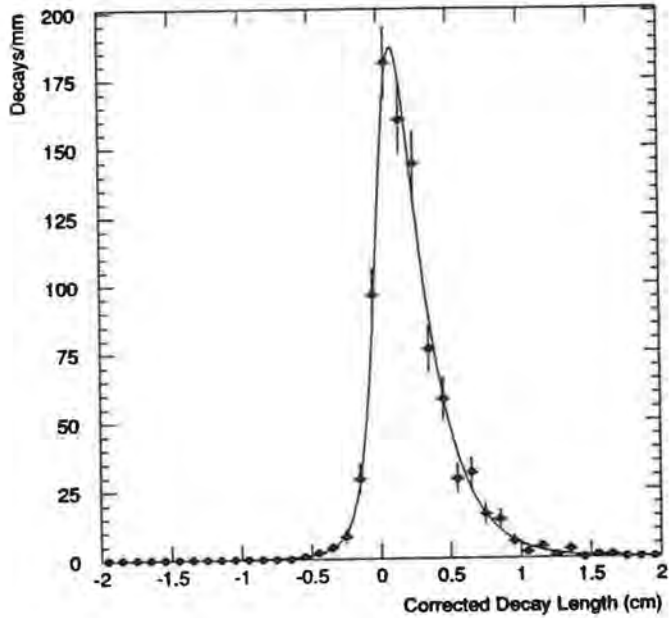

Figure 4 Distribution of decay lengths of 3-prong τ-lepton decays in OPAL, after data quality cuts (e.g. requiring silicon hits on each track, and a good vertex fit). The curve is the result of a maximum likelihood fit to determine τ_τ.

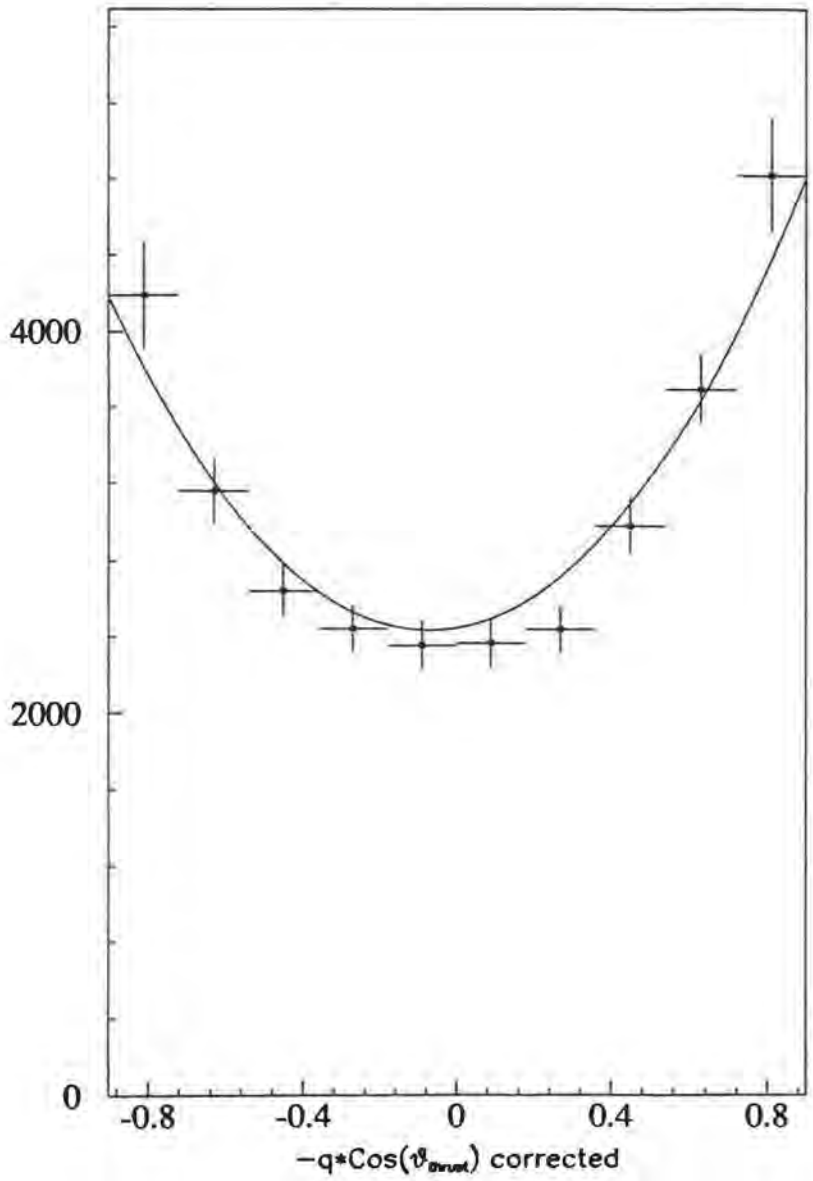

Figure 5 Angular distribution of b-quarks tagged by high p_T electrons. The charge of the b-quark is inferred from the charge of the lepton. The curve shows a least χ^2 fit to the form $1+\cos^2\theta+\frac{8}{3}A_{FB}\cos\theta$ from which A_{FB} is obtained.

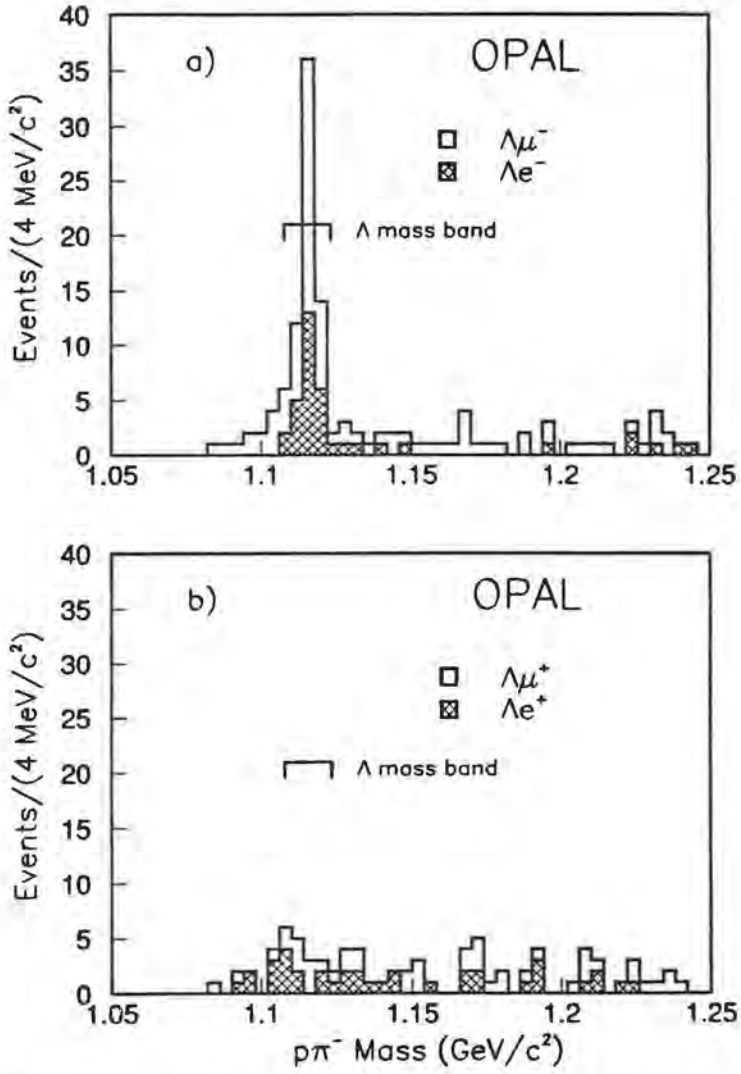

Figure 6 (6a) shows the $p\pi^-$ invariant mass distribution of the Λ candidates associated with e^-(hatched histogram) and of Λ candidates associated with μ^- (open histogram). (6b) shows the $p\pi^-$ invariant mass distribution of the Λ candidates associated with e^+ (hatched histogram) and of Λ candidates associated with μ^+ (open histogram). The observation of Λ particles correlated with ℓ^-, together with their absence in association with ℓ^+ is evidence for the decay $\Lambda_b \to \Lambda\ell^-\bar{\nu}X$.

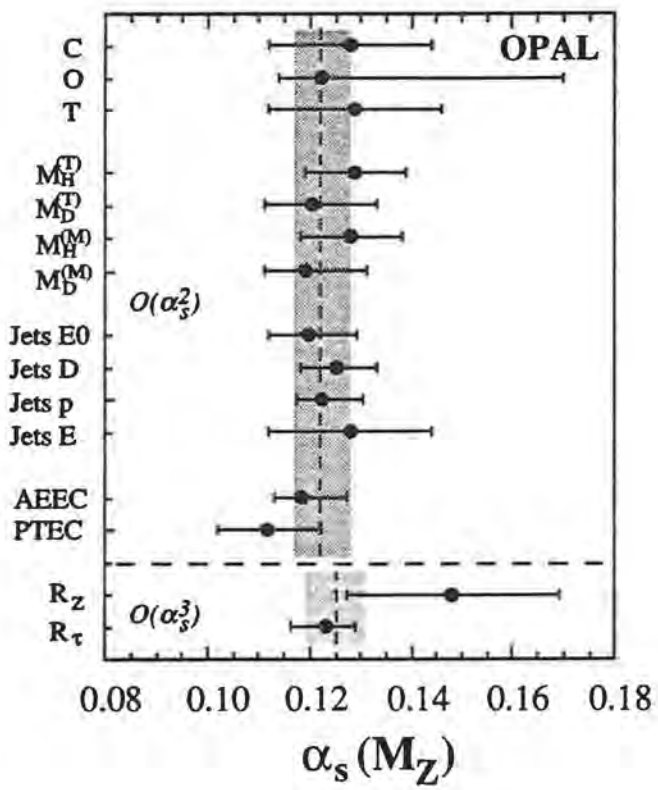

Figure 7 Compilation of measurements of $\alpha_s(M_{Z^0})$ for $\mu = M_{Z^0}$; the statistical errors are combined with experimental and theoretical systematic uncertainties. The final combined result is indicated by the shaded bands, $\alpha_s(M_{Z^0}) = 0.122^{+0.006}_{-0.005}$ from the measurements in $O(\alpha_s^2)$, and $\alpha_s(M_{Z^0}) = 0.125 \pm 0.006$ from the two $O(\alpha_s^3)$ results.

Ames; Antwerp; Athens; Bergen; Bologna; College de France; CERN; CRN (Strasbourg); Demokritos; Genova; Helsinki; IIHE (Brussels); JINR Dubna; KFK (Karlsruhe); Krakow; LAL (Orsay); Lisbon; **Liverpool**; LPNHE (Paris VI); Lund; Milano; Mons; NBI (Copenhagen); NIKHEF (Amsterdam); Oslo; **Oxford**; Padova; **RAL**; Rio de Janeiro; Saclay; Sanita (Rome); Santander; Serpukhov; Stockholm; Tech Univ Athens; Torino; Trieste; Udine; Uppsala; Valencia; Vienna; Warsaw; Wuppertal.

Physics Results in 1992:

Publications on physics topics studied with the DELPHI detector this year have covered 1) tests of the Standard Model by measuring the Z^0 peak cross section, line shape and forward-backward asymmetry for leptonic and hadronic final states[1,12], and by measuring the polarisation of the τ lepton[14] produced in $Z^0 \to \tau^+\tau^-$ decay; 2) explicit searches for neutral Higgs bosons[5], excited charged leptons[2], heavy neutrinos[6], heavy scalar leptoquarks[7] and unexpected multi-photon final states[3]; 3) detailed studies of the properties of 'normal' hadronic decays of the Z^0 [8,10,15,16,19] and a more precise determinations of α_s [9]; and 4) measurements of the coupling of the Z^0 to heavy quarks using not only high p_t leptons[17] but also the boosted sphericity product[13] and a variety of indicators combined by a neural network[20] to distinguish heavy quark from light quark production, and measurement of the forward-backward asymmetry in $Z^0 \to b\bar{b}$ production[11]; 5) measurements of the average lifetime of B hadrons[4], the detection of B_s mesons and a first estimate of their lifetime[18], and the measurement of the separate lifetimes of B^+ and B^0 mesons using events containing a reconstructed D meson and a charged lepton in the same jet[21].

In addition, approximately 40 further papers were presented at the Dallas HEP Conference in August and are currently being prepared for publication.

The following briefly summarises some of the studies in which UK physicists have been most recently and most heavily involved:

1) Standard Model Tests:

Measurements of the mass and the partial and total widths of the Z^0 together with the forward-backward asymmetries in Z^0 decay provide a powerful test of the Standard Model. Improvements in the precision of the LEP energy scale, in the understanding of systematic errors, in the statistics available and in the analysis methods combine to give substantially tighter constraints on the parameters of the Standard Model and on the possible existence of new physics. Compared with the results of a year ago, the experimental errors are now about a factor 2 smaller.

The results may be expressed in many ways.

Fits to the absolute cross sections for $e^+e^- \to$ hadrons and $e^+e^- \to$ leptons and their energy dependences ('line shapes') and the forward-backward asymmetries for $e^+e^- \to$ leptons using the data taken in 1990 and 1991 yielded the following preliminary values (reported at the Dallas conference) for the unfolded Born cross section at the Z^0 pole and the mass and the total width of the Z^0 : $\sigma_0 = 40.86 \pm 0.28$ pb, $M_Z = 91.188 \pm 0.010$ GeV, and $\Gamma_Z = 2.488 \pm 0.012$ GeV. The ratios R between hadronic and leptonic decays were found to be $R_{\mu\mu} = 20.92 \pm 0.22$, $R_{\tau\tau} = 20.69 \pm 0.30$ and $R_{ee} = 20.79 \pm 0.28$ and the forward-backward asymmetry parameters A^0 were found to be $A^0_{\mu\mu} = 0.015 \pm 0.008$, $A^0_{\tau\tau} = 0.033 \pm 0.010$ and $A^0_{ee} = 0.013 \pm 0.013$. The three R values and the three A^0 values are fully consistent with the expected universality of the coupling of the Z^0 to charged leptons. Their averaged values are $R_{\ell} = 20.82 \pm 0.16$ and $A^0_{\ell} = 0.020 \pm 0.006$.

Values can also be extracted for the squared vector and axial vector couplings of the Z^0 to charged leptons, $V_l^2 = 0.00169 \pm 0.00049$ and $A_l^2 = 0.2479 \pm 0.0016$ and for the visible and hadronic widths, $\Gamma_{\rm inv} = 512.0 \pm 10.4$ MeV and $\Gamma_{\rm had} = 1727 \pm 12$ MeV. Assuming also the value of the strong

coupling constant measured by DELPHI, $\alpha_s = 0.123^{+0.005}_{-0.006}$, and using the Minimal Standard Model to predict $R_{\ell\ell}$ gives

$$N_\nu = 3.10 \pm 0.05$$

as the number of light neutrino species. Alternatively, the value of $R_{\ell\ell}$ may be used to extract the value $\alpha_s = 0.129 \pm 0.025$.

Within the Minimal Standard Model, all electroweak observables can be predicted given the measured values of the electromagnetic and weak couplings α and G_F, the Z^0 mass M_Z and the known fermion masses, and assuming values for the top mass ($m_t = 140$ GeV) and Higgs mass ($m_H = 100$ GeV). The data are in good agreement with these predictions. New physics, as well as deviations of m_t and m_H from the values assumed, will show up in the values of ρ or $\sin^2\theta_W^{\overline{MS}}$ extracted from the data or, alternatively, in the extracted values of two related parameters S and T being non-zero. The values obtained from DELPHI data are

$$S = -1.79 \pm 1.09$$

$$T = -0.68 \pm 0.69.$$

These two values are correlated, as shown in Fig.1. The top mass value extracted is

$$m_t = 130^{+48}_{\cdots}(\text{expt})^{+21}_{-22}(\text{Higgs}) \ \text{GeV}$$

where the lower limit is below that determined by CDF and the Higgs mass is taken to be uncertain between 60 to 1000 GeV.

Going beyond the Minimal Standard Model, as the production of any new particles would contribute to the visible or invisible width of the Z^0 , these measurements also provide stringent lower limits on the masses of possible new particles that are largely independent of the assumed behaviour of these particles after their production. In many cases (eg for new quarks, squarks and excited quarks as well as for heavy neutrinos, whether they decay or not) these lower mass limits are already very close to 45 GeV, the kinematical limit for pair production at LEP.

2) Heavy quark physics:

Semileptonic decays of B hadrons give rise to leptons with high momentum and high transverse momentum. This allows a statistical separation of $Z \to b\bar{b}$ events from other $Z \to q\bar{q}$ events from the distribution in momentum p and transverse momentum p_t of leptons identified in hadronic Z^0 decays. The preliminary value obtained using high p_t muons is $(\Gamma_{b\bar{b}}/\Gamma_{q\bar{q}}) \times \text{BR}(b \to \mu) = 0.0216 \pm 0.0012$. The B$\to \ell$ decay rate was measured from the ratio of single leptons to pairs of leptons in opposite jets at high p and p_t, $\text{BR}(\text{B} \to \ell) = 0.098 \pm 0.003(\text{stat}) \pm 0.011(\text{syst})$. Combining these values, when they are finalised, will allow the measurement of the Z^0 branching ratio $\Gamma_{b\bar{b}}/\Gamma_{q\bar{q}}$, which will be a fundamental test of the Standard Model.

The ratio of same-sign to opposite-sign pairs in di-lepton events can be studied as a function of momentum and transverse momentum of the leptons in order to extract the average probability χ of a $B\bar{B}$ oscillation. The current result from the 1990+91 data is $\chi = 0.121 \pm 0.042(\text{stat}) \pm 0.017(\text{syst})$. After correction for mixing, the preliminary value obtained from the 1990+1991 data, using single electrons and muons, for the forward-backward asymmetry in $e^+e^- \to Z^0 \to b\bar{b}$ production is $A^b_{FB} = 0.126 \pm 0.026(\text{stat}) \pm 0.016(\text{syst})$. This is higher than, but still in good agreement with, the value expected from the Minimal Standard Model.

Alternatively, instead of identifying $b\bar{b}$ events using high p and p_t leptons, one can use the difference in global event shape distributions between $b\bar{b}$ and other purely hadronic Z^0 decays that is due to the large mass of B hadrons, and the different impact parameter distribution in $Z \to b\bar{b}$ events due to the B decays present. This was done using a neural network in order to use the information in a statistically optimal way. The network, with three output nodes corresponding to $b\bar{b}$, $c\bar{c}$ and light-quark final states, was trained on Monte Carlo events fully simulated in the detector. The two

dimensional distribution of the output variables obtained from the data, renormalised to sum to unity, was then fitted as a weighted sum of the distributions expected from $b\bar{b}$, $c\bar{c}$ and light-quark final states according to the full simulation. The result was

$$\Gamma_{b\bar{b}}/\Gamma_{q\bar{q}} = 0.230 \pm 0.006(\text{stat}) \pm 0.015(\text{syst}).$$

Combining this with the LEP-average value of $(\Gamma_{b\bar{b}}/\Gamma_{q\bar{q}}) \times \text{BR}(b \to \ell)$ gives $\text{BR}(\text{B} \to \ell) = 0.101 \pm 0.008$.

3) Lifetime measurements:

A very successful UK-led upgrade of the microvertex detector was effected at the beginning of 1991, involving replacement of the aluminium beam pipe by a beryllium one of smaller radius and addition of a third layer of microstrip detectors, also at smaller radius. This led to greater efficiency and reliability of track associations as well as more precise extrapolations of tracks into the vertex region. The same detector is still in place and has taken data throughout in 1992. It was instrumental in the identification of B_s [18] and Λ_b decays in the 1991 data. The exploitation of this upgraded microvertex detector to identify short-lived particles and to measure their lifetimes is currently a major focus of interest.

Measurement of the τ lifetime provides an important precise test of universality. Conceptually, the simplest method is to reconstruct the τ decay points in 3-prong decays in 2-body $Z^0 \to \tau^+\tau^-$ events and thus, knowing the average Z^0 decay point at that time, to measure the τ flight path distribution directly. The result is shown in Fig.2. Another method is to fit the distribution of the impact parameter to the beam spot in 1-prong τ decays. In events containing two 1-prong decays one can also fit the miss distance between the two tracks (the difference of their two impact parameters) thus cancelling the dependence on the Z^0 decay point reconstruction, or the correlation between the sum of the two impact parameters and the acoplanarity of the two tracks, thus avoiding dependence on Monte Carlo simulation. All four methods were used. The results are $0.303 \pm 0.013 \pm 0.007$ ps from the vertex reconstruction method, $0.304 \pm 0.011 \pm 0.006$ ps from the impact parameter fit, $0.299 \pm 0.011 \pm 0.006$ ps from the back-to-back correlation and $0.301 \pm 0.009 \pm 0.006$ ps from the miss distance fit. The results from the last three methods are of course highly correlated. Taking this into account, the combined result is

$$\tau_\tau = 0.302 \pm 0.007 \pm 0.004 \text{ ps}$$

This result is a factor 3 more precise than that of last year.

From the flight path distribution of a sample of about 44 reconstructed J/ψ mesons, corresponding to an inclusive branching ratio of $\text{BR}(Z^0 \to J/\psi) = 0.00415 \pm 0.00075 \pm 0.00053$, an average B lifetime of $1.36 \pm 0.36 \pm 0.12$ ps has been found. This is potentially a very clean measurement which will always be statistics limited.

The measurements of the average B lifetime made using 1990 data, based on fitting the impact parameter distributions of inclusive high p_t tracks as well as identified muons of high p_t, have been repeated in these improved conditions. The analysis procedures have been improved substantially in order to minimise the systematic errors. The results are $\tau_B = 1.41 \pm 0.04 \pm 0.06$ from the inclusive analysis and $\tau_B = 1.36 \pm 0.05 \pm 0.05$ from the high p_t muon analysis. The combined result, taking the correlation between these two results into account, is

$$\tau_B = 1.39 \pm 0.06(\text{stat} + \text{syst}) \text{ ps}.$$

This result is almost a factor 2 more precise than that of last year.

More interestingly, B decay vertices have for the first time been reconstructed inclusively in sufficiently clean conditions that the charge of the B could be measured. To do this, jets from hadronic Z^0 decays were selected whose tracks were not consistent with coming from a single vertex and

in which there was a unique way of forming from them two vertices, the primary Z^0 decay vertex and a secondary vertex, with good probability. The invariant mass distribution of the selected secondary vertices is shown in Fig.3. Most of those with mass above 2.2 GeV are B decays. Each such vertex was then swum back towards the primary until it could no longer be distinguished by the criteria with which it had been selected. This gave the minimum detectable flight path for that B. The excess flight path above that minimum was then plotted, separately for neutral, charged and multiply charged vertices (these measure the small degree of charge confusion and allow it to be corrected for). The mean lifetimes of charged and neutral B mesons and their ratio were then extracted:

$$\tau_{B^-} = 1.47 \pm 0.15(\text{stat}) \pm 0.15(\text{exp syst})^{+0.35}_{-0.10}(\text{composition systematic})$$

$$\tau_{B^0} = 1.41 \pm 0.10(\text{stat}) \pm 0.15(\text{exp syst})^{+0.10}_{-0.08}(\text{composition systematic})$$

$$\tau_{B^-}/\tau_{B^0} = 0.96 \pm 0.14(\text{stat}) \pm 0.15(\text{exp syst})^{+0.10}_{-0.20}(\text{composition systematic})$$

where the composition systematics reflect the uncertainty in the fractions of B_s and Λ_b in the initial charge=0 sample.

Data taking in 1992:

The above physics analyses are based mainly on the data taken in 1991.

As a result of much hard work led by UK physicists, data-taking in 1992 has proceeded even more smoothly than in 1991 and the data-taking efficiency has averaged nearly 90%, so that DELPHI had collected over 600,000 hadronic Z^0 decays by mid-October this year. This is more than twice as much data as in 1991 and brings the grand total to over 1,000,000 hadronic Z^0 decays, which is at last a significant fraction (20%) of the statistics requested at LEP100. Equally importantly, the performance and reliability of the detector continue to improve as minor problems are ironed out one by one and better understanding of the individual detectors and of DELPHI as a whole is achieved.

The hardware items for which UK groups have responsibility, namely the Outer Detector, Barrel Muon Detector and Micro-vertex Detector, all continue to perform excellently. In addition, the commissioning of the Barrel Ring Image Cherenkov (BRICH) detector and of one quadrant of the Forward RICH detector was successfully completed this year. These extremely difficult detectors are now routinely taking physics data and are being used successfully in physics analyses.

Future developments:

The Forward RICH detector will be completed before data-taking resumes in 1993.

Work is in progress towards upgrading the Micro-vertex Detector by replacing the outer and closer layer of single-sided silicon strip detectors by double-sided detectors yielding precise z as well as precise $r\phi$ coordinates. This upgrade, which will substantially improve the b-tagging capability of DELPHI and is UK-led, will be made as soon as enough double-sided detectors are available from the manufacturers. Hopefully this too can be done before data-taking resumes in 1993.

Finally a proposal has been submitted to further upgrade the Micro-vertex Detector in two years time, at the start of LEP200 running, by doubling its length and, if possible, by further reducing the beam-pipe radius. The aim is to maximise the acceptance for efficient b-tagging. This is of critical importance for the search for Higgs bosons at LEP200, in particular for distinguishing the process $e^+e^- \rightarrow$ZH from $e^+e^- \rightarrow$ZZ and $e^+e^- \rightarrow$WW since the search will then be covering Higgs masses in the range of the W and Z masses. The UK groups intend to participate in this upgrade. Other upgrades aimed at maximising the hermeticity of DELPHI, both for tracking and calorimetry, are proposed on the same time-scale.

DELPHI Publications in the last year:

1. Determination of Z^0 resonance parameters and couplings
   from its hadronic and leptonic decays
   P.Abreu et al.
   Nucl. Phys. B367 (1991) 511

2. Search for Excited Charged Leptons
   in Z^0 Decays
   P.Abreu et al.
   Zeit. Phys. C 53 (1992) 41

3. Study of Final State Photons in Hadronic Z^0 Decay
   and Limits on New Phenomena
   P.Abreu et al.
   Zeit. Phys. C 53 (1992) 555

4. Measurement of the Average Lifetime of B Hadrons
   P.Abreu et al.
   Zeit. Phys. C 53 (1992) 567

5. A Search for Neutral Higgs Particles in Z^0 Decays
   P.Abreu et al.
   Nucl. Phys. B373 (1992) 3

6. Searches for Heavy Neutrinos from Z Decays
   P.Abreu et al.
   Phys. Lett. 274B (1992) 230

7. Search for Scalar Leptoquarks from Z^0 decays
   P.Abreu et al.
   Phys. Lett. 275B (1992) 222

8. Production of Strange Particles in Hadronic Decays of the Z^0
   P.Abreu et al.
   Phys. Lett. 275B (1992) 231

9. Determination of α_s in Second Order QCD
   from Hadronic Z Decays
   P.Abreu et al.
   Zeit. Phys. C 54 (1992) 55

10. Multiplicity Dependence of Mean Transverse Momentum
    in e^+e^- Annihilations at LEP Energies
    P.Abreu et al.
    Phys. Lett. 276B (1992) 254

11. A Measurement of the $B - \bar{B}$ Forward Backward Asymmetry
    Using the Semileptonic Decay into Muons
    P.Abreu et al.
    Phys. Lett. 276B (1992) 536

12. A Measurement of $\sin^2\theta_W$ from the Charge Asymmetry
of Hadronic Events at the Z^0 Peak
P.Abreu et al.
Phys. Lett. 277B (1992) 371

13. Measurement of the Z^0 Branching Fraction to b Quark Pairs
Using the Boosted Sphericity Product
Phys. Lett. 281B (1992) 383

14. A Study of the Decays of Tau Leptons
Produced on the Z Resonance at LEP.
P.Abreu et al.
Zeit. Phys. C 55 (1992) 555

15. Charged Particle Multiplicity Distributions
for Fixed Number of Jets in Z^0 Hadronic Decays
P.Abreu et al.
Zeit. Phys. C 56 (1992) 63

16. Bose-Einstein Correlations in the Hadronic Decays of the Z^0
Phys. Lett. 286B (1992) 201

17. Measurement of the partial width of the Z^0 into $b\bar{b}$ Final States
using their Semi-Leptonic decays
P.Abreu et al.
Zeit. Phys. C 56 (1992) 47

18. Evidence for B_S^0 Meson Production in Z^0 Decays
P.Abreu et al.
Phys. Lett. 289B (1992) 199

19. Multiplicity Fluctuations in Hadronic Final States
from the Decay of the Z^0
P.Abreu et al.
CERN Report CERN–PPE/92–120
Submitted to Nucl. Phys. B

20. Classification of the Hadronic Decays of the Z^0
into b and c Quark Pairs using a Neural Network
P.Abreu et al.
CERN Report CERN–PPE/92–151
Submitted to Phys. Lett. B

21. A Measurement of B Meson Production and Lifetime
using $D\ell^-$ Events in Z^0 Decays
P.Abreu et al.
CERN Report CERN–PPE/92–174
Submitted to Zeit. Phys. C

Conference presentations by UK physicists in last year:

B Physics Results from LEP,
W. Venus,
Invited review talk at Rencontre de Physique de la Vallee d'Aoste,
La Thuile, Aosta,
March, 1992

Electroweak results from LEP,
P. Ratoff,
Invited review talk at Lancaster IOP Meeting,
April, 1992.

A Study of B→J/ψ inclusive production
in Z^0 hadronic decays with Delphi,
A. Segar,
Talk at XXVI Int. Conf. on HEP, Dallas,
August, 1992.

Lifetime and leptonic branching ratios of the τ lepton,
M. McCubbin,
Talk at XXVI Int. Conf. on HEP, Dallas,
August, 1992.

Theses completed by UK students in the last year:

K. Furnival
Heavy quark decays of the Z^0 boson in the DELPHI detector at LEP.
Liverpool (1992)

D. Johnson
A measurement of the τ lifetime using the DELPHI detector at LEP.
Liverpool (1992)

M. Richardson
Search for the Standard Model Higgs in Z^0 decays at LEP.
Liverpool (1992)

M.J. Bates
The performance of the Barrel Muon Trigger system
of the DELPHI experiment
and a study of Heavy Flavour Physics
through the semileptonic decay to muons
Oxford (1992)

C. Beeston
Study of the reaction $e^+e^- \rightarrow \mu^+\mu^-$ around the Z^0 pole.
Oxford (1992)

Fig.1 A fit of the variables S and T to the 1990 and 1991 DELPHI data on the Z^0 line shape and the lepton asymmetries. The prediction of the Minimal Standard Model for a top mass of 140 GeV and a Higgs mass of 100 GeV is S=T=0. The shaded area shows the predictions for top quark masses between 89 and 200 GeV and for Higgs masses between 50 and 1000 GeV. The contours show the experimental 68% and 95% confidence limits.

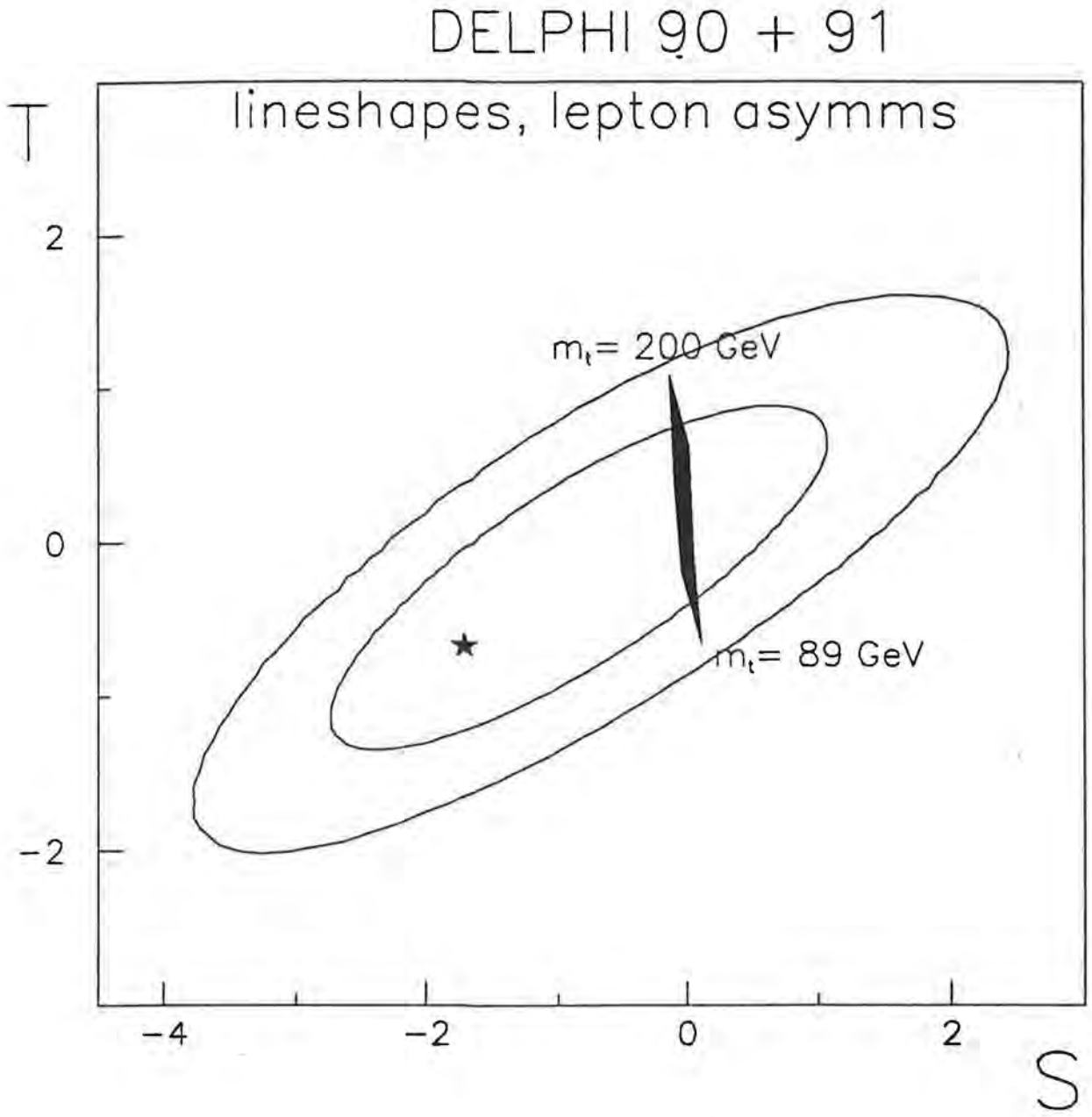

Fig.2 Distribution of the decay length in 3-prong τ meson decays. The τ decay point was reconstructed using just the main tracking detector (TPC) and the microvertex detector. Its flight path was then measured from the average position of the e^+e^- collision point in the run, reconstructed in the same way using hadronic Z^0 decays. The positive lifetime signal is clearly seen. The τ lifetime extracted from this plot, which is one of 4 methods used measure the lifetime, is $\tau_\tau = 0.303 \pm 0.013 \pm 0.007$ ps.

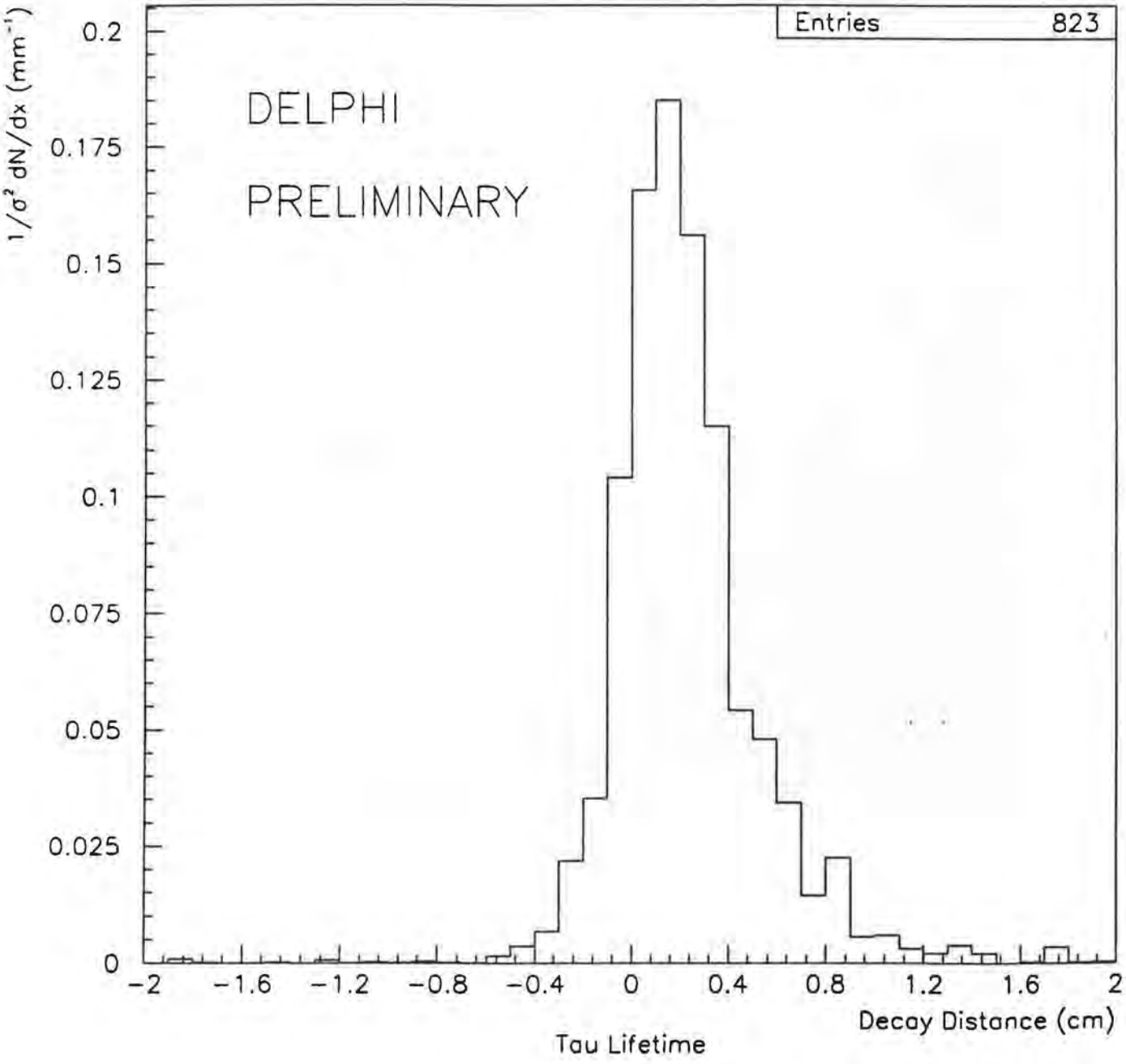

Fig.3 The invariant mass distribution of clear secondary vertices reconstructed in hadronic Z^0 decays, compared with Monte Carlo predictions. Nearly all of the vertices with mass above 2.2 GeV correspond to b decays. From the distribution of their total charge, the lifetime ratio between charged and neutral B mesons was found to be

$$\tau_{B^-}/\tau_{B^0} = 0.96 \pm 0.14(\text{stat}) \pm 0.15(\text{exp syst})^{+0.10}_{-0.20}(\text{composition systematic})$$

where the composition systematic reflects the uncertainty in the fractions of B_s and Λ_b in the charge=0 sample.

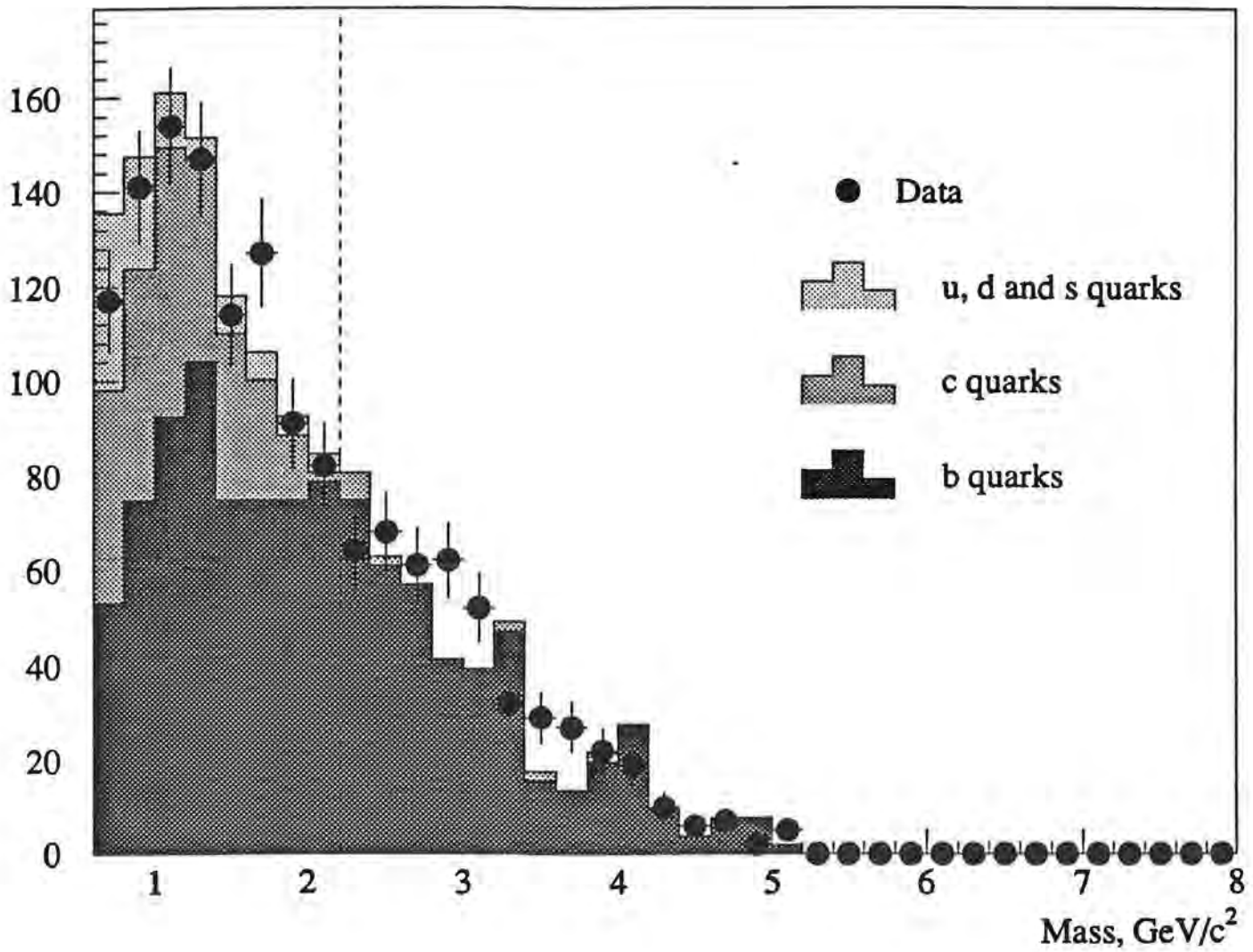

H1 - An Experiment at HERA Proposal 750

Birmingham University, Glasgow University, Lancaster University, Liverpool University, Manchester University, Queen Mary College Westfield, Rutherford Appleton Laboratory in collaboration with:

Aachen, Brussels, Cracow, Davis, Dortmund, Saclay, DESY, Hamburg, Kiel, Kosice, Lund, Moscow, Munich, Orsay, Ecole Polytechnique, Paris, Prague, Rome, Wuppertal, Zeuthen, Zurich and SLAC.

Introduction

H1 started operation in 1992 with most of the detectors in position and working. In particular, all the central and forward tracking chambers, including those built in UK have been fully operational. By the end of the year, all the electronic channels for the trackers were available.

Data taking by H1 started almost immediately when the first collisions in HERA took place on Sunday May 31st. The first physics results were presented at the International Conference in Dallas and when the HERA accelerator resumed operation in the autumn, H1 was able to increase its data base by more than a factor of 10 compared to those available for the summer conference.

At the time of writing, three papers are in print and have been submitted to journals. A few brief comments on these papers follow.

First Measurement of Hadronic Final State Characteristics in Deep Inelastic Scattering at HERA.

The energy flow and transverse momentum characteristics have been measured and are presented in both the laboratory and hadronic centre of mass frames. A comparison has been made with QCD models, distinguished by their different treatment of gluon emission. The distribution of p_T^{*2} as a function of x_F for charged tracks in the hadronic CMS is shown in Figure 1. Superimposed are the expectations of the different QCD based models.

Total Photoproduction Cross Section Measurement at HERA Energies.

These data were extracted from low Q^2 collisions between 26.7 GeV electrons and 820 GeV protons and provide measurements at γp centre of mass energies ranging from 90 to 290 GeV. The value of the cross section at an average energy of 195 GeV is:

$$\sigma_{tot}(\gamma p) = 159 \pm 6.6(\text{stat}) \pm 20(\text{syst})\ \mu\text{b}$$

This result, compared with low energy measurements using photon beams and the result from ZEUS is shown in Figure 2.

Observation of Deep Inelastic Scattering at Low x.

Measurements of the x and Q^2 distributions for inclusive neutral current deep inelastic ep scattering were measured in the range $0.025 < y < 0.6$ and $5 < Q^2 < 40\ \text{GeV}^2$. The results so far are consistent with extrapolations from available low energy fixed target data. The differential cross sections as a function of x and Q^2 are shown in Figure 3.

The H1 experiment was featured on the BBC programme "Tomorrows World" on May 1992 and again on the German ARD1 programme "Bilder aus der Wissenschaft" on August 30th. (See Figures 4 and 5).

Some parts of the detector which were completed recently are the subject of separate reports below.

The Forward Muon Trigger

Birmingham and QMW, together with the RAL electronics group, are providing the forward muon trigger which uses signals from the forward muon chambers. The staggered geometry of adjacent chamber planes makes it possible to identify the time of the beam crossing (t_o) responsible for the detected track. This is achieved using a semi-custom chip designed at RAL which acts on signals from neighbouring pairs of wires. Track segments originating from the collision point are recognised before and after the toroidal magnet using a modified version of the same chip.

The trigger control system was installed at DESY in 1991 and a prototype trigger module was operated in test mode during the first HERA runs in 1992. The full set of chips has now been delivered after some delays in production, and the complete trigger will be installed in time for high luminosity running.

The Time of Flight Scintillator Wall

The Time of Flight scintillator hodoscope is the responsibility of the QMW group and consists of a double wall of butted scintillation counters, located within the central magnetic volume of the H1 experiment. It is immediately behind and well-matched to the modularity of the backward electromagnetic calorimeter (BEMC). Since most of the H1 detectors, and especially the calorimetry, is "slow", its principal purpose is to provide a veto on most triggers when backgound associated with the proton-beam is detected. ToF has been operational since the beginning of HERA data-taking and even before the fine-tuning that is now taking place, was typically, safely, reducing the level one trigger rate by two orders of magnitude. There is no doubt that without ToF, H1 would effectively be killed by dead-time.

On average, there is of the order of 14ns between beam-associated and genuine interaction secondaries arriving at the ToF position. By examining the time difference of coincident signals from the two walls it has been determined that the (Gaussian) resolution of the whole ToF device is 2.0 ± 0.4 ns. This result folds in everything from arrival point at the scintillator, transit time, to photo-multiplier (Hamamatsu 2490-01) jitter. The real situation is complicated by rather long beam bunches and background from synchrotron radiation that takes a finite time to rise. The net effect can be roughly summarised by Figure 6 which is output from a global OR TDC. Offline analyses of such plots indicate that the ToF veto is ~98.5% efficient whilst accidentally vetoing only ~0.1% of real events.

During early analyses it was noted that despite the shielding effect of BEMC, hits in the interaction window of ToF were most useful for confirming good physics events. This has led to some proposals for another scintillator device dedicated for this purpose which may be located immediately in front of BEMC.

Throughout, both the mechanical and electrical perfomance of the present ToF has been excellent. In particular, the remote operation of pneumatic shutters that close around the beam pipe after each fill has gone without a hitch. Problems associated with the very different high voltages needed with either field-on or field-off conditions have been minimised with the automatic detection of the situation and loading of correct values from a database. There was a small difficulty in first running caused by an early failure of two of the pre-amplifiers mounted in the PM bases. We were able to survive with all channels still in operation using additional pre-amplification at the logic end of the electronics. During the summer shut-down the designed ability for ToF to separate into two halves which could be removed without splitting the beam pipe was demonstrated, and access was gained to BEMC for needed repairs. At the same time the faulty pre-amps were exchanged. In the recent run we have, for safety, used slightly lower pre-amp voltages and compensated with slightly higher PM voltages.

The QMW group is also responsible for the logic and software monitoring of the upstream Veto-Wall. Lately, we have instituted a method of plateauing the ToF counters utilising coincidence of beam-halo muons between the two devices. Not only should this speed up what was previously a tedious procedure using cosmic rays, but it should use more relevant near-horizontal tracks and enable a more meaningful detection efficiency to be established

The Data Acquisition System

The completed data acquisition system was able to cope with the challenge of *ep* collisions and performed with a relatively high level of stability considering the amount of sophisticated electronics and software involved (see Figure 7). British collaborators are responsible for the overall design and coordination of the central part of the data acquisition system and the filter "farm" together with a large fraction of the trigger control software. Several hundred microprocessing elements, embedded in the international VMEbus standard, form the backbone of one of the most powerful real-time computing engines in Particle Physics today. One of its features allows separate subdetector partitions to be independently installed as autonomous units, yet with the aid of intelligent-based fibre-optic links (VMEtaxi) the complete system can be coherently coordinated from "easy-to-operate" graphics-orientated workstations. Moreover by taking advantage of international protocols, to develop software for communication over local and wide area networks, many H1 scientists have been able to monitor the system worldwide and even witness first collisions directly relayed from the control room to their home institutes.

Thanks to the excellent collaboration with industry, the fast RISC-based processing farm was commissioned after a relatively short design and development period. The facility was not only able to filter events, at a high-level, but also provide online reconstruction of charged-particle tracks in real-time (Figure 8). Presently 14 boards are installed in just two VMEbus crates, with an equivalent power of seven IBM 3090 mainframes.

As HERA luminosity now increases towards its design value of 1.5 10^{31} cm^{-2} s^{-1}, the advantages of a modular design can be put to good effect to capitalise on recent technological advances in order to increase rates and keep flexible triggering configurations for physics investigation. With the increase in ram density, and a corresponding fall in price, coupled with the improved microprocessor clock frequencies, the central part of the acquisition system is currently being upgraded. This will primarily involve increasing the bandwidth of the optic-fibre system to boost transfer rates from a current 12 MBytes/second to 50 MBytes/second next year (Figure 9). In addition the RISC-farm will be expanded to some 32 modules with an increased performance equivalent to 20 IBM units. This will permit both higher event throughput and increased event size as more detector elements are added.

One such detector element, now being prepared, is the silicon tracker vertex detector. Presently RAL are collaborating with the institutes of DESY, Zeuthen and Zürich in building a silicon strip device ready for readout and commissioning in 1994. From the data acquisition point of view a total of 214,000 electronic channels are to be read out by purpose-built front-end amplifier chips which contain switched capacitor analogue-pipeline buffers (Figure 10). A single chip has 128 low-noise channels with a pitch of 44μm per channel storing 32 consecutive bunch crossings. Pipeline control will be synchronised to the 96 ns bunch crossing period. Each chip is fabricated in a 2μm CMOS process and prototypes have already been tested with a readout speed of 2.5 MHz, allowing a 2000:1 multiplexing within the 800 μs readout time. The total power consumption of a single chip, including the pipeline running at 10 MHz, is 38mW. An external readout unit, with a data reduction processor for hit-finding and zero-suppression, is currently under the early stages of design with a VMEbus interface.

There have been several publications in the DAQ area as follows:

(1) W.J.Haynes, *The H1 Data Acquisition System.* Presented to the International Conference "Computing in High Energy Physics '91", Tsukuba City, Japan, 11-15 March 1991. (Proceedings published by Universal Academy Press, Inc. ISBN 4-946443-09-6)

(2) A.Campbell, *A RISC multiprocessor event trigger for the data acquisition system of the H1 experiment at HERA.* Presented at the International Conference "Real Time '91", Jülich, Germany, 25-28 June 1991. (Issued as Rutherford Appleton Laboratory report RAL 91-060, September 1991).

(3) W.J.Haynes, *Experiences at HERA with the H1 Data Acquisition System.* Presented to the International Conference "Computing in High Energy Physics '92", Annecy, France, 21-25 September 1992. (Proceedings to be published).

(4) J.Coughlan et al, *Object orientated programming for online systems at H1.* Presented to the International Conference "Computing in High Energy Physics '92", Annecy, France, 21-25 September 1992. (Proceedings to be published).

(5) W.J.Haynes, *Bus-based architectures in the H1 Data Acquisition System.* Presented to the International Conference "Open Bus Systems '92", Zürich, Switzerland, 13-15 October 1992. (Also issued as RAL 92-048, August 1992).

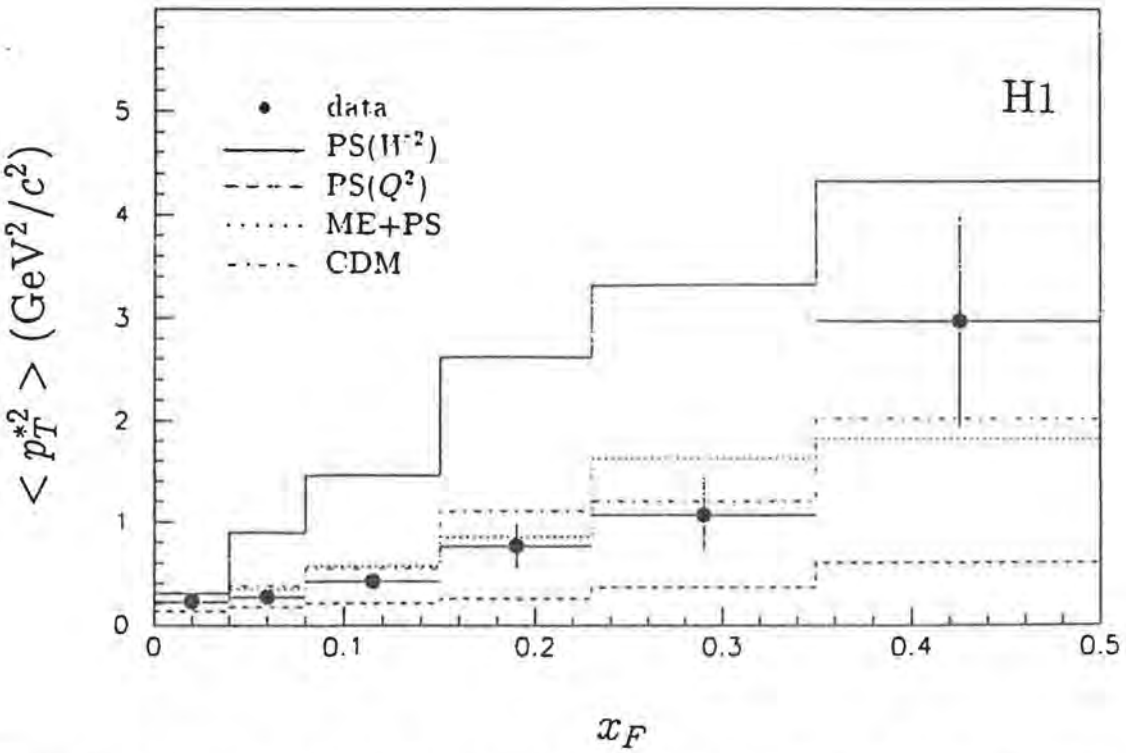

Figure 1 : The average p_T^{*2} as a function of x_F for charged tracks in the hadronic CMS, compared to the expectations of different QCD based models.

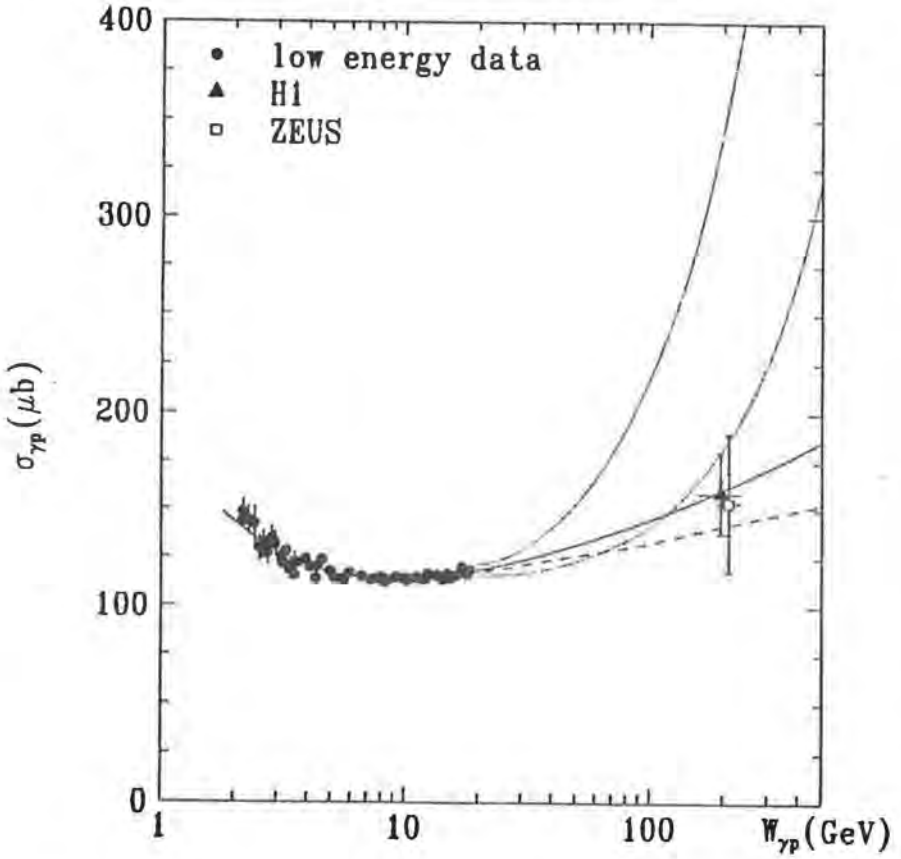

Figure 2: The total γp cross section measued by H1 (triangle) compared with ZEUS (square) and low energy measurements (circles)

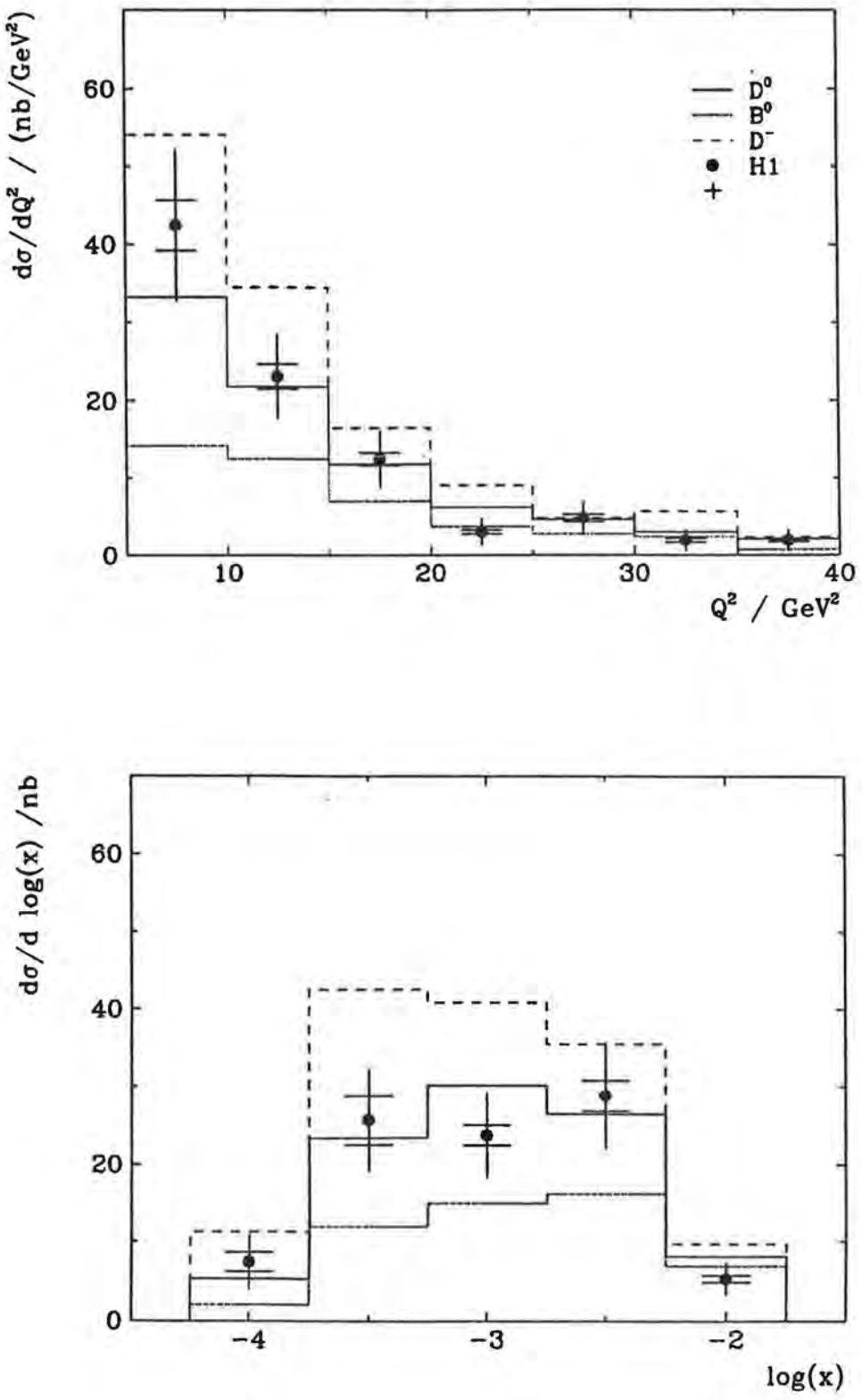

Figure 3 The differential cross section s for $d\sigma / dQ^2$ *and* $d\sigma / d\log(x)$ *in the range* $0.025 < y < 0.6$ and $5 < Q^2 < 40$ GeV^2

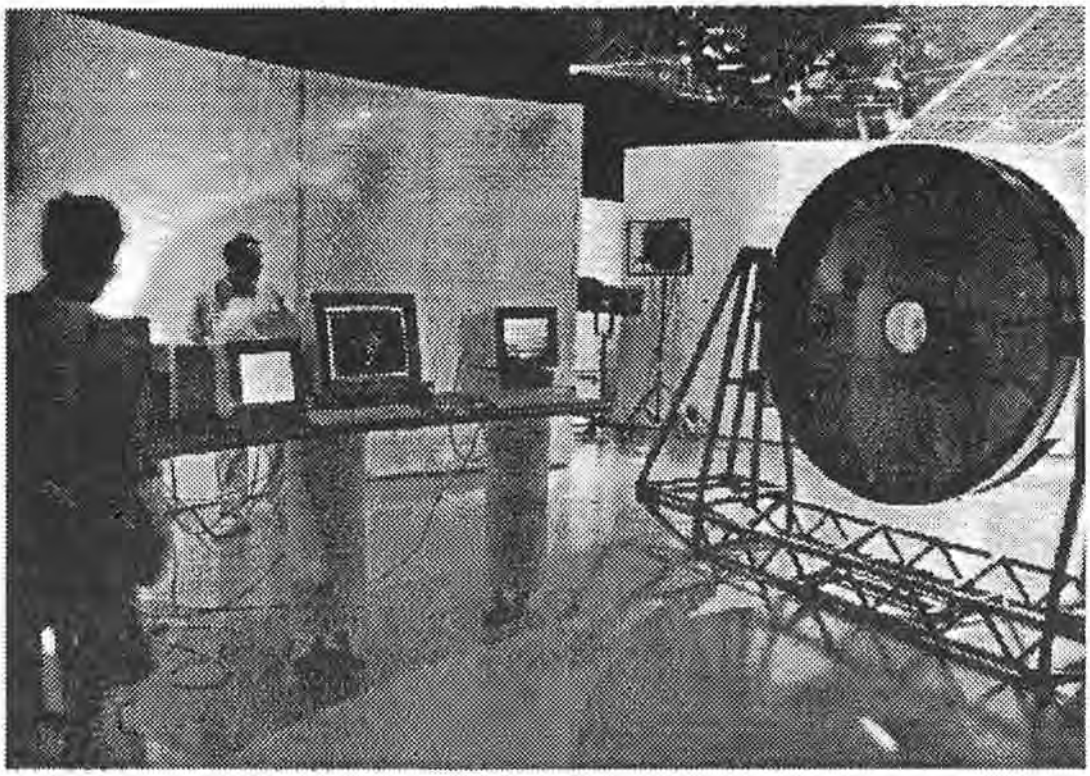

Figure 4: Scene in BBC studio during rehearsals for "Tomorrow's World", showing H1 radial chamber and the H1 event display

Figure 5: Scene from German TV Science Programme in H1 Control Room

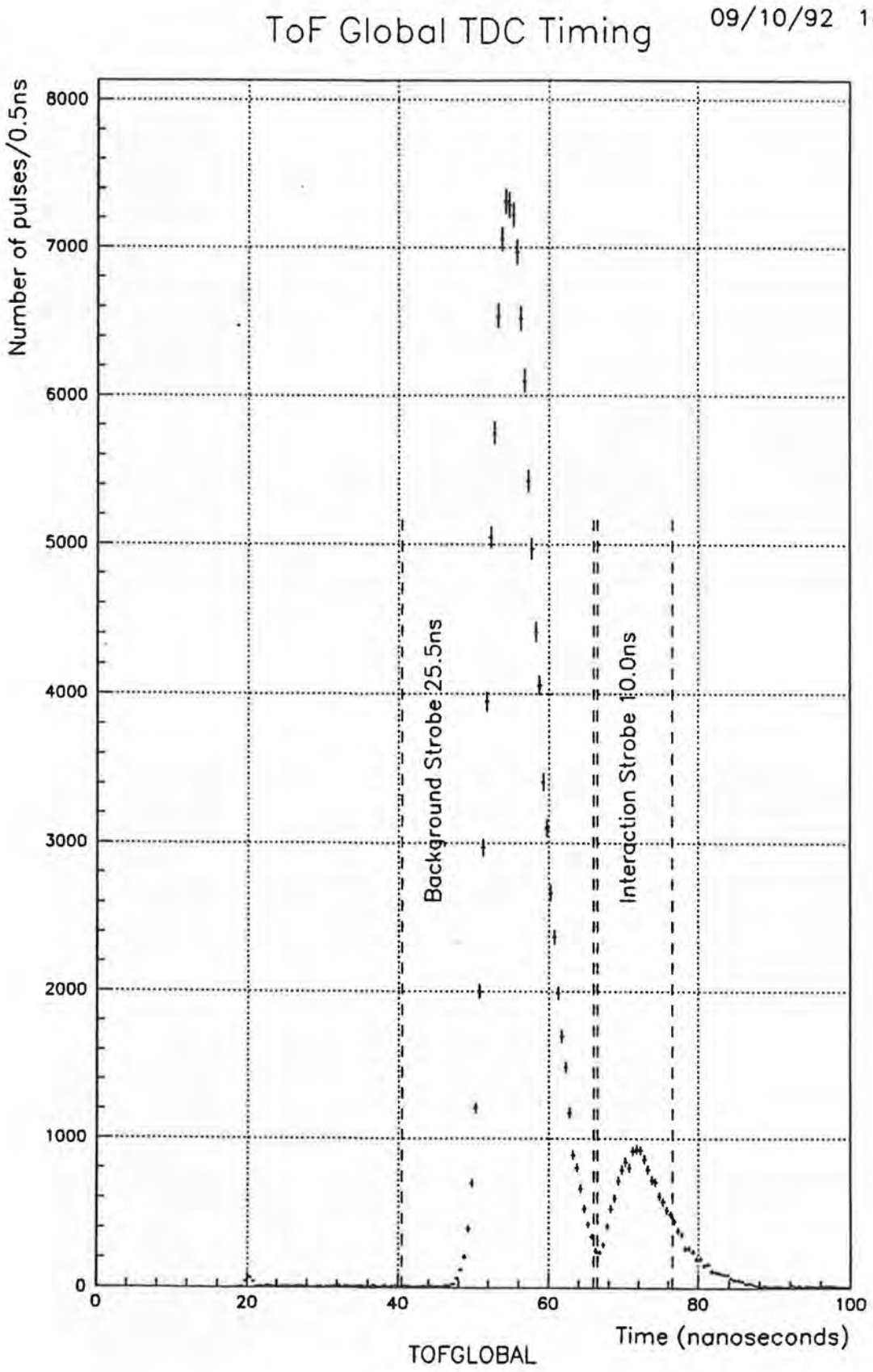

Figure 6 Output from a global OR TDC, which allows the ToF veto efficiency to be calculated

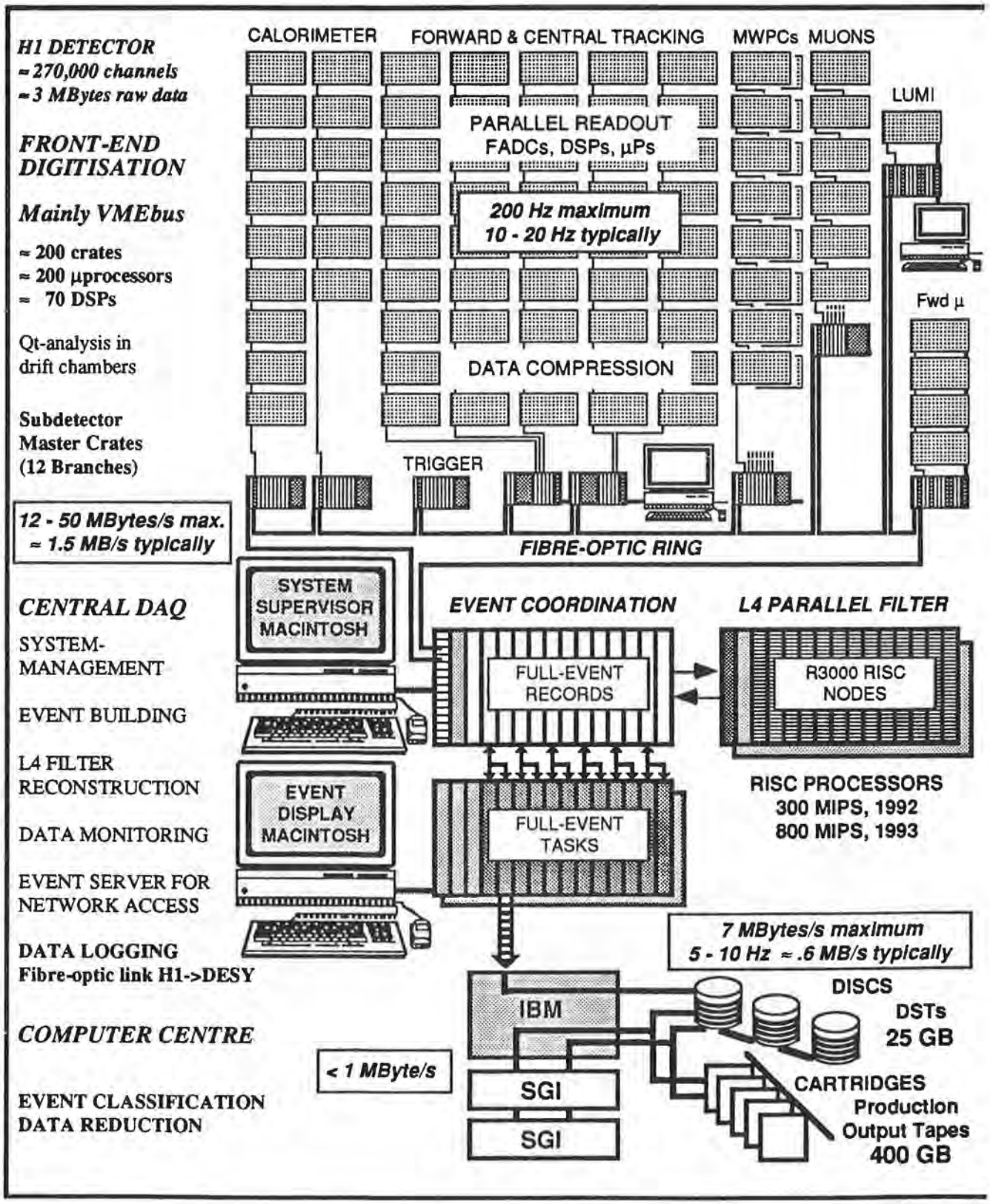

Figure 7: Key elements of the H1 Data Acquisition Layout

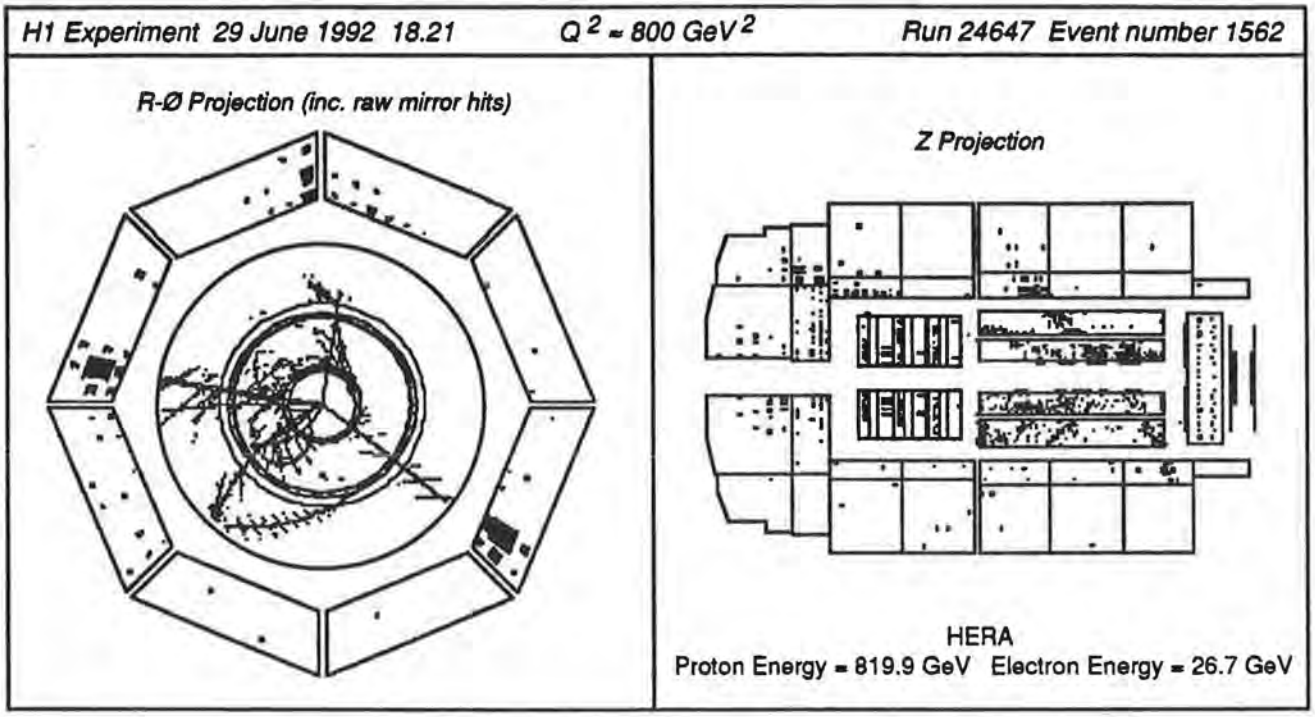

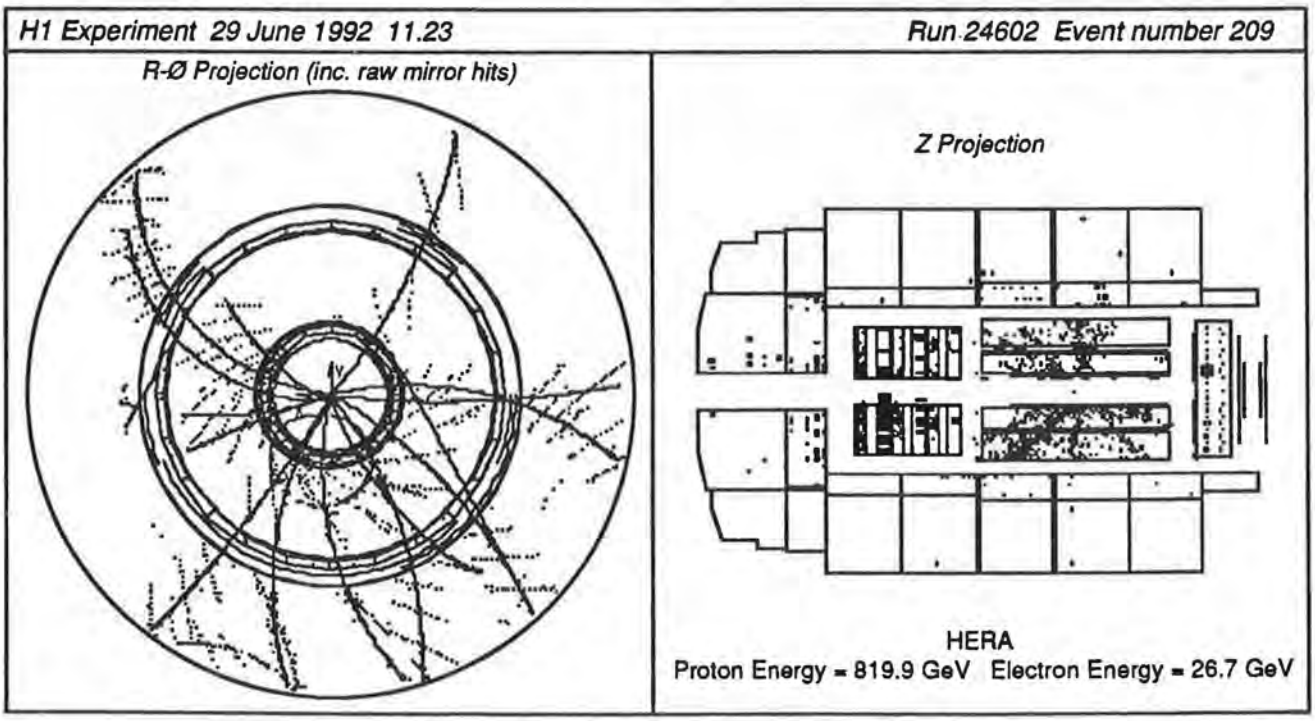

Figure 8: Some of the first deep e-p inelastic events seen from HERA and reconstructed in real-time within the H1 Data Acquisition System

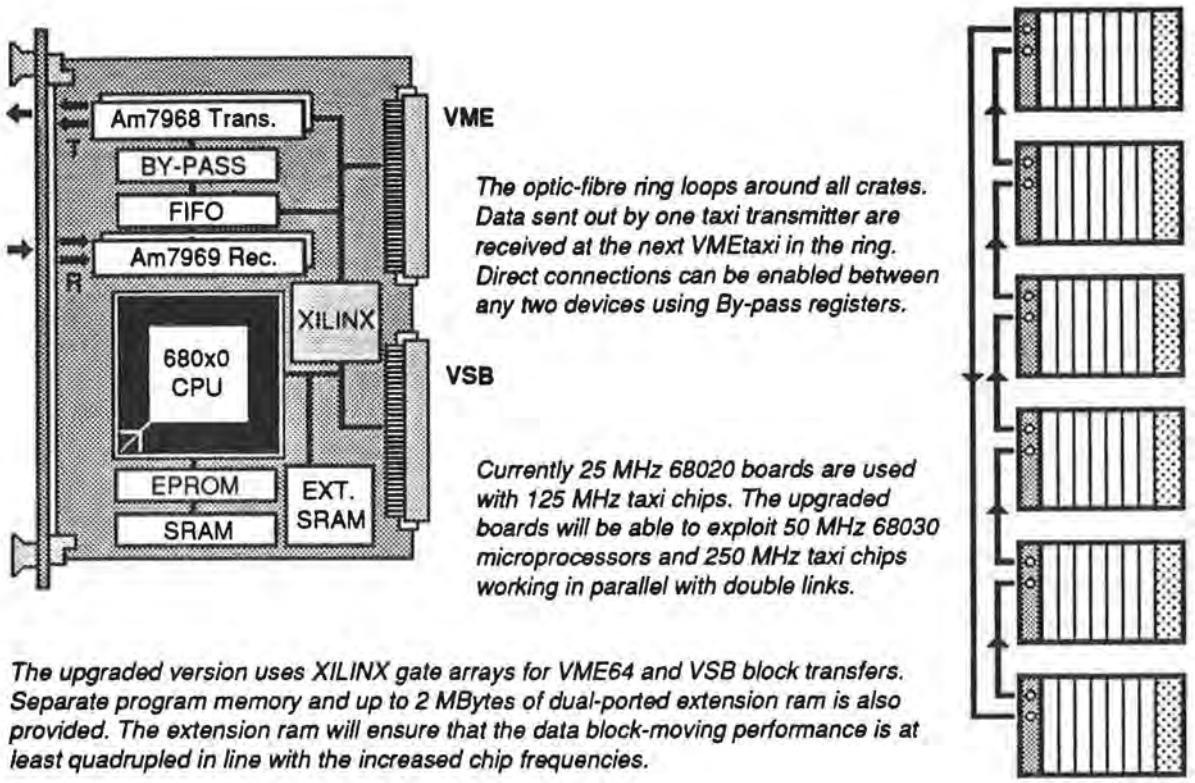

Figure 9: VMEtaxi and upgrade. As chip densities increase, so does the amount of functionality that can be condensed onto a single-width card become greater.

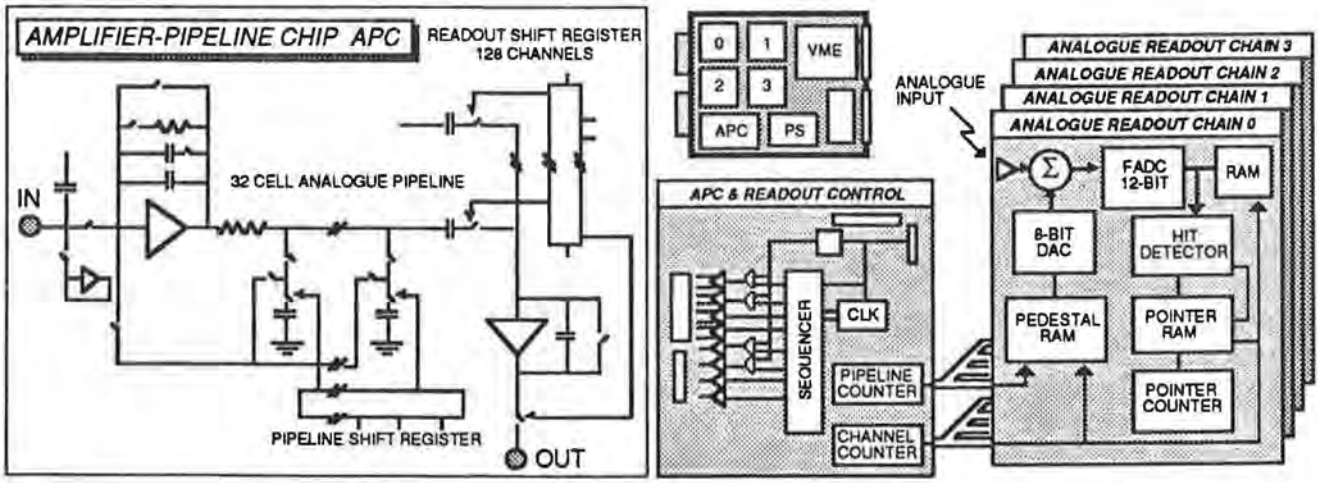

Figure 10: Readout schematics for the new silicon tracker. Each VMEbus card will be able to read out and control 8192 channels.

ZEUS - A DETECTOR FOR HERA

Proposal 760

Collaborating Institutes by Country

CANADA: MANITOBA, MC GILL, TORONTO , YORK

GERMANY: BONN, DESY, FREIBURG, HAMBURG, JUELICH, SIEGEN, ZEUTHEN

ISRAEL: WEIZMANN INSTITUTE, TEL AVIV

ITALY: BOLOGNA, CALABRIA, FIRENZE, FRASCATI, PADOVA, ROME,
TORINO

JAPAN: INS + UNIVERSITY TOKYO

NETHERLANDS: NIKHEF

RUSSIA: MOSCOW STATE UNIVERSITY

POLAND: KRAKOW, WARSAW

SPAIN: MADRID

UNITED KINGDOM: BRISTOL, GLASGOW, IC LONDON, UC LONDON, OXFORD, RAL

USA: ARGONNE NATIONAL LABORATORY, BROOKHAVEN NATIONAL LAB.,
COLUMBIA UNIVERSITY, IOWA,
LOUISIANA STATE UNIVERSITY, OHIO STATE UNIVERSITY,
PENNSYLVANIA STATE UNIVERSITY, UNIVERSITY OF CALIFORNIA SANTA CRUZ,
VIRGINIA POLYTECHNIC INST., WISCONSIN

HERA.

The period covered by this report has seen the start of data taking by the two large experiments at HERA, ZEUS and H1, and the publication of the first physics papers from this new collider.

Having successfully demonstrated e-p collisions during November 1991, HERA was shutdown from Christmas 1991 until the end of March 1992 to enable the move of the two experiments into the beam line. April and May were needed by the machine group to re-establish the previous year's conditions on both the electron and proton machines and to prepare for multi-bunch operation. Some stable single proton and electron beams were made available for background studies.

During the night of 30/31 May 1992 the first electron-proton collisons were observed in the ZEUS detector. The machine was operating in single bunch mode with 820 GeV protons (35 μA) and 26.6 GeV electrons (130 μA), with the luminosity at the ZEUS intersection estimated to be 5×10^{26} $cm^{-2}s^{-1}$. Shortly afterwards on 6 June HERA operated successfully with 10 on 10 bunches. By the beginning of July the luminosity for the experiments regularly reached 10^{28} $cm^{-2}s^{-1}$. At the end of July, when the machine was shut down for a couple of weeks access, about 2 nb^{-1} had been delivered

to each experiment. Figure 1 shows a deep-inelastic scattering candidate event recorded in the ZEUS detector during this period.

After the shutdown the first few weeks of running were devoted to machine studies and two advances were made: up to 20 proton bunches were accelerated to the maximum energy; and electron polarisation was observed at the level of about 55% at 12.0 GeV beam energy. Since the middle of September HERA has been running again for the experiments and the run will continue until the end of November 1992 with a short break during the period 1-3 October for the official celebration of the start of the HERA physics programme and DESY's public open days.

General status of ZEUS.

Before outlining the work done by the UK ZEUS groups we give a general survey of the state of the detector. As summarised in the annual report of last year, most of the major components of the ZEUS detector, including the central tracking detector (CTD), were in place by the summer of 1991. The remaining items, mostly the rest of the inner tracking system (a vertex chamber, forward and rear trackers), and the TRD system were installed during October. The Glasgow group assembled, tested and installed, with Bonn, two of the four Transition Radiation Detector modules used to identify electrons in the forward direction, where the Lorentz boost makes the spatial separation of particles smaller, and powerful identification techniques are needed. Readout modules have been tested at RAL, and the final readout system should be available for the 1993 running. At the beginning of December a cosmic ray run was undertaken to enable further integration of component readout and trigger systems.

All major components were able to participate in the data taking and particularly important for the first physics runs were the complete uranium/scintillator calorimeter and the CTD z-by-timing information. A preliminary version of the first level calorimeter trigger system was used, signals from the rear EM section being particularly important.

To begin with, the trigger thresholds were kept as low as consistent with the rate at which events could be transferred to the main DESY IBM complex for eventual writing to tape (not more than 5 Hz). We learnt very quickly that the accurate timing of the calorimeter signals was crucial for the rejection of beam related background. Signals from small counters build around a collimator (C5) just upstream on the proton side of the detector, were also important. To begin with cuts based on these signals were applied offline, but as we gained more confidence they were moved to our Silicon Graphics third level trigger farm. During the recent shutdown many of these cuts have been moved to levels one or two of the ZEUS trigger system. Figure 2(a) shows the separation of background and e-p events using calorimeter timing and figure 2(b) shows the vertex distribution from CTD tracks for e-p candidate and background events.

It is worth noting that towards the end of the first running period the CTD provided the first active component in the ZEUS second level trigger. The absence of tracks or track segments in the CTD was used to veto cosmic-ray events triggered by the barrel-muon-calorimeter coincidence trigger.

CTD as a working detector

The installation of the z-by-timing readout on the three inner axial super-layers was completed during April 1992. Very soon thereafter the CTD became a fully operational detector integrated within the ZEUS central data acquisition system under central run-control. Initially the chamber was operated at voltages slightly below optimum values until it was clear that the beam conditions were not likely to produce serious background currents. However beam induced currents have proved to be negligible at 10 on 10 bunches and so the gas gain has been increased to 10^5. The chamber is presently being operated using a "safe" argon/CO_2/ethane gas mix of 90:8:2 in a magnetic field of 1.43T.

The latest figures for the resolution of the z-by-timing system in multi-track ep interactions are $\sigma_z \sim 4$ cm and $\sigma_{r\phi} \sim 1$ mm. This compares favourably with the best resolution obtained in a test beam where the design value of 3 cm was obtained for single tracks, using an argon/ethane 50:50 gas mix. The CTD information has proved vital in all of the physics which ZEUS is currently exploring. We look forward to realising the full potential of the CTD with the completion of the electronics system in time for the next running period in spring 1993.

CTD Electronics and Trigger

The major responsibility for the CTD electronics is carried by the Bristol, Oxford and RAL groups. The RAL Electronics group provide design expertise and oversee much of the volume production. Much of the ZEUS electronics has been completed and installed in the last year. The transputer based readout controllers, crates and power supplies, z-by-timing system, second level trigger hardware and software and amplifying system are all complete.

The z-by-timing system has been operating successfully for more than 6 months. It has performed extremely reliably and formed the basis for the tracking analysis in ZEUS. The local and master timing controllers which interface the front-end readout cards to the trigger were produced by the UCL group and they have run essentially problem free during this period. After experience has been gained with the CTD first level trigger (FLT) system, the final versions of the timing boards will go into production.

The first stage of production of the CTD FLT, which uses the innermost superlayer, has now been completed. Currently 1/4 of the boards are in DESY and will be commissioned in the ZEUS system before the end of the current running period. The stage one FLT covers the full acceptance of the CTD and will be an integral part of the ZEUS trigger. Its accuracy will be improved by the addition of the stage two FLT, which uses superlayers 3 and 5. This will go into production in the next few months.

The FADC system ($r - \phi$ readout) is the remaining part of the electronics system. Each of the 4608 wires of the CTD will be instrumented with FADCs, as will the transition radiation detector in the forward region. The final preproduction boards are now undergoing tests at DESY and production of these very complex boards will begin within a month, so that the complete system can be installed early next year. The remaining parts of the system including the local and master timing controllers are already in production.

The second level trigger (SLT) is based on transputers mounted in the readout controllers. The algorithm has been adapted for use with the z-by-timing system and has formed an important part of the ZEUS trigger in the last running period. It is particularly useful in rejecting cosmic ray triggers, which are very difficult to reject using calorimeter information alone. The SLT algorithm using FADCs is also ready for installation and will be used as soon as the inner axial superlayers are instrumented with FADCs.

Software

In preparation for the first physics runs the CTD reconstruction package was modified so that it could use only z-by-timing data. A suite of offline monitor and fast analysis programmes was also prepared to ensure that the chamber itself, track trigger and reconstruction codes were operating correctly. Of particular importance for all subsequent work was accurate and fast determination of the time offsets for all signal wires. Close cooperation between the online and offline teams was essential for maintaining the quality and reliability of the CTD data.

On a more general note, the speed of reconstruction and reduction of the very large number of triggers taken was impressive. After the data was delivered to the DESY central IBM (where it was copied

to archive tape) it was then sent by a very fast data link to the ZEUS 'number-cruncher' built from Silicon Graphics work-stations. Once reconstructed the data was returned to the IBM for for first-pass physics filtering, the reduced data then being sent to the ZEUS physics analysis cluster of DEC stations. Typically data would be available for analysis within one or two days of being recorded by the detector. During the first running period of the order of 10^6 triggers were written to tape and of these about 10000 survived the first-pass selection. Correspondingly large Monte Carlo data sets were also needed for the physics analysis and these were produced by harnessing the combined CPU power of the DEC cluster overnight and at weekends.

CPU power is no longer a big issue, bottlenecks occurred because of inadequate disk space. The collaboration has approved plans to install a large capacity data server (ZARAH) connected to both the central IBM and the DEC cluster which will alleviate the problem.

Physics

Although the first run period ended only days before the Dallas International Conference on High Energy Physics, ZEUS was able to present some first physics results on e-p scattering in the HERA energy domain.

The most notable result presented was a measurement of the photoproduction total cross-section at an average CM energy of 210 GeV, an order of magnitude higher than previous measurements. Most of the data for the photoproduction analysis were taken with a special trigger in which the luminosity electron detector was used in coincidence with the main calorimeter, but the thresholds in the latter were set at lower values than for standard data taking. The ZEUS result is $\sigma(\gamma p) = 153 \pm 16(stat.) \pm 36(syst.)$ μb. Figure 3 shows data from ZEUS and earlier experiments and predictions from a variety of theoretical models. As can be seen from the figure the predictions differ by an order of magnitude. Apart from focusing theoretical studies on models at the low end of the range the result also has important implications for high energy gamma-ray astrophysics. This work has been published in Physics Letters.

Since the first results were presented at Dallas, we have found evidence in the ZEUS data for photoproduction events in which the distribution in transverse energy of the hadronic system is much harder than that needed to balance the transverse energy of the scattered electron. In addition some of the events show back-to-back 2-jet production at the rate and with the characteristics expected from hard two-body scattering between partons in the photon and those in the proton. A paper has been submitted to Physics Letters.

Results were also presented at Dallas on a first look at deep inelastic e-p scattering events. We have demonstrated that we can separate e-p events cleanly from background using calorimeter timing and energy cuts. In the candidate events we find that the electron's transverse momentum is balanced by that of the hadronic system, as one would expect for deep inelastic e-p scattering - see fig 4(a). The events are concentrated at low x and low Q^2 - see fig 4(b). The cross-section is in broad agreement with the latest structure function parameterisations that include recent μ-p data from the NMC experiment. With increased statistical precision we will be able to discriminate between the different behaviours that have been proposed at low x. The DIS analysis is being finalised for publication by the collaboration.

People from UK groups, both resident at DESY and those based in the UK, contributed to the first ZEUS physics analyses. Leading roles were taken in the photoproduction total cross-section measurement and the DIS analysis. We also have a large involvement in the exotic physics group and ZEUS will make a significant assault on existing limits when more data has been collected.

Publications.

(1) D G Cousins et al., The Design, Status and Performance of the ZEUS CTD Electronics, NIM **A315** 1992 p397.

(2 G P Heath et al., The ZEUS First Level Track Trigger, NIM **A315** 1992 p431.

(3) A T Doyle, Generators for HERA Physics, UK Workshop on Jet studies at LEP and HERA, J Phys G **17** no 10 p1596.

(4) N H Brook, Ariadne at HERA, Proceedings of the Amsterdam meeting Monte Carlo methods, May 1991 ed K Boors and R van Eijk.

(5) B Foster et al, The Performance of the ZEUS Central Tracking Detector z-by-timing Electronics in a Transputer Based Data Acquisition System, Oxford preprint OUNP-92-14, talk presented by T Khatri at the 3rd Conference on Advanced Technology and Particle Physics, Como Italy, June 1992.

(6) D Gingrich et al, Software Tools for Transputer Networks, talk presented by D Gingrich at the Second International Workshop on Software Engineering, Artificial Intelligence and Expert Systems, L'Agelonde France, January 1992, to be published in the proceedings.

(7) J Butterworth et al, Initial Experience with the ZEUS Central Tracking Detector Second Level Trigger and Data Acquisition System, talk presented by D Gingrich at the 1992 Conference on Computing in High Energy Physics, Annecy, France, September 1992, to be published in the proceedings.

(8) G A Blair et al, The Design and Construction of the ZEUS Central Tracking Detector, paper in preparation.

(9) ZEUS Collaboration (M Derrick et al) , A Measurement of $\sigma_{tot}(\gamma p)$ at $\sqrt{s} = 210$ GeV, DESY preprint DESY 92-127, Physics Letters **B293** 1992 p465.

(10) ZEUS Collaboration (M Derrick et al) , Observation of Hard Scattering in Photoproduction at HERA, DESY preprint, submitted to Physics Letters B.

(11) ZEUS Collaboration (M Derrick et al) , First Observation of Deep Inelastic Scattering with ZEUS at HERA, paper in preparation.

(12) The following items were included in the proceedings of the Workshop on HERA Physics held at DESY, October 1991 (DESY 1992, edited by W Buchmüller and G Ingelman):
- A M Cooper-Sarkar et al, Measurement of $F_L(x, Q^2)$ at low-x and extraction of the gluon distribution, Vol I p 155.
- N Brook et al, QCD cascades in deep inelastic scattering, Vol I p 275.
- P J Bussey, Photon-photon processes at HERA, Vol I p 629.
- Ch Berger N Harnew et al, An introduction to physics beyond the Standard Model at HERA, Vol II p1029.
- D Gingrich & T Khatri, Sensitivity to leptoquarks at ZEUS, Vol II p1074.
- J Butterworth & H Dreiner, Finding supersymmetry via R-parity violation, Vol II p1079.
- (N Magnussen),N brook et al, Generators for deep inelastic scattering, Vol III p1167.
- N Brook et al, Photoproduction generators at HERA, Vol III p 1221.
- D Gingrich & N Harnew, LQUARK2.1 MC Generator for leptoquark production, Vol III p 1542.
- N Brook, RADIATE1.0 - An interface to ARIADNE3.0, Vol III p 1446.
- N Brook et al, RAYPHOTON2.0 - An interface for HERA photoproduction physics, Vol III p1453.

Ph.D. Theses.

T.L. Short: " The design of the ZEUS Regional First Level Trigger Box and associated trigger studies", (Bristol 1992), RALT-133

C.J.S. Morgado: "The design of the FADC readout system for the ZEUS central tracking detector", (Bristol 1992), RALT-135

J Giddings: "Electron drift in the ZEUS central tracking detector", (ICSTM 1992)

D McQuillan: "Calibration from data of multiwire drift chamber particle detectors", (ICSTM 1992)

M Lancaster: "The design of a First Level Tracking Trigger for the ZEUS Experiment and Studies for Low-x Physics", (Oxford 1992), RALT-138

Figure Captions.

Fig. 1: A deep inelastic e-p scattering event in the ZEUS detector.

Fig. 2(a): The time difference between the forward and rear calorimeter signals versus the time of the rear calorimeter signals, for e-p and background events.

Fig. 2(b): The distribution of primary event vertices reconstructed using CTD tracks for NC candidate and background events.

Fig. 3: $\sigma(\gamma p)$ as measured by ZEUS and previous experiments compared to various theoretical predictions.

Fig. 4(a): The difference in transverse momentum versus the difference in azimuthal angle between the scattered electron and the hadronic system in a sub-sample of DIS ep events.

Fig. 4(b): The distribution in x and Q^2 of the DIS ep events.

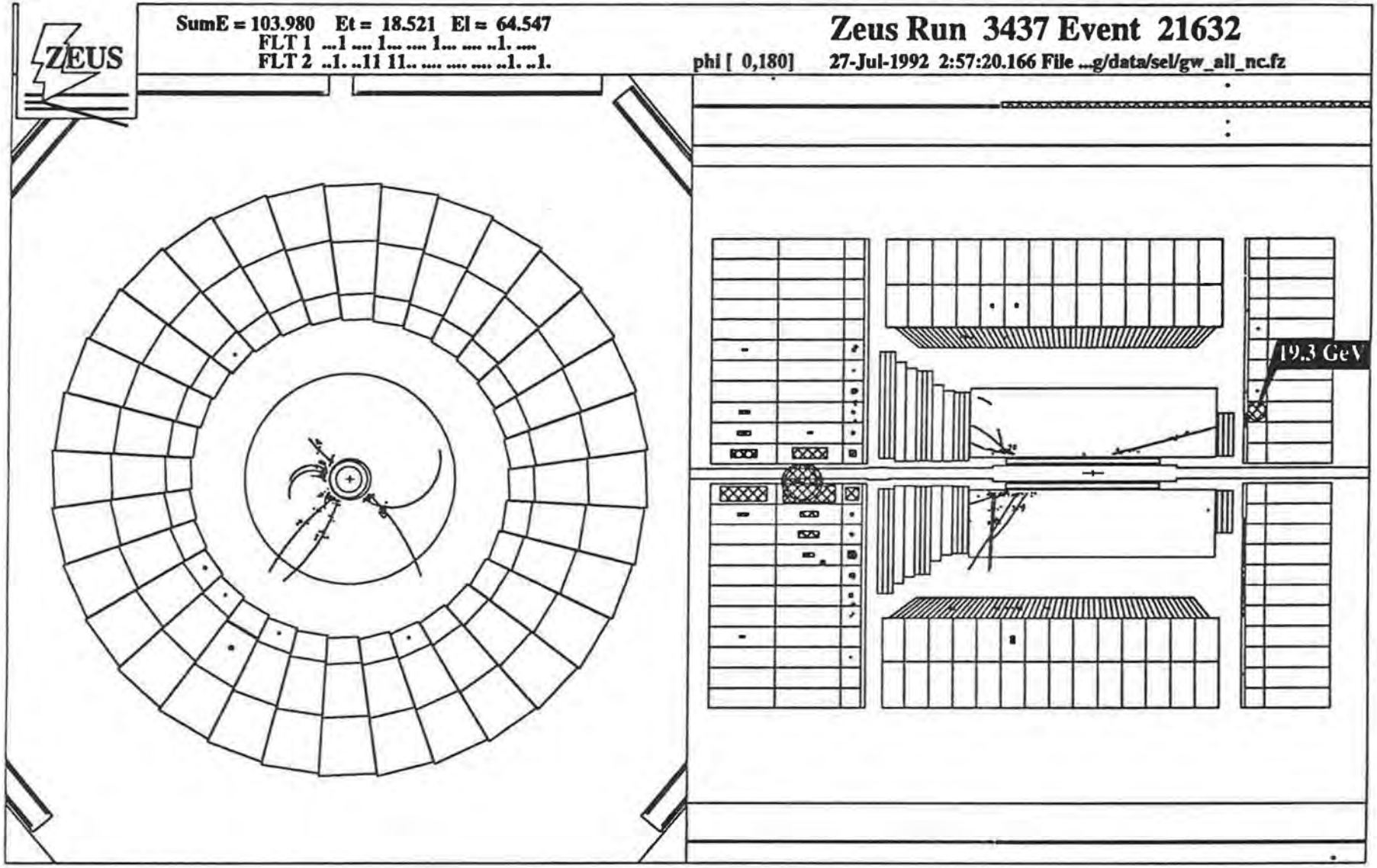
ZEUS
SumE = 103.980 Et = 18.521 El = 64.547
FLT 1 ...1 .... 1... .... 1... .... ..1. ....
FLT 2 ..1. ..11 11.. ....1. ..1.
Zeus Run 3437 Event 21632
phi [0,180] 27-Jul-1992 2:57:20.166 File ...g/data/sel/gw_all_nc.fz
19.3 GeV

Fig. 1

Fig. 2(a)

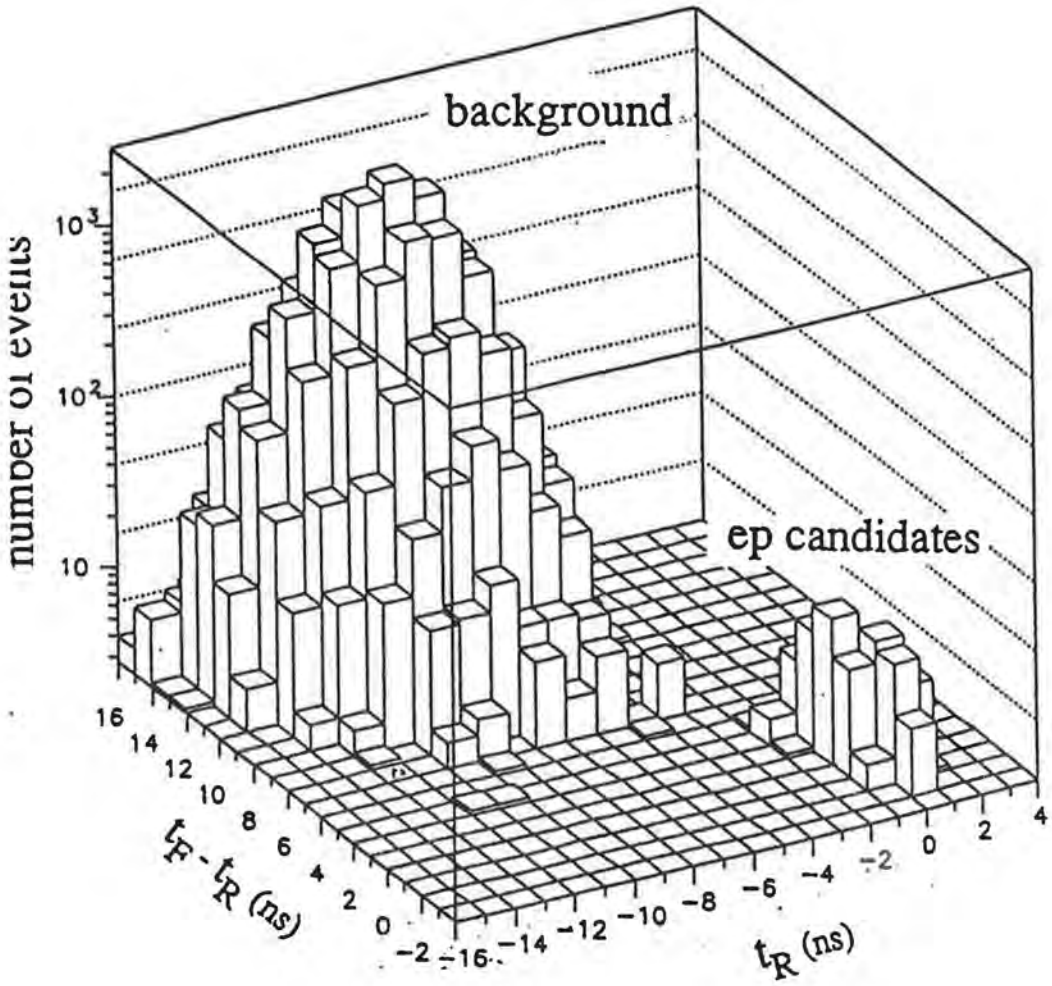
background
ep candidates
number of events
10^3
10^2
10
16
14
12
10
8
6
4
2
0
−2
−16
−14
−12
−10
−8
−6
−4
−2
0
2
4
$t_E - t_R$ (ns)
t_R (ns)

Fig. 2(b)

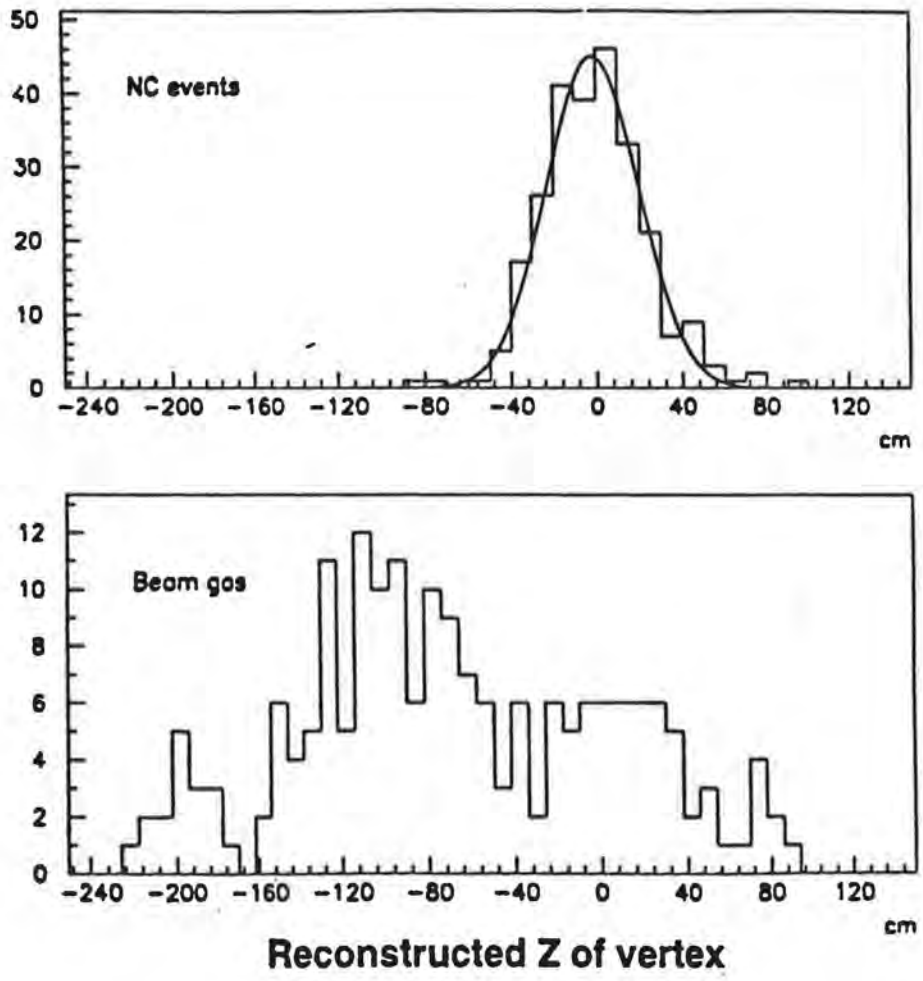
NC events
Beam gas
cm
cm
Reconstructed Z of vertex

Fig. 3

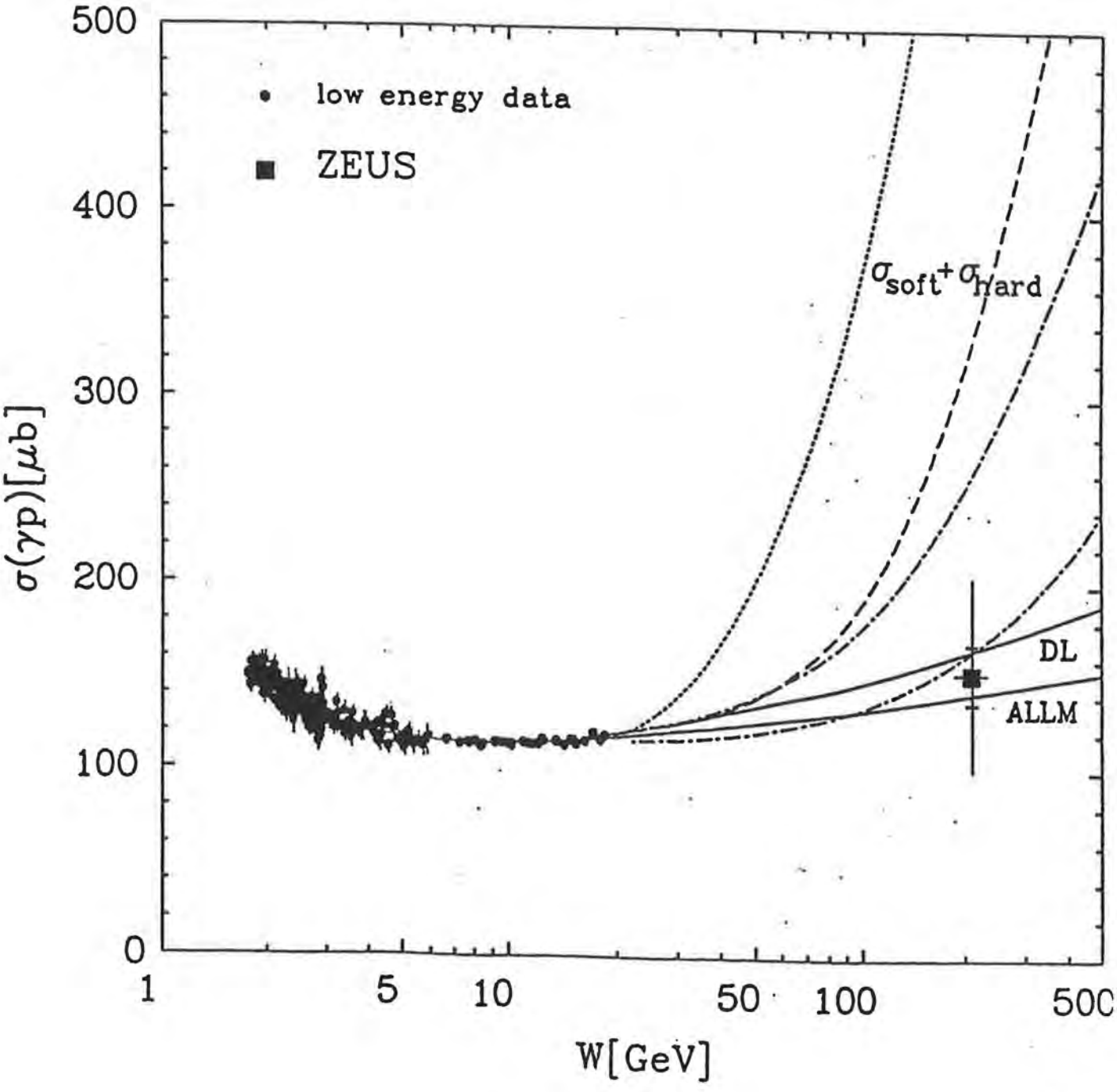
low energy data
ZEUS
$\sigma_{soft}+\sigma_{hard}$
DL
ALLM
$\sigma(\gamma p)[\mu b]$
W[GeV]
500
400
300
200
100
0
1
5
10
50
100
500

Fig. 4(a)

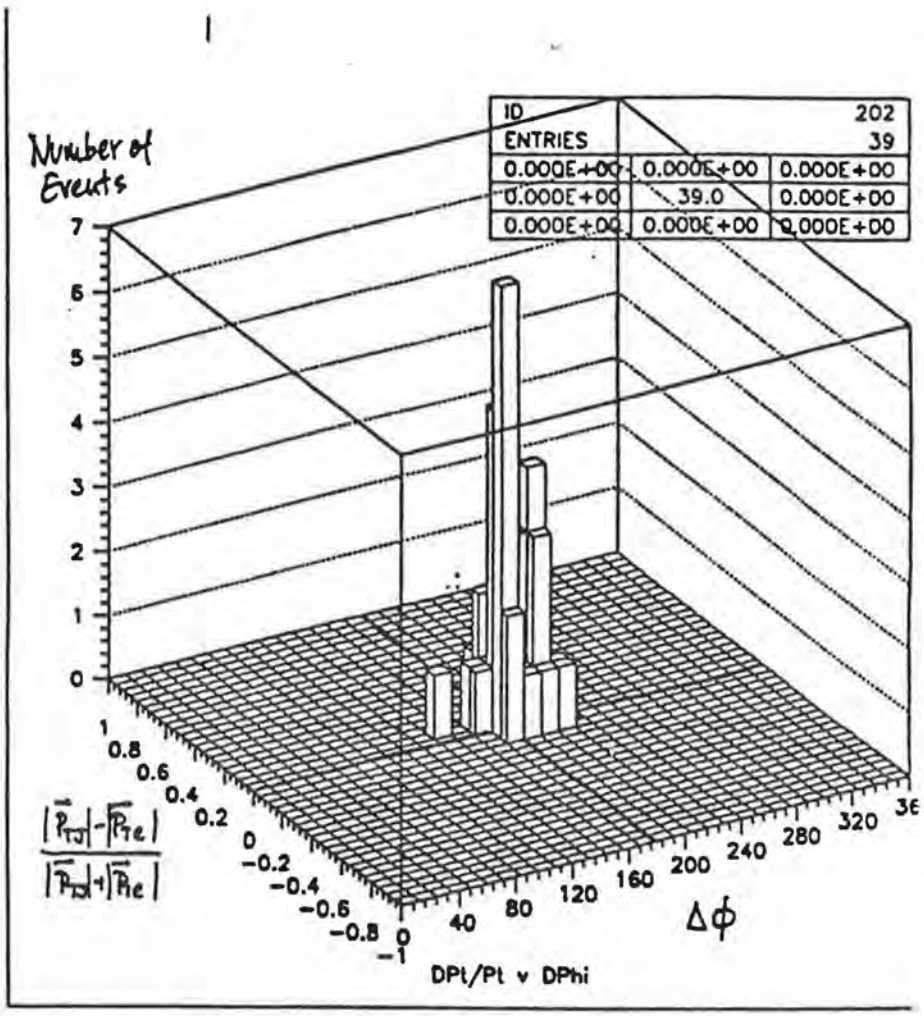
ID 202
ENTRIES 39
0.000E+00 0.000E+00 0.000E+00
0.000E+00 39.0 0.000E+00
0.000E+00 0.000E+00 0.000E+00
Number of Events
DPt/Pt v DPhi
Δφ

Fig. 4(b)

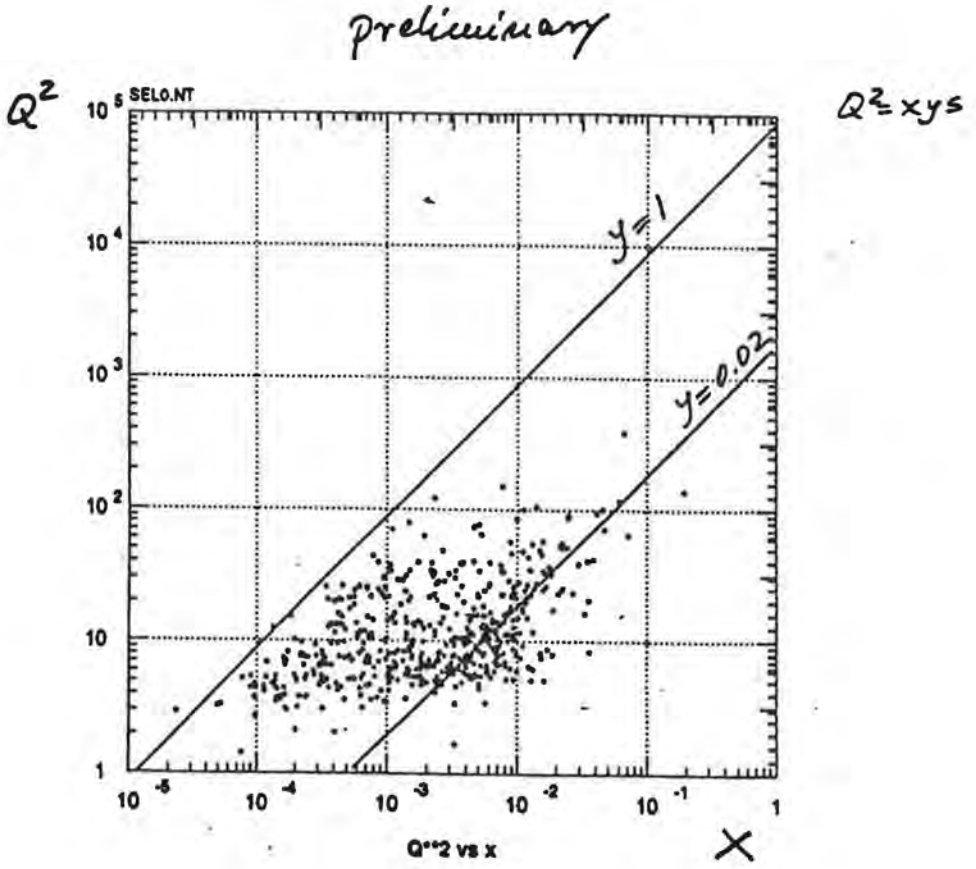
preliminary
Q²
SELO.NT
Q²=xys
y=1
y=0.02
Q**2 vs x
X

SITP: A Silicon Tracker/Preshower Detector for the LHC

RD2 Proposal 801

Cambridge University, CERN, Dortmund University, Geneva University, Hamburg University, Melbourne University, Montreal University, Oslo University, Oxford University, Perugia University and INFN, Rutherford Appleton Laboratory, Saclay CEN.

Introduction

The high luminosity at the LHC and the required detection of signatures of both expected and unexpected rare physics processes impose severe constraints on any tracking detector. We have studied the relevant aspects of silicon detectors and our results lead to a viable design (SIT) for a tracking detector for the proposed Atlas experiment. We assume that the detector will be integrated into one of the Atlas designs which includes a liquid argon electromagnetic calorimeter and an embedded cold preshower. The SIT would then perform as an outer barrel tracker, used i) as part of a combined central tracker, ii) as part of the electron identification by track preshower matching, iii) as part of the muon identification by providing the crucial measurement of the muon entry point to the calorimeter material, and iv) as a high p_T track trigger.

In the event of a warm EM calorimeter being the preferred option, the SIT layout can be easily reconfigured to provide a precision preshower layer (see the original SITP proposal). Many studies have in fact been made with this configuration.

Preshower test programme

The major activity this year was in the completion of the preshower test beam programme. Many improvements were made by the Oxford group to the readout electronics, which resulted in a big improvement in reliability. The Cambridge group is responsible for the design and fabrication of the silicon detectors. All the silicon counters and electronics used in the test beam were then tested with a laser diode system at Oxford. The complete system was tested in the low energy proton beam at ISIS before being sent out to CERN where a large number of runs was taken with different particles ($e^-/\pi^-/\gamma$'s) and different impact points and angles on the counters. The analysis of this data is still in progress.

Simulation

There was a large amount of work done on simulation studies of the use of the SIT to make a second level track trigger. This study involved the generation of about 200000 jets which included the calorimeter and level 1 trigger simulation. The CPU power for this work was provided by a set of DECstations at Oxford. The performance of the level 2 trigger algorithm was tested on the subsample of these jet events which passed the level 1 trigger and on samples of isolated electrons (including the effect of pileup of 20 minimum bias events). The efficiency of the trigger as a function of p_t is shown in fig.1. An overall rejection power of about 100 could be achieved against the jets passing the level 1 trigger for an electron efficiency of about 90%. Studies were also performed on the performance of the SIT as part of an overall tracking system, including a silicon vertex detector (SITV). The pattern recognition performance is excellent, with negligible rates of fake tracks even at the highest luminosities. Electron identification efficiencies of ~96% were found, with algorithms which reduced background from conversions and Dalitz pairs to <10% of the $W\rightarrow e\nu$ signal for $p_T^e>30$ GeV.

Engineering studies

Work at Oxford has recently started on the mechanical design for the SIT detector. To begin with finite element analysis calculations were done for the support cylinder. The deformations caused by the loading of the readout boards was calculated for different parameters of the support cylinder (e.g. thickness of skin etc.) allowing for an optimisation of this support cylinder.

The mechanical design studies will continue at Oxford. More detailed studies including thermal effects will be performed. The question of integrated SIT and SITV mechanics will be investigated jointly with RAL.

Electronics

A programme of work at RAL has been started to develop an Analogue pipeline chip suitable for processing the signals from the Fast Silicon Detectors proposed for future LHC or SSC experiments. The

key feature of these designs is the addressable analogue memory array used for temporary data storage. The analogue memory array is based on switch capacitor techniques which offer large dynamic range, static charge storage, random access addressing, simultaneous reading and writing of data even at different frequencies and low power consumption.

Two Analogue pipeline chips APC1 and APC3, have been developed. The input circuits on these chips are charge-sensitive and integrate continuously. Inputs amplify charge collected by a silicon detector connected to their inputs. After amplification the charge is sampled at periodic intervals and stored in an analogue memory cell. Memory management Logic on the chips keeps track on these samples until it is desired to readout or discard them.

As a first stage in the development of an Analogue Pipeline Chip, a 4 channel analogue pipeline chip, APC1 was designed and manufactured. This chip incorporated an analogue memory array with 64 memory cells for each channel and all the digital control logic necessary to control the storage and retrieval of data from the analogue memory array. This chip was fabricated in a 1.5 micron CMOS process and was subsequently tested and its performance measured. The results of tests on this chip showed that there was a pedestal non-uniformity of 20mV r.m.s. from cell to cell and the linearity range of the output was from -1.0 volt to 1.5 volts, which corresponds to 10 bits of accuracy.

APC3 is a development of APC1. APC3 has 32 channels and an analogue memory array with 128 memory cells for each channel. Improvements were made to the design of the analogue memory cell to reduce pedestal variation. In addition the digital control logic was redesigned to reduce its power consumption to less than 1mW per channel and to cope with the increased size of the array. This was achieved with only a 50% increase in the size of the chip. This chip has been fabricated in a 1.5 micron double metal double poly bulk CMOS process and will be tested in the near future both at the chip level and in a system with source, detector and readout.

Future Electronics Developments

Three major aspects of the chip's performance need to be addressed for the project to meet its design goals. The first of these is the need to make the chip capable of operating reliably after a high radiation dose. This requirement is being addressed by fabricating a version of the APC3 chip in an IC process resistant to radiation damage. Such a process has been identified and work is well advanced on preparing the design for manufacture in Spring 1993.

The second requirement to be addressed is the need to add circuitry to perform data sparcification, digitisation and readout. Work on the logic for sparcification has started at Oxford. A simple chip has been designed and submitted for production using ES2. This chip uses the front-end chip, ADC and discriminator to output space data (i.e. hits above threshold). Work is taking place at CERN on the design of an ADC to perform the digitisation. Subject to the successful completion of this work we would aim to incorporate this functionality into a future chip to be fabricated in Autumn 1993.

Finally improvements need to be made in the performance of the Analogue circuitry on the chip, to reduce its noise, power consumption and to improve its speed and linearity. A programme of work aimed at addressing these issues on the rad-hard developments is being pursued with our partners at CERN.

All groups plan to be involved in the board level testing of the new front end chips. The first tests will use the new RAL/CERN front end chip APC3 and a sparcification chip designed at Oxford. Oxford will be responsible for the front end board to mount these chips together with a discriminator, ADC and buffer memory. This will allow system level tests of these chips and so help in the integration of these components into one chip. Cambridge will supply software support for the VME board DAQ chain for these tests.

The design of the sparcification chip will be transferred to a full custom design so that it can be integrated into future front-end chips. At the same time different sparcification schemes and data buffering and readout schemes will be studied at Oxford and RAL.

Counter Design and Radiation Studies

Extensive studies of irradiated detectors have been undertaken by the Cambridge group and their collaborators, using the RAL ISIS facility for neutrons and the PS at CERN for protons. The expected bulk damage due to neutrons, at the SIT radius, is much greater than that caused by charged particles. The predicted neutron fluxes believed to be reliable to within a factor 2, are in the range 2-4 $10^{12}cm^{-2}\ yr^{-1}$ for the proposed rapidity range; this assumes a 10cm thick neutron moderator which reduces the fluence in the relevant energy range by a factor 10.

The CV and IV characteristics of silicon diodes after neutron irradiation have been extensively investigated. We have shown that the devices can continue to work at LHC levels of irradiation. When the

effective donor concentration N_{eff} is plotted against neutron fluence ϕ_n, the values drop to near zero and then increase again as shown in Fig.2. This is interpreted as an "inversion" of the material from n-type to apparent p-type. We have shown that there is a decrease in inter-pad resistance at the same time but that is still remains high enough for the detector to continue functioning, despite the type inversion. Typical values of interpad resistance at depletion voltage are shown in Fig.3 for neutron fluences up to ~10^{14} cm^{-2}. Little difference in inter-pad resistance was seen between different manufacturer's or detector passivation type. Values scale simply with the size and separation of the pads, and thus the measurements are normalised to the same size for comparison.

Preliminary indications from proton irradiations show that the detectors can also be expected to survive the expected charged particle flux.

The Cambridge group will be responsible for the design and fabrication of detectors optimised for a tracking geometry. This will include the investigation of passive fan-in structures needed for orthogonal strip readout, and further simulation studies.

Publications

"The development of a silicon detector for the LHC, 1st year Ph.D. report, S.J. Bates, Cambridge University, Sept. 1991.

"RD2 Status Report to the DRDC", RD2 Collaboration, CERN/DRDC/92-4, 1992.

"A 66 MHz, 32-Channel Analog Memory Circuit with Data Selection for Fast Silicon Detectors", RD2 Collaboration, presented by F. Anghinolfi, Sixth European Symposium on Semiconductor Detectors, Milan, Feb. 1992, also CERN/ECP 92-3.

"Neutron Irradiation of silicon diodes at temperatures of + 20°C and -20°C, RD2 Collaboration, Sixth European Symposium on Semiconductor Detectors, Milan, Feb. 1992.

"RD2: Silicon Tracker and Preshower - Technical Description", Eagle Internal note INDET-NO-003, Feb. 1992.

"Electrical Properties and charge collection efficiency for neutron irradiated p and n-type silicon detectors", RD2 Collaboration, presented by F. Lemeilleur, 3rd International Conference on Advanced Technology, Particle Physics, Como, July 1992.

"The Design and Function of a Radiation Tolerant Silicon Tracker for an LHC Experiment", RD2 Collaboration, presented by S.J. Bates, 3rd International Conference on Advanced Technology, Particle Physics, Como, July 1992, also Cambridge Preprint HEP 92/8.

"Implementation of a 66 MHz Analog Memory as a Front End for LHC Detectors', RD2 Collaboration, presented by R. Bonino, Dallas Conference, August 1992.

"Electron Identification using Energy Momentum Matching in the Ascot/Eagle Inner Detector". Ascot/Eagle Internal Note INDET-NO-015, Sept. 1992.

"Second Level Electron Triggering In The Atlas A Detector", Atlas Internal Note INDET-NO-013, Oct. 1992.

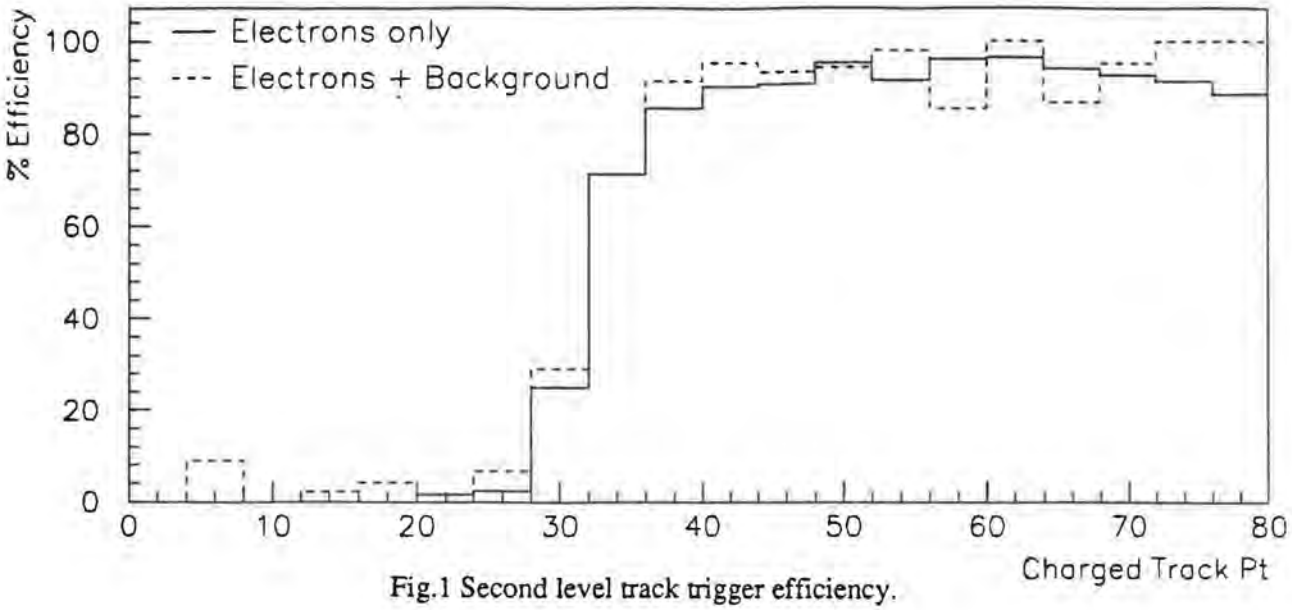

Fig.1 Second level track trigger efficiency.

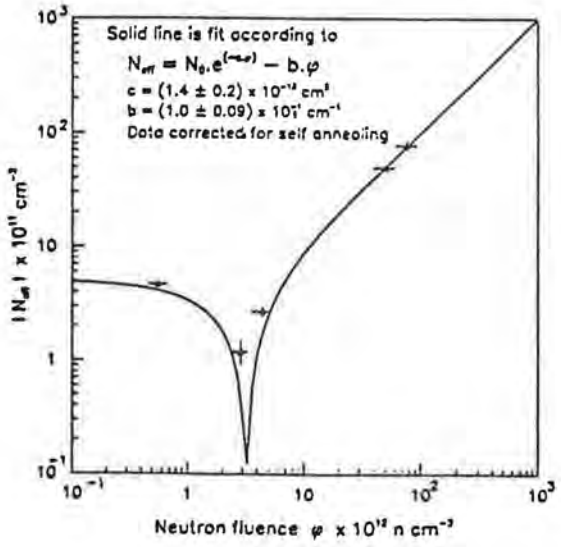

Fig.2 Effective doping concentration of a typical silicon detector versus neutron fluence.

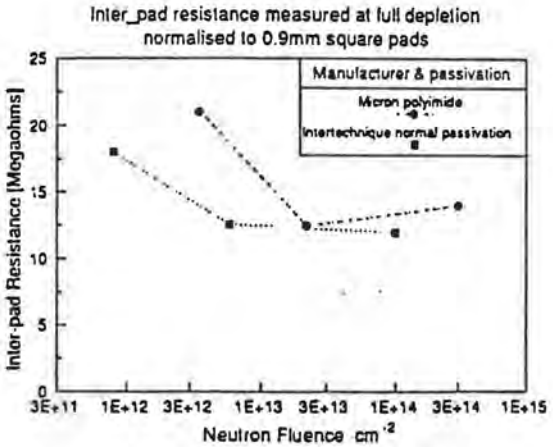

Fig.3 Interpad resistance for different segmented silicon test structures after neutron irradiation.

Integrated Transition Radiation and Tracking Detector for LHC

Glasgow and RAL
with Brookhaven, Dubna, Cracow, Lund, Moscow (Lebedev), Moscow (MEPHI), Munich (Max-Planck) and St Petersburg.

This development project is dedicated to producing a detector subsystem for highest energy pp collisions with the following properties:

Robust internal track-finding with adequate redundancy
Electron signals cleanly visible in the presence of large backgrounds
Operation at luminosities well above 10^{34} cm^{-2} s^{-1} for many years
Provides independent level-2 trigger for electrons
Suppresses jet backgrounds below 10^{-5} level using a method independent of calorimeter or track isolation.
Minimal material. Photon conversions both outside and within the detector are identified and rejected.

The principles of single-wire straw tube TRD systems for electron tracking and triggering have already been demonstrated by this collaboration [1], and in the 1991 test beam running and analysis we optimised the Xenon fraction to provide high TRD photon capture probability, and therefore excellent hadron rejection, with a short maximum drift time. The gas mixture selected is Xe-CO_2-CF_4 70:10:20, which gives a maximum drift time of 34ns.

The 1992 running investigated hadron, jet and photon-conversion rejection in a magnetic field, together with the backsplash of particles from an electromagnetic calorimeter. An LHC solenoidal detector was simulated at a rapidity of 1.75 in a magnetic field of 0.78T. In addition, the performance of the detector was enhanced by reading out drift times as well as hit and two-level pulse height information. Position resolutions of 138 microns were achieved, with systematic error control to better than 50 microns. This means that a TRD system alone, with knowledge of the beam spot position, can measure momenta to a fractional precision of $8.10^{-4}p$ (p in GeV/c). In the UK we are presently setting up to measure the electron drift velocity and Lorentz angles in a field of 2T, as required at LHC.

TRD systems have been proposed for LHC detectors [2,3]. The main focus of present effort is to build realistic elements of an LHC forward-tracker subsystem [4] in which 50cm long straws are placed at fixed ϕ and z. A detector wheel contains 16 layers, each of 600 straws, the layers being interspersed with sheets of polypropylene radiator material. The whole detector is constructed to have minimum mass. As well as a mechanical prototype we are building a series of sector prototypes with electronic readout to test an

LHC-like device with a realistic operating system (RD13 collaboration). The British groups have taken responsibility for the front-end electronics and two ASIC chips have been designed for on-detector signal processing.

The RAL 118 (TRDA) chip is an analogue device handling the input from eight channels of detector. Pulses are shaped with a 10ns peaking time and pole-zero shaping falling to 5% in 25ns. There are two discriminators, a low-range controlled in 50eV steps from 200eV to 1550eV energy deposit on the straw, and a high level running in 250eV steps from 1 keV to 7.75 keV. The low-threshold is designed to detect minimum ionising particles and provide drift time information on all particles. The high threshold detects the conversion of TR photons. The two outputs drive a ternary-encoded balanced differential output, and test pulse inputs are provided to pulse odd and even channels.

The RAL 117 (TRDS) chip controls eight chips. Five-bit serial digital control input from the DAQ system provided DC currents which set the TRDA thresholds. It also converts the ternary coded outputs to CMOS levels and drives the test pulses. The TRDA and TRDS functions are placed on separate chips to isolate the analogue system from digital level-switches.

It is intended to place complete sector prototypes in a test beam at CERN in 1993, to demonstrate a functioning subsystem suitable for incorporation into an LHC experiment [5].

Publications

1 J T Shank et al, Nucl Inst Meth A309 (1991) 377.
2. EAGLE Expression of Interest (Evian meeting) 1992.
3. ASCOT Expression of Interest (Evian meeting) 1992.
4. V A Polychronatos et al CERN DRDC/91-47.
5. ATLAS Letter of Intent for a general-purpose pp experiment at the Large Hadron Collider at CERN, CERN/LHC/92-4.

Optoelectronic Readout from LHC detectors 803

J.D. Dowell, M.S. Haben, R.J. Homer, P.M. Hattersley, P. Jovanovic, I.R. Kenyon, R. Staley, B.M. Waugh and K.A. Webster

School of Physics and Space Research, Birmingham University, P.O. Box 363, Birmingham B15 2TT.

Progress Report 1992

HFOX

The joint program (HFOX) embarked on with CERN and Hewlett-Packard in 1990, although not funded by the SERC, is mentioned here because it has brought relevant experience, as well as some material support and a CASE studentship. HFOX is an acronym for HiPPI Fibre Optics Extender. HiPPI is the IEEE High Performance Parallel Interface protocol designed for data links on copper based connections up to 25 metres length. HFOX provides a serial fibre link which extends the use of HiPPI to 10 Km. The performance is specified by an IEEE document. The link was designed to connect computers at CERN and is now coming to fruition. Figure 1 shows the link within a planned HiPPI network being installed at CERN. At the computer interface the data rate is 800 Mb/s, while the the data transfer rate over the optical link is 1.5 Gb/s. The difference is accounted for by the HiPPI protocol information and 16/20 IEEE NRZI coding scheme. The link is currently installed and undergoing tests at CERN. Figure 2 shows the components of the link in more detail. Backup multiplexer/coder and demultiplexer/decoder cards using Gigabit and Vitesse chips have been built at Birmingham and will be tested within the next few months. The HFOX project is extending our electronic design experience to ultra-high data rates equal to or exceeding those likely to be met at LHC.

Optoelectronic readout

Optoelectronic methods are seen as a necessary component of data transfer at LHC. The generic advantages of optical fibre based readout are: freedom from electromagnetic interference; high potential bandwidth; a technology adequately radhard for LHC applications [1]; negligible signal attenuation and dispersion over monomode fibre links of the length needed on an LHC detector; low volume, mass and number of radiation lengths compared to a copper wire based readout, with a corresponding gain in detector hermeticity; lower fibre cost per metre than shielded twisted pair cable.
Both passive and active modulation are of potential interest when considering how to transform the electrical signals at the detector elements into optical signals. These optical signals are then carried by fibre to the Electronics Barrack/Rucksack, where they are reconverted to electrical signals. In an active modulation scheme the electrical signal at the detector is used to directly modulate the current and hence the light output of a laser diode or LED. By contrast, in a passive modulation scheme, the sources of light are lasers located in the Electronics Barrack, and the light is piped by fibre to passive modulators located at the detector. The detector signals are used to modulate the light passing through the modulators, and the output light is carried by fibre to the Electronics

Barrack/Rucksack where the electrical signals are recovered.
Passive modulators can be based on the electro-optic effect where the refractive index of the material is altered by an applied electric field; or an electro-absorptive effect where the optical absorption of the material is altered by an applied electric field. When the electro-optic effect is used, two optical paths through the modulator are provided, as in a Mach-Zehnder interferometer. Then the change in phase between the two arms produced by applying the electric field across one arm alone will lead to interference where the paths recombine and so modulate the amplitude and intensity of light transmitted through the device. Signals from the detector applied to either type of passive modulators will then modulate the light intensity transmitted by the modulator, the modulation level being proportional to the electric signal. Passive modulation offers certain advantages: firstly, the long term reliability of the components mounted on the detector is enhanced, because these are purely passive; secondly, both the electrical power and heat load on the detector are reduced.
Several technologies are of interest for the passive modulators. The first of these are Lithium Niobate amplitude modulators [2]. They use a Mach-Zehnder configuration, with the two arms being optical waveguides formed in the lithium niobate surface layer by implanting titanium. This is a mature technology, with single channel devices being manufactured in small batches by several companies including GEC-Marconi. The competitive technology is based on Multi-Quantum Well (MQW) devices built from III/V materials, such as GaAs, InP and compounds. The MQW modulators made by GEC-Marconi are reflective devices with the absorption of the material determining the quantity of light reflected [3]. When an electric field is applied across the material Stark effect shifts in the electron and hole quantum levels are observed. Thus for incident radiation near the absorption edge in wavelength, a change in the applied field can alter the absorption coefficient considerably. This effect is amplified first by having many layers (eg 50) of quantum wells and secondly by making the outer faces of the device reflective so that they constitute a Fabry-Perot cavity. MQW modulators are very similar to unpowered MQW lasers, so that the manufacturing techniques and production lines now exist. Compared to lithium niobate modulators the MQW modulators have attractions because they are so compact. Also their construction makes monolithic integration into the electronics and even, in the case of GaAs detectors, into the detector itself a real possibility.

RD 23 Collaboration

In February this year the CERN DRDC approved our proposal made with a CERN group, Ecole Polytechnique Federale de Lausanne, GEC-Marconi, Lund, Oxford, IC(London) and RAL to investigate optoelectronic analogue signal transfer for LHC detectors. The team includes an industrial partner, a microlelectronics/optoelectronics group and representatives of the approved RD2, RD6 and RD20 teams building prototype tracking detectors for LHC as well as Stefanini's group at CERN and the electronics group at RAL. Funds for the UK component of the RD23 committment have been granted by the PPGSC for the year 92/3. The RD23 collaboration [4] is engaged in making quantitative studies of single and multi-channel modulators in the lithium niobate and MQW technologies. Up to 64 optical channels are envisaged on a single lithium niobate or MQW substrate, with correspondingly 64 electrical inputs and 64 output fibres carrying the modulated light sig-

nals. Tests are forseen with Silicon (RD2 and RD20), with liquid argon preshower (RD3), with TRD (RD6), and with GaAs (RD8) detector prototype modules. Direct modulation of laser diodes or LEDs is being considered in parallel by Nickerson at Oxford, who is also involved in the RD23 activity. The RD23 programme is extensive: the characterization of the single- and multi-channel devices will include the measurement of dynamic range, linearity, and the effects of temperature variation, applied magnetic fields and irradiation. A crucial facet of this work, which is described below, is the study of a fully connectorized optical circuit, to obtain experience in a system as near to the setup at LHC as possible. Radiation hardness of lithium niobate modulators has been validated [5]; members of RD23 have also exposed MQW devices to neutron levels expected for a decade of running at LHC with negligible change seen in device characteristics. Related work, but not part of RD23, at Brookhaven by Tsang, Radeka and colleagues [6] has shown that the lithium niobate devices function well in liquid Argon and undergo no physical damage. MQW devices have also been studied at low temperatures by GEC-Marconi and these too function satisfactorily; however the wavelength of operation must be shifted to follow the displacement of the absorption edge with temperature [7].

Characterization of single channel Modulators at Birmingham

1) Lithium Niobate Mach-Zehnder Modulator

Figure 3 shows the optical testbench at Birmingham used to characterize a GEC lithium niobate Mach-Zehnder modulator. The modulator response to DC levels is shown in figure 4; the y-coord is the output voltage of the photodiode receiving the light passing through the modulator; and the x-coord is the voltage applied to the modulator. The sinusoidal response is the characteristic of phase modulated devices. It is possible to make the response to signals linear by designing the devices so that the quadrature point (point of inflection on figure 4) occurs at a bias of zero volts. The response to rectangular pulses applied to the modulator electrodes has also been studied, and the dynamic range for 20ns long pulses over which the response is linear was found to be around 50:1. By using the fully connecterized optical circuit of figure 3, as opposed to one having segments of the light path in air, it has been possible to gain valuable insight into the importance of the various noise sources and their impact on dynamic range. A standard expression for the minimum detectable signal when working at the quadrature point is the following [see 8]:

$$\Delta V = (V_\pi/\pi)\sqrt{RIN.\Delta f}(SNR)$$

where RIN is the equivalent noise as expressed as a Relative Intensity Noise of the laser source, Δf is the receiver bandwidth (related to pulse width), V_π is the voltage required to change the phase difference between the two optical paths by π, and SNR is the minimum acceptable signal/noise ratio. Figure 5 shows the expected contributions of the more obvious noise sources: laser RIN noise (from spontaneous emission), photodiode receiver noise and shot noise. The noise level observed without the modulator in the optical circuit matches the noise predicted from figure 5. At a photocurrent of 0.1 mA, it is -140 ± 2 dB/Hz, being dominated by the laser RIN noise. However, when the modulator

is included in the optical circuit, the noise level rises to -130 ± 5 dB/Hz. The source of this additional noise is the conversion of phase noise in the laser light beam to amplitude noise. This occurs whenever standing waves can be set up between reflective components in the optical circuit. Possible sources of reflection were measured directly with a different optical test bench setup. The culprit responsible for the the noise increase is found to be the large reflection coefficient (-14dB) at the interfaces of the modulator; explicitly the interfaces between the lithium niobate and the optical fibres taking light in and out. Reflection coefficients at all the interfaces along the optical circuit have been measured. Then using these measured reflection coefficients the equivalent RIN due to phase/amplitude noise within the optical circuit has been estimated to be -130 dB/Hz [9]. Inserting the values of parameters appropriate to our optical circuit into the previous equation; namely a RIN of -130 dB/Hz, Δf of 25 MHz and requiring the SNR to remain above 3:1, gives $\Delta V = 0.0016V_\pi$. At the other extreme, the maximum recognizable signal when working at the quadrature point is $V_\pi/2$. Hence the maximum dynamic range achievable, $V_\pi/2\Delta V$, is 300:1. If signal linearity is also required the maximum acceptable signal is reduced. Requiring a departure from linearity of less than 1% means that only voltage swings of $V_\pi/12$ from quadrature can be tolerated. This reduces the usable dynamic range predicted for our optical circuit to 50:1, which agrees well with the result of our direct measurement of the dynamic range requiring linear response. As part of this study we have tried out both DFB and FP diode lasers (temperature controlled and uncontrolled), and several photodiode detectors. We have also measured the optical spectra of all the laser diodes used and correlated this information with the observed noise of the laser. Our work has highlighted the importance of reducing phase/amplitude noise conversion, and this factor is being taken into account in the design of the integrated optical circuits containing the multichannel modulators. It has certainly justified our plan of studying a system which is fully connectorized and therefore as similar as possible to a layout practicable for LHC usage.

The radiation resistance of auxiliary components in the optical circuit, such as connectors, is less well studied than the radiation resistance of lasers, fibre and modulators. A programme of irradiations of a range of such components is to begin shortly at the RAL ISIS neutron facility. Similar work will be undertaken at CERN.

2) Multi-Quantum Well Modulator

Work in this area has recently started. GEC-Marconi have supplied us with two items: a prototype chip carrying an array of eight MQW modulators whose absorption edge lies at 1610nm; and a laser diode operating at the same wavelength. Figure 6 is a mechanical drawing of the MQW chip layout showing the $30\mu m$ diameter quantum wells spaced at $100\mu m$ intervals. Our optical bench for testing this array is shown in figure 7. Light from the laser diode is passed to the modulator where part is reflected; the reflected beam intensity depending on the voltage bias applied across the individual MQW modulator illuminated. Then the reflected beam travels back along the same fibre to the SIFAM splitter where about half the reflected light is transmitted to the photodiode. Figure 8 shows an area scan of the reflectivity of the region around one modulator (seen as the plateau at the centre) for a fixed voltage bias on the modulator. A line scan across the modulator is shown in figure 9; during the scan a time varying voltage was applied to the modulator. The extent of the sensitive region is clearly defined by the level of modulation.

Note that the image of the beam on the modulator has a diameter of $8\mu m$, so the apparent diameter of the sensitive region is the sum in quadrature of the beam diameter and the MQW modulator diameter. Figure 10 shows the response of the MQW modulator to rectangular 20ns long pulses as a function of the voltage amplitude of the pulse. Shortly we intend to carry out tests of the modulator operation in field up to 2T.

Collaboration List

1) HFOX Collaboration: Birmingham University, CERN and Hewlett-Packard. Construction and installation of a GHz optical link between computers at CERN carrying the full HiPPI protocol.
2) RD23: Birmingham University, CERN, Ecole Polytechnique Federale de Lausanne, GEC-Marconi, Imperial College (London), University of Lund, Oxford University and Rutherford Appleton Laboratory. Optoelectronic Signal Transfer for LHC Detectors (see reference 4).

Figures

1) The HFOX Optical Link within the HiPPI network at CERN.
2) Block Schematic showing the components of HFOX.
3) Optical test bench used at Birmingham to study the Lithium Niobate Modulator.
4) DC response of the Lithium Niobate Modulator.
5) Noise sources for the optical circuit shown in figure 3 (excluding the phase/amplitude noise conversion).
6) Mechanical drawing of the GEC-Marconi chip carrying an array of eight MQW modulators (and also eight unused photodiodes).
7) Optical test bench used at Birmingham to study the MQW Modulator array.
8) Result of an area scan of reflectivity around a single MQW modulator from the array shown in figure 6; a fixed voltage was applied across the MQW modulator.
9) Line scan of reflectivity across a single MQW modulator with a time-varying (triangular) voltage applied across the MQW modulator.
10) Response of the MQW modulator to 20ns pulses as a function of the amplitude of the pulse.

References

1) 'Radiation Effects on Optical Transmission Systems' B. Leskovar, Workshop on Triggering and Data Acquisition for Experimants at the Superconducting Super Collider, Toronto, January 1989.
2) 'Integrated Optics in $LiNbO_3$: Recent Developments in Devices for Telecommunications', L. Thylen, Journal of Lightwave Technology 6, 847 (1988).
3) 'Semiconductor Quantum-Well Structures for Optoelectronics - Recent Advances and Future Prospects', H. Okamoto, Japanese Journal of Applied Physics 26, 315 (1987).

4) 'Optoelectronic Analogue Signal Transfer for LHC Detectors' J.D. Dowell, P.M. Hattersley, R.J. Homer, P. Jovanovic, I. Kenyon, R. Staley and K.Webster (Birmingham), C. Da Via, J. Feyt, P. Nappey and G. Stefanini (CERN), B. Dwir and F.K. Reinhart (EPFL-Lausanne), J. Davies, N. Green, W. Stewart and T. Young (GEC-Marconi), G. Hall (Imperial College), T. Akesson, G. Jarlskog and S. Kroll (Lund), G. Nickerson (Oxford) and S. Jaroslawski (Rutherford-Appleton Labs); CERN/DRDC/91-41; DRDC/P31 October 9, 1991.
5) Private Communication from V. Radeka and W. Willis (BNL) and 'High Sensitivity 1.32 μm External Modulator Links for High Energy Physics Particle Detector Diagnostics'; M. Lowry, K. McCammon, Y-H. Chang, B. Wyslouch, U. Becker and P. Parker; presented at Conference on Electronics for Future Accelerators, May 1992.
6) BNL Report: T. Tsang, V. Radeka, T. Srinavasan-Rao and W. J. Willis (1992); see also 'A study of Electro-Optical Modulators for Transfer of Detector Signals by Optical Fibres', BNL-45393 (1990) by the same authors.
7) Private Communication from A. J. Moseley (GEC-Marconi Materials Research Centre, Caswell, Northants, England).
8) A. Yariv, 'Optical Electronics' (4th edition) pp436 on, Sanders Publishing, Philadelphia (1991).
9) M.M. Choy et al., Electronics Letters 23, 1152 (1987).

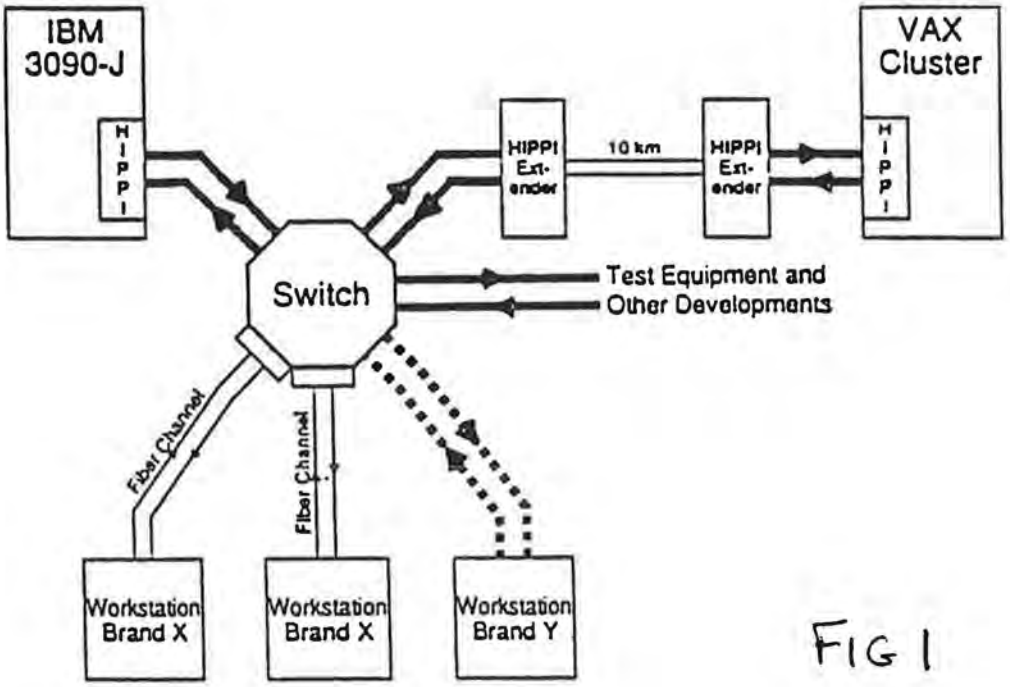
IBM
3090-J
HIPPI
HIPPI Ext-ender
10 km
HIPPI Ext-ender
VAX Cluster
HIPPI
Switch
Test Equipment and
Other Developments
Fiber Channel
Fiber Channel
Workstation Brand X
Workstation Brand X
Workstation Brand Y

FIG 1

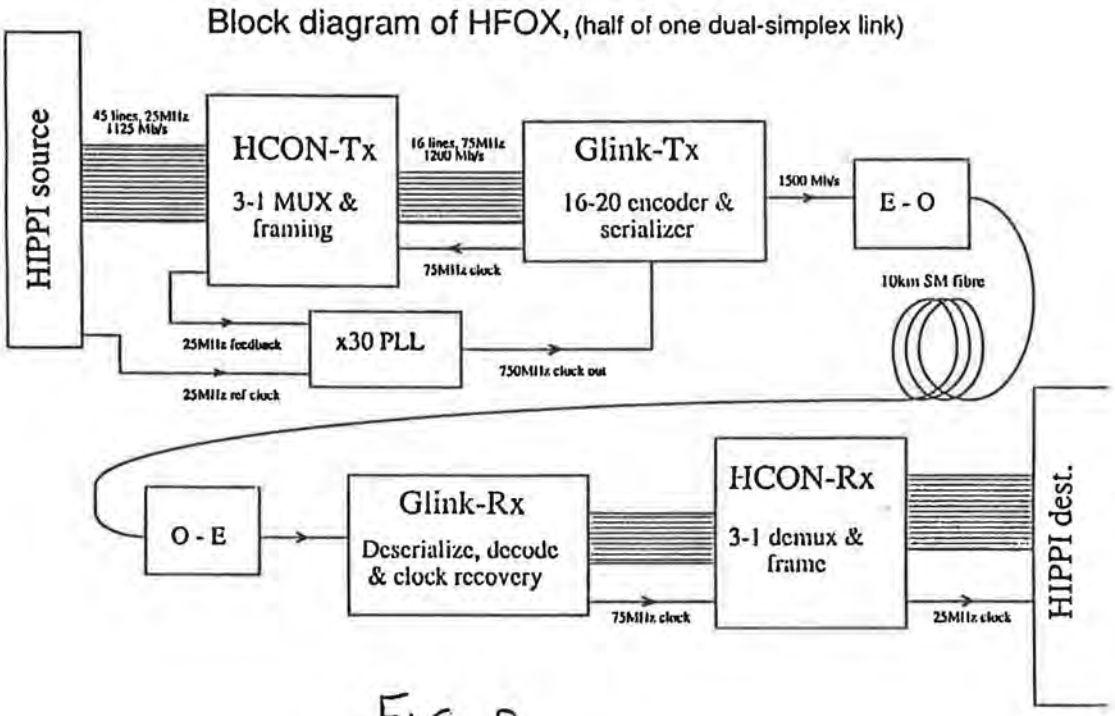
Block diagram of HFOX, (half of one dual-simplex link)
HIPPI source
45 lines, 25MHz
1125 Mb/s
HCON-Tx
3-1 MUX & framing
16 lines, 75MHz
1200 Mb/s
Glink-Tx
16-20 encoder & serializer
1500 Mb/s
E - O
10km SM fibre
75MHz clock
25MHz feedback
x30 PLL
750MHz clock out
25MHz ref clock
O - E
Glink-Rx
Deserialize, decode & clock recovery
HCON-Rx
3-1 demux & frame
75MHz clock
25MHz clock
HIPPI dest.

FIG 2

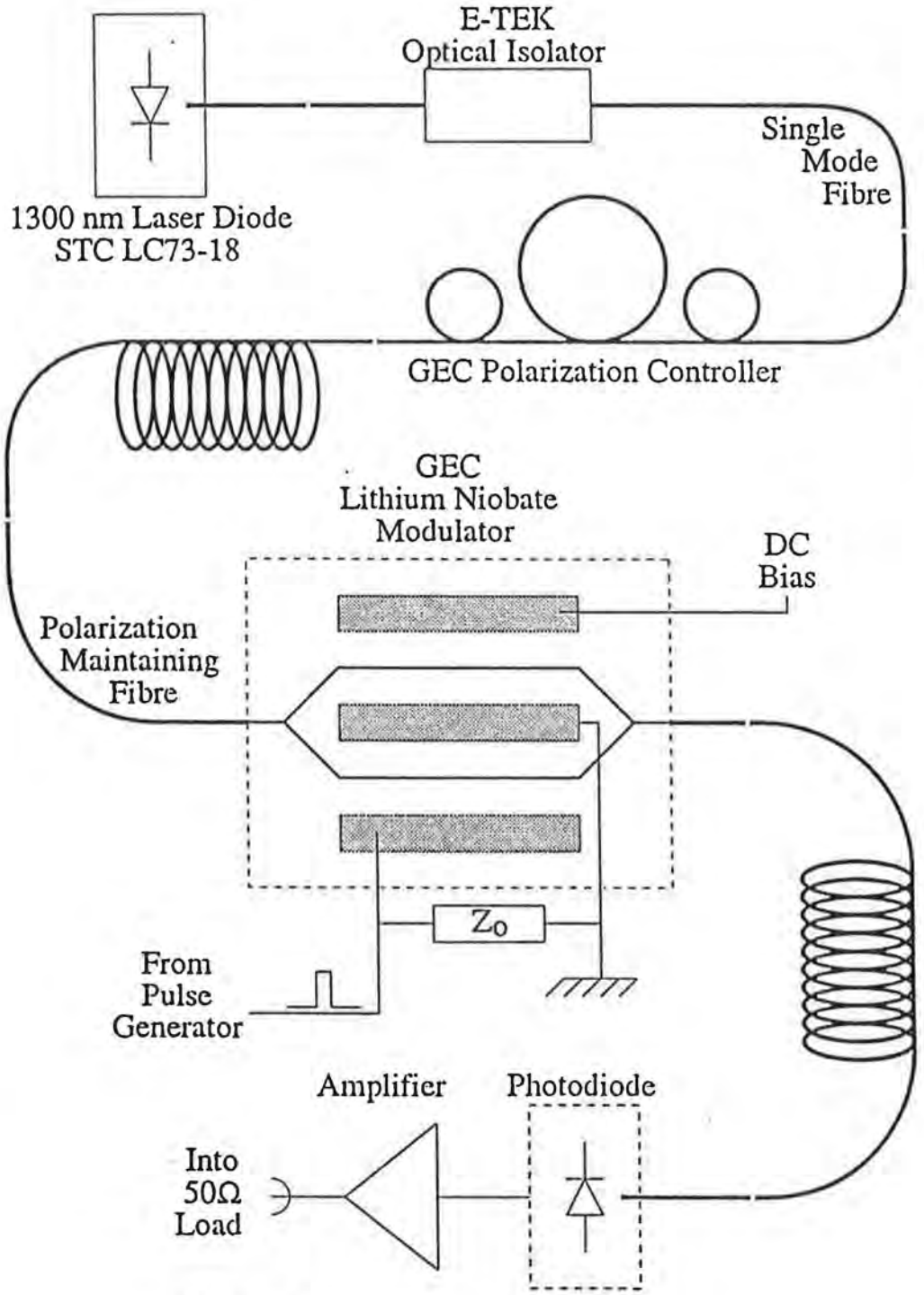
E-TEK
Optical Isolator
Single
Mode
Fibre
1300 nm Laser Diode
STC LC73-18
GEC Polarization Controller
GEC
Lithium Niobate
Modulator
DC
Bias
Polarization
Maintaining
Fibre
Zo
From
Pulse
Generator
Amplifier
Photodiode
Into
50Ω
Load

FIG 3.

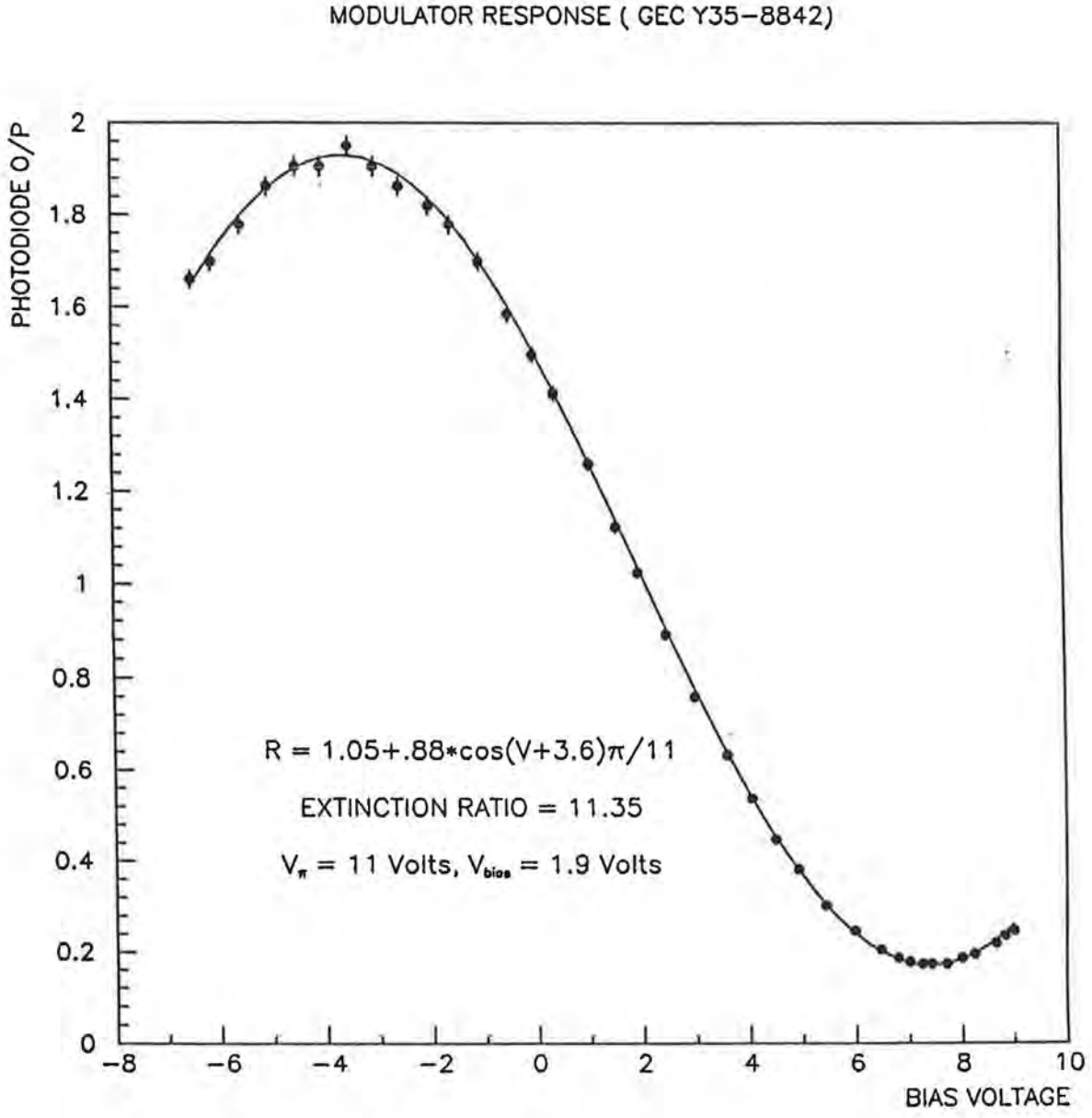
MODULATOR RESPONSE (GEC Y35-8842)
PHOTODIODE O/P
2
1.8
1.6
1.4
1.2
1
0.8
0.6
0.4
0.2
0
-8
-6
-4
-2
0
2
4
6
8
10
BIAS VOLTAGE
R = 1.05+.88*cos(V+3.6)π/11
EXTINCTION RATIO = 11.35
V_π = 11 Volts, V_{bias} = 1.9 Volts

FIG 4

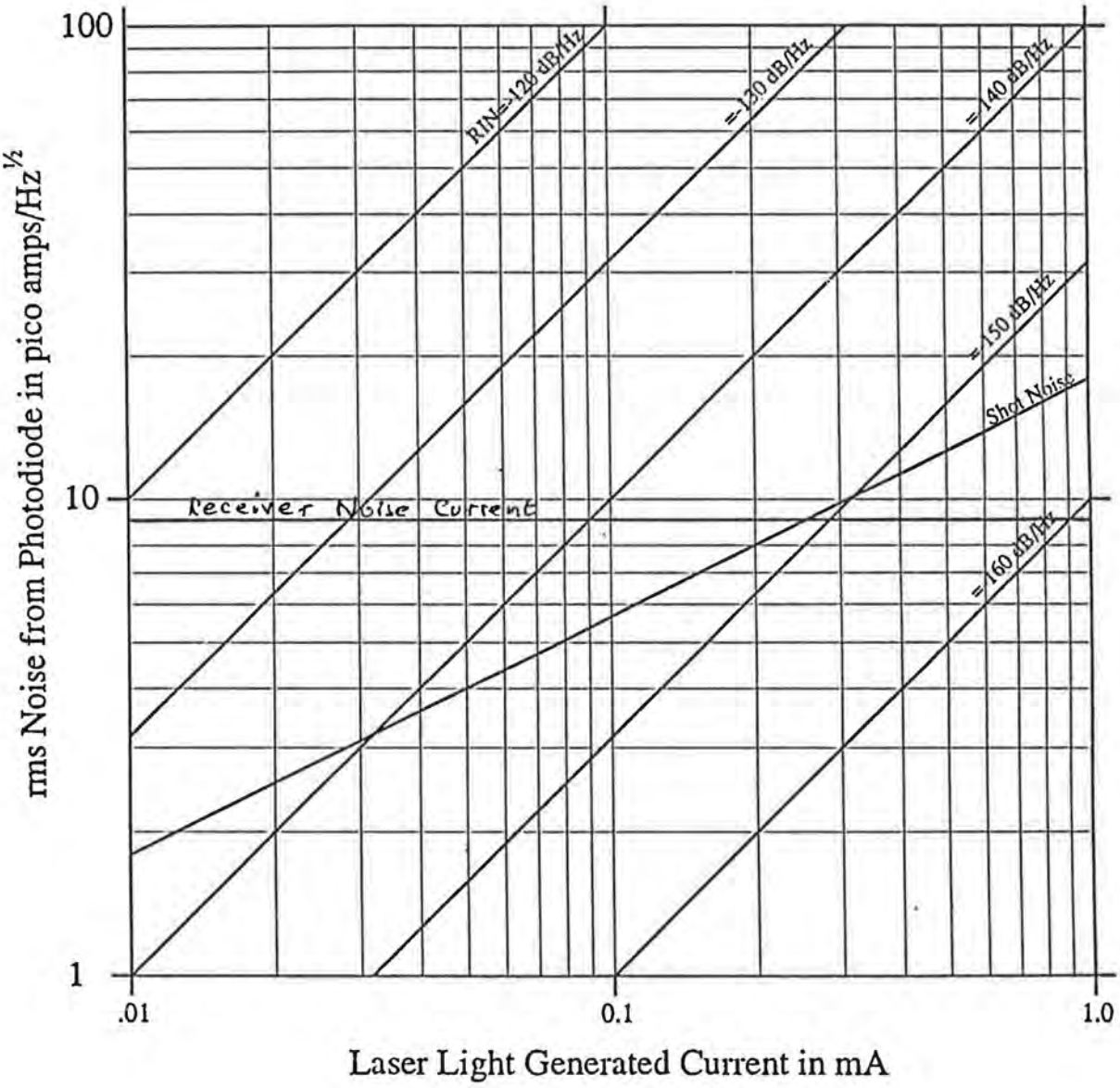
100
10
1
.01
0.1
1.0
RIN=-120 dB/Hz
=-130 dB/Hz
=140 dB/Hz
=150 dB/Hz
Shot Noise
=160 dB/Hz
Receiver Noise Current
rms Noise from Photodiode in pico amps/Hz^½
Laser Light Generated Current in mA

FIG 5

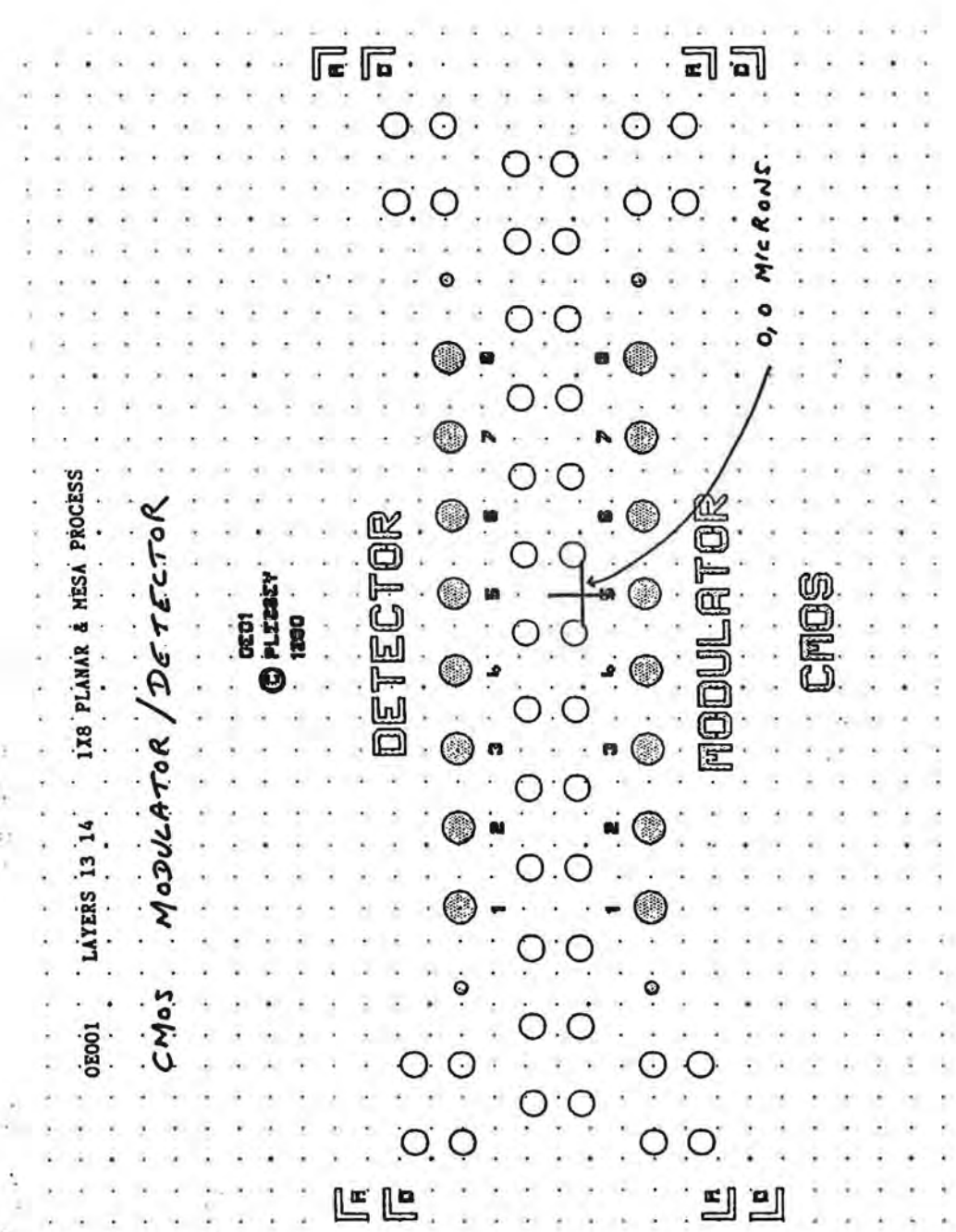
OE001 LAYERS 13 14 1X8 PLANAR & MESA PROCESS
CMOS MODULATOR /DETECTOR
OE01
PLESSEY
1990
DETECTOR
MODULATOR
CMOS
0,0 MICRONS

FIG 6

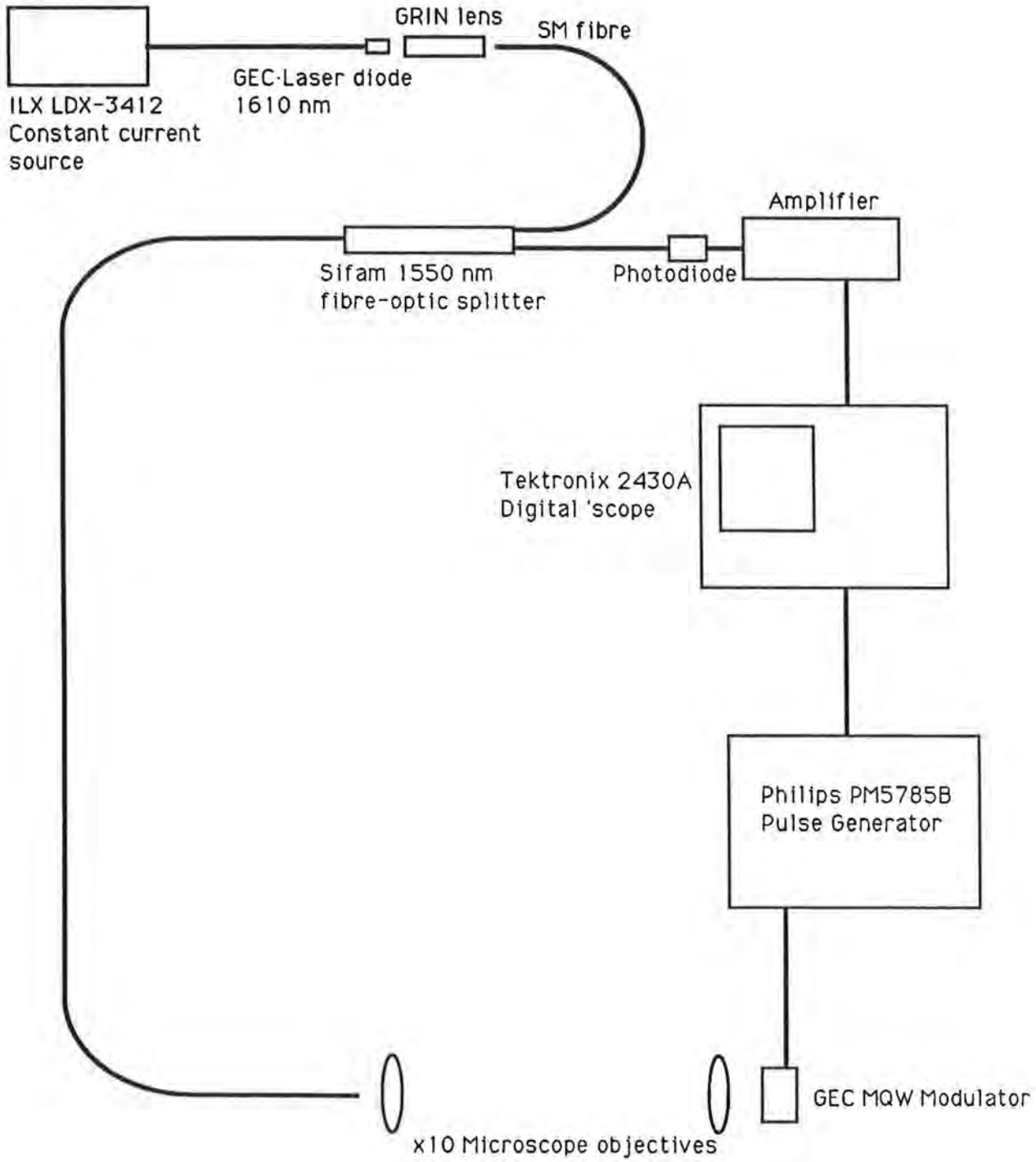

FIG 7

MQW Modulator Test Setup

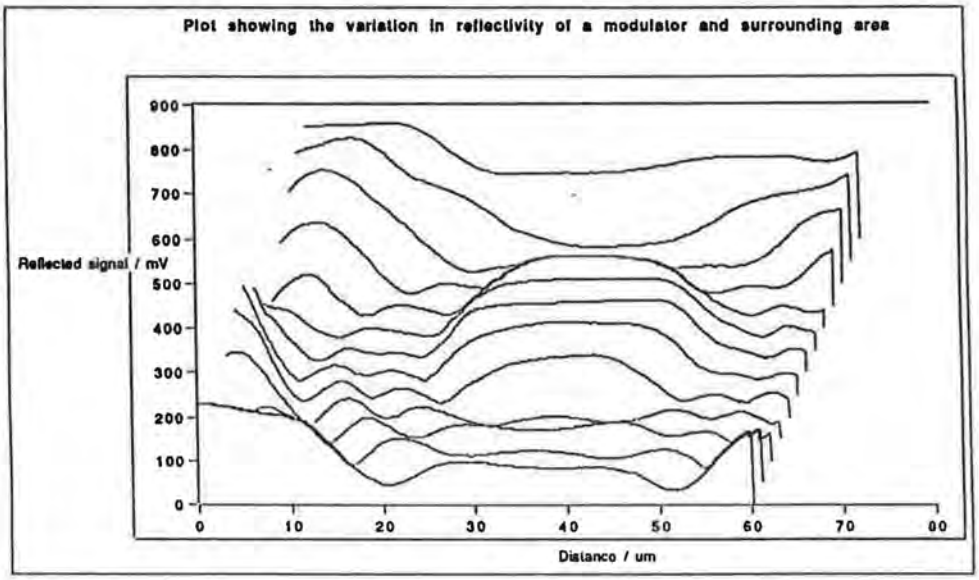
Plot showing the variation in reflectivity of a modulator and surrounding area
Reflected signal / mV
900
800
700
600
500
400
300
200
100
0
0
10
20
30
40
50
60
70
80
Distance / um

FIG 8

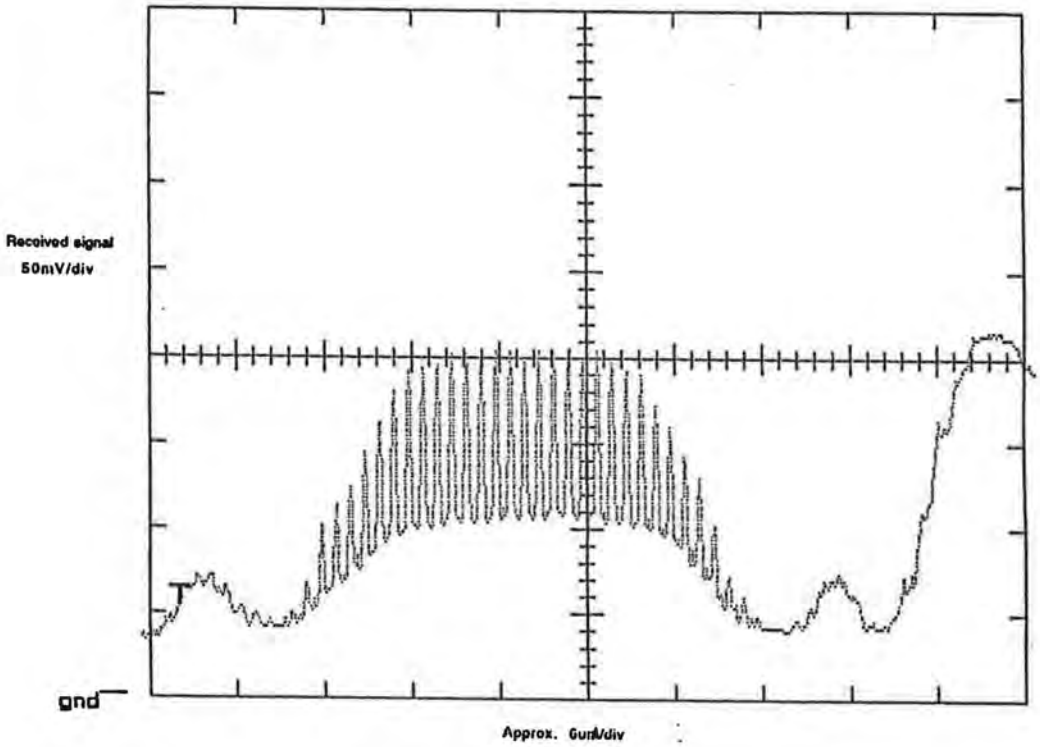
Received signal
50mV/div
gnd
Approx. 6um/div

FIG 9

Front Panel

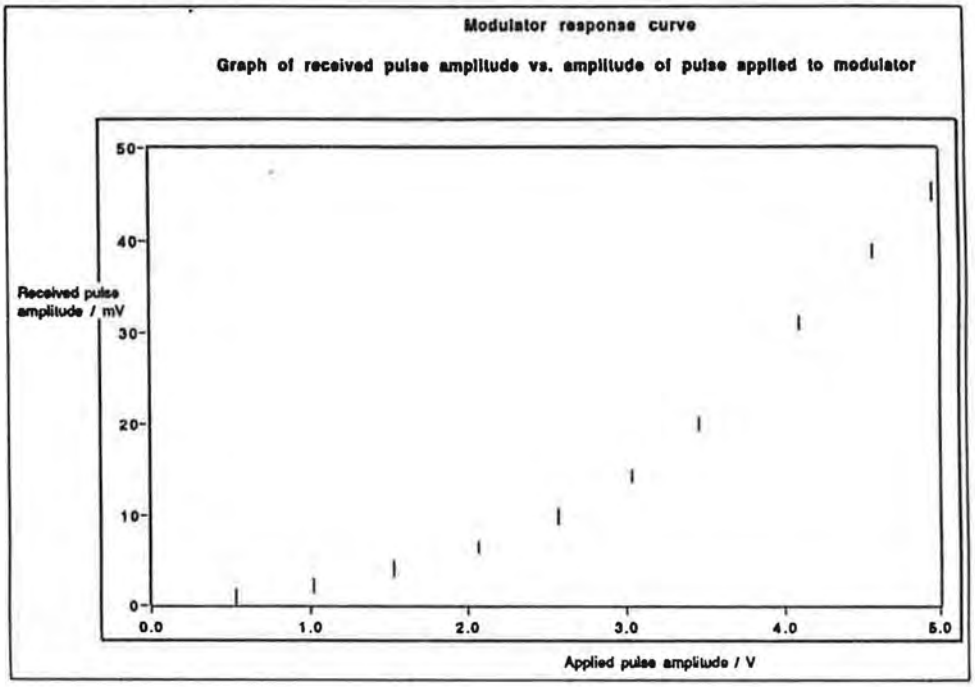

FIG 10

Progress Report of GaAs Collaboration

- Dipartimento di Fisica dell'Universita' and INFN Bologna, Italy
- CERN, Geneva, Switzerland
- Dipartimento di Fisica dell'Universita' and INFN Florence, Italy
- Dept. of Electrical and Electronic Engineering, University of Glasgow, U.K.
- Dept. of Physics and Astronomy, University of Glasgow, U.K.
- Dept. of Physics, University of Lancaster, U.K.
- Dipartimento di Fisica dell'Universita and INFN Modena, italy
- Rutherford - Appleton Laboratory, Chilton, Didcot, Oxon., U.K.
- Dept. of Physics, University of Sheffield, U.K.
- Dept.of Electrical Engineering, University of Sheffield, U.K.

The collaboration membership has grown in the last year with the addition of groups from Freiburg(University and Fraunhofer Institute), Bratislava, (Comenius University), ANSTO (Sydney) and Vilnius (Institute of Semiconductor Physics, Lithuanian Academy of Science). The emphasis of the research programme has been on improving our understanding of semi- insulating GaAs substrate material and on demonstrating that efficient detectors for minimum ionising particles can be made from this material for LHC applications.

Our original Schottky - ohmic detector fabrication recipe has now been largely replaced by one in which the contacts on both sides of the wafer are now Schottky barriers. This has the advantage of simplifying the wafer processing, thereby reducing processing costs, and does not appear to introduce significant degradation in performance. In the course of investigating these double Schottky detectors, it has become clear that the quality of surface polish on the wafer has a marked influence on the properties of the resulting detectors. This dependence is now being more closely studied. It has also been possible, using the double Schottky approach, to fabricate the first double-sided microstrip detector, which was tested satisfactorily in a test beam at CERN during 1992. Prototype detectors for application in the ATLAS forward tracking system at the LHC were also tested. These are microstrip detectors, with a 60 micron pitch and 384 channels of 50mm length on one 200 micron thick detector "tile", fabricated in Glasgow. Commercial microstrip detector prototypes from GEC-Marconi, 25mm square with 128 double-Schottky channels on a 200 micron thick wafer, were also tested during the summer of 1992. Simple pad detectors of various thicknesses were prepared in a commercial production facility by Alenia, an Italian company, and proved to have the best performance which we have obtained to date for such pad detectors. This is illustrated in Figure 1, which shows the variation of charge collection efficiency with reverse bias voltage when Alenia detectors of differing thickness were traversed by minimum ionising particles. The limiting value of this efficiency is around 80% at a bias of the order of 1V/micron.

Microstrip detector performance has not yet achieved a correspondingly high level, although the analysis of the data from the test beam running is still at an early stage. At the present stage of the analysis, it does seem that the thinner detectors which we have been testing provide almost as much of a signal charge as the thicker detectors which were evaluated in last year's test beam runs. This is consistent with the understanding which we have been building up on the nature of the charge transport and charge trapping mechanisms in the various laboratories of the collaboration. From measurements of the response to alpha particles, X-rays and penetrating beta particles, (in Bologna, CERN, Sheffield and Glasgow), from detailed analysis of the time variation of the current pulse in simple detectors illuminated with pulsed laser and with alpha particles, (at Lancaster), and from electron microscope studies of the behaviour of such simple detectors, it has emerged that the electrons and holes created by ionising particles are separated and collected as output signal only in the region of the detector where the electric field is sufficiently high, and that this tends to be only in the region close to the reverse-biased Schottky contact. Although the sensitive region grows in thickness with reverse bias voltage, there tends to be a limitation to the maximum reverse bias from the limited breakdown strength of the material, so that the greatest charge collection efficiencies are only obtained in practice with thin detectors. At present we are attempting to quantify these effects and to understand fully the implications on the optimum design of LHC forward tracker detectors. The limit to how thin the detectors can be made, (and to the resulting minimum number of radiation lengths), is determined on the one hand by the mechanical strength of the GaAs, together with any suitable backing layer, and on the other to the limit on the charge signal amplitude which may be adequately resolved from the noise of a low-power, low cost multiplexed preamplifier system. With an equivalent noise charge from currently-available systems around 1000 electrons, a GaAs detector of 100 microns thickness would probably be near the limit to the useful thickness, and 200 microns would give a

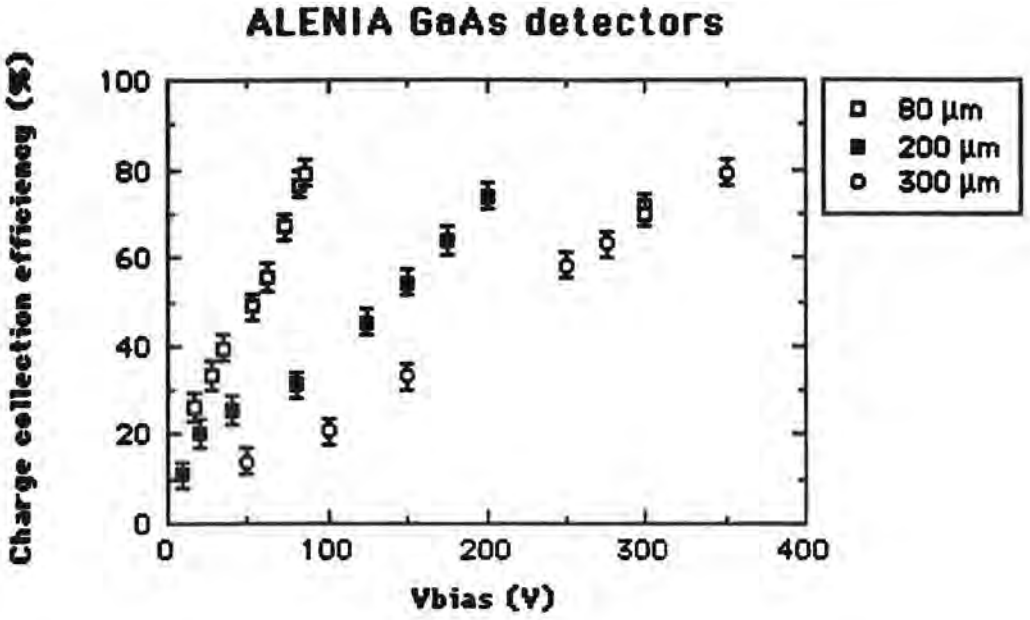

Figure 1: Charge collection efficiency for Alenia diodes of various thickness, as a function of reverse bias voltage

reasonable safety margin for efficient detection with high yield during the production process.
The detailed evaluation of the cost components in a complete LHC detector design, including mechanical supports, alignment, cooling and electronics, the Monte Carlo simulation to optimise the design and the continuing evaluation of different materials, including various types of semi-insulating substrate material and epitaxial layers are being actively pursued in of our laboratories. We look forward to being able to take up the challenge of building the GaAs forward tracker wheels for the ATLAS collaboration.

Publications and Conference Reports

S.P.Beaumont et al., *Nucl. Instr. and Meth. A321 (1992) 172-179*
S.D'Auria, *Contribution to the Como Instrumentation Conference, June 1992*
C.Buttar, *Contribution to the XXVIth International High Energy Physics Conference, Dallas, Texas, August 1992*
C.del Papa, P.-G.Pelfer and K.M.Smith (eds.), *Proceedings of the Eloisatron Workshop on GaAs Detectors and Associated Electronics, Erice, January 1992, (To be published by World Scientific)*

SDC Experiment

Bristol, Liverpool and Oxford Universities, and RAL (Plus 112 Institutes World Wide)

SDC (Solenoid Detector Collaboration) is an experiment in preparation for physics at the end of this decade at the SSC (Superconducting Super Collider) in Dallas, Texas, USA. Its design is aimed at a detector capable of studying the physics of pp collisions at the new (multi-TeV) energy scale where the underlying mechanisms responsible for the framework of today's "Standard Model" of the universe are likely to be manifest.

SDC is thus a precision experiment capable of measuring well the particles and energy flow and lepton (electron, positron and muon) fragments from these violent pp collisions over as large an angular range as possible. To do so it incorporates charged particles tracking detectors in the magnetic field of a large superconducting solenoid, a large calorimeter for electromagnetic and hadronic energy measurement, and an array of muon detectors (fig 1).

The design of SDC is presently in its final stages. Many of the details can only be specified as the results of a substantial detector R&D program become available. In July 1992, the experiment gained stage 1 approval by the Physics Advisory Committee in the US after scrutiny of the Technical Proposal which had been prepared and submitted. In October 1992 the SDC sought stage 2 approval from the DOE to proceed to the construction phase.

The UK groups in SDC are concerned with the tracking detectors in SDC. Oxford University, in collaboration with RAL, have designed and laid out a level 1 trigger logic chip suitable for use with either silicon or gas microstrip detectors in the inner silicon tracker or the outer intermediate angle track detector. Bristol and Oxford Universities have designed and simulated the trigger system for charge tracks at levels 1 and 2. Oxford University have developed with industrial collaboration a new fibre optic data transmission system which is radiation hard, is cheaper than alternatives, and is well suited to SDC (and other HEP experiments) read-out.

Liverpool University and RAL have been concerned with the design of the intermediate angle track detector. The infant detector technology of Microstrip Gas Avalanche Chambers (MSGC) is presently envisaged as the basis of the ITD. Annuli of MSGC "tiles" with a "keystone" geometry are laid out on a lightweight cone structure (fig 2) in a scheme which ensures both efficient and accurate track reconstruction and acceptable level 1 trigger p_T threshold. The development of the MSGC tiles and the design of the ITD support infrastructure are taking place in both Liverpool and RAL, and also in collaboration with Carleton University, Canada.

The contributions of the UK groups outlined above is already well enough advanced to mean that they are well placed to be responsible for the construction and operation of these major parts of SDC. The construction phase of the experiment will begin in earnest as funding is approved by the agencies of all countries with institutes in SDC.

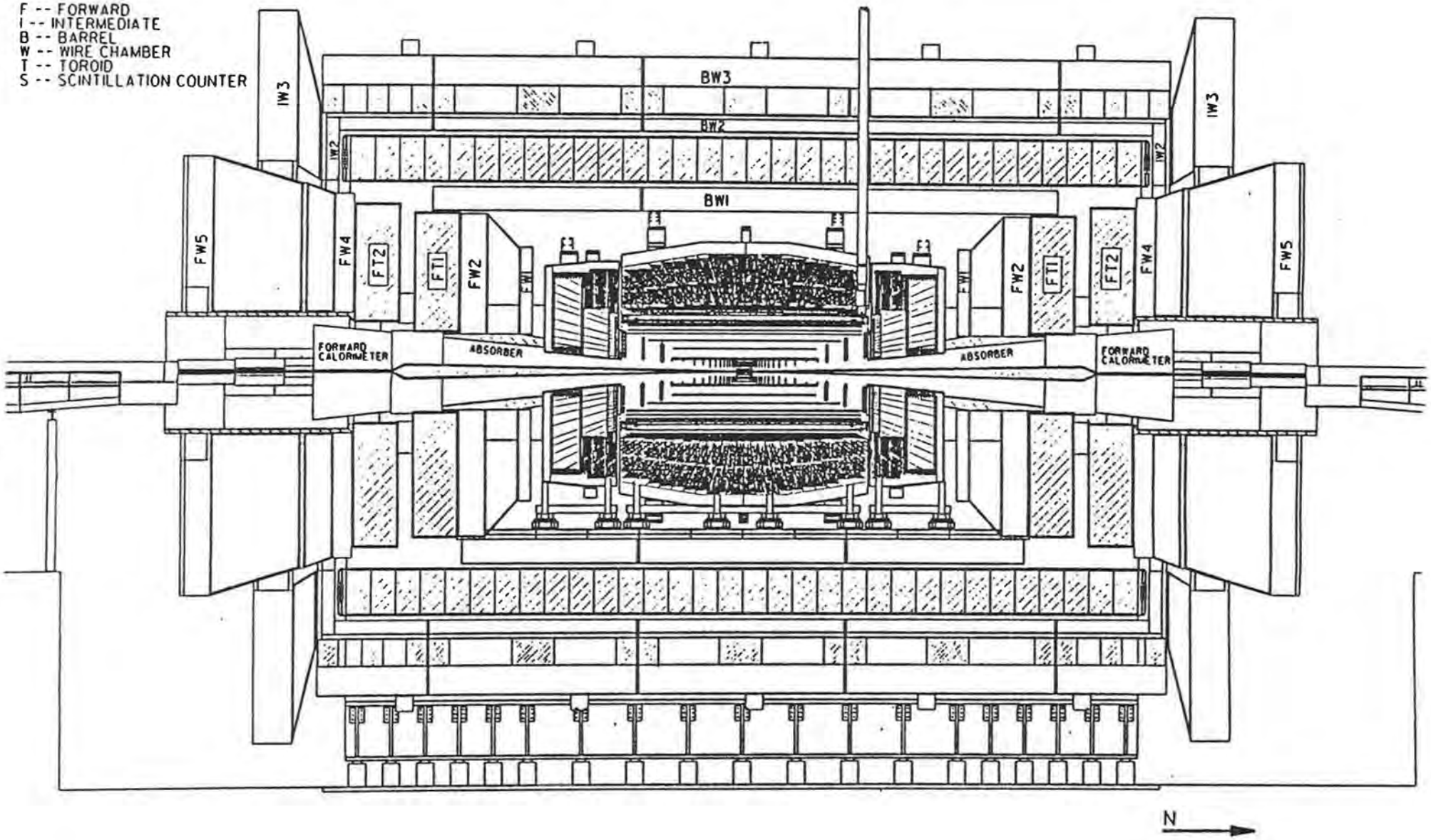

1. Schematic lay-out of the SDC experiment at SSC.

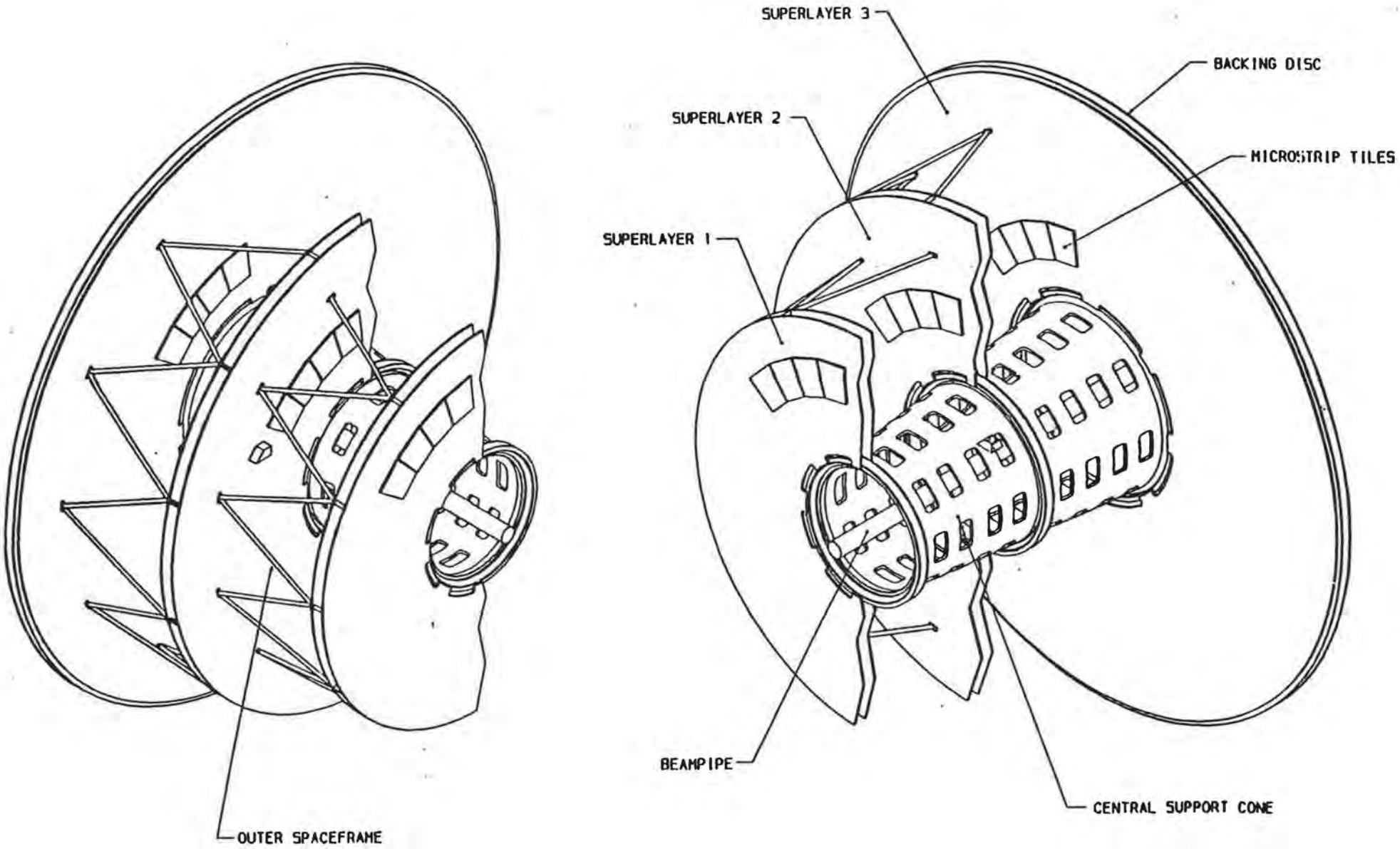

2. Schematic (3D) view of the essential features of the ITD showing the lightweight conical structure supporting MSGC tile annuli.

Development of High Resolution Silicon Strip Detectors for Experiments at High Luminosity at LHC

RD20 **Proposal 807**

CERN, INP Cracow, INPT Cracow, SEFT Helsinki, University of Liverpool, Imperial College London, CPPM Marseille, University of Oslo, SI Oslo, INFN Roma (Sanità), Rutherford Appleton Laboratory, LEPSI Strasbourg, INFN Torino, University of Uppsala, IHEP Vienna, PSI Villigen, Yale University, Cambridge University, Comenius University, Bratislava, Brunel University, London , INFN Padova

Introduction

The aim of this R&D project is to develop a high spatial precision tracking detector for an LHC experiment. The strongest candidate for inner tracking close to the beam is silicon because of its fast charge collection, probable radiation tolerance, demonstrated performance and past experience with both detectors and microelectronic readout.

The goals of RD20 are to demonstrate sufficiently radiation tolerant microstrip detectors and the essential electronic elements of a front end system with adequately low noise, precise timing and minimum power, which will be essential for cooling. It should be possible to implement in radiation hard form using a low mass mechanical support structure.

However, LHC operation will not be easy since some aspects of performance are expected to change over several years. The most obvious are detector leakage currents, and thus shot noise, but other less well measured parameters, such as charge collection speed and microstrip electrical characteristics, such as capacitance and interstrip isolation, are also expected to be influenced by irradiation.

Detectors

There is a staged programme of prototype fabrication under way to evaluate radiation tolerance of microstrip detectors and their sub-elements systematically. From irradiations of existing devices a large body of data now exists [1,2].

Both p-side and n-side prototypes detectors have been designed and submitted for fabrication. The p-side structures have been delivered and are being tested before and after a wide range of irradiations; the n-side structures are being fabricated. On the basis of the results so far, design of a single sided LHC detector will begin shortly. The design of a double sided LHC detector will be undertaken when results from n-side structures will be available.

Irradiations using by neutrons, high energy gammas and electrons have been carried out. Data on annealing of leakage currents and changes in doping

concentrations in the bulk silicon after radiation damage have been accumulated. These are the limiting factors to long term LHC operation. Recent results show an increase in detector capacitance after ionising irradiation which has important implications for front end electronics. Successful demonstration of high interstrip isolation on both surfaces of double sided readout detectors after irradiation has been demonstrated.

Electronics

Front end electronics were included in the programme since the performance of the amplifying system is inseparably related to the properties of the detectors. High speed operation with low noise in a hostile radiation environment is essential. An LHC system will have several million electronic channels and thus large power dissipation. An initial goal was therefore to emphasise low power electronics since minimal power dissipation is mandatory.

A CMOS preamplifier with 45 nsec CR-RC shaper has been tested with ENC≈ 400 +65e/pF and power dissipation of 1.6mW. A version of the RD20 preamplifier and shaper has been designed in the Harris 1.2 μm hardened CMOS process now available through Rutherford Appleton Lab. The process is believed to be hard to at least 1Mrad and 10^{14} n.cm^{-2}.

An analogue data pipeline buffer after the amplifier stores the data until a Level 1 trigger. It is followed by an signal processor employing analogue deconvolution to retrieve the impulse like input signal from the shaped pulse[3,4]. This is a novel signal processing concept for a front end system and has been thoroughly evaluated, including a substantial development of the underlying theoretical basis. It has been demonstrated using data from the prototype amplifier using a CMOS switched capacitor circuit with <0.1 mW/channel. All the essential elements of the front end system now exist as working prototypes and a total power consumption of 1-2mW/channel can be confidently envisaged.

Mechanical structure

For good spatial measurements it will be necessary to construct a stable but low mass mechanical support structure which must permit removal of the large amount of heat produced.

There has been a great deal of progress in the cooling and material studies which have been undertaken. Liquid and gas cooling schemes have been studied as well as properties of coolants and structural materials after irradiation. No conclusion has yet been drawn on the best method of cooling but water based systems appear to be capable of adequate performance. This work will provide a basis for more substantial work which will gradually be aimed more directly at individual LHC experiments.

Role of the UK groups in RD20

The work of the UK participants spans the entire range of activities. Imperial College has designed all the prototype detectors and test structures so far fabricated and has been closely involved in the electronic developments, particularly in the analysis of the novel signal processing ideas, experimentally and theoretically. These include measurements of detectors with RD20 prototype electronics after radiation damage. Radiation damage studies have been carried out using neutrons at ISIS, with Rutherford Appleton Laboratory, and electrons with LEPSI, Strasbourg. Liverpool has recently, with Cambridge and Rutherford Appleton Laboratory, designed new prototype detectors to be fabricated at Micron Semiconductor and has been carrying out neutron damage studies at ISIS, as well as contributing to the analogue pipeline developments. Rutherford Appleton Laboratory has been heavily involved in the mechanical studies, including demonstration of a potential method of water cooling of the system, and studies of the materials likely to be employed in a tracking system where the radiation hardness of components is of great importance.

Cambridge and Brunel Universities joined RD20 recently at the start of the second year. Both expect to contribute particularly to detector studies of radiation effects and Brunel plans to work also on the design of a mechanical support structure.

Future plans

In the next year construction of an LHC module will be undertaken which should demonstrate a mounted detector coupled to readout electronics in a realistic prototype. This should include a method of cooling the module to the proposed operating temperature of the system which is expected to be in the range 5-10°C.

References

[1] H. Borner et al. CERN/DRDC/91-10 (1991)
RD20 status report. CERN/DRDC/92-28 (1992)

[2] *Radiation damage by neutrons and photons to silicon detectors*
K. Gill, G. Hall, S. Roe, S. Sotthibandhu, R. Wheadon, P. Giubellino, L. Ramello. IC/HEP/92/7 (May 1992).
To be published in Nucl. Instr. & Meths.

[3] *The deconvolution method of fast pulse shaping at hadron colliders.*
S. Gadomski, G. Hall, T.Høgh, P. Jalocha, E. Nygård, P. Weilhammer.
CERN-PPE/92-24 (1992). Nucl. Instr. & Meths. A320 (1992) 217-227.

[4] *A novel technique for fast pulse shaping using a slow amplifier at LHC.*
N. Bingefors, S. Bouvier, S. Gadomski, G. Hall, T.Høgh, P. Jalocha, H. vd. Lippe, J. Michel, E. Nygård, M. Raymond, A. Rudge, R. Sachdeva, P. Weilhammer, K. Yoshioka. CERN-PPE/92-70 (April 1992)
To be published in Nucl. Instr. & Meths.

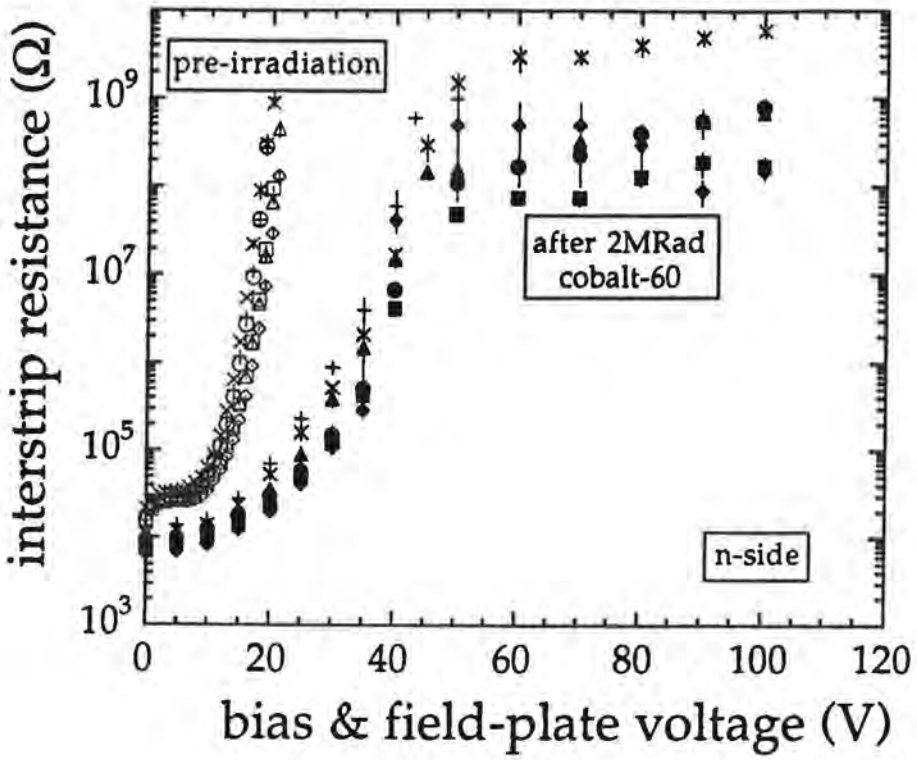

Fig. 1.
The interstrip resistance several strips of a microstrip detector measured on the ohmic (n-type) strip surface before and after gamma irradiation. The detector uses a field plate isolation method. Oxide charging has decreased the interstrip resistance but it remains sufficiently high for long term LHC operation.

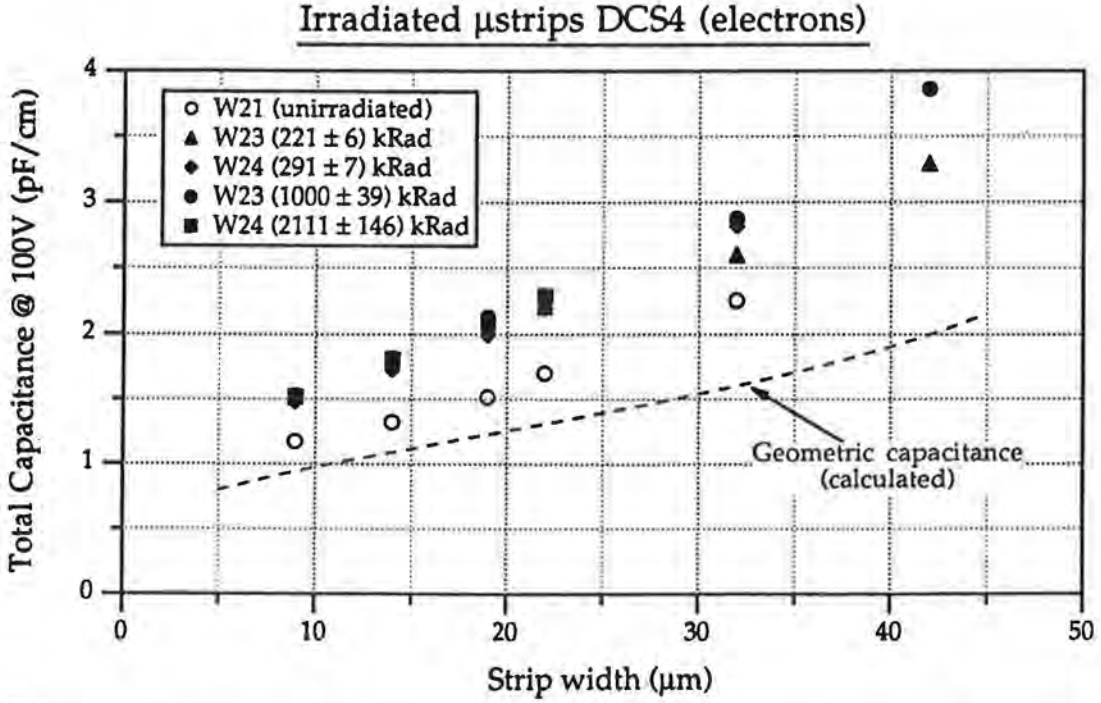

Fig. 2.
The capacitance of prototype microstrip detectors as a function of the strip width for 50μm pitch strips. After ionising irradiation the detector capacitance is observed to increase at doses up to several hundred krad.

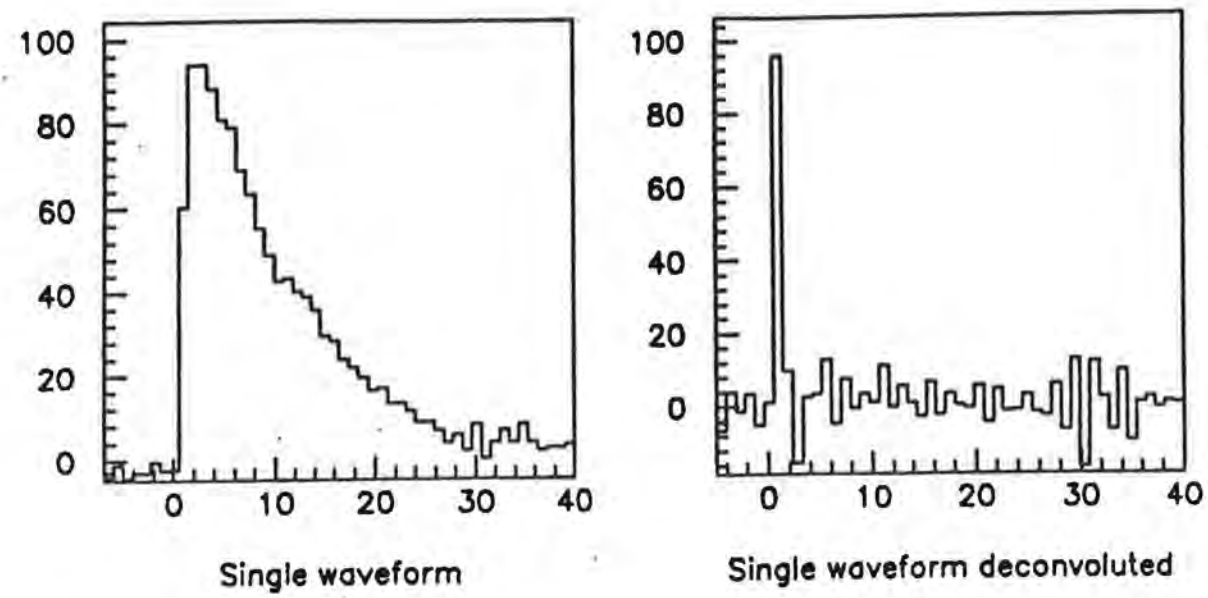

Fig. 3.
A simulated detector signal processed with a CMOS prototype amplifier, using a 45nsec time constant, as it could be observed at LHC. (a) shows the shaped amplifier output; each interval is 15nsec. (b) shows the result of an analogue deconvolution of the pulse and displays the precise event timing obtained.

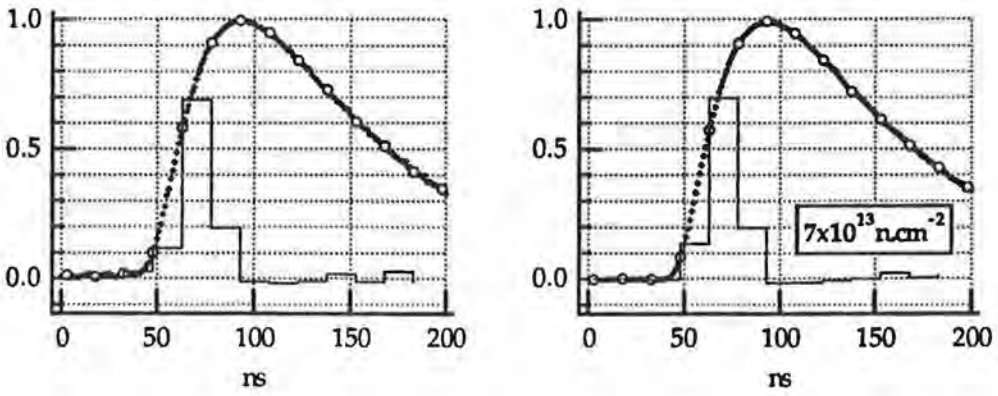

Fig. 4.
Beta electron signals measured in detectors connected to RD20 prototype electronics, before and after neutron irradiation, and deconvoluted off-line. The results show only small changes after heavy neutron damage provided the detectors are operated fully depleted.

GAS MICROSTRIP DETECTORS R & D
(CERN DRDC RD28)

UK participants: Birmingham, Liverpool, Manchester, RAL and UC London

Introduction

This collaboration was formed in Jan 1992 to establish the feasibility of constructing gaseous microstrip detectors (GMSDs) capable of operating as tracking devices in the LHC/SSC collider environment. In July 1992, the collaboration participated in the formation of a CERN DRDC project (RD28) with the same goals.

Background

A GMSD is based on the same principles as the wire proportional chamber but with the wires replaced by finely pitched alternating anode and cathode strips laid down on an insulating substrate. Above the substrate incident charged particles pass through a narrow region of gas (typically 3mm). A drift field carries the released electrons to the microstrip plane where avanlanche multiplication takes place. Most of the positive ions produced travel the short distance across the anode-cathode gap, typically 100 microns, giving very rapid recovery from any space charge effects. Thus, in principle these detectors can tolerate the very high fluxes expected at LHC/SSC, and approach the spatial resolutions and fast timing properties normally associated with more expensive Silicon detectors.

Current Status

Measurements on candidate substrate materials have continued in Engineering Science Division at RAL, mainly focussing on glass plates with differing electrical conducting properties. The standard electrode pattern is a grouped anode structure with a pitch of 300 microns produced from a 0.5 micron thick aluminium metallised surface by wet-etch techniques. To date, working detectors have been built from 10cm square substrates after processing in the Electron Beam Lithography Unit at RAL. All detectors are tested in collimated X-ray beams which generate up to 3×10^4 conversions per mm^2 in the detector gas. This enables rate and ageing effects to be studied. Detectors made from ionically conducting glasses such as 'Tempax' require HV conditioning when first switched on before stable gas-gain is observed. Further losses in gain are seen depending on the incident particle flux and voltage applied. These effects can be partially attributed to dynamic changes in the surface resistivity of the substrate with electric field. Conditioning does not seem to be necessary for semiconducting glasses with suitable resistivities but, contrary to expectations, a sample device built from these materials still shows rate dependences similar to those seen for 'ionic' glasses. This may

indicate that currrent processing techniques are partially responsible for the behaviour observed. Alternative methods of metallisation and pattern fabrication are being actively studied both at RAL and other institutes in the RD28 collaboration.

Relatively few measurements exist of the response of GMSDs to minimum ionising particles. A simple detector built from 'Tempax' glass with a grouped anode structure was exposed to a low intensity 5-7Gev pion beam at CERN. Using Argon (70%)-Isobutane (30%) gas mixture and fast low noise transimpedance amplifiers , the time structure and size of the anode signals were studied in detail. Running with a gas gain of $3x10^3$ the detector was found to be quite efficient ; however, large variations in the pulse shapes were observed attributed to random fluctuations in the collection of the amplified charge in the gas with time. These first measurements point to the importance of selecting 'fast' gas mixtures with good primary yield of ion pairs.

Preparations are well in hand to carry out much more sophisticated tests with minimum ionising particles in very high intensity beams at CERN which are capable of exceeding the flux densities anticipated at the Hadron Colliders. For this purpose, several modular detectors have been constructed in which hybridized fast front-end electronics is connected to the individual anode strips at 300 micron spacing by wire bonds. This will enable the clustering of deposited charge to be studied with angle of incidence, and more detailed measurements of the pulse structure made with flash ADCS connected to neighbouring channels. A first test run is planned before the end of 1992, followed by further periods in the North Area at CERN in 1993. During this time, it is planned that custom designed monolithic circuits followed by analogue or digital pipelining can be incorporated. This choice will depend on the perceived needs of the future experiments.

The aims are to develop stable detectors with minimal thickness materials (0.5 mm glass equivalent) capable of withstanding sustained rates of more than 10^4 mm-2 sec-1 for at least 10^8 secs without ageing. The latter requirement is probably the greatest challenge in the project matching the need to develop within the next year working detectors having larger area substrates with non-parallel strips.

A Calorimeter-Based Level-One Electromagnetic Cluster Trigger for LHC

N Ellis, I Fensome, J Garvey, P Jovanovic, R Staley, A Watson
University of Birmingham, Birmingham, UK
E Eisenhandler
Queen Mary and Westfield College, University of London, London, UK
C N P Gee, A Gillman, R Hatley, V Perera, S Quinton
Rutherford Appleton Laboratory, Chilton, Didcot, Oxon, UK

Abstract

Level-one triggering at LHC will be very challenging. We have studied the problem of recognition of electromagnetic clusters and have developed an algorithm based on the transverse energy distribution in an electromagnetic calorimeter. This receives 8-bit digitised energies from a 4 X 4 window in the calorimeter. Two cluster thresholds and two isolation thesholds are provided, all of which are programmable. The algorithm has been been implemented as a gate array in 0.8 μm CMOS technology, and is performed using pipelined processing at 67 MHz. The gate array has been tested at full speed, and is being incorporated into a small prototype trigger processor to be tested with beam in conjunction with prototype calorimeters.

INTRODUCTION

At the LHC design luminosity of 1.7×10^{34} $cm^{-2}s^{-1}$ the proton-proton interaction rate will be approximately 1.5×10^9 Hz. If the beam bunches cross every 15 ns this is equivalent to 20 interactions per crossing. Most of these interactions will contain no interesting physics. The function of the trigger is to select the small fraction in which a hard process may have occurred. Signatures for such processes are the production of high p_T leptons, partons or gammas and therefore triggers must recognise these particles in the detectors of the experiment. Selection of potentially interesting interactions is made in several steps or levels, as shown in fig. 1. At level one every interaction is examined and a rejection factor of between 10^4 and 10^5 is required to reduce the input rate into level two to a value where microprocessors can be used. This reduction must be achieved with no deadtime and requires a hard-wired processor operating in a pipelined mode at a clock frequency of 67 MHz. In this paper we describe such a processor, designed to recognise electromagnetic energy clusters in a calorimeter. The dominant background to such triggers comes from jets. The effectiveness of a cluster trigger is measured not only by the efficiency with which it detects real clusters but also by how well it can reject false triggers from jets.

TRIGGER ALGORITHMS

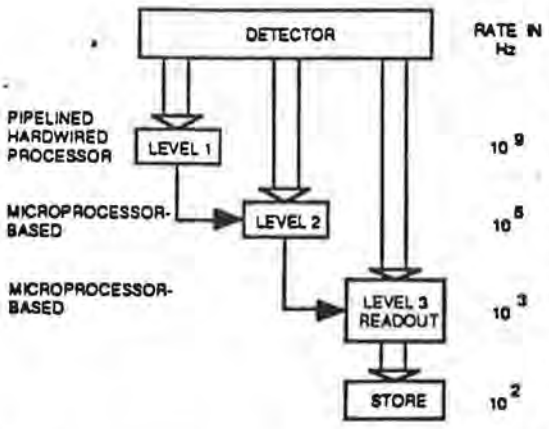

Fig. 1 Conceptual trigger system for a LHC experiment

The effectiveness of various trigger algorithms has been tested using Monte Carlo data simulating p-p collisions at 16 TeV [1]. Results of such a study are shown in fig. 2. Various rates are given as a function of transverse energy, (E_T), threshold. Curve (a) gives the rate of events containing a QCD jet anywhere in phase space having a transverse energy greater than the threshold indicated. Curve (d) gives the rate of events containing a π^0 in the pseudorapidity range $|\eta| < 2.5$ having a transverse energy greater than the threshold indicated. For an electromagnetic cluster trigger, this curve represents the minimum rate realistically achievable at level one. This is a guide to the limit to which one should attempt to reduce the false

electromagnetic trigger rate from jets. The other three curves represent the results of applying specific algorithms to the distribution in the calorimeter. These are described below.

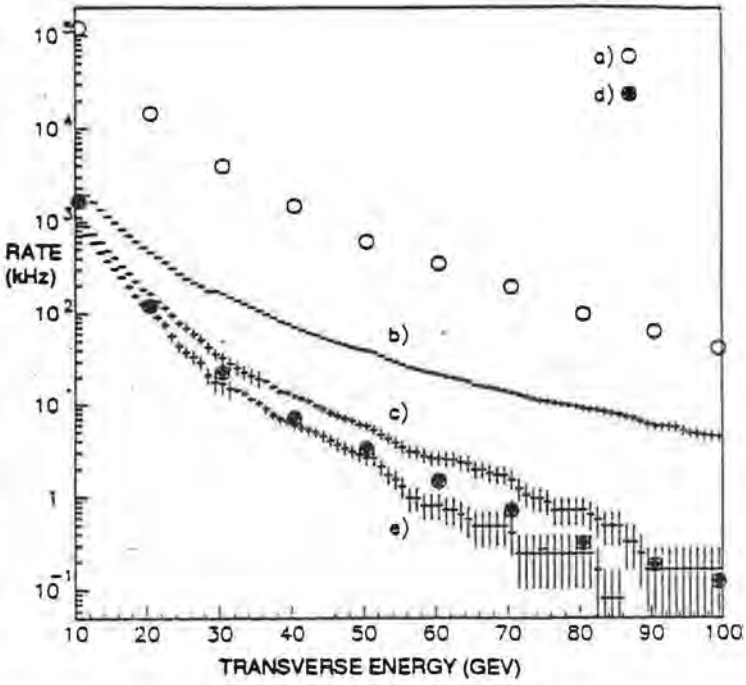

Fig. 2 Various rates as a function of transverse energy threshold for an LHC luminosity of 1.7×10^{34} $cm^{-2}s^{-1}$.

The inputs to the trigger algorithm are the transverse energies contained in calorimeter trigger cells each covering an area 0.1 X 0.1 in $\eta - \phi$ space, where η is pseudorapidity and ϕ is the azimuthal angle around the beam. A 4 X 4 array of both electromagnetic and hadronic cells is shown in fig. 3. For the simulations the electromagnetic part consists of 29 radiation lengths and the hadronic part 8 interaction lengths. The reference cell for this particular block of electromagnetic calorimetry is labelled (2.2). The distribution of transverse energy in this volume of the calorimeter is examined by the algorithm to determine if there is an electromagnetic energy cluster spanning the reference cell. The process is duplicated, using each electromagnetic trigger cell in the calorimeter as the reference cell, over the pseudorapidity range $|\eta| < 2.5$. The algorithm calculates the sum of the transverse energies in the reference cell and the one above it (2.2+3.2), and in the reference cell and the one to its right (2.2+2.3). The event rate where the larger value of E_T is above threshold is plotted as curve (b) in fig. 2. Addition of adjacent trigger cells is important to provide sharp E_T thresholds, especially for large values of η. Rejection of hadronic jets is improved by requiring that the electromagnetic energy cluster is isolated. Thus the algorithm also calculates the sum of the transverse energies in the surrounding cells and requires this sum to be below a certain threshold. For curve (c) in fig. 2 the ring of electromagnetic cells surrounding the reference cell (as shown in fig. 3) provides the isolation energy sum, and the threshold is 3 GeV transverse energy. For curve (e) this ring of electromagnetic cells and the sum of all 16 hadronic cells are used, and the threshold is 5 GeV transverse energy. In both cases the electron detection efficiency is greater than 95%.

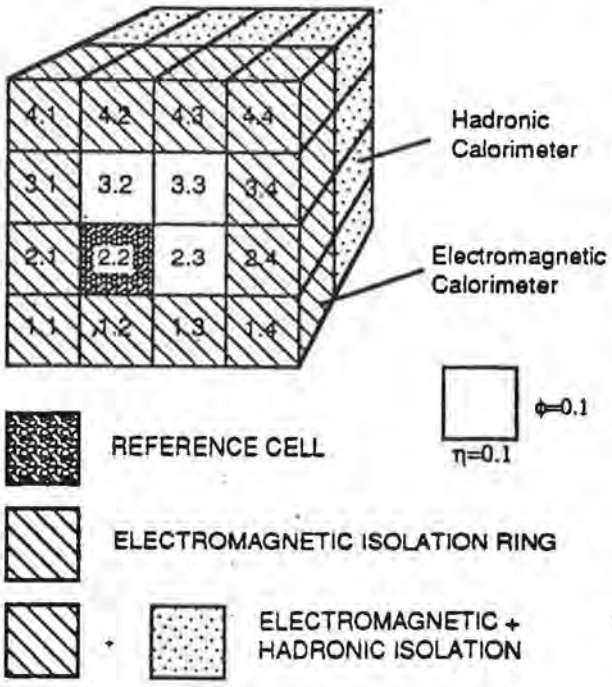

Fig. 3 Block of calorimetry used to study the jet rejection and electromagnetic cluster acceptance algorithm.

The granularity of 0.1 x 0.1 in $\eta - \phi$ space represents a compromise between jet-rejection power and complexity. This granularity with isolation brings the trigger rate down to a level similar to that of the π^0 rate. It is interesting that the full isolation requirement does produce a trigger rate lower than that of the π^0s, and this is because the π^0s are themselves part of jets.

THE IMPLEMENTATION OF THE ALGORITHM

An ASIC using a gate array in 0.8 μm CMOS has been designed and manufactured to perform the algorithm corresponding to the results shown in curve (c) of fig. 2 [2]. This algorithm was chosen in preference to that corresponding to curve (e) (which requires hadronic information as well) to simplify the prototype ASIC design. The ASIC operates in a pipelined manner with 15 ns between pipeline steps. The ASIC takes in the 16 digitised 8-bit pulse heights from a block of electromagnetic calorimetry. The steps in the pipeline are indicated in fig. 4. It is possible to apply two separate thresholds to the electromagnetic cluster and two separate thresholds to the ring of isolation cells. The ASIC outputs two hit-bits corresponding to the two thresholds, and also the 12-bit sum of the total tranverse energy in all 16 cells. From fig. 4 it can be seen that the latency of the ASIC is 7 clock cycles, ie 105 ns. The ASIC was manufactured by Fujitsu and has been tested up to the full LHC frequency of 67 MHz.

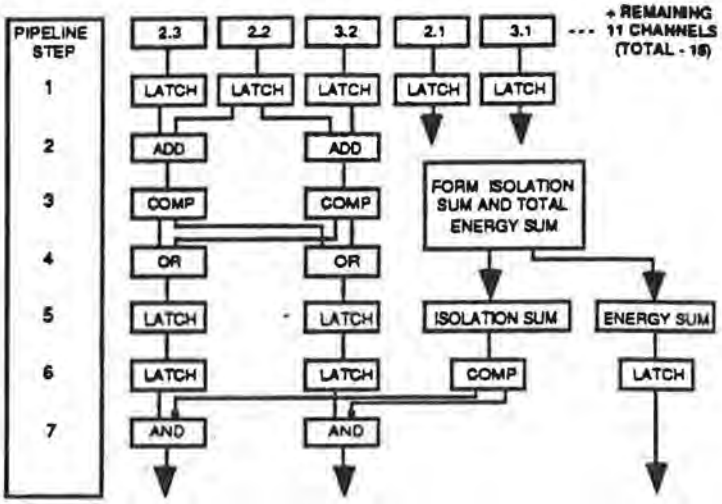

Fig. 4 Pipelined steps performed by the cluster finding ASIC using the electromagnetic trigger cells indicated in fig. 3.

A PROTOTYPE TRIGGER PROCESSOR

We are at present assembling a prototype processor which is designed to handle completely a 3 X 3 array of electromagnetic trigger reference cells. The nine cluster-finding ASICs are mounted on one cluster-finding module into which are brought the digitised pulse heights from a 6 X 6 array of electromagnetic trigger cells. The configuration of trigger cells is shown in

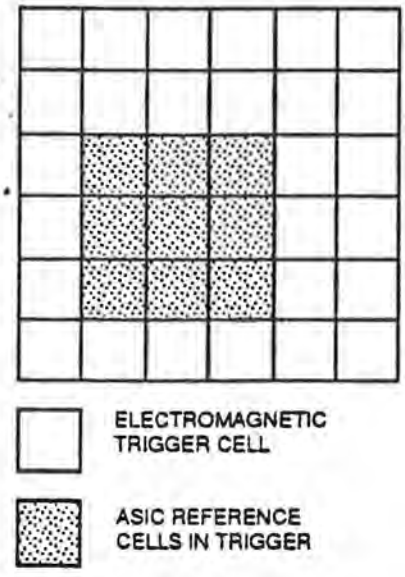

Fig. 5 Configuration of trigger cells processed by a cluster-finding module.

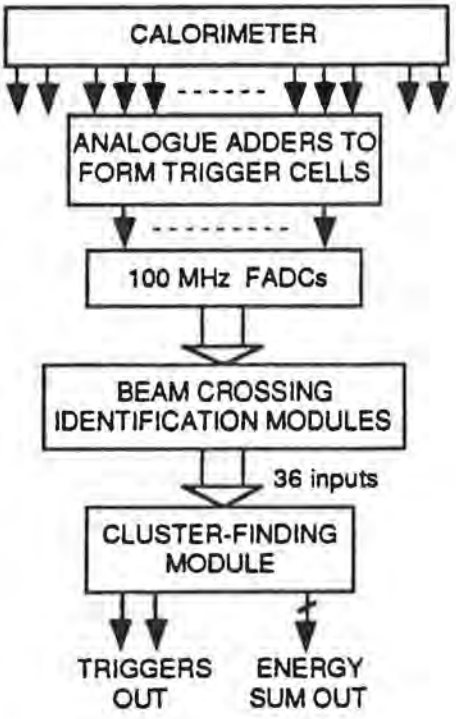

Fig. 6 Components of the prototype trigger processor.

fig. 5. The cluster-finding module is equipped with fast memory on its input and output, to allow it to be tested in an off-line mode. The components of the prototype processor are shown in fig. 6. The crossing identification module will be crucial for the level one trigger at LHC, since the calorimeter pulses will probably be longer than one bunch crossing period. The level one processor must know on a crossing-by-crossing basis which 8-bit words to include in performing the algorithm. The function of the beam-crossing identification module is to compute the peak calorimeter signal and identify the beam crossing responsible for it. Digitisations corresponding to all other crossings will be suppressed. This module has not yet been designed. Its role in beam tests is not crucial, as the activity in any one trigger cell will be low. The other components indicated in fig. 6 are being built. We intend installing the processor on the Accordion calorimeter barrel prototype [3] for beam tests at CERN.

PROGRESS TOWARDS A FULL TRIGGER PROCESSOR DESIGN

This work is now part of the RD27 project to study all aspects of level-one triggering. For the calorimeter trigger the most serious problem is the large number of interconnections between trigger cells required to implement the cluster-finding algorithm we have described. The modularity of the present cluster-finding module results in each calorimeter signal being fanned-out to 4 modules. The module takes in (36 X 8) bits of signal information which is easily achieved using present connector technology. The problem is that this modularity requires about 400 modules to cover the region $\eta < 3.0$ and in a crate-based system results in a very complex inter-crate connection matrix.

We are therefore investigating the implications of increasing the trigger channel density on a single module, which would reduce the number of modules and the number of crates required for the complete processor. A design study is under way of a larger ASIC which would fully process a 2 X 2 array of electromagnetic trigger cells, by taking in a 5 X 5 array of electromagnetic cells and the matching 5 X 5 hadronic cell array. In order to minimise the ASIC I/O requirements, several techniques to reduce the data bandwidth are being studied. These include time-multiplexing the inputs at 134 MHz, and dynamic allocation of tagged above-threshold data to a limited number of transmission paths. Asynchronous systems incorporating zero suppression and data compression are also under consideration. The effects on the various physics processes of implementing these techniques in the trigger processor are being investigated by simulation. The results of these studies so far indicate that an ASIC based on a 100 K gate array in 0.8 μm CMOS, with 179 pins might provide a solution to the problem.

Using such techniques, eight ASICs could be assembled on a 9U cluster-finding module, of which about 120 would then be required to fully process the entire calorimeter. It is currently estimated that only ten crates would be sufficient to accommodate all the necessary processing hardware.

Acknowledgements

We are grateful to many people of the technical staffs at Birmingham and RAL for expert help on this project. This work has been funded by the Science and Engineering Research Council (UK).

References

[1] N Ellis et al., *Level-1 trigger system*, ATLAS note DAQ NO 005.

[2] V Perera, *Data on the LHC Electromagnetic cluster finding ASIC* (RAL 114) Rutherford Appleton Laboratory, Systme Design Group, 1992.

[3] B Aubert et al., *Hadronic and electromagnetic liquid argon LHC prototype calorimeter with pointing geometry*, CERN/DRDC/91-21.

[4] N Ellis et al., *First-level trigger systems for LHC experiments*, CERN/DRDC/92-17.

PROTOTYPE NEUTRINO DETECTOR

Oxford University

Project 894

The major effort of the group this year has been devoted to detailed preparations for an experiment (Proposal P282) on the 17-keV neutrino. This will be the first particle physics experiment carried out utilizing the new cryogenic phonon detector devices developed by the group. In this experiment the β-source (^{63}Ni, Q=67 keV) is electroplated onto a small area of a Si wafer, and covered by a second wafer in close contact as indicated in Fig.1. This geometry ensures that all of the kinetic energy of the β-particles regardless of back-scattering or back-diffusion is deposited in the Si wafers. Approximately 70% of the kinetic energy is transformed into phonons which propagate to the outer surfaces where they are absorbed by Cooper-pair breaking in the Al films of series-connected arrays of Al-AlOx-Al superconducting tunnel junctions (SASTJ's). Each phonon absorbed produces at least two electronic excitations (called quasiparticles) which are detected as an increase in the tunneling current from its thermal equilibrium value. Since the phonons are confined, those which are not absorbed in the first encounter with a surface are subsequently absorbed in further encounters (reverberation). We have obtained energy resolutions substantially better than 1 keV (FWHM) with such detector devices.

These devices require an operating temperature of about 100 mK and to this end we have installed and commissioned a small dilution refrigerator in a screened room. The tunneling current pulses are extracted from the cryogenic environment using battery-powered biasing circuity and preamplifying electronics operated at room temperature.

A new data acquisition system has been designed and implemented. This system consists of 12-bit waveform digitizers connected to a digital signal processor and a work station, and an auxiliary trigger generator. Such a system is required because of the complicated shape of the phonon signals and because of the need to operate at high counting rates where effects due to pulse pileup must be precisely assessed. In addition to the hardware implementation, effort has gone into modelling of β-particle scattering in the detector and phonon propagation.

We have extended the radioactive source preparation technique, based on the adsorption of chemically produced precipitates which is extensively used in Oxford, to give highly uniform electroplated deposits directly on the detector devices. Source thicknesses have been checked with a scanning electron microscope and are in agreement with those determined by Faraday's Law during deposition.

We have succeeded in dramatically improving the quality and uniformity of the tunnel junction arrays by switching from a shadow mask, thermal evaporation procedure

to a magnetron sputtering and photolithographic patterning technique. Figure 2 shows an example of the junction uniformity achieved with this technique. The most important result so far of this change in fabrication procedure is a much improved biasing stability of the tunnel junction arrays.

At the time of writing preliminary data have been taken only with a ^{57}Co source not directly on a detector device. This source provides X-rays, γ-rays and internal conversion electrons spanning the energy range 6.4 keV to 129 keV. Preliminary measurements give a non-linearity of less than 0.5% over this range.

Serious data-taking with ^{63}Ni is about to commence, and we expect to have a conclusive result during the first half of 1993.

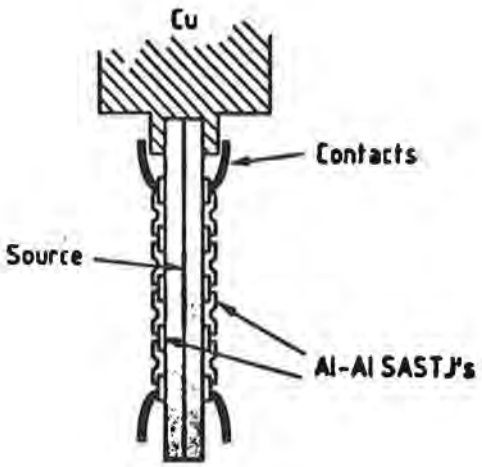

Figure 1. Schematic arrangement of beta-ray spectrometer for a precision experiment on the 17-keV neutrino. The Cu heat-sink is fastened to the mixing chamber of a small dilution refrigerator.

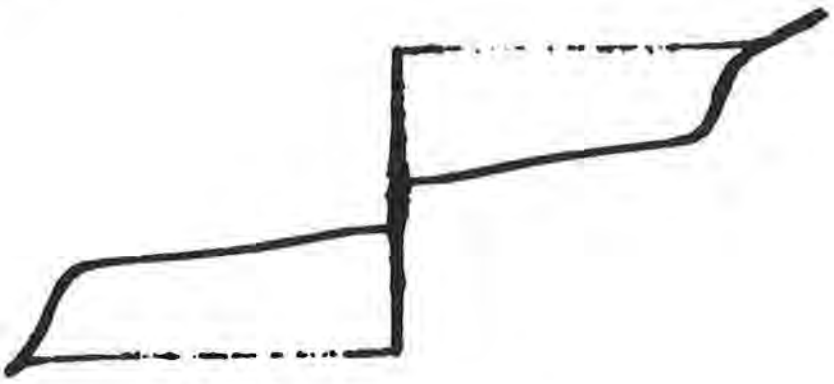

Figure 2. Current voltage characteristic of a series connected array of 700 Al-AlOx-Al tunnel junctions exhibiting a high degree of uniformity of the Josephson critical current.

Publications

N E Booth, R J Gaitskell, D J Goldie, C Patel and G L Salmon
"Single crystal superconductors as X-ray detectors"
in **X-Ray Detection by Superconducting Tunnel Junctions**, ed. by A Barone, R Cristiano and S Pagano (World Scientific, 1991) p.125.

D J Goldie, *"Energy resolved γ-ray detection using tunnel junction arrays on single crystal silicon"*
in **X-Ray Detection by Superconducting Tunnel Junctions**, ed. by A Barone, R Cristiano and S Pagano (World Scientific, 1991) p.98.

R J Gaitskell, D J Goldie, N E Booth and G L Salmon
"Low temperature superconducting detectors for dark matter and solar neutrino experiments"
in **Massive Neutrinos Tests of Fundamental Symmetries**, XIth Moriond Workshop, ed. by O. Fackler, G. Fontaine and J. Trân Thanh Vân (Editions Frontieres, Gif-sur-Yvette, France, 1991) p.191.

A C Howman, C Patel, G L Salmon, N E Booth with G J White and A T Scivetti, Queen Mary and Westfield College, and F Goodall and J O'Donnell, Rutherford Appleton Laboratory
"Frequency conversion with superconducting tunnel junctions"
Extended abstracts of the International Superconductive Electronics Conference, ISEC '91, Glasgow (1991) p.528

N E Booth, R J Gaitskell, D J Goldie, A C Howman, C Patel and G L Salmon
"Cryogenic detectors for experiments in elementary particle physics"
(Invited paper presented at Frontier Detectors for Frontier Physics, 5th Pisa meeting on advanced detectors, Elba, Italy, May 1991)
Nucl. Instr. and Meth. **A315**, 201 (1992)

N E Booth, R J Gaitskell, D J Goldie, A C Howman, C Patel and G L Salmon
"Cryogenic detectors based on superconducting tunnel junction arrays for elementary particles"
in **The Vancouver Meeting, Particles and Fields '91**, ed. by D Axen, D Bryman and M Comyn (World Scientific, 1992) p.922

D J Goldie, N E Booth and G L Salmon
"Particle detection with tunnel junction arrays on InSb"
in **Low Temperature Detectors for Neutrinos and Dark Matter IV**, ed. by N E Booth and G L Salmon (Editions Frontières, 1992) p.245

R J Gaitskell, N E Booth and G L Salmon
"Prospects for dark matter detection with a large superconducting niobium absorber"
ibid. p.435

N E Booth, R J Gaitskell, D J Goldie, A C Howman, C Patel , G L Salmon and P Valko
"Plans for a cryogenic detector experiment on the 17-keV neutrino"
ibid. p.407

D J Goldie, N E Booth, R J Gaitskell and G L Salmon
"Particle Detection with Superconducting Tunnel Junctions — Modelling the Non-Equilibrium State Generated by Particle Interactions"
(Invited paper at SQUID '91, published in **Superconducting Devices and Their Applications'**, ed. by H Koch and H Lübbig (Springer-Verlag, 1992) p.474.

Particle Acceleration

Introduction

High amplitude plasma waves driven by lasers (Beat Waves) are promising candidates for achieving particle acceleration for applications in fundamental high energy physics research. Researchers at UCLA have used 10μ CO_2 laser radiation to produce relativistic plasma waves with associated longitudinal electric field amplitudes of 10 MV cm^{-1}, and have demonstrated acceleration of electrons by these waves. However, the long laser wavelength restricts the ultimate acceleration obtainable.

The programme at RAL, based on the 1μm Vulcan glass laser facility has already reported the generation of Beat Waves at 6.10^6 $V.cm^{-1}$. It was found that the wave amplitude saturated at less than the value suggested by relativistic de-tuning. This has been attributed to the modulational instability, which caused premature break-up of the plasma wave. This has been confirmed by modelling using a PIC code, and by very recent experiments by co-workers at Ecole Polytechnique.

The growth time of the modulational instability under the experimental conditions produced in the RAL programme is in the 10ps regime. Recent work at RAL has concentrated on developments to enable Beat Waves to be generated on the ps timescale, thereby avoiding the problems associated with plasma instability.

Plasma production with ultra-short pulses

The production of large scale, homogeneous, fully ionised plasmas at a pre-defined density is essential to Beat Wave experiments. Since interest is now focused on high intensity, ultra-short pulse irradiation as explained above, it is important to demonstrate that such plasmas can be produced. Pending the availability of picosecond pulses from Vulcan, experiments have been performed using the 268nm, 12 ps laser output from the Sprite facility. This work used Thomson scattering to demonstrate that 100% ionisation of He_2 was achievable over the pressure range of interest (1 - 10 torr). With 2 ps pulses now available from the Vulcan laser, these experiments will be repeated at 1μm using H_2 during the early part of 1993.

Laser development

Work has commenced on a two-year upgrade programme to the Vulcan glass laser facility to provide 50TW, 1 ps operations in support of user experiments including the Beat Wave programme. The work is well advanced, and ultra-short pulses at the 10TW level will be made available to users from January 1993, with 50TW operations planned for the following year.

Ultrashort high power pulses can not be produced directly from glass lasers because at such high intensities, non-linear self focussing effects would cause severe degradation of the laser beam quality, leading to beam break-up and catastrophic damage to the optics. Chirped Pulse Amplification, or CPA, is a suitable technique for overcoming these problems. A low intensity, ultra-short pulse (~1-2 ps) is generated in an advanced oscillator, followed by pulse stretching to ~100ps using a pair of diffraction gratings prior to amplification to the 10 - 50 J level. The pulse is then re-compressed to its original duration using a second pair of gratings. The CPA technique was successfully demonstrated on Vulcan at the end of 1991 at the 5J, 3TW level; the next stage of development to 20J, 10TW is currently under way.

At the intensities generated in the final re-compressed pulse, the non-linear effects due to propagation of the beam in air would cause significant beam distortion, and consequently the final grating must be maintained in vacuum. The photograph shows the vacuum chamber which has been constructed for this purpose, coupled to an existing target chamber which houses the focusing optics and target mechanism.

The Beat Wave programme is undertaken by scientists from RAL, Imperial College, and Ecole Polytechnique in Paris.

The Vulcan upgrade is a collaboration between RAL, the Blackett Laboratory, and the Optoelectronics Research Centre at Southampton University.

cbe 22/10/92